MSc (Clinical Immunology)

Vaginal microbial diversity of the genital tract of South African adolescent females

---

AERIN OLIVIA BREETZKE
BRTAER001

Supervisor: Associate Professor Jo-Ann Passmore
Co-supervisor: Dr. Heather Jaspan
Co-supervisor: Dr. Katie Lennard

Department of Clinical Immunology
Division of Pathology
Faculty of Health Sciences

University of Cape Town
South Africa

Plagiarism Declaration

I, Aerin Olivia Breetzke, hereby declare that the work on which this dissertation/thesis is based is my original work (except where acknowledgements indicate otherwise) and that neither the whole work nor any part of it has been, is being, or is to be submitted for another degree in this or any other university.

I empower the university to reproduce for the purpose of research either the whole or any portion of the contents in any manner whatsoever.

Signed by candidate

Signature Removed

Signature: _____

Date: 10/11/2016

Masters of Science Degree – Clinical Immunology

Vaginal microbial diversity of the genital tract of South African adolescent females

By

Aerin Olivia Breetzke

BRTAER001

Dissertation submitted in fulfillment for the requirements of the degree in Medical Masters in Clinical Immunology.

Table of Contents Page

Acknowledgements

First and foremost I would like to thank Dr. Heather Jaspan, Department of Clinical Immunology, Pathology, for her supervision and encouragement throughout the entire process of my MSc project.

I would like to thank Assistant Professor Jo-Ann Passmore and Dr. Katie Lennard for all of their assistance and guidance throughout my laboratory work and write up.

My gratitude goes to both the Clinical Immunology staff and students for their guidance and help throughout my work, and for the constant support during my write up. Further thanks to everyone who helped and guided me with learning new laboratory techniques and equipment.

Thanks to the Clinical Virology staff and students, for their help and encouragement during this project.

Thank you to the UCT Clinical Immunology, Department of Pathology for the funding laboratory framework and the opportunity to work on the WISH samples and study this interesting topic in relation to adolescent health in South Africa.

Jake my love, my family, and friends, thank you for consistently supporting and holding me throughout the last two years, and for being there for me through the good days and the bad!

List of Tables

Chapter 1: Literature Review

Chapter 2: Cohort Characteristics

Chapter 3: Laboratory Methods and Materials

Chapter 4: Results

List of Figures

Chapter 1: Literature Review

Chapter 3: Laboratory Methods and Materials

Chapter 4: Results

the standard curve is generated based on the amplification curve of the standard positive controls ranging from 10^6 to 10^0 copies/µL. Red and brown indicate positive amplification in the unknown samples and the positive control standards respectively, blue indicates uncertainty and green indicates negative amplification in the wells.

Figure 4.2.1: Box plot comparison of the copies of each bacterial species of interest quantified in the DNA extracted from WISH participants' lateral wall swabs; showing the entire cohort reported as copies/ng total DNA for *L. gasseri* (red), *L. jensenii* (orange), *L. crispatus* (green), *L. iners* (blue), and *G. vaginalis* (purple) and *P. bivia* (pink). The 'box' component of each plot indicates the interquartile range (IQR) of the data set and the 'whiskers' which are the two lines (bottom and top) extending from the box component of each block that end with a horizontal stroke, indicate the range from the smallest and largest non-outliers to the 25% and 75% percentile components, respectively. The middle line indicates the median value for each data set.

Figure 4.3.1A: Box-plot of *L. gasseri* (red), *L. jensenii* (orange), *L. crispatus* (green), *L. iners* (blue), and *G. vaginalis* (purple) quantities for BV positive participants. The 'box' component of each plot indicates the interquartile range (IQR) of the data set and the 'whiskers' which are the two lines (bottom and top) extending from the box component of each block that end with a horizontal stroke, indicate the range from the smallest and largest non-outliers to the 25% and 75% percentile components, respectively. The middle line indicates the median value for each data set.

Figure 4.3.1B: Box-plot of *L. gasseri* (red), *L. jensenii* (orange), *L. crispatus* (green), *L. iners* (blue), and *G. vaginalis* (purple) quantities for BV intermediate participants. The 'box' component of each plot indicates the interquartile range (IQR) of the data set and the 'whiskers' which are the two lines (bottom and top) extending from the box component of each block that end with a horizontal stroke, indicate the range from the smallest and largest non-outliers to the 25% and 75% percentile components, respectively. The middle line indicates the median value for each data set.

Figure 4.3.1C: Box-plot of *L. gasseri* (red), *L. jensenii* (orange), *L. crispatus* (green), *L. iners* (blue), and *G. vaginalis* (purple) quantities for BV negative participants. The 'box' component of each plot indicates the interquartile range (IQR) of the data set and the 'whiskers' which are the two lines (bottom and top) extending from the box component of each block that end with a horizontal stroke, indicate the range from the smallest and largest non-outliers to the 25% and 75% percentile components, respectively. The middle line indicates the median value for each data set.

Figure 4.3.1.1: Comparison of the quantities of *L. crispatus* (copies/ng DNA) measured in the DNA extracted from vaginal lateral wall swabs from participants in the WISH study, between BV positive, intermediate and negative groups. All p-value comparisons were based on an

unpaired, non-parametric Dunn's Multiple Comparison test. Each point in the figure represents an individual participant. The three horizontal bars represent the median value (middle bar), upper interquartile range (top bar) and lower interquartile range (bottom bar).

Figure 4.3.1.2: Comparison of the quantities of *L. gasseri* (copies/ng DNA) measured in the DNA extracted from vaginal lateral wall swabs from participants in the WISH study, between BV positive, intermediate and negative groups. All p-value comparisons were based on an unpaired, non-parametric Dunn's Multiple Comparison test. Each point in the figure represents an individual participant. The three horizontal bars represent the median value (middle bar), upper interquartile range (top bar) and lower interquartile range (bottom bar).

Figure 4.3.1.3: Comparison of the quantities of *L. jensenii* (copies/ng DNA) measured in the DNA extracted from vaginal lateral wall swabs from participants in the WISH study, between BV positive, intermediate and negative groups. All p-value comparisons were based on an unpaired, non-parametric Dunn's Multiple Comparison test. Each point in the figure represents an individual participant. The three horizontal bars represent the median value (middle bar), upper interquartile range (top bar) and lower interquartile range (bottom bar).

Figure 4.3.1.4: Comparison of the quantities of *L. iners* (copies/ng DNA) measured in the DNA extracted from vaginal lateral wall swabs from participants in the WISH study, between BV positive, intermediate and negative groups. All p-value comparisons were based on an unpaired, non-parametric Dunn's Multiple Comparison test. Each point in the figure represents an individual participant. The three horizontal bars represent the median value (middle bar), upper interquartile range (top bar) and lower interquartile range (bottom bar).

Figure 4.3.1.5: Comparison of the quantities of *G. vaginalis* (copies/ng DNA) measured in the DNA extracted from vaginal lateral wall swabs from participants in the WISH study, between BV positive, intermediate and negative groups. All p-value comparisons were based on an unpaired, non-parametric Dunn's Multiple Comparison test. Each point in the figure represents an individual participant. The three horizontal bars represent the median value (middle bar), upper interquartile range (top bar) and lower interquartile range (bottom bar).

Figure 4.3.2A: Box-plot of the low inflammation for *L. gasseri* (red), *L. jensenii* (orange), *L. crispatus* (green), *L. iners* (blue), and *G. vaginalis* (purple). The 'box' component of each plot indicates the interquartile range (IQR) of the data set and the 'whiskers' which are the two lines (bottom and top) extending from the box component of each block that end with a horizontal stroke, indicate the range from the smallest and largest non-outliers to the 25% and 75% percentile components, respectively. The middle line indicates the median value for each data set.

Figure 4.3.2B: Box-plot of the high inflammation for *L. gasseri* (red), *L. jensenii* (orange), *L. crispatus* (green), *L. iners* (blue), and *G. vaginalis* (purple). The 'box' component of each plot indicates the interquartile range (IQR) of the data set and the 'whiskers' which are the two lines

(bottom and top) extending from the box component of each block that end with a horizontal stroke, indicate the range from the smallest and largest non-outliers to the 25% and 75% percentile components, respectively. The middle line indicates the median value for each data set.

Figure 4.3.2.1: Comparison of the quantities of *L. crispatus* (copies/ng DNA) measured in the DNA extracted from vaginal lateral wall swabs from participants in the WISH study, between women with high and low genital inflammation. All p-value comparisons were based on an unpaired, non-parametric Mann-Whitney t-test statistic. Each point in the figure represents an individual participant. The three horizontal bars represent the median value (middle bar), upper interquartile range (top bar) and lower interquartile range (bottom bar).

Figure 4.3.2.2: Comparison of the quantities of *L. gasseri* (copies/ng DNA) measured in the DNA extracted from vaginal lateral wall swabs from participants in the WISH study, between women with high and low genital inflammation. All p-value comparisons were based on an unpaired, non-parametric Mann-Whitney t-test statistic. Each point in the figure represents an individual participant. The three horizontal bars represent the median value (middle bar), upper interquartile range (top bar) and lower interquartile range (bottom bar).

Figure 4.3.2.3: Comparison of the quantities of *L. jensenii* (copies/ng DNA) measured in the DNA extracted from vaginal lateral wall swabs from participants in the WISH study, between women with high and low genital inflammation. All p-value comparisons were based on an unpaired, non-parametric Mann-Whitney t-test statistic. Each point in the figure represents an individual participant. The three horizontal bars represent the median value (middle bar), upper interquartile range (top bar) and lower interquartile range (bottom bar).

Figure 4.3.2.4: Comparison of the quantities of *L. iners* (copies/ng DNA) measured in the DNA extracted from vaginal lateral wall swabs from participants in the WISH study, women with high and low genital inflammation. All p-value comparisons were based on an unpaired, non-parametric Mann-Whitney t-test statistic. Each point in the figure represents an individual participant. The three horizontal bars represent the median value (middle bar), upper interquartile range (top bar) and lower interquartile range (bottom bar).

Figure 4.3.2.5: Comparison of the quantities of *G. vaginalis* (copies/ng DNA) measured in the DNA extracted from vaginal lateral wall swabs from participants in the WISH study, between women with high and low genital inflammation. All p-value comparisons were based on an unpaired, non-parametric Mann-Whitney t-test statistic. Each point in the figure represents an individual participant. The three horizontal bars represent the median value (middle bar), upper interquartile range (top bar) and lower interquartile range (bottom bar).

Figure 4.3.3A: Box-plot of the 16-18 years for *L. gasseri* (red), *L. jensenii* (orange), *L. crispatus* (green), *L. iners* (blue), and *G. vaginalis* (purple). The 'box' component of each plot indicates the interquartile range (IQR) of the data set and the 'whiskers' which are the two lines (bottom

and top) extending from the box component of each block that end with a horizontal stroke, indicate the range from the smallest and largest non-outliers to the 25% and 75% percentile components, respectively. The middle line indicates the median value for each data set.

Figure 4.3.3B: Box-plot of the 19-22 years for *L. gasseri* (red), *L. jensenii* (orange), *L. crispatus* (green), *L. iners* (blue), and *G. vaginalis* (purple). The 'box' component of each plot indicates the interquartile range (IQR) of the data set and the 'whiskers' which are the two lines (bottom and top) extending from the box component of each block that end with a horizontal stroke, indicate the range from the smallest and largest non-outliers to the 25% and 75% percentile components, respectively. The middle line indicates the median value for each data set.

Figure 4.3.3.1: Comparison of the quantities of *L. crispatus* (copies/ng DNA) measured in the DNA extracted from vaginal lateral wall swabs from participants in the WISH study, between the two 16-18 years old and 19-22 years old age groups. All p-value comparisons were based on an unpaired, non-parametric Mann-Whitney t-test statistic. Each point in the figure represents an individual participant. The three horizontal bars represent the median value (middle bar), upper interquartile range (top bar) and lower interquartile range (bottom bar).

Figure 4.3.3.2: Comparison of the quantities of *L. gasseri* (copies/ng DNA) measured in the DNA extracted from vaginal lateral wall swabs from participants in the WISH study, between the two 16-18 years old and 19-22 years old age groups. All p-value comparisons were based on an unpaired, non-parametric Mann-Whitney t-test statistic. Each point in the figure represents an individual participant. The three horizontal bars represent the median value (middle bar), upper interquartile range (top bar) and lower interquartile range (bottom bar).

Figure 4.3.3.3: Comparison of the quantities of *L. jensenii* (copies/ng DNA) measured in the DNA extracted from vaginal lateral wall swabs from participants in the WISH study, between the two 16-18 years old and 19-22 years old age groups. All p-value comparisons were based on an unpaired, non-parametric Mann-Whitney t-test statistic. Each point in the figure represents an individual participant. The three horizontal bars represent the median value (middle bar), upper interquartile range (top bar) and lower interquartile range (bottom bar).

Figure 4.3.3.4: Comparison of the quantities of *L. iners* (copies/ng DNA) measured in the DNA extracted from vaginal lateral wall swabs from participants in the WISH study, between the two 16-18 years old and 19-22 years old age groups. All p-value comparisons were based on an unpaired, non-parametric Mann-Whitney t-test statistic. Each point in the figure represents an individual participant. The three horizontal bars represent the median value (middle bar), upper interquartile range (top bar) and lower interquartile range (bottom bar).

Figure 4.3.3.5: Comparison of the quantities of *G. vaginalis* (copies/ng DNA) measured in the DNA extracted from vaginal lateral wall swabs from participants in the WISH study, between the two 16-18 years old and 19-22 years old age groups. All p-value comparisons were based on an unpaired, non-parametric Mann-Whitney t-test statistic. Each point in the figure represents an

individual participant. The three horizontal bars represent the median value (middle bar), upper interquartile range (top bar) and lower interquartile range (bottom bar).

Figure 4.3.4A: Box-plot of hormonal contraceptive use of DMPA for *L. gasseri* (red), *L. jensenii* (orange), *L. crispatus* (green), *L. iners* (blue), and *G. vaginalis* (purple). The 'box' component of each plot indicates the interquartile range (IQR) of the data set and the 'whiskers' which are the two lines (bottom and top) extending from the box component of each block that end with a horizontal stroke, indicate the range from the smallest and largest non-outliers to the 25% and 75% percentile components, respectively. The middle line indicates the median value for each data set.

Figure 4.3.4B: Box-plot of hormonal contraceptive use of the Implanon for *L. gasseri* (red), *L. jensenii* (orange), *L. crispatus* (green), *L. iners* (blue), and *G. vaginalis* (purple). The 'box' component of each plot indicates the interquartile range (IQR) of the data set and the 'whiskers' which are the two lines (bottom and top) extending from the box component of each block that end with a horizontal stroke, indicate the range from the smallest and largest non-outliers to the 25% and 75% percentile components, respectively. The middle line indicates the median value for each data set.

Figure 4.3.4C: Box-plot of hormonal contraceptive use of Nur Isterate for *L. gasseri* (red), *L. jensenii* (orange), *L. crispatus* (green), *L. iners* (blue), and *G. vaginalis* (purple). The 'box' component of each plot indicates the interquartile range (IQR) of the data set and the 'whiskers' which are the two lines (bottom and top) extending from the box component of each block that end with a horizontal stroke, indicate the range from the smallest and largest non-outliers to the 25% and 75% percentile components, respectively. The middle line indicates the median value for each data set.

Figure 4.3.4.1: Comparison of the quantities of *L. crispatus* (copies/ng DNA) measured in the DNA extracted from vaginal lateral wall swabs from participants in the WISH study, between the hormonal contraceptives DMPA, Nur Isterate and the Implanon. All p-value comparisons were based on an unpaired, non-parametric Dunn's Multiple Comparison test. Each point in the figure represents an individual participant. The three horizontal bars represent the median value (middle bar), upper interquartile range (top bar) and lower interquartile range (bottom bar).

Figure 4.3.4.2: Comparison of the quantities of *L. gasseri* (copies/ng DNA) measured in the DNA extracted from vaginal lateral wall swabs from participants in the WISH study, between hormonal contraceptives DMPA, Nur Isterate and the Implanon. All p-value comparisons were based on an unpaired, non-parametric Dunn's Multiple Comparison test. Each point in the figure represents an individual participant. The three horizontal bars represent the median value (middle bar), upper interquartile range (top bar) and lower interquartile range (bottom bar).

Figure 4.3.4.3: Comparison of the quantities of *L. jensenii* (copies/ng DNA) measured in the DNA extracted from vaginal lateral wall swabs from participants in the WISH study, between

hormonal contraceptives DMPA, Nur Isterate and the Implanon. All p-value comparisons were based on an unpaired, non-parametric Dunn's Multiple Comparison test. Each point in the figure represents an individual participant. The three horizontal bars represent the median value (middle bar), upper interquartile range (top bar) and lower interquartile range (bottom bar).

Figure 4.3.4.4: Comparison of the quantities of *L. iners* (copies/ng DNA) measured in the DNA extracted from vaginal lateral wall swabs from participants in the WISH study, between hormonal contraceptives DMPA, Nur Isterate and the Implanon. All p-value comparisons were based on an unpaired, non-parametric Dunn's Multiple Comparison test. Each point in the figure represents an individual participant. The three horizontal bars represent the median value (middle bar), upper interquartile range (top bar) and lower interquartile range (bottom bar).

Figure 4.3.4.5: Comparison of the quantities of *G. vaginalis* (copies/ng DNA) measured in the DNA extracted from vaginal lateral wall swabs from participants in the WISH study, between the hormonal contraceptives DMPA, Nur Isterate and the Implanon. All p-value comparisons were based on an unpaired, non-parametric Dunn's Multiple Comparison test. Each point in the figure represents an individual participant. The three horizontal bars represent the median value (middle bar), upper interquartile range (top bar) and lower interquartile range (bottom bar).

Figure 4.3.5A: Box-plot of the absence of any one STI for *L. gasseri* (red), *L. jensenii* (orange), *L. crispatus* (green), *L. iners* (blue), and *G. vaginalis* (purple). The 'box' component of each plot indicates the interquartile range (IQR) of the data set and the 'whiskers' which are the two lines (bottom and top) extending from the box component of each block that end with a horizontal stroke, indicate the range from the smallest and largest non-outliers to the 25% and 75% percentile components, respectively. The middle line indicates the median value for each data set.

Figure 4.3.5B: Box-plot of the presence of any one STI for *L. gasseri* (red), *L. jensenii* (orange), *L. crispatus* (green), *L. iners* (blue), and *G. vaginalis* (purple). The 'box' component of each plot indicates the interquartile range (IQR) of the data set and the 'whiskers' which are the two lines (bottom and top) extending from the box component of each block that end with a horizontal stroke, indicate the range from the smallest and largest non-outliers to the 25% and 75% percentile components, respectively. The middle line indicates the median value for each data set.

Figure 4.3.5.1: Comparison of the quantities of *L. crispatus* (copies/ng DNA) measured in the DNA extracted from vaginal lateral wall swabs from participants in the WISH study, where the samples have been separated based on absence or presence of any one of the WISH cohort STIs present. All p-value comparisons were based on an unpaired, non-parametric Mann-Whitney t-test statistic. Each point in the figure represents an individual participant. The three horizontal bars represent the median value (middle bar), upper interquartile range (top bar) and lower interquartile range (bottom bar).

Figure 4.3.5.2: Comparison of the quantities of *L. gasseri* (copies/ng DNA) measured in the DNA extracted from vaginal lateral wall swabs from participants in the WISH study, where the samples have been separated based on absence or presence of any one of the WISH cohort STIs present. All p-value comparisons were based on an unpaired, non-parametric Mann-Whitney t-test statistic. Each point in the figure represents an individual participant. The three horizontal bars represent the median value (middle bar), upper interquartile range (top bar) and lower interquartile range (bottom bar).

Figure 4.3.5.3: Comparison of the quantities of *L. jensenii* (copies/ng DNA) measured in the DNA extracted from vaginal lateral wall swabs from participants in the WISH study, where the samples have been separated based on absence or presence of any one of the WISH cohort STIs present. All p-value comparisons were based on an unpaired, non-parametric Mann-Whitney t-test statistic. Each point in the figure represents an individual participant. The three horizontal bars represent the median value (middle bar), upper interquartile range (top bar) and lower interquartile range (bottom bar).

Figure 4.3.5.4: Comparison of the quantities of *L. iners* (copies/ng DNA) measured in the DNA extracted from vaginal lateral wall swabs from participants in the WISH study, where the samples have been separated based on absence or presence of any one of the WISH cohort STIs present. All p-value comparisons were based on an unpaired, non-parametric Mann-Whitney t-test statistic. Each point in the figure represents an individual participant. The three horizontal bars represent the median value (middle bar), upper interquartile range (top bar) and lower interquartile range (bottom bar).

Figure 4.3.5.5: Comparison of the quantities of *G. vaginalis* (copies/ng DNA) measured in the DNA extracted from vaginal lateral wall swabs from participants in the WISH study, where the samples have been separated based on absence or presence of any one of the WISH cohort STIs present. All p-value comparisons were based on an unpaired, non-parametric Mann-Whitney t-test statistic. Each point in the figure represents an individual participant. The three horizontal bars represent the median value (middle bar), upper interquartile range (top bar) and lower interquartile range (bottom bar).

Figure 4.3.6.1: Comparison of the quantities of *L. crispatus* (copies/ng DNA) measured in the DNA extracted from vaginal lateral wall swabs from participants in the WISH study, where the samples have been separated based on none, one, two (or more <) of the WISH cohort Bacterial (B) versus Viral (V) STIs being present. All p-value comparisons were based on an unpaired, non-parametric Dunn's Multiple Comparison test. Each point in the figure represents an individual participant. The three horizontal bars represent the median value (middle bar), upper interquartile range (top bar) and lower interquartile range (bottom bar).

Figure 4.3.6.2: Comparison of the quantities of *L. gasseri* (copies/ng DNA) measured in the DNA extracted from vaginal lateral wall swabs from participants in the WISH study, where the

samples have been separated based on none, one, two (or more <) of the WISH cohort Bacterial (B) versus Viral (V) STIs being present. All p-value comparisons were based on an unpaired, non-parametric Dunn's Multiple Comparison test. Each point in the figure represents an individual participant. The three horizontal bars represent the median value (middle bar), upper interquartile range (top bar) and lower interquartile range (bottom bar).

Figure 4.3.6.3: Comparison of the quantities of *L. jensenii* (copies/ng DNA) measured in the DNA extracted from vaginal lateral wall swabs from participants in the WISH study, where the samples have been separated based on none, one, two (or more <) of the WISH cohort Bacterial (B) versus Viral (V) STIs being present. All p-value comparisons were based on an unpaired, non-parametric Dunn's Multiple Comparison test. Each point in the figure represents an individual participant. The three horizontal bars represent the median value (middle bar), upper interquartile range (top bar) and lower interquartile range (bottom bar).

Figure 4.3.6.4: Comparison of the quantities of *L. iners* (copies/ng DNA) measured in the DNA extracted from vaginal lateral wall swabs from participants in the WISH study, where the samples have been separated based on none, one, two (or more <) of the WISH cohort Bacterial (B) versus Viral (V) STIs being present. All p-value comparisons were based on an unpaired, non-parametric Dunn's Multiple Comparison test. Each point in the figure represents an individual participant. The three horizontal bars represent the median value (middle bar), upper interquartile range (top bar) and lower interquartile range (bottom bar).

Figure 4.3.6.5: Comparison of the quantities of *G. vaginalis* (copies/ng DNA) measured in the DNA extracted from vaginal lateral wall swabs from participants in the WISH study, where the samples have been separated based on none, one, two (or more <) of the WISH cohort Bacterial (B) versus Viral (V) STIs being present. All p-value comparisons were based on an unpaired, non-parametric Dunn's Multiple Comparison test. Each point in the figure represents an individual participant. The three horizontal bars represent the median value (middle bar), upper interquartile range (top bar) and lower interquartile range (bottom bar).

Figure 4.3.7A: Box-plot of the negative HPV group for *L. gasseri* (red), *L. jensenii* (orange), *L. crispatus* (green), *L. iners* (blue), and *G. vaginalis* (purple). The 'box' component of each plot indicates the interquartile range (IQR) of the data set and the 'whiskers' which are the two lines (bottom and top) extending from the box component of each block that end with a horizontal stroke, indicate the range from the smallest and largest non-outliers to the 25% and 75% percentile components, respectively. The middle line indicates the median value for each data set.

Figure 4.3.7B: Box-plot of the low risk HPV group for *L. gasseri* (red), *L. jensenii* (orange), *L. crispatus* (green), *L. iners* (blue), and *G. vaginalis* (purple). The 'box' component of each plot indicates the interquartile range (IQR) of the data set and the 'whiskers' which are the two lines (bottom and top) extending from the box component of each block that end with a horizontal

stroke, indicate the range from the smallest and largest non-outliers to the 25% and 75% percentile components, respectively. The middle line indicates the median value for each data set.

Figure 4.3.7C: Box-plot of the high risk HPV group for *L. gasseri* (red), *L. jensenii* (orange), *L. crispatus* (green), *L. iners* (blue), and *G. vaginalis* (purple). The 'box' component of each plot indicates the interquartile range (IQR) of the data set and the 'whiskers' which are the two lines (bottom and top) extending from the box component of each block that end with a horizontal stroke, indicate the range from the smallest and largest non-outliers to the 25% and 75% percentile components, respectively. The middle line indicates the median value for each data set.

Figure 4.3.7.1: Comparison of the quantities of *L. crispatus* (copies/ng DNA) measured in the DNA extracted from vaginal lateral wall swabs from participants in the WISH study, between the negative, low risk and high risk HPV groups. All p-value comparisons were based on an unpaired, non-parametric Dunn's Multiple Comparison test. Each point in the figure represents an individual participant. The three horizontal bars represent the median value (middle bar), upper interquartile range (top bar) and lower interquartile range (bottom bar).

Figure 4.3.7.2: Comparison of the quantities of *L. gasseri* (copies/ng DNA) measured in the DNA extracted from vaginal lateral wall swabs from participants in the WISH study, between the negative, low risk and high risk HPV groups. All p-value comparisons were based on an unpaired, non-parametric Dunn's Multiple Comparison test. Each point in the figure represents an individual participant. The three horizontal bars represent the median value (middle bar), upper interquartile range (top bar) and lower interquartile range (bottom bar).

Figure 4.3.7.3: Comparison of the quantities of *L. jensenii* (copies/ng DNA) measured in the DNA extracted from vaginal lateral wall swabs from participants in the WISH study, between the negative, low risk and high risk HPV groups. All p-value comparisons were based on an unpaired, non-parametric Dunn's Multiple Comparison test. Each point in the figure represents an individual participant. The three horizontal bars represent the median value (middle bar), upper interquartile range (top bar) and lower interquartile range (bottom bar).

Figure 4.3.7.4: Comparison of the quantities of *L. iners* (copies/ng DNA) measured in the DNA extracted from vaginal lateral wall swabs from participants in the WISH study, between the negative, low risk and high risk HPV groups. All p-value comparisons were based on an unpaired, non-parametric Dunn's Multiple Comparison test. Each point in the figure represents an individual participant. The three horizontal bars represent the median value (middle bar), upper interquartile range (top bar) and lower interquartile range (bottom bar).

Figure 4.3.7.5: Comparison of the quantities of *G. vaginalis* (copies/ng DNA) measured in the DNA extracted from vaginal lateral wall swabs from participants in the WISH study, between the negative, low risk and high risk HPV groups. All p-value comparisons were based on an

unpaired, non-parametric Dunn's Multiple Comparison test. Each point in the figure represents an individual participant. The three horizontal bars represent the median value (middle bar), upper interquartile range (top bar) and lower interquartile range (bottom bar).

List of Abbreviations

˚C	Degrees Celsius
AIDS	Acquired Immune Deficiency Syndrome
ANOVA	Analysis of Variance
ATCC	American Type Culture Collection
BLAST	Basic Local Alignment Search Tool
Bp	Base pairs
BV	Bacterial Vaginosis
BVAB	BV associated bacteria
COC	Combined oral contraceptive pill
DMPA	Depot Medroxyprogesterone Acetate
DNA	Deoxyribonucleic Acid
dsDNA	Double stranded DNA
FGT	DNA Female Genital Tract
gDNA	Genomic DNA
GM-CSF	Granulocyte-macrophage colony stimulating factor
HC	Hormonal contraceptive
HIV	Human Immunodeficiency Virus
HPV	Human Papilloma Virus
IFN	Interferon
IL	Interleukin
IL-1ra	IL-1 receptor antagonist
IP-10	IFN-gamma inducible protein 10
IQR	Interquartile Range
IUD	Intra-Uterine Device
LTR	Long terminal repeats
MD-2	Myeloid differentiation factor 2
MIP	Macrophage inflammatory protein
MIQE	Minimum Information for Publication of Quantitative Real-Time PCR Experiments
NCBI	National Center for Biotechnology Information
NFW	Nuclease Free Water
NGS	Next Generation Sequencing
NOD	Nucleotide Oligomerization Domain
NTC	None Template Control
PAM	Partitioning Around Medoids
PCR	Polymerase Chain Reaction
pDC's	Plasmacytoid dendritic cells
POP	Progestin-only contraceptive pill
PSA	Prostate-specific antigen

rDNA	Ribosomal DNA
RICK	Receptor-Interacting serine/threonine protein Kinase 2
RNA	Ribonucleic Acid
rRNA	Ribosomal RNA
SNP	Single nucleotide polymorphism
SSU	Small Subunit
STI	Sexually Transmitted Infection
TGF	Transforming growth factor
TLR	Toll-like Receptor
TNF	Tumor necrosis factor
QIIME	Quantitative Inference In Microbial Ecology
qPCR	Quantitative Real-Time Polymerase Chain Reaction
WISH	Women's Initiative in Sexual Health

List of Units

℃	Degrees Celsius
sec	Seconds
min	Minutes
h	Hour
RPM	Revolutions per minute
v/v	Volume per volume
V	Volts
bp	Base pair
µL	Microliter
mg/L	Milligrams per liter
g/L	Grams per liter
mL	Milliliter
µM	Micromole
pg	Pico-gram
ng/µL	Nano-gram per microliter
copies/µL	Copies of bacteria per microliter
copies/ng	Copies of bacteria per nano-gram

Abstract

Young, reproductive-aged women are at highest risk of acquiring human-immunodeficiency virus (HIV). The Women's Initiative in Sexual Health (WISH) study was designed to investigate potential biological reasons for this high risk in HIV negative, South African adolescent females. Little is known about the 'normal' microbiome of this population. As such, the aim of this sub-study was to quantify specific bacterial species (*L. crispatus, L. jensenii*, *L. gasseri, L. iners, G. vaginalis* and *P. bivia)* by quantitative real time PCR (qPCR) from adolescent female lateral vaginal wall swabs, and to assess associations between the quantities of these bacteria and bacterial vaginosis (BV) status, inflammation levels, age, hormonal contraceptive usage, and sexually transmitted infections (STIs). Samples were collected from 143 participant adolescent females in total, aged between 16 and 22 years of age, with a median of 18 years of age, from the Masiphumelele Youth Clinic in Cape Town, South Africa.

Bacterial DNA was extracted from lateral vaginal wall swabs using the MoBio Powersoil® DNA Isolation Kit after enzymatic digestion. Positive bacterial reference strains were cultured in MRS buffer and Schwedler's broth, after which the DNA was extracted using the Qiagen Blood and Tissue DNA Maxi Extraction Kit. The quality and concentration of the DNA was confirmed using Qubit technology. The positive control DNA was amplified with PCR using species specific primers and the product run on an agarose gel to confirm primer specificity. The positive control DNA was serially diluted from 10^{6} to 10^{-2} copies/µL to form a standard curve for absolute quantification through qPCR. Multiple steps were taken in order to optimize the qPCR experiments in terms of protocols, initial denaturation and annealing temperatures, cycle length and number, primers, and serial dilutions of the positive control DNA. The optimization for the *P. bivia* qPCR protocol presented the most issues, with the final quantification results being unreliable and requiring further work. Once the qPCR conditions were optimized for each bacterium; all samples, non-template control and standards were run in triplicate to quantify the number of bacterial copies per ng of DNA for each participant. The average of the three values were used as the final quantities and then used for downstream analyses.

The bacterium *L. crispatus, L. jensenii* and *L. gasseri,* had median readings of 3.957 copies/ng, 1.568 copies/ng, and 17.58 copies/ng, respectively, with increased *L. iners* (2807 copies/ng) and *G. vaginalis* (8540 copies/ng). BV negative participants had increased levels of *L. crispatus*

(p=0.0004, p=0.0002) and *L. gasseri* (p=0.0016, p<0.0001) in comparison to both BV intermediate and BV positive participants. *L. jensenii* (p<0.0001) and *L. iners* (p=0.0461) readings were increased in BV negative participants compared with BV positive and BV intermediate participants, respectively. BV positive participants had increased levels of *G. vaginalis* in comparison with both BV intermediate (p=0.0059) and BV negative (p<0.0001) adolescents. The 47 immunological factors, assessed via luminex, were categorized into high and low genital inflammation based on the unsupervised analysis by partitioning around medoids (PAM) using an R package 'cluster' with a k-value of 2. The inflammation-low group had increased levels of *L. crispatus* (p=0.0005), *L. gasseri* (p=0.033) and *L. jensenii* (p=0.0046) in comparison to the genital inflammation-high group.

In participants with two viral STIs (Herpes Simplex Virus 2 and Human Papilloma Virus), there were increased copies/ng of *G. vaginalis* in comparison with participants with none (p=0.0098) or one viral STI (p=0.0324). Participants with high-risk HPV subtypes had significantly higher copy numbers of *L. crispatus* in comparison to the participants with low risk HPV subtypes (p=0.0181). Further, the only association demonstrated between the qPCR-based bacterial levels and the hormonal contraceptive prescribed was indicated by *L. jensenii* (ANOVA p=0.0222), possibly due to the low copy number readings.

In conclusion, BV status, low levels of genital inflammation and the presence of two viral STIs indicate an association with bacterial copy numbers reported in this study, with increased median levels of *L. iners* and *G. vaginalis* across all adolescent participants compared to the other reported bacterial copy numbers. This indicates a possible alternate 'normal' microbiota profile of the FGT in adolescents in Masiphumelele.

Chapter 1: Literature Review

1.1 Human-Immunodeficiency Virus in South Africa

In sub-Saharan Africa, the Human immunodeficiency virus (HIV) is an epidemic (Byrne et al. 2016; Cohen et al. 2012; Mitchell & Marrazzo 2014; Murphy et al. 2014; Roberts et al. 2012). Within the high risk reproductive-age adolescent population, there are approximately 7000 young women infected weekly in sub-Saharan Africa (Roxby et al. 2016). In South Africa in 2015, an estimated 7 million people were living with HIV, of which 4 million were women aged 15 years and over, with 180 000 Acquired Immune Deficiency Syndrome (AIDS) related deaths (UNAIDS 2015). Such high numbers have been attributed to poverty, as well as the lower status of women in some cultures, social instability and inequality, high levels of sexually transmitted infections (STIs), limited access to medical care, and sexual violence (AFSA 2011). These factors are further aggravated by the limited knowledge surrounding HIV infection and transmission in a large proportion of the population (AFSA 2011). South Africa has one of the highest rates of HIV with 15% of the young women and close to 5% of young men between the ages of 15-24 years infected. Females aged between 18 and 24 years are at highest risk of HIV acquisition which can be attributed to sexual activity and associated factors such as either heavier or thin vaginal discharge, thought to be in conjunction with the use of hormonal contraceptives, older male sexual partners as well as high numbers of sexual partners and inconsistent condom use (Pettifor et al. 2005; Seutlwadi et al 2012). Programs such as the loveLife campaign are designed to incorporated education, multi-media awareness, sexual health and outreach services for adolescents in order to lower HIV prevalence and related risk behaviors (loveLife 1999). Due to multiple factors such as socio-economic variables and potentially biological factors, black South African women have an increased risk of HIV acquisition in comparison to other races (Pettifor et al. 2005).

HIV infects and dysregulates multiple key innate and adaptive immune cell populations. Infection results in severe damage to mucosal barriers within the female genital tract (FGT) and leads to infiltration of symbiotic bacteria present within the FGT into the tissue, which could potentially cause opportunistic infections and activation of the systemic immune system (Reis Machado et al. 2014). The induction of an inflammatory response results in spreading of the virus to specific HIV target cells, such as activated $CD4^+$ T-cells expressing CXCR4 and CCR5

HIV co-receptors, which promote viral infection. In addition to activated T cells, HIV can also infect proliferating and resting T cells (Reis Machado et al. 2014; Xu et al. 2013; Zhang et al. 2004).

Antigen presenting $CD4^+$ T-cells present a particular challenge as their preferential targeting by HIV results in their possible impairment or elimination from the immune response. Increased levels of inflammatory cytokines that promote $CD4^+$ T-cell activation result in increased sources of target cells for HIV. This results in the hyper-activation of $CD8^+$ T cells and over production of antibodies which can lead to a poor specific antibody response, lack of cytotoxic T lymphocytes and an overall impairment of the immune system. High levels of these activated $CD4^+$ T-cells within the FGT mucosa further facilitate shedding of HI-virus and overall depletion of $CD4^+$ T-cells. HIV infection is further facilitated by Langerhans cells which act as transmission channels for the HI-virus within the FGT (Jaspan et al. 2011; Riou et al. 2012; Xu et al. 2013).

1.2 The female genital tract (FGT) immune response

The FGT is comprised of the upper and lower FGT, with the upper FGT including the uterus body, fallopian tubes, endocervix, which are lined by type I mucosa with columnar epithelial cells, while the lower FGT includes the ectocervix, vagina and type II mucosa with squamous epithelial cells (Xu et al. 2013; Reis Machado et al. 2014). The FGT immune system includes all cell types associated with innate and adaptive immune functions (Xu et al. 2013). The activity and numbers of T cells, B cells, neutrophils, monocytes, macrophages, dendritic and other antigen presenting cells, along with other components of the mucosal immune system, is hormonally controlled with oestradiol and progesterone. These two hormones are involved in the regulation of cytokine levels, cell population distributions, immunoglobulin transport and antigen presentation and production during immune response (Beagley & Gockel 2003; Mestecky & Fultz 1999; Wira, Fahey, et al. 2005). FGT hormones further regulate the immune system in such a way as to favour optimal conditions and functions for fecundity, such as sperm migration and implantation (Reis Machado et al. 2014).

Columnar epithelial cells play an important role in innate and adaptive immunity by forming a physical barrier and, through the secretion of specific cytokines and chemokines which link the adaptive immune system, are antimicrobial and play a role in tissue physiology and differentiation for support of the fetus during gestation (Wira, Grant-Tschudy, et al. 2005). Epithelial cells further prevent pathogenic and opportunistic bacteria from entering the body through the secretion of mucus which lines the cervix and vagina, trapping any unwanted pathogenic microbes. The mucus which contains antimicrobial defensin proteins, in conjunction with the epithelial cells which express TLRs, myeloid differentiation factor 2 (MD-2) and major histocompatibility complex molecules, ensures the innate and adaptive immune systems are fully functional and efficient within the FGT (Wira, Fahey, et al. 2005; Mirmonsef et al. 2011).

The FGT has a multi-layered immune defense system composed of mucus lining, antimicrobial peptide secretions, tight epithelial barriers, and cytokines monitored by innate and epithelial immune cells, which bridge the gap of cell-mediated and pathogen-specific humoral adaptive immunity (Hickey et al. 2011; Reis Machado et al. 2014; Ochiel et al. 2008). Mucosal immunity plays a specific role in female reproductive organ functioning and embryonic development during pregnancy. Mucosal immunity is specifically active against the multitude of microorganisms that access the FGT and that can cause dysbiosis and infection while maintaining a balance with commensal bacteria, preventing unnecessary inflammation. The FGT defends against microorganisms via toll-like receptors (TLRs) such as TLRs 7-9 in the uterine and fallopian tubes, ectocervix and cervix as well as Nucleotide Oligomerization Domain (NOD) like receptors such as NOD1 and NOD2 along with Receptor-Interacting serine/threonine protein Kinase 2 (RICK) which are all expressed within the FGT tissues. These receptors induce pro-inflammatory CXCL8 and aid in the removal of pathogens (Reis Machado et al. 2014; Xu et al. 2013). Additionally the squamous epithelium forms a physical barrier of defense as a result of tight junctions, desmosome proteins, and adherens junctions to reduce permeability to the HI-virus (Reis Machado et al. 2014; Mestecky & Fultz 1999; Xu et al. 2013).

The release and concentration of pro-inflammatory and anti-inflammatory cytokines secreted by the cellular components of the FGT affects the functionality of the immune-competent tissues which comprise the mucosal immune defense system (Anjuère et al. 2012). Cytokines are signaling molecules that allow information exchange between the immune system and tissue

network. Cytokines bind to their cognate receptors, which results in a change in function or phenotype of the recipient cell upon acceptance of the antigen signal through antigen receptors (Firestein et al. 2013; Su et al. 2012). Cytokines can be anti- or pro-inflammatory, potentially modulating multiple pathways throughout the immune system. Common anti-inflammatory cytokines include interleukin-4 (IL-4), IL-6, IL-10, IL-11, IL-13, alpha-interferon (IFN-α), Transforming growth factor-beta (TGF-β), and IL-1 receptor antagonist (IL-1ra). Anti-inflammatory cytokines act through various pathways in order to combat infections, such as IL-4, IL-10 and IL-13 which activate B lymphocytes during infection (Dinarello 2000). Common pro-inflammatory cytokines include IL-7, tumor necrosis factor alpha (TNF-α), IFN-γ, IL-12, IL-18, granulocyte-macrophage stimulating factor (MG-CSF), IL-23/17, and IL-1β (Arnold et al. 2015; Cavaillon 2000; Jung et al. 1995; Su et al. 2012; Sultani et al. 2012). In addition to the role of cytokines, the inflammatory response may be further modulated by the nature and quantity of target cells and cytokine activating signals, the timing, sequence of cytokine action, as well as cytokine polymorphisms, which can have a further impact on the magnitude of the response (Cavaillon 2000). Chemokines control the differentiation and development of immune precursor cells in the thymus and bone marrow as they are chemotactic cytokines which influence the positioning and migratory patterns of the immune cells. Common cytokines include IFN-gamma inducible protein 10 (IP-10) involved in TH1 response and natural killer cell trafficking, RANTES, MIP-1α and MIP-1β which play a role in the migration of macrophage and natural killer cells, as well as interactions between dendritic cells and T cells (Griffith et al. 2014).

Several pro-inflammatory cytokines have been associated with STIs in high-risk HIV uninfected adult women and can therefore be used as a possible indicator of infection and HIV susceptibility (Mlisana et al. 2012). Increased levels of Th17 cells ($CD3^+$ $CD4^+$ $IL\text{-}17^+$) have been associated with chlamydia and gonorrhea (Masson et al. 2015). Inflammatory cytokines can inhibit HIV replication and disease progression and as such play an important role in disease prevention (Breen 2002), with certain cytokines, including IFN-γ, IL-2, IL-4 and IL-5 predominantly associated with T-cell effector function which direct participation in the immune response to foreign bodies (Firestein et al. 2013). Inflammatory cytokines such as IL-10, have been associated with the inhibition of long terminal repeats (LTR)-directed HIV gene expression through cyclin T1 proteolyis induction in human macrophages (Wang & Rice 2006), while IL-16 is associated with inhibition of HIV replication in acutely infected T cells and the suppression of

lymphocyte activation (Idziorek et al. 1998). Circulating T-lymphocytes, bone marrow and thymus T-cell precursors, macrophages and monocytes, eosinophils, dendritic and microglial cells have been identified as targets for HIV replication and their increased levels with STI infections have been associated with increased activation of target cells and susceptibility to HIV acquisition (Fanales-Belasio et al. 2010; Hunt et al. 2011; Masson et al. 2015). The possible cause of this susceptibility is the decreased production of IL-21, IL-22, IL-1β, IL-17, IL-18 and Macrophage inflammatory protein-3α (MIP-3α), which is associated with the promotion of tight junctions, barrier functions, proteases and production of mucin by the mucosal epithelial cells of the FGT. The interruption of the FGT epithelial cell wall functions results in mechanical errors leading to the entry of HIV across the cellular barrier. A possible mechanism for the entry of, and efficient infection by, HIV, could be the increase in the frequency of endocervical $CD4^+$ T-cells upon any mechanical damage within the FGT mucosal lining (Arnold et al. 2015).

The FGT is equipped to remove foreign substances and microbes such as fungi, viruses, parasites and bacteria, but is also colonized by commensal bacteria, predominantly *Lactobacillus* species, which aid in its immune defense (Mirmonsef et al. 2011). The innate and adaptive immune systems interact with uterine epithelial cells and microbiota to optimize the FGT health through the removal of harmful infections while maintaining inflammation to prevent self- responses (Mirmonsef et al. 2011). Thus the FGT microbiota, in conjunction with the immune system and vaginal environment as a whole, plays a major role in women's health (Jespers et al. 2016a; Ravel et al. 2011; Anahtar et al. 2015), which also has important implications for fetal and neonatal health (Srinivasan et al. 2010; Srinivasan et al. 2012).

1.3 FGT Microbiota

The FGT microbiota is a combined community of commensal microbes co-existing together, with changes within the balance resulting in changes in health which occur due to colonization with pathogenic microbes (Salipante et al. 2013; Srinivasan & Fredricks 2008). A ‘healthy’ microbiome is dominated by Gram-positive bacteria such as the commensal *Lactobacillus* species (Selle et al. 2014), that play an important role in the FGT due to their numerical dominance (Lamont et al. 2011), production of lactic acid and hydrogen peroxide which reduce

the pH of the genital tract to maintain the optimal conditions for commensal bacteria. Furthermore, lactobacilli prevent the growth of pathogens, compete for adherence to the vaginal epithelium and for nutrients, thus making the vagina less hospitable to pathogens (Vitali et al. 2007; Mirmonsef et al. 2011), STIs, yeast, and urinary tract infections (Balkus et al. 2012). The reduction of lactobacilli present within the FGT, and the increase in BV associated anaerobes has been associated with increased risk of HIV acquisition and seroconversion (Atashili et al. 2008; Myer et al. 2005). Lactobacilli influence HIV by playing a role in the control in the genital shedding of newly reproduced HIV to another part of the body or another person (Balkus et al. 2012). Lactobacilli species further maintain an inhospitable environment for pathogenic bacteria by acting as probiotics, producing bacteriocins and antibiotic toxic hydroxyl radicals (Lamont et al. 2011). The loss of lactobacilli species results in the overgrowth of anaerobic and facultative bacteria which can lead to dysbiosis of the FGT microbiome (Jespers et al. 2012; Lopes dos Santos Santiago et al. 2012; Srinivasan et al. 2012; Ravel et al. 2011). Although it is understood that a 'healthy' microbiome is lactobacilli -dominated, the microbiome diversity and structure is strongly influenced by geographical location, ethnicity, age and culture (Ravel et al. 2011; Jespers et al. 2012).

Common lactobacilli found within the FGT include *L. crispatus, L. gasseri, L. jensenii,* as well as *L. iners*; however, *L. iners* has been shown to be present during the intermediate phase between dysbiosis and a healthy microbiome within the FGT and thus is not as strongly associated with what is considered to be a 'healthy' FGT microbiome (Jespers et al. 2012; Mayer et al. 2015; Macklaim et al. 2013; Roxby et al. 2016; Srinivasan & Fredricks 2008). In contrast, common facultative and anaerobic bacterial species associated with the loss of lactic acid producing bacteria include *Gardnerella vaginalis* and *Prevotella bivia*, whose presence within the FGT microbiome is concomitant with Bacterial Vaginosis (BV), which is the dysbiosis of the FGT microbiome and considered to be 'unhealthy' (Mayer et al. 2015; Fredricks et al. 2007; Fredricks et al. 2015; Lopes dos Santos Santiago et al. 2012; Saito et al. 2006). Some bacteria present within the FGT associated with BV are further associated with the change in vaginal pH and influence the inflammatory status of the FGT mucosa (Roy et al. 2006). This is achieved through the production of microbial products such as short chain fatty acids, which can inhibit pro-inflammatory cytokines secretion, affect phagocytosis and migration of immune cells (Mirmonsef et al. 2011).

Although the exact protective mechanisms of lactobacilli are partially unknown, H_2O_2 production creates a hostile acidic environment, which inhibits the growth of many harmful micro-organisms (Jespers et al. 2012). There is much debate about what constitutes a 'normal' FGT microbiome, as different cultures and races such as Hispanic, black, white and Asian populations have been found to have different predominant species present depending on BV status as well as pH (Ravel et al. 2011).

1.4 Bacterial vaginosis (BV)

Bacterial vaginosis (BV) is an alteration within the vaginal flora, with an increase in anaerobic and facultative bacteria, and overall diversity, and a concomitant decrease in the relative abundance of *Lactobacilli*. The most common bacteria associated with BV include *Gardnerella vaginalis, Prevotella bivia, Atopobium vaginae, Shuttleworthia sp.,* BV associated bacteria 2 (BVAB2), BVAB3*, Sneathia sp., Megasphaera sp.* Phylotype 1, and *Leptotrichia sp.* (Jespers et al. 2012; Lopes dos Santos Santiago et al. 2012; Srinivasan et al. 2010; Srinivasan et al. 2012). In healthy, BV-negative women, lactobacilli predominate the FGT microbiome, with a distinct reduction in their colonization upon the initiation of BV (Fredricks et al. 2007; Srinivasan et al. 2012).

BV is commonly diagnosed based on Amsel's clinical criteria, which include the presence of clue cells, vaginal fluid pH of greater than 4.5, a positive amine odor whiff test and a thin, homogenous milky discharge. A woman is classified as being BV positive if at least three of these four criteria are positive (Amsel et al. 1983; Eschenbach et al. 1988). BV can also be classified by Nugent scoring, which is based on the presence of specific morphotypes with different associated scores where the *Lactobacillus* morphotypes have a score of 4-0 (large gram-positive rods), the *G. vaginalis* and *Bacteroides* spp. morphotypes have a score of 0-4 (small gram-variable and gram negative rods) and *Mobiluncus* spp. morphotypes are scored 0-2 (curved gram-variable rods) (see Table 1.1 for scoring system) (Gad et al. 2014; Nugent et al. 1991; Spiegel et al. 1983). The vaginal smear is graded according to the presence of each morphotype to calculate the final Nugent score. A Nugent score of 0-3 is considered BV negative, a score of 4-6 is considered BV intermediate and a Nugent score between 7-10 is considered BV positive

(Srinivasan et al. 2010; Lopes dos Santos Santiago et al. 2012; Jespers et al. 2012; Srinivasan & Fredricks 2008).

Table 1.1: Nugent scoring system for Gram-stained vaginal smears

Score[a]	Lactobacillus morphotypes	*G. vaginalis* and *Bacteroides* spp. morphotypes	*Mobiluncus* spp. morphotypes
0	4+	0	0
1	3+	1+	1+ or 2+
2	2+	2+	3+ or 4+
3	1+	3+	
4	0	4+	

[a]0 - no morphotypes present; 1 - <1 morphotype present; 2 – 1 to 4 morphotypes present; 3 – 5 to 30 morphotypes present; 4 – 30 or more morphotypes present.

Risk factors for BV include new and multiple sexual partners, vaginal douching, as well as a slight association with wearing tight trousers more than once a week. BV incidence and recurring infection could be reduced by decreasing unprotected sexual encounters and increased in condom use (Chiaffarino et al. 2004; Fethers et al. 2008). Further factors, such as the presence of Prostate-specific antigen (PSA), age, sexual preference or point in the menstrual cycle have yet to be successfully associated with BV status (Jespers et al. 2012). BV has been associated with increased risk of pelvic inflammatory disease and acquisition of HIV (Fredricks et al. 2007; Fredricks et al. 2009). In pregnancy specifically it has been associated with the multiple complications such as early and late miscarriage, recurrent abortion, post-abortal sepsis, preterm pre-labor rupture of membranes, spontaneous preterm labor, preterm birth, postpartum endometriosis and histological chorioamnionitis (Lamont et al. 2011; Malaguti et al. 2015). In a study performed by Petricevic et al. (2014), it was shown that most *Lactobacillus* species were associated with full term gestation periods in healthy pregnant women, whereas *L. iners* specifically was shown to be present in 85% of the women who delivered preterm.

The dysbiosis and increase in diversity of the FGT microbiome, change in pH and loss of defensive lactobacilli due to the onset of BV have been associated with an increased risk of sexually transmitted and upper genital tract infections. Further, BV has been associated with HIV (Lamont et al. 2011; Srinivasan et al. 2010; Srinivasan et al. 2012).

1.5 Sexually Transmitted Infections (STIs)

There multiple different types of STIs with the most infamous viral STI being HIV (Hunt et al. 2011; Patterson et al. 2002; O'Farrell 2008). Common bacterial sexually transmitted infections include *Mycoplasma genitalium,* Chlamydia caused by *Chlamydia trachomatis*, Gonorrhea caused by *Neisseria gonorrhea*, and Syphilis caused by *Treponema pallidum*. Parasitic infections such as Trichomoniasis are caused by *Trichomonas vaginalis*, while the human papilloma virus (HPV) and herpes simplex virus (HSV-2) are two of the most common viral infections. Candidiasis is a yeast overgrowth that is not sexually transmitted, yet often co-occurs with other STIs (Reproductive Health and Research & Who 2005; Reis Machado et al. 2014; Anahtar et al. 2015; Chinsembu 2009; Ohene & Akoto 2008).

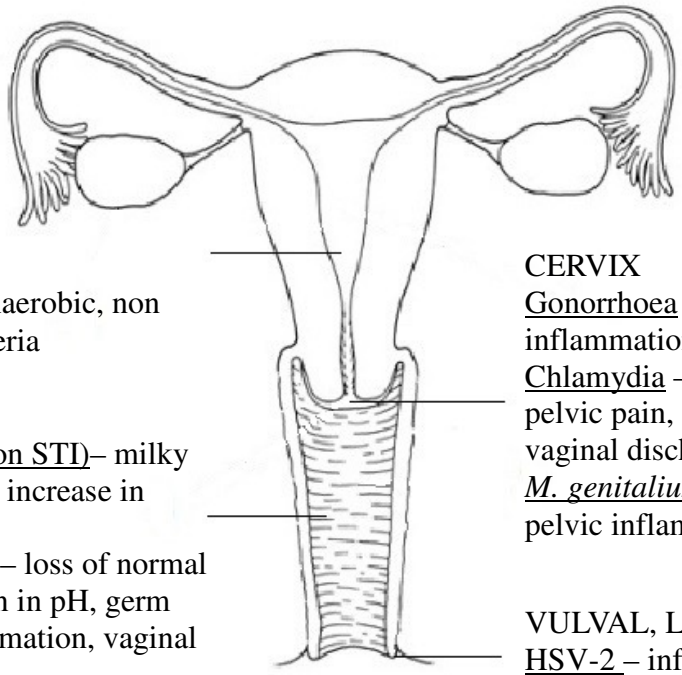

UTERUS
Vaginal bacteria – Anaerobic, non H_2O_2 producing bacteria

VAGINA
Bacterial Vaginosis (non STI)– milky discharge, amine odor, increase in vaginal pH
Candidiasis (non STI) – loss of normal vaginal flora, reduction in pH, germ tube formation, inflammation, vaginal discharge
Trichomoniasis – premature birth and membrane rupture, infertility, cervical cancer, vaginal discharge

CERVIX
Gonorrhoea – vaginal discharge, inflammation
Chlamydia – infertility, chronic pelvic pain, ectopic pregnancy, vaginal discharge
M. genitalium – cervicitis, urethritis, pelvic inflammatory disease

VULVAL, LABIA, VAGINA
HSV-2 – inflammation, genital ulcers
Human Papilloma Virus – genital warts, cervical cancer

Figure 1.1: Adaptation from Reproductive Health and Research (WHO) sites of infection in the FGT and the associated STIs and other infections with associated sequela (Reis Machado et al. 2014; Chinsembu 2009; Reproductive Health and Research & Who 2005; Minnesota 2005; CDC 2014a; CDC 2014b; CDC 2014c; CDC 2014d).

Adolescents in particular are at higher risk of STI acquisition, with a ratio of 2:1 adolescent females to their male counterparts (Chinsembu 2009). This increased ratio is thought to be partially due to increased cervical ectopy, cognitive, biological and socio-cultural factors. STIs can be asymptomatic or symptomatic in adolescents, and can further cause tubal pregnancy, infertility, and cervical cancer (Chinsembu 2009; Ohene & Akoto 2008). Further factors associated with the acquisition of STIs in adolescents include drug and alcohol use, unavailability and lack of condom use, as well as an early initiation age of sexual activity and multiple sexual partners (Ohene & Akoto 2008; Reproductive Health and Research & Who 2005).

Importantly, STIs have been shown to increase the risk of HIV acquisition by three fold or more (Mlisana et al. 2012; Newman et al. 2013; Ohene & Akoto 2008) with 16.3% co-infection between genital inflammatory diseases and HIV (Reis Machado et al. 2014). HIV positive individuals have reduced immune function and favor the colonization of STIs as local infections within the FGT. This facilitates local replication of HIV within the FGT through HIV shedding (Reis Machado et al. 2014). One important issue in Southern Africa is that STIs are treated by the syndromic approach, yet up to 50% of the women infected with an STI are asymptomatic and therefore remain untreated. STIs may have subclinical manifestations such as elevated cytokines due to genital tract inflammation. However, due to the lack of diagnosis, under- and over-treatment of STIs is common, further increasing adolescent HIV risk (Mlisana et al. 2012).

1.6 Hormonal Contraceptives

Several different types of contraceptives are currently licensed, including Intra-Uterine Devices (IUD's), barrier methods, hormonal contraception, spermicides and operative sterilization, with other methods including fertility cycle awareness methods, situational methods such as coitus interruptus, douching and abstinence (Draper 2006; Mitchell 2008). Hormonal contraception and condom use are two of the most commonly used methods (Smit et al. 2002).

The two hormones oestradiol and progesterone play a major role in the regulation and defensive immunity of the FGT, along with controlling the monthly menstrual cycle. Synthetic version of these two hormones are used in contraceptives, administered as a daily oral pill, injection, patch,

or inserted in the form of a rod to adjust the monthly menses and FGT conditions in order to prevent pregnancy (Murphy et al. 2014; van de Wijgert et al. 2013). Hormonal contraceptives can contain one or a combination of hormones in various doses, and usually suppress ovulation, increase the viscosity of cervical mucus to impair sperm movement, or induce morphological changes to the endometrium lining to prevent nidation of the egg in the cervix (Family Planning Western Australia 2012; Murphy et al. 2014; Organon Pharmaceuticals USA 2011; Pfizer 2011; Pharmaceutical/Industry 2005).

In Sub-Saharan Africa, the three hormonal contraceptives (HCs) Depo-Provera, Implanon and Nur-Isterate are particularly popular as they do not require daily administration, can go unnoticed due to the manner and frequency in which they are administered, as well as do not require coital-dependent insertion or use (Organon Pharmaceuticals USA 2011; Pharmaceutical/Industry 2005; Pfizer 2011). These three HCs contain progestogens only with the active agents of Depot Medroxyprogesterone acetate (DMPA), Norethisterone Enantate and Progestin Etonogestrel in Depo-Provera, Nur-Isterate and Implanon respectively. Depo-Provera lasts for 12 weeks, Nur-Isterate are injections for 8 weeks, while Implanon is an ethylene vinyl acetate rod that is inserted under the subdermal connective tissue in the arm and can remain for up to three years. The three HCs have similar side effects, such as irregular or prolonged bleeding as well as heavy bleeding or amenorrhea, weight gain, headaches and mood changes. They differ in that Depo-Provera can cause an allergic reaction, albeit rare, as well as loss of bone density. Nur-Isterate can cause dizziness and loss of glucose tolerance while the Implanon can cause bruising, breast pain and acne (Mitchell 2008; Organon Pharmaceuticals USA 2011; Pharmaceutical/Industry 2005; Pfizer 2011).

Progestin-only hormonal contraceptives are favoured in Sub-Saharan Africa due to their privacy, convenience, low cost and efficacy. They were used by an estimated 8 million women in 2015, with specific popularity in South Africa (Byrne et al. 2016; Murphy et al. 2014; Smit et al. 2002; van de Wijgert et al. 2013). In South Africa, male and female condoms, hormone patches, intrauterine devices, sterilization, hormonal pills and contraception injections are available. There are two combined oral contraceptive (COC) and progestin-only contraceptive pills (POP), as well as two progestin only contraceptive injections Nur-Isterate and Depo Provera (DMPA)

(Department of Health 2012; Dr Manto Tshabalala-Msimang 2013; Western Cape Government 2015).

Much observational and pre-clinical research has been conducted to determine the relationship between progestin-only hormonal contraceptives and HIV acquisition (Smit et al. 2002; van de Wijgert et al. 2013). Exogenous progestin's found in hormonal contraceptive injections such as DMPA reportedly could accelerate $CD4^+$ T cell depletion in HIV positive women through the physiological functions of the glucocorticoid receptor within the immune system and apoptosis (Govender et al. 2014; Tomasicchio et al. 2013). Increased progestin levels have been linked to an increased frequency of activated CCR5+ CD4 T cells within the cervix, which are HIV target cells, illustrating a link between the contraceptives and HIV acquisition (Byrne et al. 2016). Further research, originally performed on macaques, indicates that hormonal contraceptives may interfere with cervical cellular immune function by thinning the vaginal epithelial cell layers, which exposes the vaginal junctions to disruption and may therefore allow access to pathogenic bacteria and STIs (Murphy et al. 2014).

Further, HIV acquisition has been linked to progestin-only contraceptives due to their proposed inhibition of TLR-9-induced Interferon (IFN) production by plasmacytoid dendritic cells (pDC's) along with other innate and adaptive soluble factors, potentially hampering immune responses within the cervix against HIV infection (Murphy et al. 2014). A specific association has been indicated with the active agent of Depo-Provera, DMPA and the sustained decrease in Interleukin-8 (IL-8), Interleukin-6 (IL-6), and the Interleukin-1a receptor antagonist (IL-1a) within women over a prolonged period of Depo-Provera use (Borgdorff et al. 2015). Further studies have been conducted to determine if there is a link between the FGT microbiome, progestin-only contraceptives, and HIV within African women given the widespread contraceptive use and HIV acquisition (FSRH Clinical Effectivesness Unit 2017; Polis et al. 2016; World Health Organization 2017). The use of injectable hormonal contraceptives have been implicated in the increased risk of STI acquisition, which are further associated with increased HIV acquisition (Grabowski et al. 2015; Noguchi et al. 2015). The prolonged use of DMPA resulted in a 100 fold decrease in *G. vaginalis* in the vaginal fluid in a study by Roxby et al. (2016), with the suggested explanation linking amenorrhea and the requisite for iron for *G. vaginalis* growth. The bacterial species *L. crispatus* and *L. jensenii* were below detection level

for most participants on DMPA with little or no change to *L. iners.* The total bacterial load was further shown to decrease over time with DMPA administration, with no correlation indicated with BV in vaginal health (Borgdorff et al. 2015; Roxby et al. 2016).

1.7 Technical analysis of FGT bacteria

Several techniques exist to quantify bacteria in a diverse range of samples. Although growth media has been used to culture many organisms within the FGT, some are more difficult to cultivate and therefore Polymerase chain reaction (PCR) is one of the most commonly used techniques for quantifying target DNA that does not depend on the culturability of the bacteria. The DNA is amplified through the use of primers, which can be custom designed and species-specific or universal, for instance targeting all bacteria via genes targeting the hypervariable regions of the 16S rRNA gene. The DNA goes through an initial denaturation cycle most commonly at 95℃, followed by a number of cycles of denaturation, annealing and extension after which the DNA product is run on an agarose gel with a DNA size marker to confirm expected amplicon size. PCR is a rapid, automated and when performed in a 384 well qPCR plate- high throughput quantitative technology used as an important tool for basic research (Lambert et al. 2013; Pabinger et al. 2014).

Real-time quantitative PCR (qPCR) is an advancement of PCR where simultaneous amplification and quantitation of a target gene is possible. The initial amount of template DNA can be quantified based on the relationship between cycle number and fluorescent threshold signal level where the higher the initial DNA concentration, the fewer cycles required to reach the threshold level (Pabinger et al. 2014; Pfaffl 2004; Pfaffl & Wittwer 2015). qPCR can be used for relative quantitation of bacteria through the use universal bacterial 16S rRNA primers, followed by sequencing in order to identify the species present. qPCR can be used for absolute quantification through the use of species specific primers in relation to a standard curve constructed through serial dilution of DNA extracted from a positive control reference bacterium. This technique allows absolute quantification of the bacteria of interest (copies/µL), which can be converted to bacterial copy numbers based on the reference bacteria's genome size (see Methods Chapter 3 for details) (Grunenwald & Kramer n.d.; Hermann-bank et al. 2013;

Roche 2003; Smith & Osborn 2009). With the increased use of this technique as a tool for gene expression, pathogen detection and biomolecular diagnostics, it is important to have stringent quality control measures in place. As such the Minimum Information for Publication of Quantitative Real-Time PCR Experiments (MIQE) has been established in order to maintain the standard of qPCR for all research (Bustin 2010; Pabinger et al. 2014).

Next Generation Sequencing (NGS) is used for 16S rRNA, small subunit rRNA, hypervariable regions, rDNA, and metagenomics sequencing. NGS has multiple clinical applications such as forensic genetics, infectious disease surveillance, pathogen outbreaks and is in the early stages of clinical diagnostics (Jones et al. 2015; Illumina 2013; Voelkerding et al. 2010). NGS involves the sequencing of stretches of target DNA in order to identify the relative abundance of bacteria present. Sanger sequencing was the first form of sequencing and since, the advent of NGS has progressed to 454 pyrosequencing, Illumina MiSeq, Illumina HiSeq and Ion Torrent sequencing (Tan et al. 2015). NGS is a high throughput analysis technique which has a diverse set of applications above DNA sequencing such as re-sequencing, microsatellite analysis and Single nucleotide polymorphism (SNP) genotyping, multiplexing and whole-genome sequencing with tunable resolution, target sequencing and enrichment (Czerniecki & Wołczyński 2011; Illumina 2013; Wienkoop & Weckwerth 2006).

In this study, we aimed to compliment Illumina MiSeq relative abundance analysis of the vaginal microbiota of adolescent females by development and application of qPCR. This study aimed to identify the presence of a relationship between the factors such as high risk HPV subtypes, high genital inflammation BV positive, older adolescent age groups, DMPA hormonal contraceptives and the presence of an STI in relation to increased quantities of the key bacterial species which may influence HIV acquisition as discussed in the literature review.

1.8 Aims of this Study

1. To develop an assay for absolute quantitation of *L. jensenii, L. gasseri, L. crispatus L. iners, G. vaginalis* and *P. bivia* in adolescent genital tract in HIV negative South African adolescent females.

2. To analyze relationships between the copies/ng of the bacteria, and relate the absolute quantities to BV status, inflammation, age, hormonal contraceptive and STIs.

1.9 Objectives of this Study

1. In HIV negative adolescent females in South Africa, to asses any associations between the copies/ng of bacterial species of interest *L. jensenii, L. gasseri, L. crispatus L. iners, G. vaginalis* and *P. bivia* and;
    a. High and Low Inflammatory cytokine levels,
    b. BV Positive, Intermediate and Negative based on Nugent scores,
    c. Age (stratified as 16-18 years old vs 19-22 years old),
    d. DMPA, Nur Isterate, and Implanon hormonal contraceptives,
    e. The presence or absence of STIs (*N. gonorrhea, C. trachomatis,* HSV-2, *T. vaginalis, M. genitalium, T. pallidum, H. ducreyi*)

1.10 Hypothesis

We hypothesize that *L. jensenii, L. gasseri,* and *L. crispatus* will be more abundant in HIV negative female adolescent vaginal samples that contain low levels of inflammatory cytokines and/or are BV negative and/or have no STI, and/or are using the hormonal contraceptives Nur Isterate or Implanon between the ages of 16-18 years old.

We further hypothesized that *L. iners, G. vaginalis* and *P. bivia* will be more abundant in HIV negative adolescent female vaginal samples that contain high levels of inflammatory cytokines and/or are BV positive and/or have one or more STIs and/or using the hormonal contraceptive DMPA between the ages of 19-22 years old.

Chapter 2: Cohort Characteristics

2.1 Study Design

The research group working under the Women's Initiative in Sexual Health (WISH) cohort (HREC REF 267/2013) aimed to look at the relationship between inflammatory cytokines, BV, STI's and genital tract microbiome in the FGT in HIV negative adolescent females in South Africa at high risk for HIV. The ethical approval of this MSc project (HREC REF: 678/2015) was granted on the 17 September 2015 as part of the WISH cohort ethical approval. Here, we aimed to identify the composition of the vaginal microbiome in the mucosa of the female genital tract, and to relate these to the composition of cervical target cells for HIV infection and levels of inflammation in the cervix. Next Generation Sequencing of 16S rRNA was previously performed by our group for this cohort to profile the FGT microbiome – mostly to genus level, with some species level identification (Lennard, manuscript in preparation). Participants were drawn from the Masiphumelele Youth Centre based in Masiphumelele, Cape Town, Western Cape. Participants were chosen from this area since there is a high HIV prevalence (21.9% in 2004 (Lawn et al. 2006)) and thus an applicable population to assess adolescent HIV risk.

2.2 Recruitment of participants

HIV-negative, sexually active, adolescent females aged 16-22 years were recruited from the Masiphumelele Youth Centre. Participants provided written consent if >= 18 years old, or for participants < 18 years old, their guardians provided written consent while the adolescent provided signed assent.

2.3 Exclusion criteria

Participants were excluded according to the following criteria:

1. Participants younger than 16 years or older than 22 years old.
2. Participants who had a positive pregnancy test or had used anything that contained spermicide within 48 hours prior to sampling.
3. Participants were excluded if they had inserted anything in their vagina within 24 hours before sampling (including but not limited to protected or unprotected vaginal intercourse).

4. Participants who had douched within 48 hours before sample collect, or were menstruating.
5. Participants were excluded if they had taken antibiotics within the two weeks prior to sampling.
6. HIV positive participants were excluded and referred for care.

2.4 Participants and sample collection

The cohort participants were sexually active female adolescents between the ages of 16 and 22 who were enrolled in the WISH study at the Masiphumelele Youth Centre. A detailed questionnaire was completed by each participant in order to establish sexual practices, demographics, menstrual cycle, antibiotic used, STI symptoms and adherence in terms of condom and contraceptive use for the study. Samples were collected in the luteal phase of the menses cycle from participants taking no HC. A physical exam was performed and the following vaginal specimens were collected;

1. A softcup to collect vaginal secretions for measurement of cytokines,
2. A lateral wall swab for 16S microbiome profiling,
3. An endocervical swabs or cervical mucous plug for HPV testing,
4. A vulvovaginal swab for STI's and BV testing
5. Two Digene cervical cytobrushes for cervical immune and epithelial cells.

2.5 Human-immunodeficiency virus (HIV) testing

HIV testing was performed using a Rapid assay on a blood sample retrieved through a prick to a finger, the result of which was verified using a second, Rapid test for positive samples. Intermediate results were sent for ELISA confirmation.

2.6 Bacterial vaginosis (BV) testing

BV was diagnosed based on Nugent Scoring on a vaginal swab slide where a Nugent score of 0-3 and was considered BV-negative, a Nugent score of 4-6 BV-intermediate and a Nugent score of 7-10 BV-positive. The pH was noted during the sampling process, as well as symptoms such as the presence of heavy discharge and the colour of the patients discharge. The presence of

"Clue" cells were taken into account when determining Nugent Scores. All symptomatic BV cases were treated through the Masiphumelele Youth Centre.

2.7 Sexually Transmitted Infections (STIs) testing

All female participants who consented to this study provided vulvovaginal swabs, which were tested for *N. gonorrhea, C. trachomatis,* HSV-1, HSV-2, *T. vaginalis, M. genitalium, T. pallidum,* and *H. ducreyi* at the mucosal sampling visit. The results of the tested samples were made available for all participants who tested positive for one or more of the infections. These participants were prescribed treatment as well as counseling on site. *T. pallidum* was not included in the categorization of viral versus bacterial STI comparisons as there were no positive results.

STI screening was performed by multiplex PCR on the DNA extracted from vulvovaginal swabs (Lewis 2000). HSV-1, HSV-2, *T. pallidum,* and *H. ducreyi* were identified through M-PCR using targeted gene primers. Physical exams were performed as part of the identification of *T. pallidum* and no ulcers were present. Overall there were no *T. pallidum* results. HSV-1 and HSV-2 were identified as a result of both the serology and M-PCR positive results, however, only PCR results were used for this analysis (i.e. only active shedding was taken into account). The serology results for HSV-1 and HSV-2 were not incorporated into the results such that analyses were performed based on the presence of absence HSV-1 and HSV-2 alone. Slides were prepared to identify candida hyphae and spores.

2.8 Next Generation Sequencing (NGS) of 16S rRNA

NGS was carried out through the extraction of microbial DNA using a MoBio Ultraclean microbial DNA extraction kit from cervical swabs in order to identify the bacteria present within the female genital tract. The following universal primers were used to amplify the SSU rRNA gene;

515F 5'-GTGCCAGCMGCCGCGGTAA-3' and 907R 5'- CCGTCAATTCCTTTRAGTTT-3'. These universal primers allow identification of bacteria present within the participant samples by Illumina Miseq (V3 chemistry 300 bp paired end).

The data analysis was performed by Katie Lennard (PhD) using UPARSE, Quantitative Inference In Microbial Ecology (QIIME) and custom R scripts.

2.9 Cohort characteristics

Cohort characteristics are summarized in Table 2.9.

Table 2.9: Summarized characteristics of the WISH cohort according to the following categories.

Category	Sample Size	Classification type	Score	Groups	Participants (%)
BV	143	Nugent Scoring	0-3	Positive	56 (39.16)
			4-6	Intermediate	17 (11.89)
			7-10	Negative	70(48.95)
Inflammation	140	Unsupervised hierarchical clustering analysis	Partitioning around medoids (PAM) using an R package 'cluster' with a k-value of 2	Low	42 (30)
				High	98 (70)
Age	143	Age in years	Years	16-18	75 (52.45)
				19-22	68 (47.55)
Hormonal Contraceptives	136	Type	Prescribed	DMPA	25 (18.38)
				Nur Isterate	102 (75)
				Implanon	9 (6.62)
STI	140	Presence/absence of any one STI	*N. gonorrhea, C. trachomatis,* HSV-2, HPV, *T. vaginalis, M. genitalium*	None	62 (44.29)
				Present	78 (55.71)
Bacterial STI	143	Absence, presence of one, presence of two or more	*Chlamydia trachomatis, Neisseria gonorrhea,*	None	77 (53.85)
				One	51 (35.66)
				Two<	15 (10.49)

			Mycoplasma genitalium		
Viral STI	143	Absence, presence of one, presence of two	HSV-2, HPV	None One Two	46 (32.17) 91 (63.63) 6 (4.20)
HPV	90	Absence, presence of low or high risk subtypes	6, 11, 40, 42, 54, 55, 61, 62, 64, 67, 69, 70, 71, 72, 81, 83, 84, 89 (CP6109), IS39	None Low Risk	29 (32.22) 27 (30)
			16, 18, 26, 31, 33, 35, 39, 45, 51, 52, 53, 56, 58, 59, 66, 68, 73, 82	High Risk	34 (37.78)

Chapter 3: Laboratory Methods and Materials

In this chapter, the protocols used in laboratory for processing and analysis of the WISH vaginal samples will be discussed.

We used qPCR to quantify the presence of six microbes in the genital tract of South African adolescents. In addition to providing absolute quantitative data, the qPCR-based data complements the 16S rRNA-based microbiome data previously generated for this cohort by providing data on species-level taxonomic annotation for specific bacteria of interest that were only identified to genus level via 16S sequencing.

3.1. Bacterial reference strains

The ATCC reference strains *Lactobacillus gasseri* (ATCC 9857), *Lactobacillus crispatus* (ATCC 33197), and *Lactobacillus jensenii* (ATCC 25258) were kindly provided by Remy Froissart PhD., from the Division of Virology, University of Cape Town. The ATCC reference strains *Lactobacillus iners* Strain UPII 143-D (Product sheet HM-126), *Gardnerella vaginalis* Strain UPII 315-A (Product sheet HM-133) and *Prevotella bivia* Strain DNF00188 (Product sheet HM-1088) were obtained from BEI Resources, Manassas USA.

The bacterial reference strains were used as positive controls and to perform absolute quantification by constructing standard curves with genomic DNA extracted from there strains.

3.1.1 Bacterial Culturing

3.1.1.1 *Lactobacillus spp. growth conditions*

Lactobacillus gasseri (ATCC 9857)*, L. jensenii* (ATCC 25258) and *L. crispatus* (ATCC 33197) were cultured in a sterile broth composed of 51 g/L of De Man, Rogosa, Sharpe broth (MRS, Sigma), 50 mg/l of L-Cysteine (Merck) and 1 ml of Tween 80 (Sigma) for a minimum of 48 hours at 37°C. The ATCC *Lactobacillus* strains were allowed to thaw for 20 minutes on ice, after which a sterile tooth pick was used to culture 1.4 mL of MRS Broth in a 1.5 mL Eppendorf Tube and incubated at 37°C. After 48 h of growth, the 1.5 mL Eppendorf with cultured MRS Broth were vortexed briefly and transferred to a sterile 50 mL Falcon tube, which was topped up with

additional MRS Broth. The 50 mL Falcon tube was vortexed briefly and incubated at 37°C to be used for DNA extraction.

A 1.5 mL Eppendorf Tube containing 1.4 mL cultured broth was centrifuged at 5500 RPM for 5 minutes and 900 µL of supernatant was discarded. After vortexing the pellet, 250 µl of 60% glycerol (v/v) was added and vortexed briefly three times and subsequently stored at -80°C for future use.

3.1.1.2 *Lactobacillus iners, Prevotella bivia* and *Gardnerella vaginalis.* growth conditions

*Lactobacillus iners (*UPII 143-D), *Prevotella bivia* (DNF00188) and *Gardnerella vaginalis* (UPII 315-A) were cultured individually in reduced Schaedler Broth with 5% horse blood for a minimum of 48 hours at 37°C. The three strains were allowed to thaw for 20 minutes on ice, after which a sterile tooth pick was used to collect bacterial stock and culture 1.4 mL Schaedler Broth with 5% horse blood in a 1.5 mL Eppendorf tube and incubated at 37°C for 48 h, followed by brief vortexing and transferred to a sterile 50 mL Falcon tube which was topped up with additional Schaedler Broth with 5% horse blood. The 50 mL Falcon tube was vortexed briefly and incubated for a minimum of 48 hours at 37°C to be used for DNA extraction.

3.1.2 DNA Extraction

DNA was extracted from vaginal lateral wall swabs and bacterial cultures using two different kits, both designed to lyse the cell walls of Gram positive and Gram negative bacterium.

The MoBio Powersoil® DNA Isolation Kit (MoBio Laboratories, Inc., USA, Biocom Biotech, SA) was used to extract bacterial DNA from the vaginal lateral wall swabs. Briefly, bacterial cell walls were lysed with buffer C1 which contains sodium dodecyl sulfate (SDS) detergent that breaks down fatty acids and disrupts the bacterial cell walls, and by mechanical disruption (bead beating). Buffers C2 and C3 contain inhibitors that remove sample contaminants including non-DNA organic and inorganic material and proteins. Buffer C4 selectively binds DNA to the silica filters thus further excluding contaminants during the wash step. The final ethanol-based wash buffer C5 is the final step in removing any excess contaminants within the sample DNA.

The Qiagen Blood and Tissue DNA Maxi Extraction Kit with buffers B1 and B2 (Whitehead Scientific (Pty) Ltd, Cape Town), was used to extract DNA from bacterial cultures. Proteinase

K, which cleaves peptide bonds, was used to digest proteins, and RNase A to digest RNA (at the C and U residues). Lysozyme was used to lyse bacterial cell walls – more specifically peptidoglycan, which is found in both Gram-negative and –positive bacteria, but is most effective against the latter. Buffer B1 contains Tween 20 and Triton X-100, which are polyethylene and polyethylene oxide surfactants respectively, which act in conjunction with lysozyme to lyse bacterial cell walls. Buffer B2 contains Tween 20 and guanidine hydrochloride, a chaotropic agent that denatures proteins.

The quality and concentration of the DNA was confirmed with Qubit Fluorometric Quantitation (ThermoFisher Scientic Inc, 200 Smit Street, Fairland, 2195 Johannesburg, South Africa), using the Picogreen target-specific fluorescent dye, High Sensitivity dsDNA assay as per the user manual.

3.1.3 Primer Design

The species-specific primers used for the detection of each of the bacterial species of interest within this study were either sourced from the literature or designed de novo (Table 3.1.1). The specificity for all primers was confirmed using NCBI Primer BLAST website (National Center of Biotechnology Information, National Institute of Health, Bethesda, MD), Ribosomal Database Project Probe Design (http:// www.rdp.cme.msu.edu/) and PriSM Primer Designing Tool. All primers were obtained from Integrated DNA Technologies Inc., Coralville, IA.

Table 3.1.3: Primers of the target genes for detection of bacteria of interest and protocol source of PCR and qPCR.

Bacteria	Primers		Reference
	Forward (5'-3')	Reverse (5'-3')	
Lactobacillus crispatus	TGCGACGCAAAG CTGAAACA	AATGCTTCACGCG CAAGGTT	(Byun et al. 2004; Jespers et al. 2012)
Lactobacillus jensenii	AAGTCGAGCGAG CTTGCCTATAGA	CTTCTTTCATGCGA AAGTAGC	(Jespers et al. 2012; Tamrakar et al. 2007)
Lactobacillus	GTCTGCCTTGAA	ACAGTTGATAGGC	(De Backer et al. 2007;

iners	GATCGG	ATCATC	Jespers et al. 2012)
Lactobacillus gasseri	TGGAAACAGRTG CTAATACCG	CAGTTACTACCTC TATCTTTCTTCACT AC	(Jespers et al. 2012; Malaguti et al. 2015; Tamrakar et al. 2007)
Gardnerella vaginalis	TTACTGGTGTAT CACTGTAA	CCGTCACAGGCTG AACAGT	(Jespers et al. 2012; Malaguti et al. 2015)
Prevotella bivia	TGGGGATAAAGT GGGGAACG	ACAACACGCTTAC CAAACGG	(Premaraj et al. 1999); followed by Aroutcheva *et al.,* 2008; followed by (Dumonceaux et al. 2009)

3.2 Polymerase Chain Reaction

3.2.1 Polymerase Chain Reaction (PCR) of ATCC reference strains (Primer confirmation)

PCR was run on DNA extracted from the pure cultures of each bacterium of interest to ensure primer specificity and to confirm the expected amplicon size. A total of 10 µL Roche LightCycler® 480 SYBR Green I Master Mix was used per reaction, with 0.5 µL of each 10 µM primer, 3 µL template gDNA of the serially diluted positive standard controls and 6 µL nuclease-free water for a total volume of 20 µL (Table 3.2.1). Difference cycle conditions were optimized and used for each bacterium (Table 3.2.2)

Table 3.2.1: PCR mixture components.

Reagents for PCR	Volume (µL)
Master mix	10
Forward Primer	0.5
Reverse Primer	0.5
Template DNA	3
Nuclease-free H_2O	6
Total	20

Table 3.2.2: PCR conditions and amplicon size of the target gene for the six bacteria of interest.

Bacteria	Initial Denaturation		Denaturation		Annealing		Extension		Cycles	Amplicon size (bp)
	Time (min)	Temp (℃)	Time (sec)	Temp (℃)	Time (sec)	Temp (℃)	Time (sec)	Temp (℃)		
Lactobacillus crispatus	15	95	15	95	60	60	20	72	45	172
Lactobacillus jensenii	15	95	15	95	55	60	60	72	40	160
Lactobacillus iners	15	95	15	95	55	60	60	65	35	158
Lactobacillus gasseri	15	95	15	95	60	57	60	65	40	322
Gardnerella vaginalis	15	95	45	95	45	55	45	72	50	330
Prevotella bivia	5	95	20	95	120	60	300	74	35	156

3.2.2 Gel electrophoresis

Gel electrophoresis was used to confirm accuracy of the primers based on the size of the PCR product and the presence of a single band. Amplified DNA (4 µL) was separated on 1.6% agarose gel (Whitehead Scientific Agarose, #D1-LE) by electrophoresis in 1X TAE buffer (40 min, at 120 V). DNA was visualized with GelRed and viewed under a UV-Trans-illuminator. A ThermoFisher O'Gene Ruler® 100 bp ladder was used for sizing of the PCR amplicon bands.

3.2.3 Serial dilution calculations for the known standard controls

In order to calculate the number of copies/µL of bacteria present in the extracted DNA for each standard control, the method described by Dolezel et al., (2003) was used. Briefly, the assumptions made are that the average weights for the nucleotide pairs AT and GC are 615.3830 and 616.3711 respectively, which can be converted to an absolute value through the

multiplication by the atomic mass unit (1 u) which is the equivalent of ^{12}C (1.660539×10^{-27} kg). Thus, the average weight of a single nucleotide pair can be calculated at 1.023×10^{-9} pg, where a single picogram of DNA would be equivalent to 0.978×10^{9} base pairs.

Genome size (bp) = (0.978×10^{9} bp) x DNA content (pg)

DNA content (pg) = Genome size (bp) / (0.978×10^{9} bp)

Therefore, as an example, for *L. crispatus* the complete genome size is 2195108.667 bp (Table 3.2.5) DNA content (pg) = 2195108.667 bp / (0.978×10^{9} bp)

= 0.002244487 pg

1 ng DNA from *L. crispatus* contains = 1000 pg / DNA content (pg)

= 1000 pg / 0.002244487 pg

= 445,536.0296 copies

L. crispatus DNA concentration = 290 ng/µL

The number of copies of DNA per µL = Number of copies DNA x DNA concentration (ng/µL)

= 445,536.0296 copies x 290 ng/µL

= 129 205 448.6 copies/µL

$C_1V_1 = C_2V_2$

(129 205 448.6 copies/µL) x V_1 = (10^6 copies/µL)x(1000 µL)

V_1 = ((10^6 copies/µL) x (1000 µL)) / (129 205 448.6 copies/µL)

V_1 = 7.739 µL

Therefore 7.739 µL of *L. crispatus* DNA was added to 992.261 µL distilled water to dilute it to 10^6 copies/µL. From there the DNA was serially diluted from 10^6 copies/µL down to 10^{-2} copies/µL.

The calculations for the six bacterial reference strains can be seen below in Table 3.2.3. See table 3.5.2 for data transformation software.

Table 3.2.3: Serial dilution calculation summary table.

Bacteria	ID Code	[DNA] (ng/µL)	DNA content (pg)	Copies in 1 ng DNA	Copies of DNA/µL	Volume of DNA into 1 mL for 10^6 copies/µL
L. crispatus	33820	290	0.00224449	445536.030	129205449	7.739611688
L. jensenii	25258	870.6	0.00169902	588576.408	512414620	1.951544629
L. gasseri	9857	321	0.00201423	496468.302	159366325	6.274851359
L. iners	UPII 143-D	19.72	0.00132327	755703.271	14902469	67.10297695
G. vaginalis	UPII 315-A	4.28	0.00163010	613458.066	2625600.5	380.8652505
						Volume of DNA into 40 µL for 10^6 copies/µL
P. bivia	DNF00188	2.773	0.00254910	392295.603	1087966.47	36.7658

*For all calculations, 1 pg of DNA was considered to have 0.97×10^9 bp as per the explanation above in 3.2.3. See table 3.5.2 for data transformation software.

Table 3.2.4: Calculation and source for the whole genome size for each bacterium.

Bacteria	Source	NCBI Accession Number	Number of sources	Average whole genome size (bp)
L. crispatus	ATCC	PRJNA30641, PRJNA37951, PRJNA38361, PRJNA38513, PRJNA36325, PRJNA42533, PRJNA52107, PRJNA52105, PRJNA222257, PRJNA200566,PRJNA267549, PRJNA213996, PRJDB800, PRJEA46813, PRJNA40665,	15	2195108.67
L. jensenii	ATCC	PRJNA31205, PRJNA37953, PRJNA38515, PRJNA38645,PRJNA231005,PRJNA231005,PRJNA 231005,PRJNA231005, PRJNA231005,	14	1661636.43

		PRJNA231005, PRJNA222257,PRJNA34097, PRJNA213997, PRJNA31493, PRJNA219715, PRJNA31487,		
L. gasseri	ATCC	PRJNA42535, PRJNA42543, PRJNA203137, PRJNA36379, PRJNA163367,PRJNA208361, PRJDB635, PRJNA267549, PRJNA267549, PRJNA31203, PRJNA40683, PRJNA84, PRJNA53061, PRJNA52039, PRJNA52037,	14	1969914.29
L. iners	BEI	PRJNA52035, PRJNA52033, PRJNA52031, PRJNA43549, PRJNA52041, PRJNA52043, PRJNA52045, PRJNA52047, PRJNA60373, PRJNA60375, PRJNA222257,PRJNA288563,	16	1294158.75
G. vaginalis	BEI	PRJNA31001, PRJNA51067, PRJDB63, PRJNA52029,PRJNA181326,PRJNA181325, PRJNA181324,PRJNA181323,PRJNA181322, PRJNA181321,PRJNA181320,PRJNA181319, PRJNA181318,PRJNA181317,PRJNA181316, PRJNA181315, PRJNA181314,PRJNA181313, PRJNA181312, PRJNA53359, PRJNA53893, PRJNA40893, PRJNA40895, PRJNA52049, PRJNA42431, PRJNA42443, PRJNA42445, PRJNA42451, PRJNA42435, PRJNA42437, PRJNA42441, PRJNA42447,PRJNA42449,PRJNA42453, PRJNA42455,PRJNA267549, PRJNA294071, PRJNA46675, PRJNA267549,PRJNA267549, PRJNA267549, PRJNA42439	43	1594241
P. bivia	BEI	PRJNA31377, PRJNA187523, PRJNA219670, PRJNA219665, PRJNA50753	5	2493018

3.3 qPCR Optimization

Optimization was undertaking by adjusting the following parameters of the previously published qPCR protocols (Table 3.1.3):

1. Protocol

   Protocols- for each bacterial species of interest were found in the literature and run as published for the first trial run. Thereafter, parameters were manipulated; including primer concentration, annealing temperature, cycle number and sequence as a last step in order to achieve acceptable standard curves with low levels of primer dimers, error values and high efficiency values, as outlined below. If the protocol could not be improved upon by manipulating these parameters, a new protocol from another published article was used and the same steps followed as mentioned below to optimize.

2. Primer optimization

   Prior to use in the wet lab, primers were first tested *in silico* using NCBI Primer BLAST to ensure primer specificity and a low level of self-complementarity. Thereafter, a PCR trial run was performed. If the primers amplified the correct product size in a PCR trial run they were kept for further qPCR optimization. If the primers were found to be consistent and sensitive, they were used to construct a standard curve.

   The primer concentration was further optimized by applying different starting concentrations. The optimum primer concentration was determined based on lower error and higher efficiency values in the standard curves.

3. Annealing temperature optimization

   The annealing temperature used in the literature was used for the first qPCR trial run. If the DNA started amplifying at a later cycle number than anticipated, the temperature was then increased slightly to try and improve on protocol sensitivity.

4. Cycle number optimization

   The first trial run qPCR was run with the number of cycles specified in the literature. If the DNA amplified at a later cycle number than anticipated, of which a possible cause is low DNA concentration, the cycle number was increased to by no more than 20 cycles to ensure complete amplification of the sample and standard DNA.

5. Initial denaturation

   The initial denaturing temperature was found to be 95℃ in all protocols used. The temperature was kept the same when optimizing, however, the time the denaturation cycle ran was adjusted when it was found the DNA did not amplify sufficiently after the initial and cycle denaturation.

6. Serially diluted standards

   Positive controls (DNA extracted from each reference strain) were diluted to 10^6 copies/µL from the stock DNA and then serially diluted down to 10^0 copies/µL. If there were issues with the precision or accuracy of the standard replicates, the DNA was re-serially diluted in order to improve the standard curve error and efficiency. The goal error and efficiency values were $\leq$0.05 and 2, respectively.

After optimization for each bacterium, the final qPCR cycle conditions were determined (Table 3.2.7).

3.3.1 qPCR Optimization Outcomes

Multiple plates were run with different conditions until the error and efficiency values were as close to 0.05 and 2 respectively, as could be optimized. A summary of the plate errors and efficiencies for each step in the optimization process can be found in Table 3.3.1. All optimization plates are named as V1 with the point number indicating the number of plate replicate for each bacterium.

Table 3.3.1: Summary table for the optimization statistics for the following bacteria.

Bacteria	qPCR Plate	Error	Efficiency
L. crispatus	V1.1	0.565	1.705
	V1.2	2.322	0.00
	V1.3	1.141	1.717
	V1.4 (750 nM)	1.301	1.358
	(500 nM)	0.221	1.628
	(250 nM)	0.223	1.985
	V1.5	0.219	1.783
	V1.6	0.731	1.699
	V1.7	0.177	1.890
L. gasseri	V1.1	0.0223	1.828
	V1.2	0.0436	1.851
	V1.3	0.0442	1.839
L. jensenii	V1.1	0.312	1.864
	V1.2	0.0210	1.921
L. iners	V1.1	0.0335	2.022
	V1.2	0.0805	1.953
G. vaginalis	V1.1	0.370	1.835
	V1.2	0.248	1.733
	V1.3	0.351	1.671
	V1.4	0.242	1.719
	V1.5	0.157	1.875
	V1.6	0.204	1.766
P. bivia	V1.1	1.191	0.997
	V1.2	0.306	2.393
	V1.3	0.823	1.714
	V1.4	0.589	1.765
	V1.5	0.283	1.983
	V1.6	0.0376	1.904
	V1.7	0.210	2.089
	V1.8	0.419	2.294
	V1.9	0.393	2.049
	V1.10	0.628	1.550
	V1.11	0.618	2.922
	V1.12	0.0830	2.039
	V1.13	0.0608	1.993

The qPCR optimization process outcomes for the three bacterium *L. crispatus, G. vaginalis* and *P. bivia* have been included as an example. The optimization process outcomes for the other bacterium have been recorded in Appendix C, qPCR Optimization.

3.3.2 *Lactobacillus crispatus*

A total of seven qPCR plates were run in order to optimize the cycle conditions for *L. crispatus* to get the error close to 0.05, the efficiency to 2.00, single melt curve peaks and clear amplification curves for the standard control. The first trial plate run for *L. crispatus* (V1.1) contained 10 µL SYBR Green I master mix, 1.5 µL of both the forward and reverse 10 µM primers to give a final concentration of 750 nM, 5 µL for each positive controls and corresponding amounts of Nuclease Free Water (NFW) to make up the total volume to 20 µL. The positive control was diluted from 10^6 copies/µL to 10^{-2} copies/µL. Each sample was run in triplicate, with the NTC containing all the reagents minus the template gDNA or the known standard DNA. The participant sample W132 V1 A was run in triplicate of initial concentrations of 10 ng/µL, 7 ng/µL, 5 ng/µL, 2.5 ng/µL and 1 ng/µL. The following qPCR conditions were followed, 95℃ for 15 min initial denaturation, followed by 40 cycles of 95℃ for 15 s, 60℃ for 1 min and 72 for 20 s (Figure 3.3.2.1 A, Figure 3.3.2.2 A). However, the error and efficiency values for the standard curve were not specific enough and the triplicates of the positive control DNA did not amplify neatly where the replicates started amplifying at different cycles.

Therefore a few changes were made to the second trial plate for *L. crispatus* (V1.2) which was run with the same volumes and concentrations of reagents, standard control dilutions and participant sample W132 V1 A as mentioned in V1.1 except for the standard positive controls which were run in triplicate, but two of the triplicates had gDNA that had gone through PCR amplification using the same primers prior to qPCR and one replicate had gDNA that had not gone through qPCR prior to amplification in order to ensure the starting concentrations were sufficient. Furthermore, two different primer concentrations were run, 3 µM and 0.5 µM which resulted in final primer concentrations of 225 nM and 37.5 nM respectively to determine the ideal concentration of primer for amplification. The following qPCR conditions were followed, 95℃ for 5 min initial denaturation, followed by 40 cycles of 95℃ for 20 s, 60℃ for 45 s and 72

for 15 s (Figure 3.3.2.1 B, Figure 3.3.2.2 B). This resulted in the positive control DNA forming odd amplification curves with only the two highest dilutions amplifying sufficiently, as well as a standard curve with poor error and efficiency values.

The third trial plate for *L. crispatus* (V1.3) contained the same reagent conditions as V1.1, except for the use of 1 µL of each primer, 3 µL of the standard control and sampled DNA was used. The participant sample W132 V1 A DNA concentrations were also varied; 1 ng/µL and 0.5 ng/µL to determine the minimum concentration for amplification. The ATCC positive bacterial control standards included dilutions from 10^6 copies/µL to 10^1 copies/µL. The following qPCR conditions were followed, 95℃ for 5 min initial denaturation, followed by 40 cycles of 95℃ for 15 s, 60℃ for 20 s and 72℃ for 10 s (Figure 3.3.2.1 C, Figure 3.3.2.2 C). This led to a high error rate and differences in the replicates for the positive control dilutions. The fourth trial plate for *L. crispatus* (V1.4) had the same cycle conditions and reagent volumes as V1.3 with some changes. Varying volumes of both the forward and reverse 10 µM primers, 0.5 µL, 1 µL and 1.5 µL were used to give a final concentration of 250 nM, 500 nM and 750 nM, in order to determine the most ideal primer concentration as well as the inclusion of sample W037 V1 which had high levels of lactobacilli bacteria present with 16S sequencing (Figure 3.3.2.1 D, Figure 3.3.2.2 D). The dilution of the primers to 250 nM resulted in the best error and efficiency readings for the standard curve.

For the fifth trial plate for *L. crispatus* (V1.5), the same cycle conditions were used as in V1.4 with 0.5 µL of both the forward and reverse 10 µM primers, positive controls diluted from 10^6 copies/ L to 10^{-2} copies/µL and the annealing temperature was reduced from 60℃ to 58℃ to try reduce the formation of primer dimers with the remaining conditions the same as V1.4 (Figure 3.3.2.1 E, Figure 3.3.2.2 E). The error value was higher than ideal with the replicates of the standards failing to amplify at concurrent cycles. The sixth trial plate for *L. crispatus* (V1.6) was run with the same reagent concentration and volumes, as well as the conditions with the adjusted annealing temperature as were used for V1.5. The positive control DNA was re-diluted to try improve accuracy and prevent the delay in the amplification between 10^5 copies/µL and 10^4 copies/µL (Figure 3.3.2.1 F, Figure 3.3.2.2 F). The second dilution did not improve replicate accuracy, and resulted in an increase in the standard curve error value. The seventh and final trial plate for *L. crispatus* (V1.7) used the same reagents and DNA in the same concentrations as used

in V1.6 with the standard control dilutions from 10^6 copies/µL to 10^0 copies/µL. New species specific primers for *L. crispatus* were designed targeting the transcription start site, tested with a PCR by running the product on a gel and confirming the product size and presence of a single band (Figure 3.3.2.1 G, Figure 3.3.2.2 G). This resulted in error and efficiency values of sufficient readings with the replicates of the positive control dilutions amplifying more accurately.

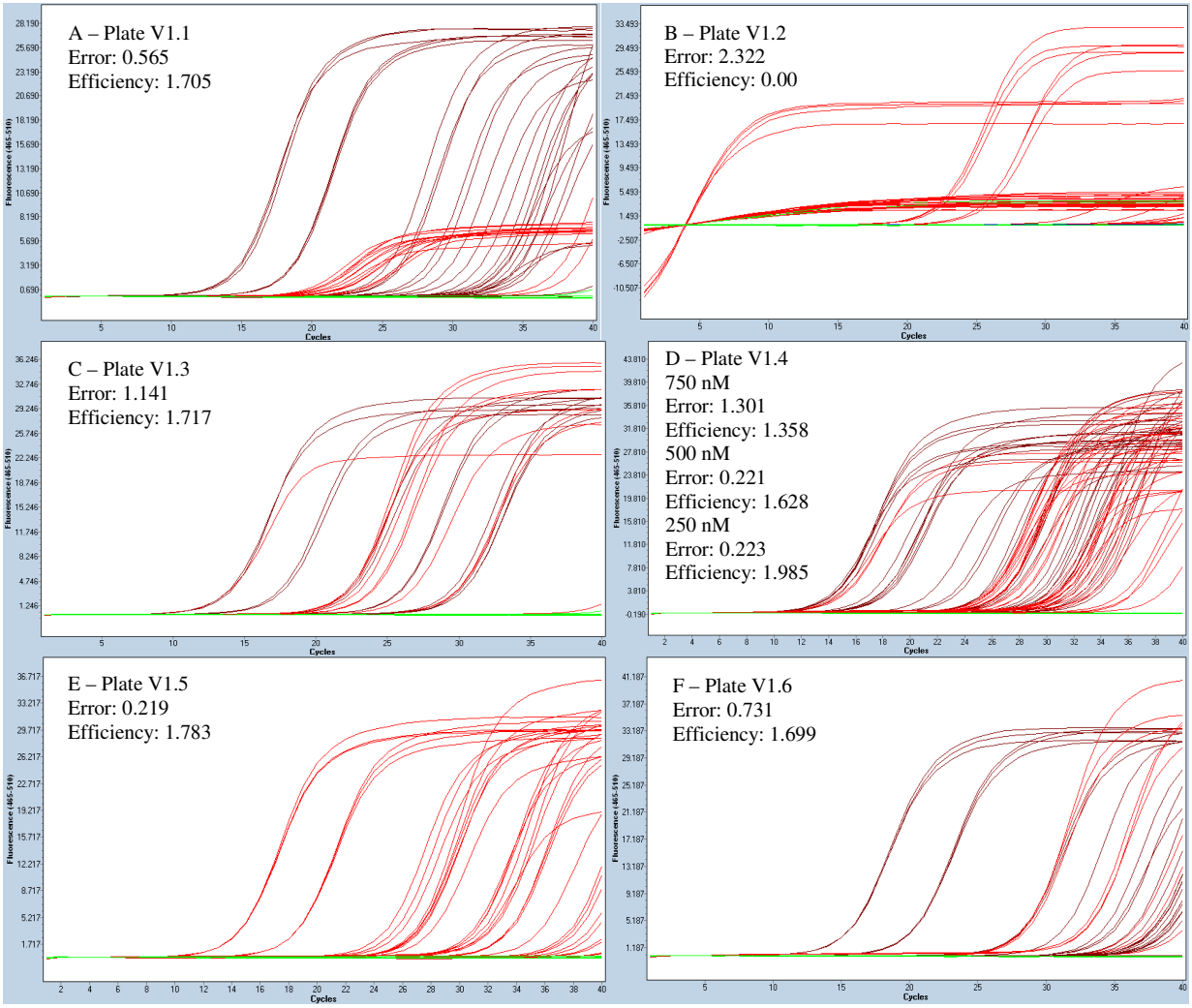

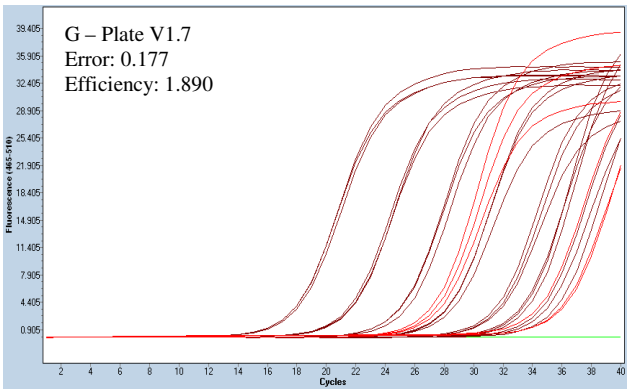

Figure 3.3.2.1: Roche LightCycler® 480 absolute quantitative derivative max amplification curve for each of the seven *L. crispatus* optimization plates (V1.1-V1.7). The fluorescence (465-510 nm) is indicated on the y-axis and the number of cycles is indicated on the x-axis. Red and brown indicate positive amplification in the unknown sample and the positive control standards respectively, and green indicates negative amplification in the wells.

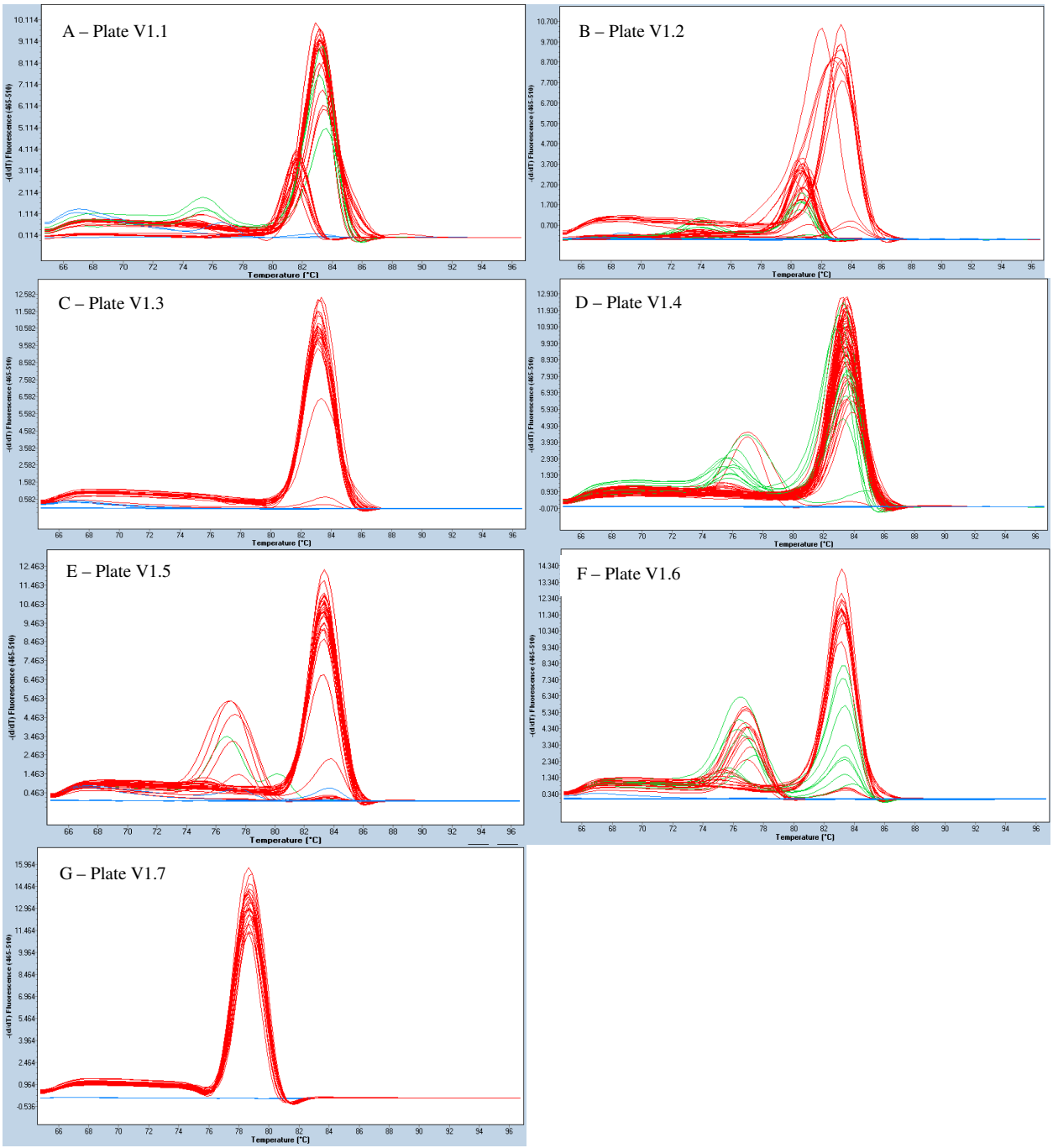

Figure 3.3.2.2: Roche LightCycler® 480 melt curve for each of the seven *L. crispatus* optimization plates (V1.1-V1.7). The –d/dT fluorescence (465-510 nm) is indicated on the y-axis and the temperature (℃) is indicated on the x-axis. Red indicates a single peak (product), green indicates two peaks and blue indicates no peak for each well.

A similar process was followed for *L. gasseri, L. jensenii* and *L. iners*. The first optimization plate for *L. gasseri, L. jensenii* and *L. iners* was run using the final reagent concentration and

volumes as those in the seventh plate of *L. crispatus* V1.7 as the lactobacilli species have very similar optimal qPCR conditions. Optimization for the other lactobacilli species required far less trouble-shooting. (See appendix C, qPCR Optimization).

3.3.3 *Gardnerella vaginalis*

In order for the qPCR conditions of *G. vaginalis* to be optimized, six different trial plates were run to get the best error and efficiency values. The first trial plate for *G. vaginalis* (V1.1) was run using the same reagent and DNA volumes and concentrations as used in the *L. crispatus* final trial plate (V1.7) with the following qPCR conditions; 95℃ for 15 min for the initial denaturation of the DNA followed by 50 cycles if 95℃ for 45 s, 55℃ for 45 s, and 65℃ for 45 s (Figure 3.3.3.1 A, Figure 3.3.3.2 A). The first six serial dilutions of the positive control amplified well, however the lower dilutions did not reach the same amplification and the replicates did not at consistent cycles. The second trial plate (V1.2) was run with a final extension temperature of 72℃ for 45 s in order to try improve primer specificity (Figure 3.3.3.1 B, Figure 3.3.3.2 B) with little improvement and high levels of primer dimerization, while the third trial plate (V1.3) was run using the same conditions as the previous trial plate (V1.2), but for 40 cycles in an attempt to accurately amplify the lower dilutions of the positive control DNA (Figure 3.3.3.1 C, Figure 3.3.3.2 C). Since tis did not seem sufficient, the fourth trial plate (V1.4) was run using the same conditions for 60 cycles (Figure 3.3.3.1 D, Figure 3.3.3.2 D). The increase in cycle number did not amplify the low dilutions of the positive control DNA to the same degree as the higher dilutions with an increase in primer dimers and thus the fifth trial plate (V1.5) was run using the same conditions as used in the first trial plate (V1.1), with a change in cycle conditions. The following qPCR conditions were followed, 95℃ for 15 min for the initial denaturation of the DNA followed by 50 cycles if 95℃ for 30 s, 60℃ for 1 min, and 72℃ for 45 s (Figure 3.3.3.1 E, Figure 3.3.3.2 E). This change improved the height of the amplification curves for the lower dilutions, but not the accuracy of replicate starting cycle number. The sixth trial plate (V1.6) served as a repeat for the fifth trial plate (V1.5) to confirm the error and efficiency values (Figure 3.3.3.1 F, Figure 3.3.3.2 F). The error and efficiency values were the most consistent and as close to the ideal conditions as possible with a decent standard curve.

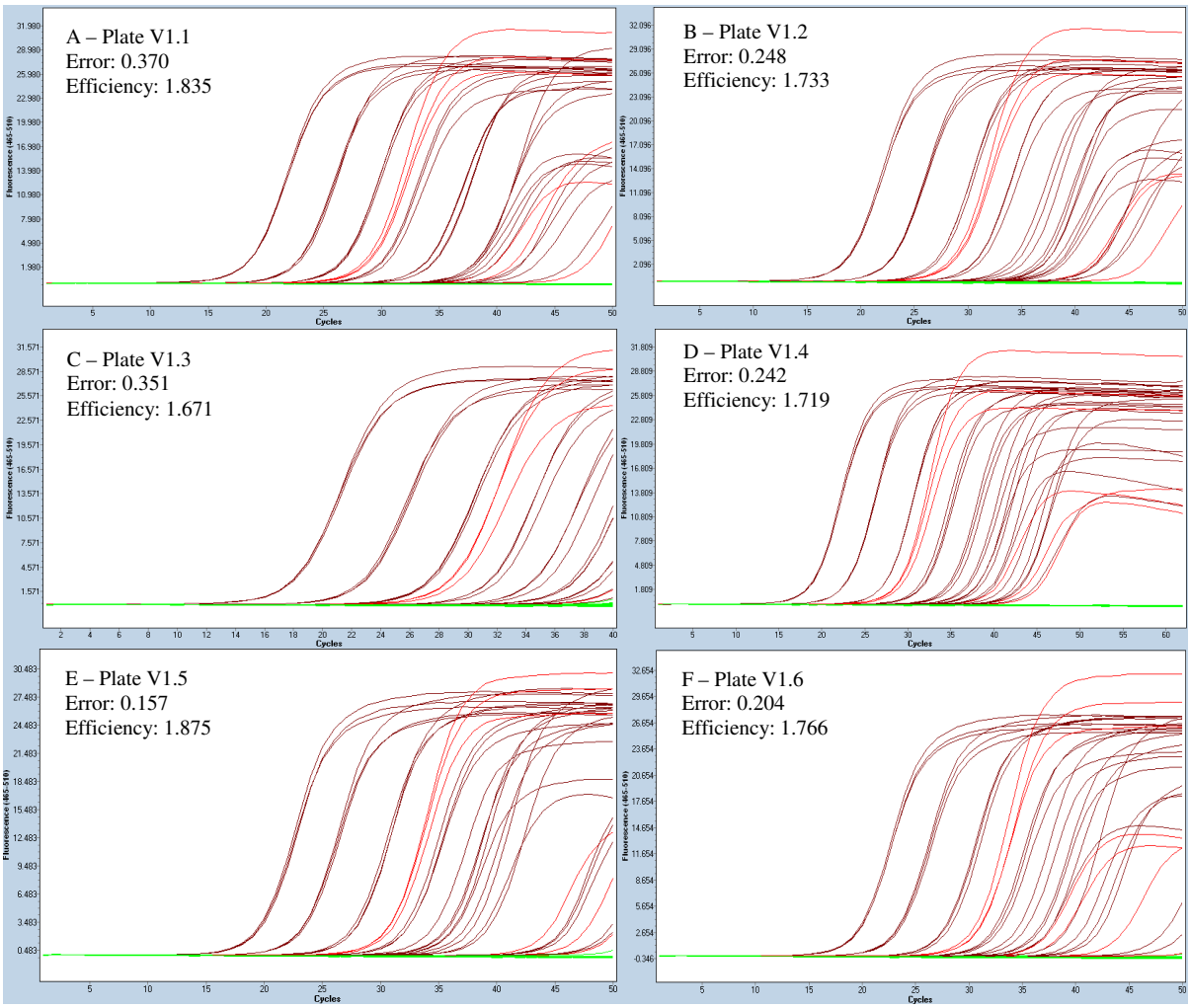

Figure 3.3.3.1: Roche LightCycler® 480 absolute quantitative derivative max amplification curve for each of the six *G. vaginalis* optimization plates (V1.1-V1.6). The fluorescence (465-510 nm) is indicated on the y-axis and the number of cycles is indicated on the x-axis. Red and brown indicate positive amplification in the unknown sample and the positive control standards respectively, and green indicates negative amplification in the wells.

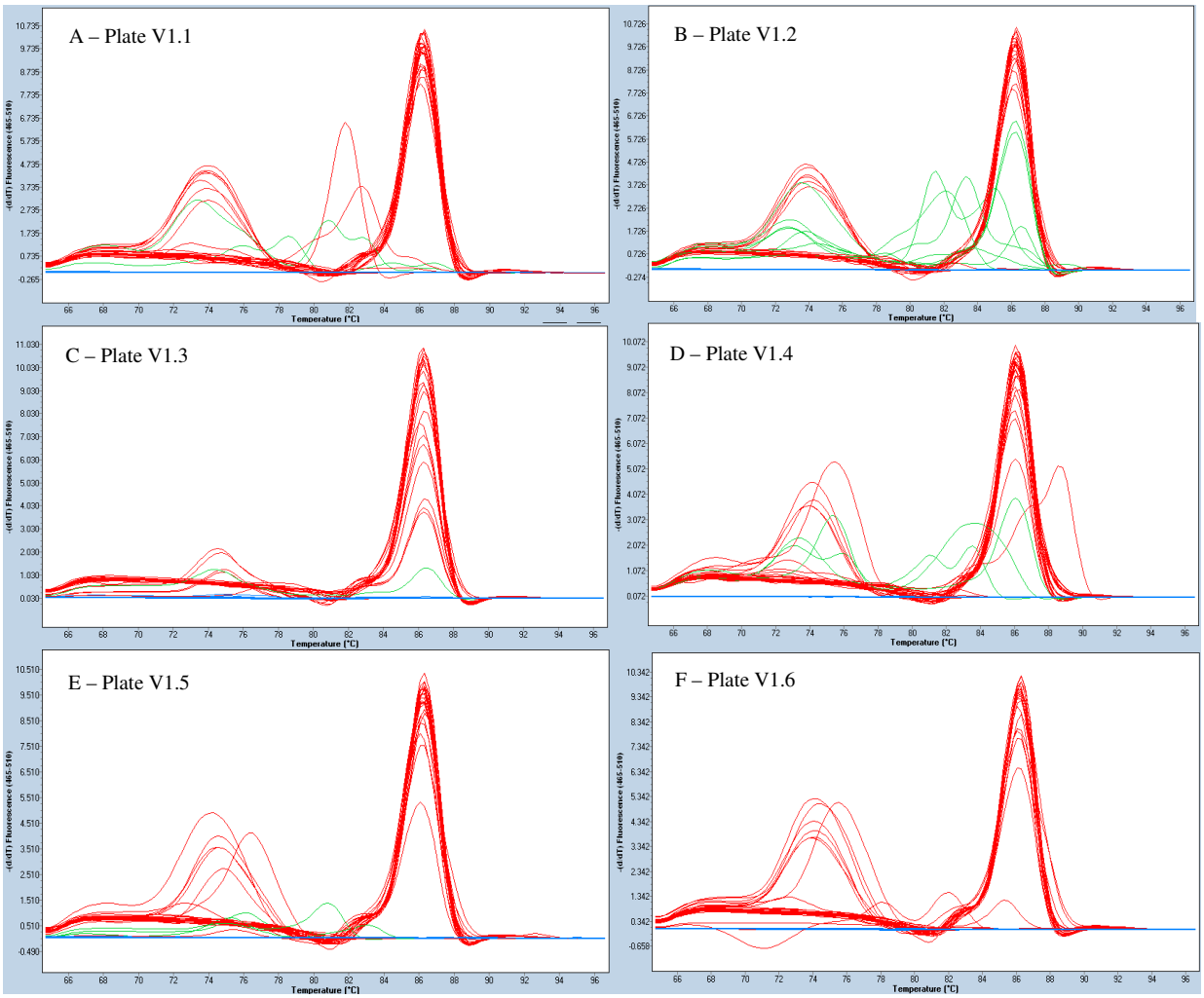

Figure 3.3.3.2: Roche LightCycler® 480 melt curve for each of the six *G. vaginalis* optimization plates (V1.1-V1.6). The –d/dT fluorescence (465-510 nm) is indicated on the y-axis and the temperature (℃) is indicated on the x-axis. Red indicates a single peak (product), green indicates two peaks and blue indicates no peak for each well.

3.3.4 *Prevotella bivia*

A total of thirteen trial plates were necessary to optimize the cycle conditions for *P. bivia*. The first trial plate for *P. bivia* (V1.1) was consistent with the other five bacterium in that it was run using the same reagent volumes and concentrations as the final trial plate for *L. crispatus* (V1.7) with the adjusted qPCR cycles conditions of 95℃ for 15 min as the initial denaturation of the DNA followed by 35 cycles of 95℃ for 20 s, 60℃ for 2 min and 74℃ for 5 min using the first set of primers F 5' GAACGATTTAGAGATAATGAGGTCC 3' and R 5'

CCCCAGTCCGAACTGAGAAT 3' (Figure 3.3.4.1 A, 3.3.4.2 A). The second trial plate (V1.2) was run using the different conditions of 95℃ for 15 min as the initial denaturation of the DNA followed by 50 cycles of 95℃ for 5 s, 60℃ for 20 s and 72℃ for 20 s in order to try improve the standard curve values (Figure 3.3.4.1 B, 3.3.4.2 B). This resulted in a lower error but unreliable efficiency as well as insufficient amplification of the positive control DNA. Since the improvement was minimal, the third trial plate (V1.3) was run the same as the second except the denaturation step was changed to 15 s, and we used a new set of primers (F5'GAACGATTTAGAGATAATGAGGTCC3' and R5'CCCCAGTCCGAACTGAGAAT3') to try improve amplification accuracy and a single melt curve product (Figure 3.3.4.1 C, 3.3.4.2 C). The same reagent volumes and concentrations were used in the fourth trial plate (V1.4) with □ew qPCR cycle co□ditio□s; 95℃ for 5 mi□, followed by 40 cycles of 95℃ for 30 s, 42℃ for 30 s and 72℃ for 30 s (Figure 3.3.4.1 D, 3.3.4.2 D). These conditions produced a high error reading and did not amplify the positive control DNA with a late starting cycle number. The fifth trial plate (V1.5) used the same conditions as V1.4 with were re-diluted positive controls from 10^6 copies/µL to 10^0 copies/µL to try improve the standard curve values and improve the starting cycle number (Figure 3.3.41 E, 3.3.4.2 E). A set of cycle conditions was used for the sixth trial plate (V1.6) where the initial denaturation was 95℃ for 5 min, followed by 50 cycles of 95℃ for 30 s, 60℃ for 30 s and 72℃ for 30 s (Figure 3.3.4.1 F, 3.3.4.2 F). Although the efficiency and error readings were good the positive control DNA was not amplifying concurrently below 10^5 copies/µL and had a high start cycle.

The seventh trial plate for *P. bivia* (V1.7) was run using the same conditions as V1.6; except for a change in the annealing temperature to 50℃ to try amplify the standard control DNA more consistently (Figure 3.3.4.1 G, 3.3.4.2 G). This shifted the standard curve readings and produced come primer dimers and separate peaks. The eight trial plate (V1.8) was a repeat of V1.7 with re-serially diluted standard controls from 10^9 copies/µL down to 10^0 copies/µL to try amplify the DNA at a lower C_P value than 25 cycles (Figure 3.3.4.1 H, 3.3.4.2 H). This positive control DNA did amplify more successfully, however the error reading showed a big increase. In the ninth trial plate (V1.9) the same qPCR conditions were followed as mentioned in V1.8, except the annealing temperature was 48℃ and the cycle number was changed to 60 (Figure 3.3.4.1 I, 3.3.4.2 I). The replicates of the positive control DNA serial dilutions did not amplify concurrently and the melt curve illustrated more than a single peak with primer dimers present.

The tenth trial plate (V1.10) was a repeat of V1.9 with the alteration of the annealing temperature to 46℃ (Figure 3.3.4.1 J, 3.3.4.2 J) which resulted in a slight improvement in replicate accuracy but not in the primer dimers and separate peaks within the melt curve. The eleventh trial plate (V1.11) is a further repeat of V1.9 with newly designed primers F 5' TGGGGATAAAGTGGGGAACG 3' and R 5' ACAACACGCTTACCAA 3' (Figure 3.3.4.1 K, 3.3.4.2 K). This lead to the positive control DNA serial dilutions amplifying closer to each other and the production of two distinct peaks in the melt curve. For the twelfth trial plate (V1.12) same qPCR conditions as V1.9 were used, with the change of the annealing temperature to 48℃, and two sets of serially diluted standard DNA were run. *P. bivia* was re-cultured, DNA extracted and serially diluted as well as the standards from 10^9 copies/µL were diluted down to 10^0 copies/ µL (Figure 3.3.4.1 L, 3.3.4.2 L), resulting in acceptable error and efficiency values and a single main melt curve peak with a lower abundance peak slightly shift. The thirteenth trial plate (V1.13) was a repeat of V1.12 with the serially diluted standard DNA run from 10^6 copies/µL to 10^0 copies/ µL (Figure 3.3.4.1 M, 3.3.4.2 M). This final plate had sufficient error and efficiency readings with neat positive control replicates.

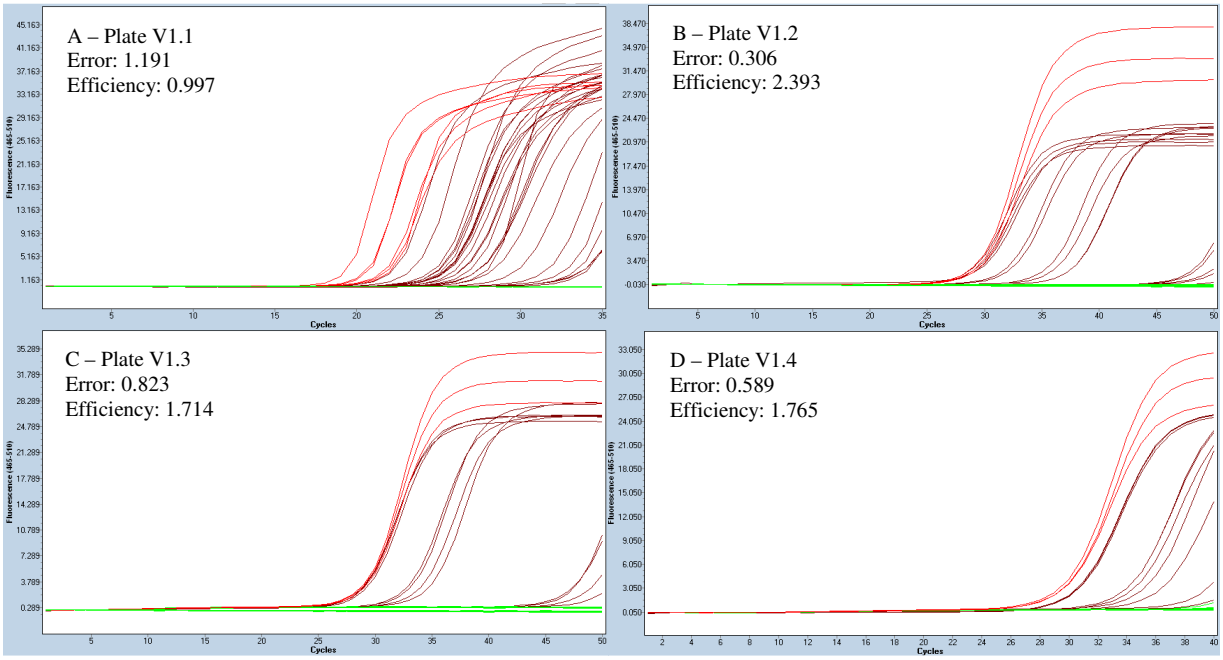

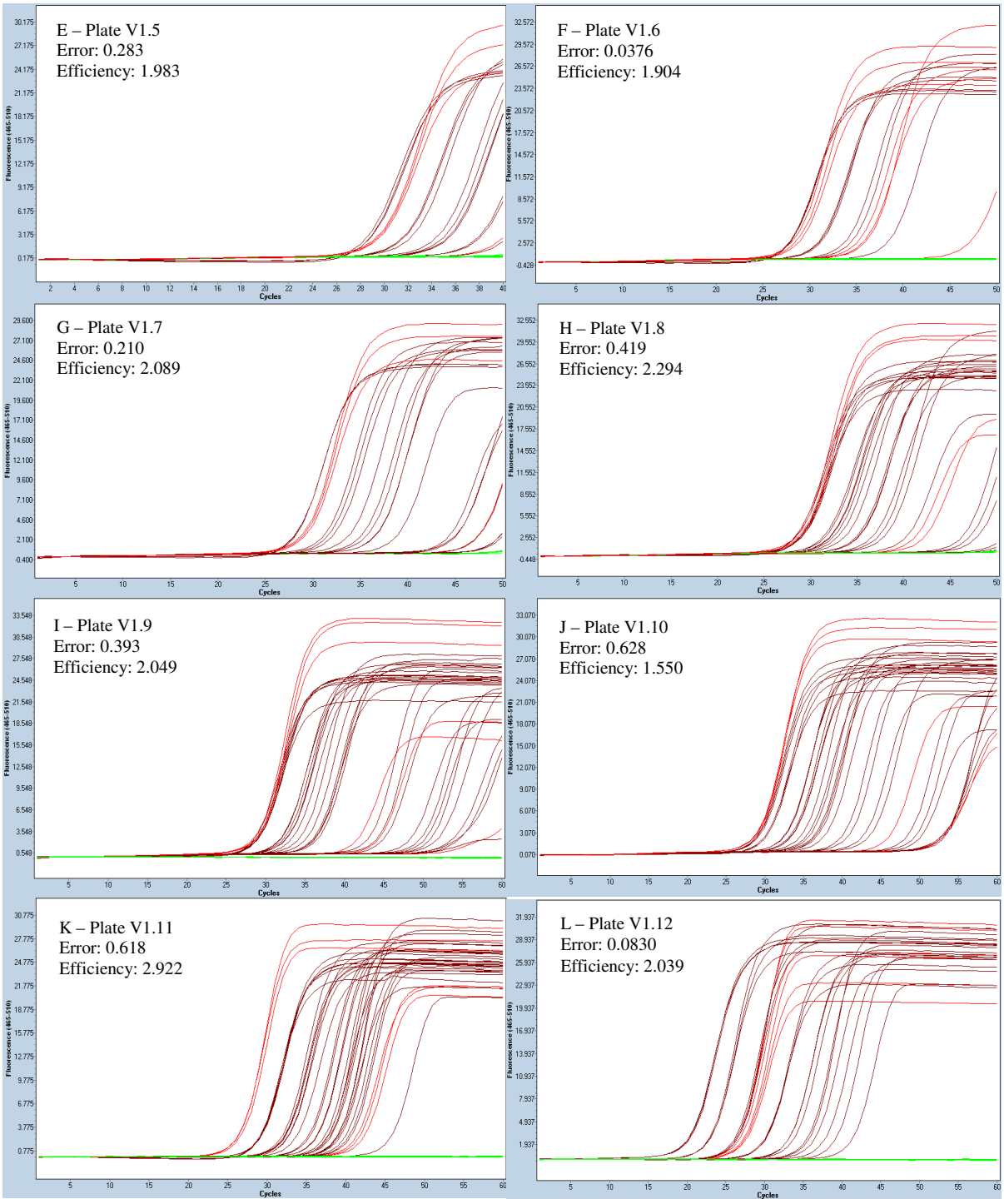
E – Plate V1.5
Error: 0.283
Efficiency: 1.983
F – Plate V1.6
Error: 0.0376
Efficiency: 1.904
G – Plate V1.7
Error: 0.210
Efficiency: 2.089
H – Plate V1.8
Error: 0.419
Efficiency: 2.294
I – Plate V1.9
Error: 0.393
Efficiency: 2.049
J – Plate V1.10
Error: 0.628
Efficiency: 1.550
K – Plate V1.11
Error: 0.618
Efficiency: 2.922
L – Plate V1.12
Error: 0.0830
Efficiency: 2.039
Cycles

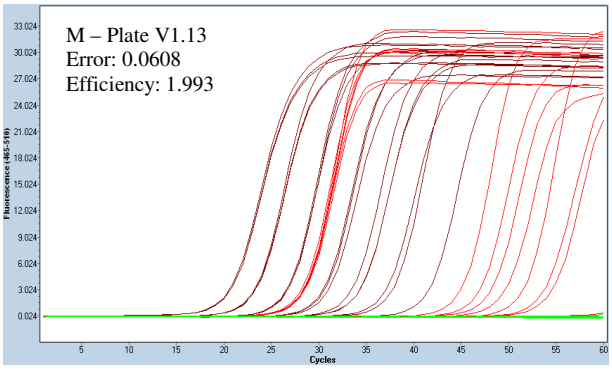

Figure 3.3.4.1: Roche LightCycler® 480 absolute quantitative derivative max amplification curve for each of the thirteen *P. bivia* optimization plates (V1.1-V1.13). The fluorescence (465-510 nm) is indicated on the y-axis and the number of cycles is indicated on the x-axis. Red and brown indicate positive amplification in the unknown sample and the positive control standards respectively, and green indicates negative amplification in the wells.

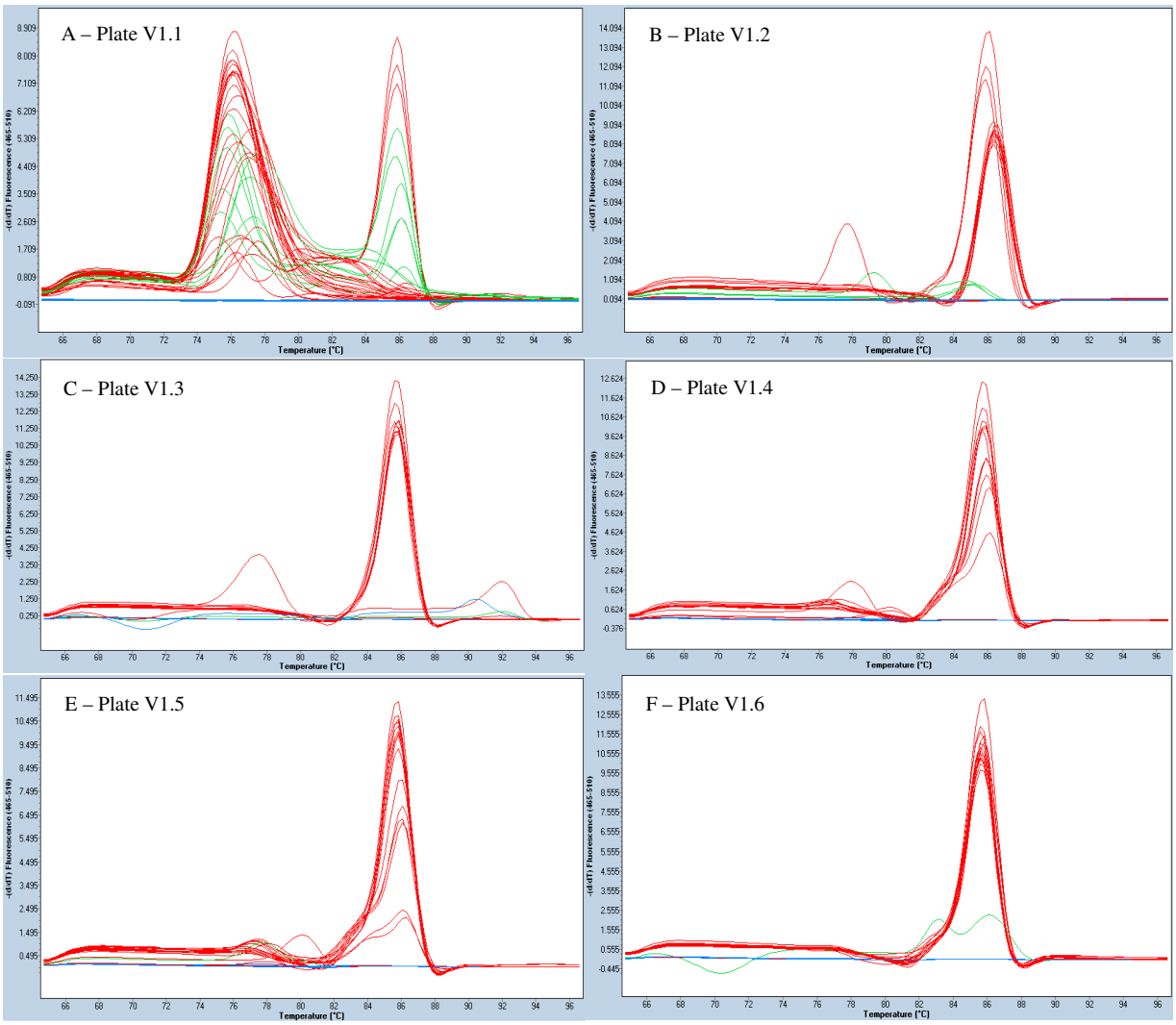

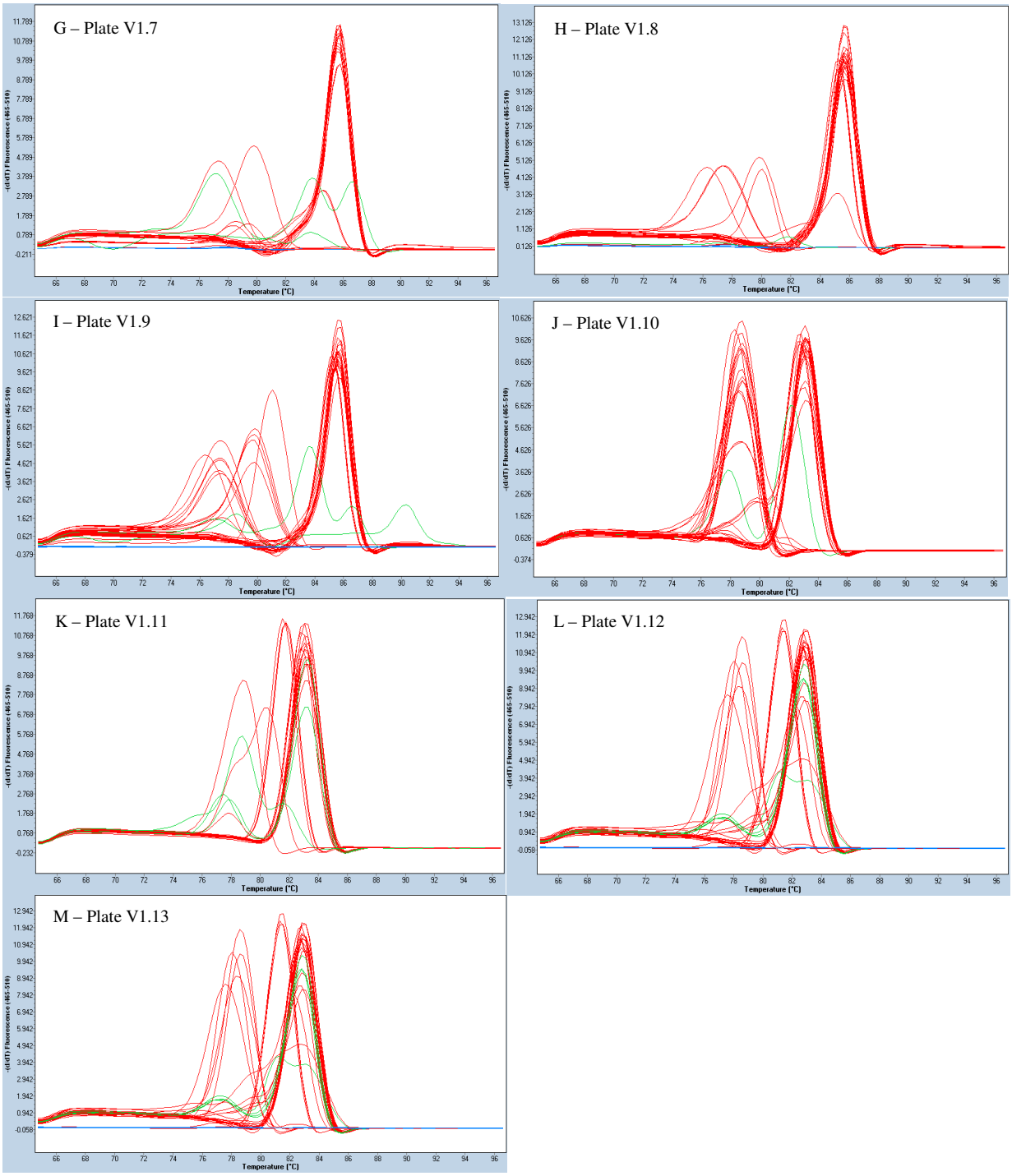

Figure 3.3.4.2: Roche LightCycler® 480 melt curve for each of the thirteen *P. bivia* optimization plates (V1.1-V1.13). The –d/dT fluorescence (465-510 nm) is indicated on the y-axis and the temperature (℃) is indicated on the x-axis. Red indicates a single peak (product), green indicates two peaks and blue indicates no peak for each well.

It should be noted that there were major limitations with the accurate amplification of *P. bivia* DNA due to the qPCR conditions coupled with inaccurate primers. The results were included in this thesis, however, they cannot be relied upon and further work and experiments will need to be run and optimized in future.

3.4 Real-Time PCR (qPCR) Protocol

Prior to PCR the laminar flow hood and pipettes were exposed to UV light to crosslink any contaminant DNA, and the master mix was kept away from any light and DNA. The qPCR master mix was prepared on ice in a 2 mL reaction tube by pipetting 10 µl of the LightCycler® 480 SYBR Green I Master Mix into each well of the LightCycler® 480 Multiwell Plate, along with the relative amounts of PCR-grade water, forward primer and reverse primer (Table 3.4.1). Reactions were mixed by aspiration.

Refer to Tables 3.1.3, 3.4.1 and 3.4.2 for qPCR conditions and primer sequences.

A 1 in 10 serial dilution of the gDNA isolated from each of the positive control reference ATCC strains was prepared, ranging from $1x10^6$ copies/µL to $1x10^0$ copies/µL. A volume of 9 µl nuclease free water for the negative control, 3 µL gDNA template standard for the positive control was added to the appropriate wells. The participant sample DNA was diluted to 0.5 ng/µL with TE Buffer, unless the DNA concentration was lower than 1 ng/µL, in which case samples were used as is. Once the master mix, positive standard control and sample DNA, and PCR-grade water had been added to the white multiwell plate, it was sealed with LightCycler® 480 Multiwell Sealing Foil. All non-template controls, positive controls and samples were run in triplicate. The Multiwell Plate was placed in the centrifuge and centrifuged at 2500 x g for 2 minutes.

After the Multiwell Plate has been spun down, the qPCR cycle is run using the Roche LightCycler® 480 based on the final conditions seen in Table 3.4.2, after optimization had been completed.

Table 3.4.1: qPCR mixture components.

Component	Final Concentration	1 reaction (µl)
Nuclease Free Water	-	6
2X Master Mix	1x	10
10 µM Forward Primer	0.25 µM	0.5
10 µM Reverse Primer	0.25 µM	0.5
Template DNA	0.075 ng/µL	3
Total	-	20

Table 3.4.2: qPCR Cycle Conditions after optimization.

Step	Cycles	Temperature (℃)	Time (sec)
Pre-incubation	1	95	5 min
Denaturation			
L. crispatus	45	95	15
L. gasseri	40	95	15
L. jensenni	40	95	15
L. iners	40	95	15
G. vaginalis	50	95	30
P. bivia	60	95	30
Primer Annealing			
L. crispatus		60	20
L. gasseri		57	60
L. jensenni		60	55
L. iners		60	55
G. vaginalis		60	60
P. bivia		48	30
Extension			
L. crispatus		72	10
L. gasseri		65	60

L. jensenni		72	60
L. iners		65	60
G. vaginalis		72	45
P. bivia		72	30
Acquire data		80	1
Melting Curve Analysis			
Denaturation	**1**	**95**	**5**
Re-Annealing		**65**	**1 min**
Melting		**97**	**0.11 ^{o}C/second**
Cooling	**1**	**40**	**30 sec**

3.5 Analysis

Triplicate values of the quantified unknown bacterial quantities (copies/µL) from the Roche LightCycler® 480 output were averaged to get a single value. Vaginal DNA samples that had one or two negative amplification readings in a triplicate, had primer dimers or showed separate peaks on the melt curve analysis (indicating more than a single product), were re-run in a qPCR through the Roche LightCycler II 480 ® to confirm the results (Table 3.5.1 and Table 3.5.2). All of the triplicate samples that were re-run were averaged again and incorporated into the results as replacement values. After the second set of qPCR, there were no further ambiguous results.

The below figure (Figure 3.5.1) illustrates an example of how the Non-Template Control, Positive reference dilutions and WISH vaginal DNA samples were set up on a 96 Multiwell plate.

	1	**2**	**3**	**4**	**5**	**6**	**7**	**8**	**9**	**10**	**11**	**12**
A	**NTC**	**NTC**	**NTC**	**10^6**	**10^6**	**10^6**	**10^5**	**10^5**	**10^5**	**10^4**	**10^4**	**10^4**
B	**10^3**	**10^3**	**10^3**	**10^2**	**10^2**	**10^2**	**10^1**	**10^1**	**10^1**	**10^0**	**10^0**	**10^0**
C	W002 V1	W002 V1	W002 V1	W004 V1	W004 V1	W004 V1	W006 V1	W006 V1	W006 V1	W007 V1	W007 V1	W007 V1
D	W008 V1	W008 V1	W008 V1	W009 V1	W009 V1	W009 V1	W010 V1	W010 V1	W010 V1	W011 V1	W011 V1	W011 V1

E	W012 V1	W012 V1	W012 V1	W013 V1	W013 V1	W013 V1	W015 V1	W015 V1	W015 V1	W016 V1	W016 V1	W016 V1
F	W017 V1	W017 V1	W017 V1	W021 V1	W021 V1	W021 V1	W022 V1	W022 V1	W022 V1	W023 V1	W023 V1	W023 V1
G	W024 V1	W024 V1	W024 V1	W025 V1	W025 V1	W025 V1	W026 V1	W026 V1	W026 V1	W027 V1	W027 V1	W027 V1
H	W028 V1	W028 V1	W028 V1	W030 V1	W030 V1	W030 V1	W031 V1	W031 V1	W031 V1	W032 V1	W032 V1	W032 V1

Figure 3.5.1: Example of a multi-well qPCR plate set out. Each non-template control (NTC), Standards diluted from 10^6 copies/µL down to 10^0 copies/µL and the WISH participant vaginal DNA are run in triplicate and the resulting value is the mean value of the three replicates.

The Roche LightCycler® quantified readings per bacteria were measured in copies/µL. The average for each triplicate was calculated, followed by the conversion to copies/ng. The WISH samples of a concentration higher than 0.5 ng/µL were standardized and diluted to 0.5 ng/µL, while any samples of a lower concentration than 1 ng/µL were used as is.

Copies/ng = copies/µL (Roche LightCycler reading) ÷ ng/µL (WISH participant reading)

= copies/µL x µL/ng

= copies/ng

For all statistical analyses, the raw values were used. For the bacterium that had zero quantified values, half the lowest value was taken for each to replace the zero values for figure representation (Table 3.4.1), after which the data was $\log_{10}$ transformed for analysis for comparison between bacterial species with contrasting median values (copies/ng). The lowest values for *L. iners* (copies/ng), *G. vaginalis* (copies/ng), and *P. bivia* (copies/ng) were above zero and thus were not altered.

Table 3.5.1 Illustration of the replacement of the zero values with the replacement of half the lowest positive quantified value (copies/ng) for each bacterium.

Quantified values (copies/ng)	*L. gasseri*	*L. jensenii*	*L. crispatus*
Positive lowest value	0.052	0.00116	0.000297334

Half positive lowest value	0.026	0.00058	0.000148667

*See table 3.6.2 for data transformation software.

The following comparisons were made in terms of the bacterial quantities (copies/ng) measured in each WISH participant sample and the following cohort characteristics: BV (positive, intermediate, negative); Inflammation (high, low); Age (16-18 years old, 19-22 years old); Hormonal contraceptive (DMPA, Implanon, Nur Isterate), and STI (none, any one), Bacterial (none, one two or more), Viral STI (none, one, two), HPV (none, low risk, high risk) (Table 3.6.2).

3.6 Statistical considerations

Three different statistical software programs were used to perform the data the data analyses as mentioned above in 3.5 Analysis.

3.6.1 Statistical software used for data analysis

Table 3.6.1: Statistical software used in this study.

Software	Objective
Roche LightCycler II 480 ®	Data acquisition
Microsoft Excel 2010	Data cleaning
STATA® Version 12 (for Windows StataCorp LP, College Station, TX77845, USA)	Inferential statistical analyses between the bacteria quantities, cytokines and level of inflammation
GraphPad Prism V5 (for Windows, GraphPad Software, San Diego California USA)	Comparison of bacterial quantities between BV groups, age groups and hormonal contraceptives

3.6.2 Statistical tests used for data analysis in this study

The software Microsoft Excel was used to calculate the triplicate average of the raw quantified data readings (copies/ng) for all participant samples as measured for each of the bacterium.

These average values were then used in all downstream analyses and the log-transformed data used to form figures.

The software STATA® V12 was used to perform a Shapiro-Wilk test to test if averaged triplicate data was normally distributed or not. The data was log transformed when not normally distributed (this was done to all the data as none of the data sets were normally distributed). STATA® V12 was used to perform Two-sample Wilcoxon rank-sum (Mann-Whitney) tests in order to compare the difference in bacterial quantities between the two group readings for each inflammation (low and high), and age (16-18 and 19-22 years). STATA® V12 was used to calculate the Spearman Rank correlation coefficient (rho) to determine if there was a correlation between bacterial quantities and the 47 immunological factors, as well as to calculate the Beta-coefficient Regression in order to determine if there was regression between bacterial quantity and cytokines.

The software GraphPad Prism V5 was used to calculate the paired, non-parametric Friedman's ANOVA statistical test to compare the distribution of bacterial quantities across each category group measured for the BV, hormonal contraceptive, bacterial and viral STI categories. GraphPad Prism V5 was used to calculate the unpaired, non-parametric Kruskal-Wallis ANOVA statistical test to compare the distribution of each bacterium across the three groups in the BV (positive, intermediate, negative), hormonal contraceptive (Implanon, DMPA, Nur Isterate), HPV (negative, low risk, high risk), bacterial (none, one, two or more) and viral STI (none, one, two) categories.

3.6.3 Conceptual Framework:

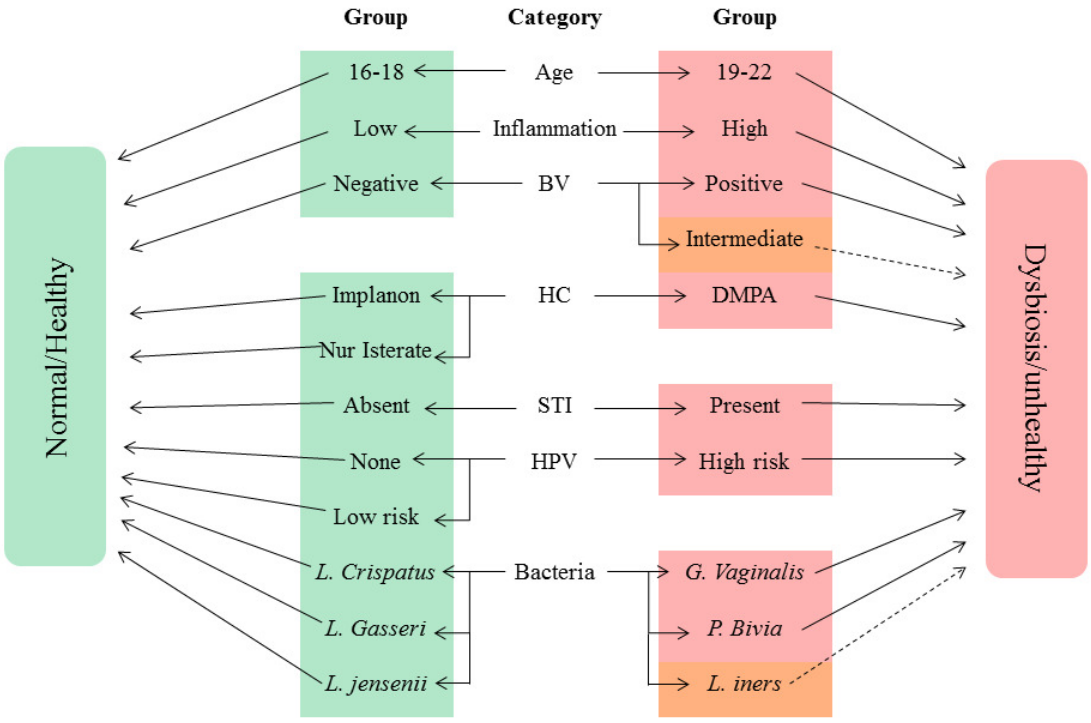

This framework has been established as a visual representation of the hypothesis studied in this thesis. As part of the first hypothesis, the green category groups on the left have been associated with a healthy/normal FGT microbiome, while the red/orange category groups have been associated with dysbiosis and an unhealthy FGT microbiome in the second hypothesis. The orange intermediate and *L. iners* groups have been associated with dysbiosis and an unhealthy FGT microbiome to a lesser degree than the other groups. These associations have been hypothesize through the knowledge provided by published literature articles.

3.7 Sequencing and Analysis

Full Service sequencing was performed by Inqaba Biotechnical Industries (Pty) Ltd. PO Box 14356, Hatfield 0028, Pretoria, South Africa (http://www.inqababiotec.co.za/).

The sequences were visualized and the reverse compliment sequences formed using SnapGene V3.2, GSL Biotech LLC (http://www.snapgene.com/).

The National Centre for Biotechnology Information (NCBI), U.S. National Library of Medicine, 8600 Rockville Pike, Bethesda MD, 20894 USA was used for two functions:

1. To Nucleotide BLAST (BLASTN) the sequences samples to determine what species they are most related to (percentage identity) (http://blast.ncbi.nlm.nih.gov/Blast.cgi?PAGE_TYPE=BlastSearch&BLAST_SPEC=MicrobialGenomes).
2. To retrieve the reference strains used for alignment using the Nucleotide search function through (http://www.ncbi.nlm.nih.gov/nucleotide).

The samples sequenced were aligned using the EMBOSS Needle Nucleotide program and the Primer BLAST program, run through European Molecular Biology Laboratory Bioinformatics Institute (EMBL-EBI), Wellcome Genome Campus, Hinxton, Cambridgeshire, CB10 1SD, UK (http://www.ebi.ac.uk/Tools/psa/emboss_needle/nucleotide.html).

Chapter 4: Results

This chapter serves as a summary of the optimization of the qPCR absolute quantification of the key species of interest namely; *L. crispatus, L. gasseri, L. jensenii, L. iners, G. vaginalis* and *P. bivia* and the subsequent results in relation to the BV status, inflammation levels, age, hormonal contraceptive and STI status, bacterial versus viral STIs and HPV. Due to the fact that not all samples had complete data, these results are based on varying samples sizes: n= 90 participants for HPV, n=140 participants for inflammation levels and STI status, n=136 participants for hormonal contraceptive, n=143 participants for BV, age, bacterial vs viral STIs and HPV adolescent female participants from the Masiphumelele Desmond Tutu Youth Centre, Masiphumelele.

The bacterium *P. bivia* could not accurately be identified at species level in this study. As such, the following section indicates the steps taken in order to analyze the results. The log transformed copies/ng readings for *P. bivia* have been included as a possible reference to the other bacterium; however, they should not be relied upon.

4.1 *P. bivia* Sequencing

The qPCR products that were formed run across the five qPCR multiwall plates using the final pair of *P. bivia* optimized primers showed increased levels of primer dimers and different products present within the melt curves. As such, a set of 7 samples in total were sent for sequencing with Inqaba Biotech in order to determine the cause of such high levels of variability. Three NTC controls, a standard positive control sample and three random samples were taken in a random selection of plates, rows, and replicate wells indicated by the number and letter combination, and version (V2.) in the sample names, respectively.

4.1.1 NCBI Blast Analysis

The first step was to perform a nucleotide NCBI BLASTN 2.5.0 using a representative genome reference sequence database for the forward and reverse compliment sequence for each sample to identify what species the primer products are most closely related to (Table 4.1.1).

Table 4.1.1: NCBI BLASTN results for the seven samples sequenced.

Sample	Sequence	Base Pairs	Number of BLASTN hits	Top two BLASTN hits	Percentage Identity (%)	Accession Number (NZ)
NTC A1 V2.0	Forward	499	NSSF	-	-	-
	Reverse Compliment	496	NSSF	-	-	-
NTC A3 V2.2	Forward	54	NSSF	-	-	-
	Reverse Compliment	36	NSSF	-	-	-
NTC A2 V2.4	Forward	156	NSSF	-	-	-
	Reverse Compliment	130	NSSF	-	-	-
10^5 A5 V2.1	Forward	147	188	*P. bivia* DSM 20514 Scfld 1	99	JH660658.1
				P. bivia DSM 20514 Scfld 3	99	JH660660.1
	Reverse Compliment	116	178	*P. bivia* DSM 20514 Scfld 1	100	JH660658.1
				P. bivia DSM 20514 Scfld 3	100	JH660660.1
W012 C8 V2.0	Forward	114	5	*P. bivia* DSM 20514 Scfld 3	100	JH660660.1
				P. bivia DSM 20514 Scfld 1	100	JH660658.1
	Reverse Compliment	427	4	*P. bivia* DSM 20514 Scfld 1	92	JH660658.1
				P. bivia DSM 20514 Scfld 3	92	JH660660.1
W125 E4 V2.3	Forward	428	12	*P. stercorea* DSM18206 Scfld41	100	Jh379355.1
				P. bivia DSM 20514 Scfld 1	100	JH660658.1
	Reverse Compliment	426	NSSF	-	-	-

W174 F11 V2.4	Forward	116	5	*P. bivia* DSM 20514 Scfld 3	94	JH660660.1
				P. bivia DSM 20514 Scfld 1	94	JH660658.1
	Reverse Compliment	412	4	*P. bivia* DSM 20514 Scfld 1	90	JH660658.1
				P. bivia DSM 20514 Scfld 3	90	JH660660.1

*Scfld – Scaffold, NSSF – No significant similarities found.

The presence of amplification peaks within the NTC of the qPCR multiwall plates indicated contamination. The contamination peaks amplified later between 40-50 cycles whereas the sample DNA amplified between 10-35 cycles on average. It can be tentatively said that there was no specific contaminating bacterial DNA amplifying within the NTC wells due to the peaks having no identity with any bacterial species with the NCBI BLASTN. Further, there are large differences in size (base pairs) between the three sets of forward and reverse compliment sequences amplified by the primers, illustrating a strong lack of specificity. This could indicate that the primer set designed was not accurate enough with non-specific products.

There was a common top hit of *P. bivia* strain DSM 20514 Scaffolds 1 and 3 as seen with the forward and reverse compliment sequence of the standard control sample 10^5 A5 V2.1 with 99% and 100% percent respectively. However, only three of the hits for the forward sequence had an alignment score above 200 with $\pm$ 120 base pairs (bp) while the rest of the hits were a combination of $\pm$ 100 bp and $\pm$ 120 bp with alignment scores between 80-200. The reverse compliment sequence differed in that the top two hits had a $\pm$ 120 bp alignment with a score above 200 while the rest were a combination of $\pm$ 120 and $\pm$ 90 bp with scores between 80 and 200. These alignments are unlikely since both the forward and reverse sequences are smaller than the primer product of 156 bp.

The forward sequence for ample W125 E4 V2.3 had 100% identity with two different Prevotella species, *P. stercorea* commonly associated with the human fecal microbiome (Hayashi et al. 2007), and *P. bivia* DSM 20514 Scaffold 1, similar to the standard control sample. However, only one alignment had a score above 200 with an alignment of $\pm$ 410 bp, far above the primer product size, with the rest of the alignments ranging from $\pm$ 40 bp to $\pm$ 230 bp with scores between 50-80 and 80-200. The forward and reverse compliment sequences were far larger than the expected primer product size. Both samples W012 C8 V2.0 and W174 F11 V2.4 had the

same top two hits of *P. bivia* DSM 20514 Scaffold 3 with a higher percentage identity for the forward sequences, 100% and 94% respectively, and *P. bivia* DSM 20514 Scaffold 1 for the reverse compliment sequences with 92% and 90% respectively. The two samples had smaller forward sequences with much larger reverse compliment sequences, with alignments between ± 40-55 bp long and scores of 50-80 and a single 80-200. The high percentage identity could be due to the small-aligned sequences.

These percentage identity differences between the different samples and the forward and reverse compliment sequences, as well the diverse set of alignment scores and sequence sizes (bp) further indicates the non-specificity of the *P. bivia* primers that were designed and further research should be done into more accurate and reliable species specific primers.

Description	Max score	Total score	Query cover	E value	Ident	Accession
Prevotella bivia DSM 20514 genomic scaffold Prebiscaffold_1, whole genome shotgun sequence	209	209	78%	2e-51	99%	NZ_JH660658.1
Prevotella bivia DSM 20514 genomic scaffold Prebiscaffold_3, whole genome shotgun sequence	209	623	78%	2e-51	99%	NZ_JH660660.1
Prevotella stercorea DSM 18206 genomic scaffold Scfld41, whole genome shotgun sequence	200	200	77%	1e-48	98%	NZ_JH379355.1
Prevotella oulorum F0390 genomic scaffold supercont1.2, whole genome shotgun sequence	183	183	77%	1e-43	96%	NZ_JH114216.1
Prevotella buccalis ATCC 35310 contig00150, whole genome shotgun sequence	182	182	76%	4e-43	96%	NZ_ADEG01000074.1
Prevotella saccharolytica JCM 17484 DNA, contig: JCM17484.contig00060, whole genome shotgun sequence	182	182	76%	4e-43	96%	NZ_BAKN01000060.1
Prevotella marshii DSM 16973 genomic scaffold SCAFFOLD2, whole genome shotgun sequence	182	182	76%	4e-43	96%	NZ_GL397215.1
Prevotella pallens ATCC 700821 genomic scaffold SCAFFOLD6, whole genome shotgun sequence	178	178	77%	5e-42	95%	NZ_GL982518.1
Prevotella dentalis DSM 3688 chromosome 2, complete sequence	178	178	77%	5e-42	95%	NC_019968.1
Prevotella dentalis DSM 3688 chromosome 1, complete sequence	178	713	77%	5e-42	95%	NC_019960.1
Prevotella copri DSM 18205 genomic scaffold Scfld4, whole genome shotgun sequence	178	496	77%	5e-42	95%	NZ_GG703856.1
Prevotella sp. S7-1-8 contig117, whole genome shotgun sequence	176	176	76%	2e-41	95%	NZ_JRNC01000117.1
Prevotella aurantiaca JCM 15754 DNA, contig: JCM15754.contig00105, whole genome shotgun sequence	176	176	74%	2e-41	95%	NZ_BAKF01000105.1
Prevotella micans F0438 genomic scaffold supercont1.4, whole genome shotgun sequence	176	176	76%	2e-41	95%	NZ_JH594524.1
Prevotella oralis ATCC 33269 genomic scaffold SCAFFOLD2, whole genome shotgun sequence	176	176	76%	2e-41	95%	NZ_GL833117.1
Prevotella oralis ATCC 33269 genomic scaffold SCAFFOLD1, whole genome shotgun sequence	176	176	76%	2e-41	95%	NZ_GL833116.1
Prevotella nigrescens ATCC 33563 genomic scaffold SCAFFOLD7, whole genome shotgun sequence	176	176	76%	2e-41	95%	NZ_GL982470.1
Prevotella bergensis DSM 17361 genomic scaffold SCAFFOLD6, whole genome shotgun sequence	176	176	76%	2e-41	95%	NZ_GG704785.1
Prevotella oris F0302 genomic scaffold Scfld3, whole genome shotgun sequence	176	176	76%	2e-41	95%	NZ_GG703886.1

Description	Max score	Total score	Query cover	E value	Ident	Accession
Prevotella bivia DSM 20514 genomic scaffold Prebiscaffold_1, whole genome shotgun sequence	207	207	96%	5e-51	100%	NZ_JH660658.1
Prevotella bivia DSM 20514 genomic scaffold Prebiscaffold_3, whole genome shotgun sequence	207	618	96%	5e-51	100%	NZ_JH660660.1
Prevotella saccharolytica JCM 17484 DNA, contig: JCM17484.contig00060, whole genome shotgun sequence	172	172	95%	2e-40	95%	NZ_BAKN01000060.1
Prevotella sp. S7 MS 2 contig097, whole genome shotgun sequence	167	167	95%	8e-39	94%	NZ_JRPT01000097.1
Prevotella oralis ATCC 33269 genomic scaffold SCAFFOLD2, whole genome shotgun sequence	167	167	95%	8e-39	94%	NZ_GL833117.1
Prevotella oralis ATCC 33269 genomic scaffold SCAFFOLD1, whole genome shotgun sequence	167	167	95%	8e-39	94%	NZ_GL833116.1
Prevotella scopos JCM 17725 DNA, contig: JCM17725.contig00095, whole genome shotgun sequence	163	163	96%	1e-37	93%	NZ_BAKP01000095.1
Prevotella melaninogenica ATCC 25845 chromosome II, complete sequence	163	163	96%	1e-37	93%	NC_014371.1
Prevotella melaninogenica ATCC 25845 chromosome I, complete sequence	163	490	96%	1e-37	93%	NC_014370.1
Prevotella multiformis DSM 16608 genomic scaffold SCAFFOLD8, whole genome shotgun sequence	161	161	95%	4e-37	93%	NZ_GL872289.1
Prevotella sp. 109 contig00071, whole genome shotgun sequence	161	161	95%	4e-37	93%	NZ_LFQU01000071.1
Prevotella denticola F0289, complete genome	161	647	95%	4e-37	93%	NC_015311.1
Prevotella ruminicola 23, complete genome	159	639	94%	1e-36	93%	NC_014033.1
Prevotella stercorea DSM 18206 genomic scaffold Scfld41, whole genome shotgun sequence	156	156	95%	2e-35	92%	NZ_JH379355.1
Prevotella dentalis DSM 3688 chromosome 2, complete sequence	156	156	95%	2e-35	92%	NC_019968.1
Prevotella dentalis DSM 3688 chromosome 1, complete sequence	156	624	95%	2e-35	92%	NC_019960.1
Prevotella oris F0302 genomic scaffold Scfld3, whole genome shotgun sequence	156	156	95%	2e-35	92%	NZ_GG703886.1
Prevotella sp. P4-76 contig42, whole genome shotgun sequence	154	154	97%	6e-35	91%	NZ_JXQI01000042.1
Prevotella sp. HUN102 P150DRAFT_scf7180000000013_quiver.3_C, whole genome shotgun sequence	150	150	95%	8e-34	91%	NZ_JIAF01000003.1

Figure 4.1.1.1: NCBI BLASTN hit results for the 147 bp forward (top) and 116 bp reverse compliment (bottom) sequences of the positive control sample 10^5 A5 V2.1

Description	Max score	Total score	Query cover	E value	Ident	Accession
Prevotella bivia DSM 20514 genomic scaffold Prebiscaffold_3, whole genome shotgun sequence	58.4	175	27%	5e-06	100%	NZ_JH660660.1
Prevotella bivia DSM 20514 genomic scaffold Prebiscaffold_1, whole genome shotgun sequence	58.4	58.4	27%	5e-06	100%	NZ_JH660658.1
Prevotella stercorea DSM 18206 genomic scaffold Scfld41, whole genome shotgun sequence	58.4	58.4	27%	5e-06	100%	NZ_JH379355.1

Description	Max score	Total score	Query cover	E value	Ident	Accession
Prevotella bivia DSM 20514 genomic scaffold Prebiscaffold_1, whole genome shotgun sequence	73.1	73.1	11%	8e-10	92%	NZ_JH660658.1
Prevotella bivia DSM 20514 genomic scaffold Prebiscaffold_3, whole genome shotgun sequence	73.1	219	11%	8e-10	92%	NZ_JH660660.1

Figure 4.1.1.2: NCBI BLASTN hit results for the 114 bp forward (top) and 427 bp reverse compliment (bottom) sequences for sample W012 C8 V2.0.

Description	Max score	Total score	Query cover	E value	Ident	Accession
Prevotella stercorea DSM 18206 genomic scaffold Scfld41, whole genome shotgun sequence	60.2	60.2	7%	6e-06	100%	NZ_JH379355.1
Prevotella bivia DSM 20514 genomic scaffold Prebiscaffold_1, whole genome shotgun sequence	60.2	60.2	7%	6e-06	100%	NZ_JH660658.1
Prevotella bivia DSM 20514 genomic scaffold Prebiscaffold_3, whole genome shotgun sequence	60.2	180	7%	6e-06	100%	NZ_JH660660.1
Rhodopseudomonas sp. B29 DNA, contig: IB029.C419, whole genome shotgun sequence	180	180	23%	5e-42	99%	NZ_BADD01000419.1
Alcanivorax hongdengensis A-11-3 contig94, whole genome shotgun sequence	171	171	34%	3e-39	87%	NZ_AMRJ01000089.1
Stenotrophomonas panacihumi strain JCM 16536 contig_136, whole genome shotgun sequence	159	159	32%	6e-36	87%	NZ_LLXU01000042.1
Alcanivorax hongdengensis A-11-3 contig71, whole genome shotgun sequence	285	778	96%	1e-73	79%	NZ_AMRJ01000070.1
Nocardia brevicatena NBRC 12119 DNA, contig: NB2_con135, whole genome shotgun sequence	196	196	51%	5e-47	83%	NZ_BAFU01000135.1

Figure 4.1.1.3: NCBI BLASTN hit results for the 428 bp forward sequences for sample W125 E4 V2.3.

Description	Max score	Total score	Query cover	E value	Ident	Accession
Prevotella bivia DSM 20514 genomic scaffold Prebiscaffold_3, whole genome shotgun sequence	73.1	219	40%	2e-10	94%	NZ_JH660660.1
Prevotella bivia DSM 20514 genomic scaffold Prebiscaffold_1, whole genome shotgun sequence	73.1	73.1	40%	2e-10	94%	NZ_JH660658.1
Prevotella stercorea DSM 18206 genomic scaffold Scfld41, whole genome shotgun sequence	73.1	73.1	40%	2e-10	94%	NZ_JH379355.1

Description	Max score	Total score	Query cover	E value	Ident	Accession
Prevotella bivia DSM 20514 genomic scaffold Prebiscaffold_1, whole genome shotgun sequence	82.4	82.4	14%	1e-12	90%	NZ_JH660658.1
Prevotella bivia DSM 20514 genomic scaffold Prebiscaffold_3, whole genome shotgun sequence	82.4	243	14%	1e-12	90%	NZ_JH660660.1

Figure 4.1.1.4: NCBI BLASTN hit results for the 116 bp forward (top) and 412 bp reverse compliment (bottom) sequences for sample W174 F11 V2.4.

Since the NTC samples did not identify with any species, no figures have been illustrated for the negative BLASTN hit results. The positive control sample 10^5 A5 V2.1 had the most diverse set of results due to such a high number of BLASTN hits, with the forward and reverse compliment sequences indicating identity with *P. bivia* as well as *P. stercorea, P. oulorum, P. buccalis, P. saccharolytica, P. marshi, P. pallens, P. dentalis, P. copro, P. oralis, P. scopos, P. melaninogenica, P. multiformis, P. denticola,* and *P. ruminicola* to name a few, with the majority being associated with the oral, gut and faecal human microbiomes (Faust et al. 2012; Filippo et al. 2010; Gupta et al. 2015; Hayashi et al. 2007; Kolenbrander et al. 2002; Scher et al. 2013; Wu et al. 2011). A single BLASTN hit was associated with the vaginal microbiome; Prevotella sp. S7 MS 2 contig097, since it has not been identified to species level no specificity is possible

(Figure 4.1.1.1). Both the forward and reverse compliment sequences for sample W012 C9 V2.0 showed high percentage identification with *P. bivia* DSM 20514 Scaffold 3 and *P. bivia* DSM 20514 Scaffold 1, with the forward sequence showing 100% identification with *P. stercorea* DSM 18206 Scaffold41(Figure 4.1.1.2) indicating possible higher levels of specificity for the sequences with *P. bivia*. Sample W125 E4 V2.3 has an increased number of BLASTN hits for the forward sequence versus the reverse compliment sequence, which had no significant similarities with any species. The forward sequence showed 100% identity with *P. stercorea* Scaffold41, *P. bivia* DSM 20514 Scaffold 1 and 3, as well as a combination of Rhodospeudomonas sp. B29, *Alcanivorax hongdengensis* A-11-13 contigs 94 and 71, *Stenotrophomonas panacihumi,* and *Nocardia brevicatena* identifying from 99% to 83% (Figure 4.1.1.3). The last sample that was sequenced showed similar results with similar percentage identities for the forward and reverse compliment sequences with the forward sequence showing 94% identity with *P. bivia* DSM 20514 Scaffold 1 and 3 and *P. stercorea* Scaffold41, while the reverse compliment sequence showed 90% for *P. bivia* DSM 20514 Scaffold 1 and 3 (Figure 4.1.1.4).

4.1.2 Sequence Alignment

The forward and reverse compliment sequences for each sample were then aligned to the ATCC *P. bivia* reference strain DNF00188 contig005 sequence (NCBI NZ_JRNF01000005.1) (Table 4.1.2.1) and the NCBI Primer BLAST Hit *P. bivia* strain DSM 20514 genomic scaffold Prebiscaffold_1, whole genome shotgun sequence (NCBI NZ_JH660658.1) (Table 4.1.2.2) for comparison using the EMBOSS Needle nucleotide alignment search tool with a gap penalty of 10.0 and an extension penalty of 0.5.

Table 4.1.2.1: Emboss Needle nucleotide alignment results using the ATCC *P. bivia* reference strain DNF00188 (138593 bp).

Sample	Sequence	Identity (%)	Similarity (%)	Gaps (%)	Score	Alignment (bp)
NTC A1 V2.0	Forward	336 (0.2)	348 (0.3)	138171 (99.7)	580	5301-6123
	Reverse	340* (0.2)	352 (0.3)	138188	577.5	6401-7316

	Compliment			(99.7)		
NTC A3 V2.2	Forward	34 (0.0)	42 (0.0)	138466 (100)	98.0	68151-68298
	Reverse Compliment	27* (0.0)	29* (0.0)	138486 (100)	71.5	32701-32797
NTC A2 V2.4	Forward	118 (0.1)	120 (0.1)	1383670 (99.9)	211.0*	126051-126345
	Reverse Compliment	98 (0.1)	101 (0.1)	138416 (99.9)	191.5	73051-73335
10^5 A5 V2.1	Forward	90 (0.1)	97 (0.1)	138421 (99.9)	165.5	34301-34574
	Reverse Compliment	82 (0.1)	82 (0.1)	138424 (9909)	171.5	77501-77738
W012 C8 V2.0	Forward	80 (0.1)	80 (0.1)	138532 (99.9)	171.5	112251-112484
	Reverse Compliment	284 (0.2)	301 (0.2)	138195 (99.7)	466.5	54851-55547
W125 E4 V2.3	Forward	312 (0.2)	319 (0.2)	138142 (99.7)	514.0	135201-136023
	Reverse Compliment	291 (0.2)	313 (0.2)	1381674 (99.7)	450.5	75101-75958
W174 F11 V2.4	Forward	76 (0.1)	78 (0.1)	1384150 (99.9)	185.5	72301-72475
	Reverse Compliment	268 (0.2)	274 (0.2)	138232 (99.7)	477.5	114851-115436

* Values that are the concurrent as the alignment in Table 4.1.2.2.

Table 4.1.2.2: Emboss Needle nucleotide alignment results using the NCBI Primer BLAST Hit *P. bivia* strain DSM 20514 (139516 bp).

Sample	Sequence	Identity (%)	Similarity (%)	Gaps (%)	Score	Alignment (bp)
NTC A1 V2.0	Forward	348 (0.2)	366 (0.3)	139067 (99.7)	580.5	119051-119940
	Reverse Compliment	340* (0.2)	353 (0.3)	139090 (99.7)	566.5	126651-127480
NTC A3 V2.2	Forward	37 (0.0)	47 (0.0)	139392 (100)	84	13301-13500
	Reverse Compliment	27* (0.0)	29 (0.0)	139412 (100)	72.5	134301-134449

NTC A2 V2.4	Forward	114 (0.1)	117 (0.1)	139326 (99.9)	221.0*	85701-85982
	Reverse Compliment	102 (0.1)	105 (0.1)	139324 (99.9)	202.5	44351-44646
10^5 A5 V2.1	Forward	124 (0.1)	125 (0.1)	139341 (99.9)	554.0	44351-44579
	Reverse Compliment	114 (0.1)	114 (0.1)	139330 (99.9)	552.0	44351-44500
W012 C8 V2.0	Forward	81 (0.1)	85 (0.1)	139364 (99.9)	223.0	44401-44534
	Reverse Compliment	283 (0.2)	300 (0.2)	139115 (99.7)	579.5	43851-44502
W125 E4 V2.3	Forward	309 (0.2)	314 (0.2)	139092 (99.7)	523.5	72601-73363
	Reverse Compliment	282 (0.2)	307 (0.2)	139128 (99.7)	483.0	43701-44496
W174 F11 V2.4	Forward	89 (0.1)	95 (0.1)	139340 (99.9)	331.5	44401-44545
	Reverse Compliment	299 (0.2)	306 (0.2)	139124 (99.7)	622.5	43751-44505

* Values that are the concurrent as the alignment in Table 4.1.2.1.

From the above tables 4.1.2.1 and 4.1.2.2 it can be seen that the two reference strains are similar in size (bp) which correlates to the same identity, similarity and gap percentages for the forward and reverse compliment sequences for the seven samples. This occurrence is mostly due to the fact that the alignment sequences are far larger than the sample sequences and if a portion of the alignment sequences could be use the percentages may identify some differences. Since the sample sequences aligned to different portions of the alignment sequences, it was not possible to focus on a specific section and whole sequences were used. The identity and similarity percentages are so low due to such a large difference in size between the sequenced samples and the reference strains. The reverse compliment sequences for the samples NTC A1 V2.0 and NTC A3 V2.2 have the same identity across the reference strains with the NTC A3 V2.2 showing the same similarity as well. The forward sequence for sample NTC A2 V2.4 has the same score in both sequence alignments. The position of the aligned sequences appears to be different for each sample, as well as between the forward and reverse compliment sequences. Further discrepancies include the different sizes of the overlapping sequences with none being the expected 256 bp.

The alignment score for each sequence indicates the quality of the samples sequences against the alignment strains, with a higher score indicating a stronger alignment. The forward and reverse compliment sequences for samples NTC A1 V2.0, NTC A3 V2.2 and NTC A2 V2.4 show similar score results, which is to be expected as they do not correlate with any species specifically. The largest difference can be seen with the positive control sample 10^5 A5 V2.1 which has scores of 165.5 and 171.5 aligned with *P. bivia* reference strain NDF00188 versus 554.0 and 552.0 with NCBI Primer Blast Hit *P.* bivia strain DSM 20514 for the forward and reverse compliment sequences respectively (Figure 4.1.2.1). The scores for the sample sequences could be skewed based on the distinct difference in size (bp) between the alignment strains and the sample sequences.

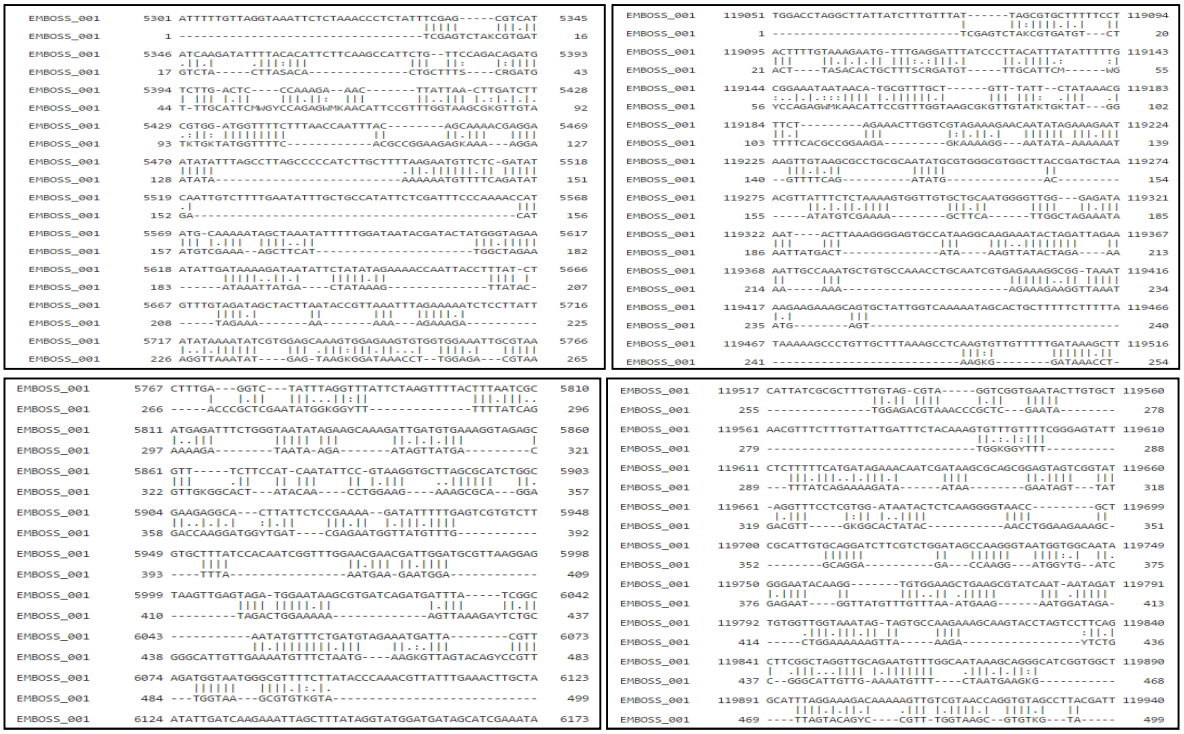

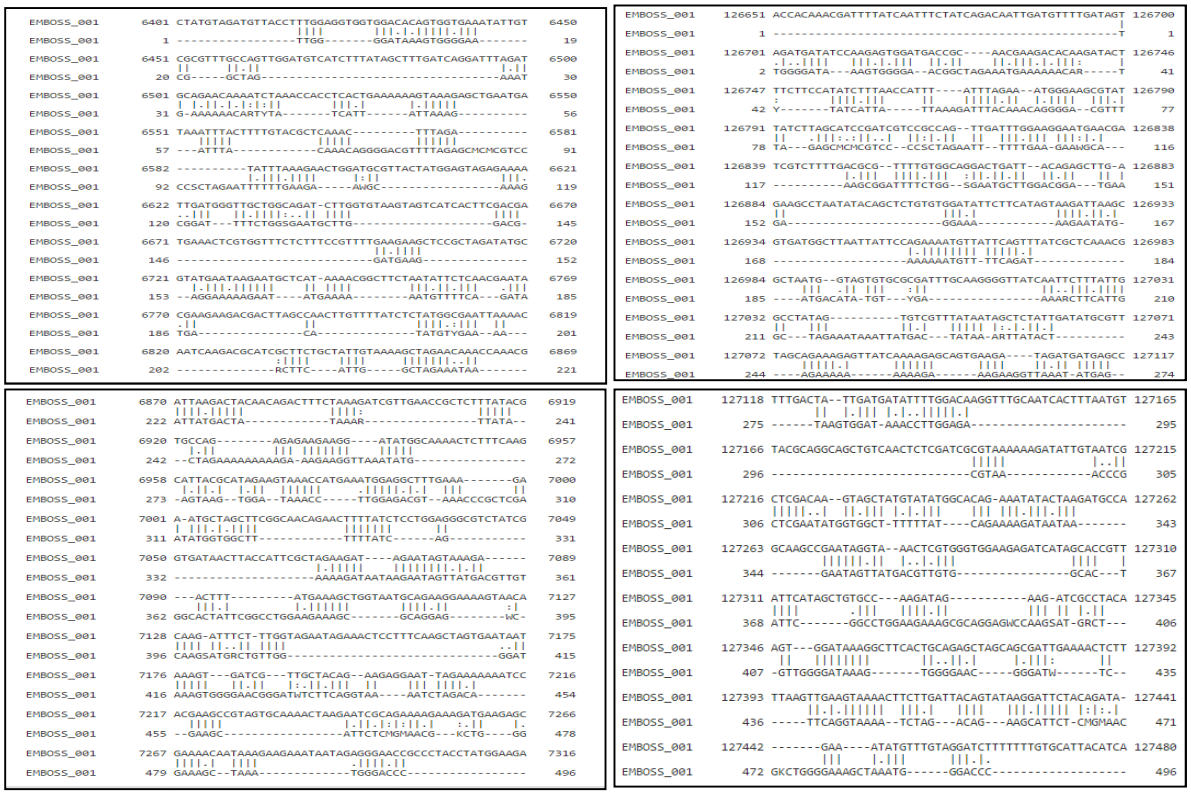

Figure 4.1.2.1: Comparison of the forward (top __ and …) and reverse compliment (bottom _ _ and __) sequence alignments for sample NTC A1 V2.0 against the ATCC *P. bivia* reference strain DNF00188 (left) and the NCBI Primer BLAST Hit *P. bivia* strain DSM 20514 (right).

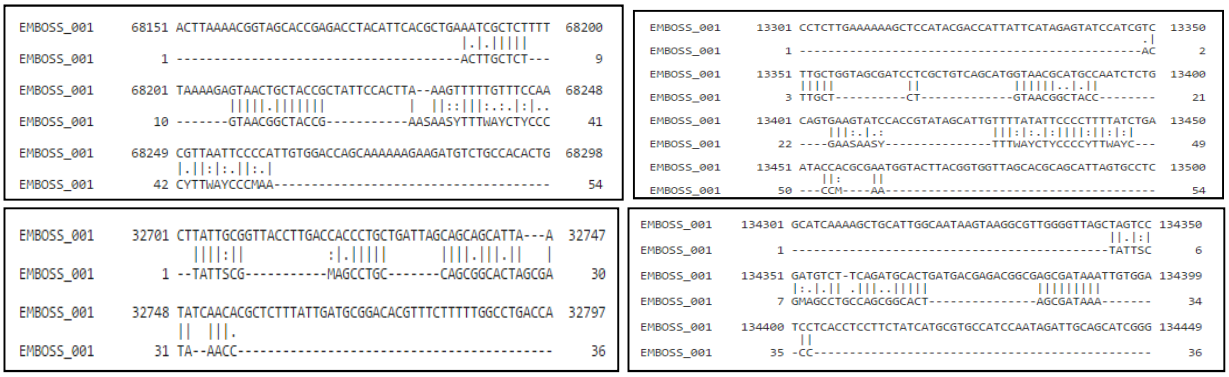

Figure 4.1.2.2: Comparison of the forward (top __ and …) and reverse compliment (bottom _ _ and __) sequence alignments for sample NTC A3 V2.2 against the ATCC *P. bivia* reference strain DNF00188 (left) and the NCBI Primer BLAST Hit *P. bivia* strain DSM 20514 (right).

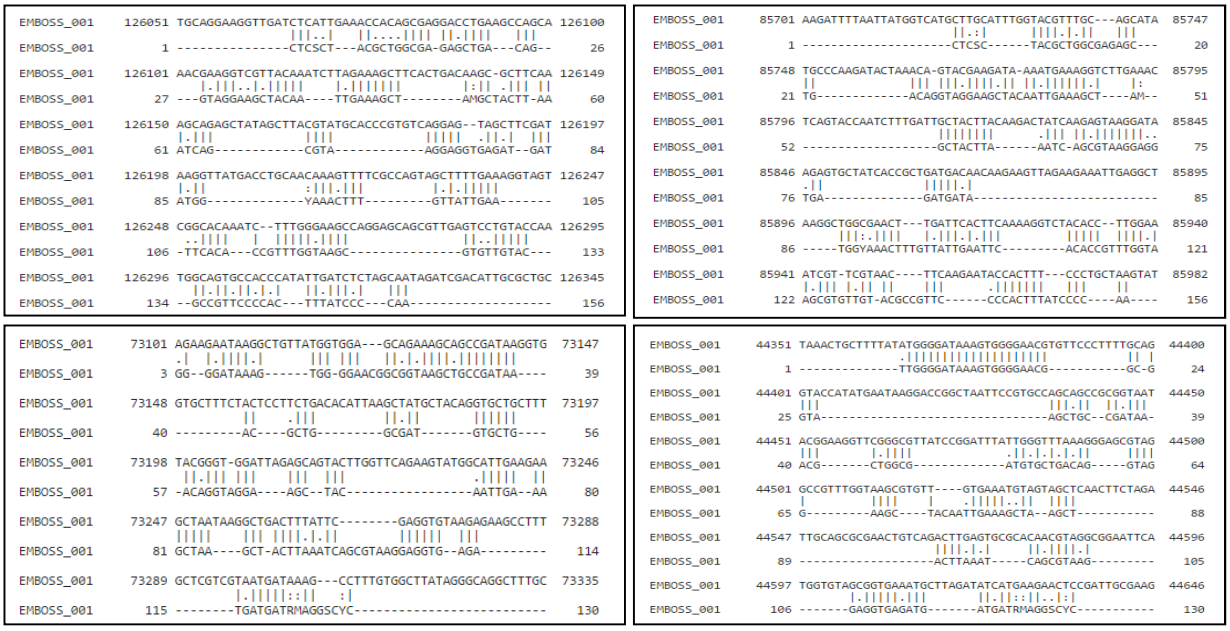

Figure 4.1.2.3: Comparison of the forward (top __ and …) and reverse compliment (bottom _ _ and __) sequence alignments for sample NTC A2 V2.4 against the ATCC *P. bivia* reference strain DNF00188 (left) and the NCBI Primer BLAST Hit *P. bivia* strain DSM 20514 (right).

The NTC samples sequences aligned against *P. bivia* reference strain NDF00188 and NCBI Primer Blast Hit *P.* bivia strain DSM 20514 show poor alignment for both the forward and reverse compliment sequences as seen for NTC A1 V2.0 (Figure 4.2.2.1), NTC A3 V2.2 (Figure 4.2.2.2) and NTC A2 V2.4 (Figure 4.2.2.3) where there are very little solid alignment stretches against the alignment sequences regardless of the length and direction.

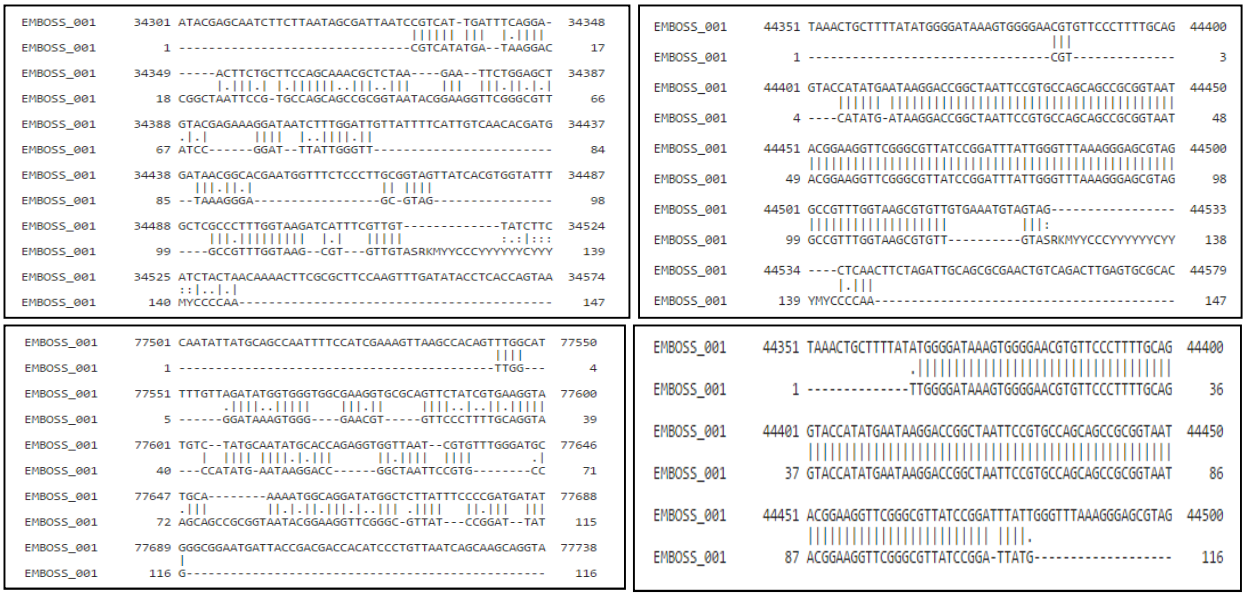

Figure 4.1.2.4: Comparison of the forward (top __ and …) and reverse compliment (bottom _ _ and __) sequence alignments for the positive standard control 10^5 copies/ng A5 V2.1 against the ATCC *P. bivia* reference strain DNF00188 (left) and the NCBI Primer BLAST Hit *P. bivia* strain DSM 20514 (right).

When the forward and reverse compliment positive standard control 10^5 copies/ng sequences were aligned against the *P. bivia* reference strain NDF00188 and NCBI Primer Blast Hit *P.* bivia strain DSM 20514, the forward and reverse compliment sequences had the same identity, similarity and gap percentages, based on different sequence lengths and alignments. The differences came through in the number of gaps in relation to the two alignment strains lengths (bp) and the position that the forward and reverse compliment sequences aligned. The forward sequence aligned between base pairs 34 301 and 34 574 of the *P. bivia* reference strain NDF00188 and aligned between base pairs 44 351 and 44 579 of the NCBI Primer Blast Hit *P.* bivia strain DSM 20514, while the reverse compliment aligned between 77 501 - 77 738 base pairs and 44 351 – 44 500 base pairs, respectively. From Figure 4.1.2.4 it can be quite clearly seen that both the forward and reverse compliment sequences of the positive standard control 10^5 copies/ng aligned better to the NCBI Primer Blast Hit *P.* bivia strain DSM 20514, which is further emphasized by alignment scores of 554.0 and 552.0 respectively, as well as a product size of 149 bp, similar to the expected size of 156 bp. In contrast, the forward and reverse compliment sequences had reasonably smaller alignment scores of 165.5 and 171.5 respectively, as illustrated by the poor alignment in Figure 4.1.2.4.

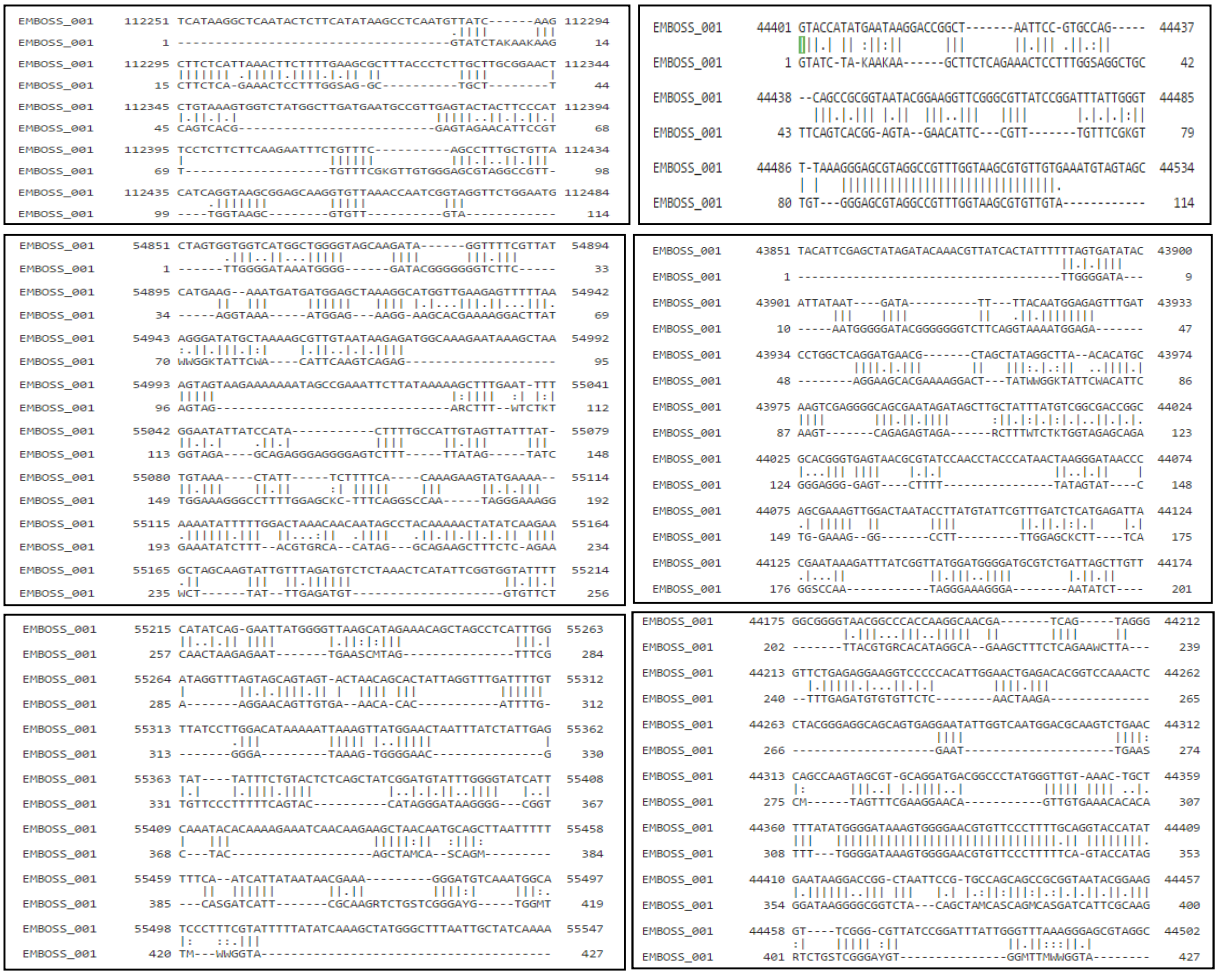

Figure 4.1.2.5: Comparison of the forward (top __ and …) and reverse compliment (bottom _ _ and __) sequence alignments for W012 C8 V2.0 against the ATCC *P. bivia* reference strain DNF00188 (left) and the NCBI Primer BLAST Hit *P. bivia* strain DSM 20514 (right).

The forward and the reverse compliment sequence of W012 C8 V2.0 when aligned against NCBI Primer BLAST Hit *P. bivia* strain DSM 20514 show improved alignment in comparison to when the sequences are aligned against ATCC *P. bivia* reference strain DNF00188 (Figure 4.1.2.5) with larger stretches of concurrent base pair alignments. Despite the increased length of the reverse compliment sequence, the alignment quality does not improve in comparison to the shorter forward sequence.

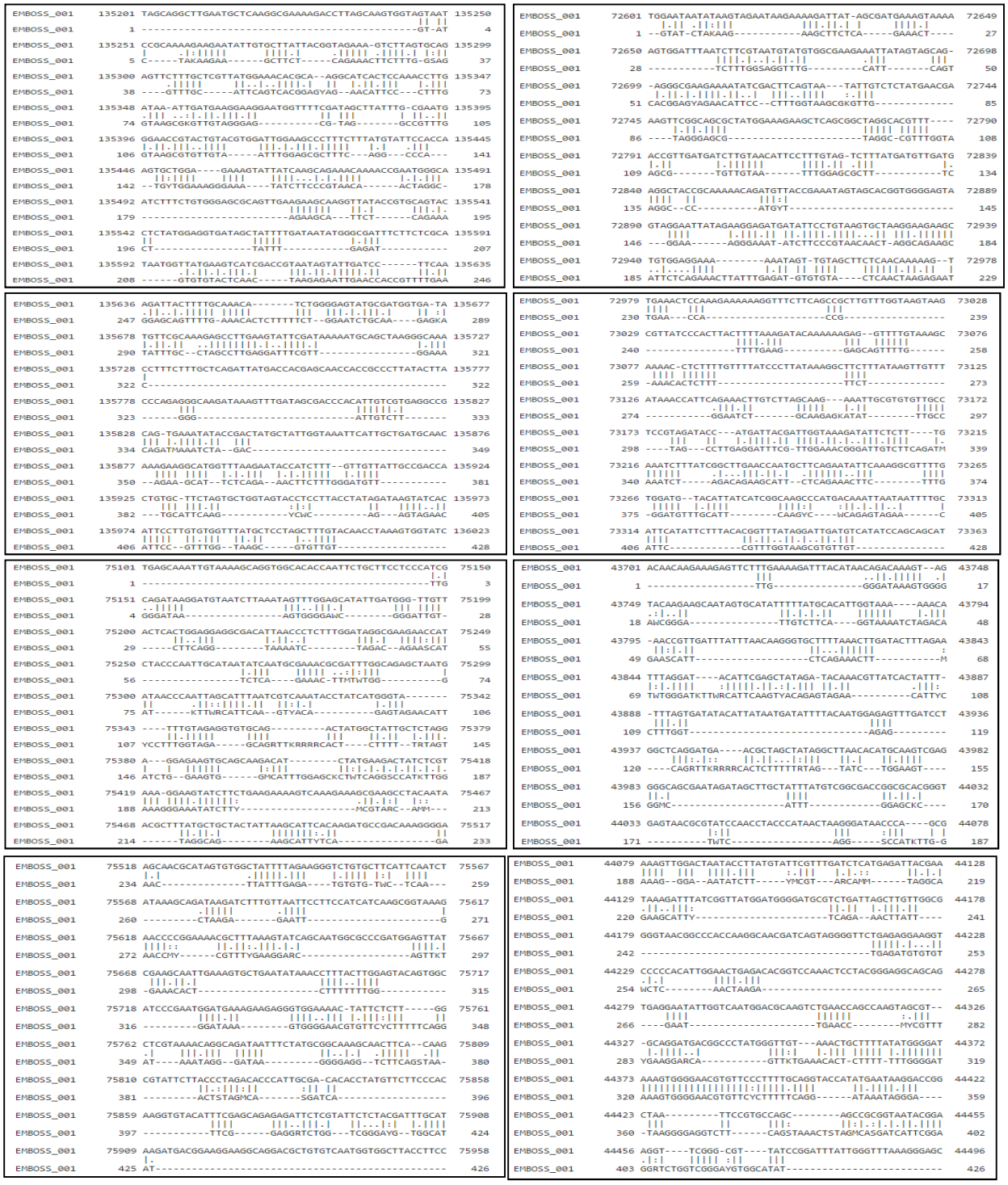

Figure 4.1.2.6: Comparison of the forward (top __ and …) and reverse compliment (bottom _ _ and __) sequence alignments for W125 E4 V2.3 against the ATCC *P. bivia* reference strain DNF00188 (left) and the NCBI Primer BLAST Hit *P. bivia* strain DSM 20514 (right).

A similar alignment pattern can be seen for sample W125 E4 V2 as W012 C8 V2.0 where the quality of alignment of both the forward and reverse compliment sequences to the NCBI Primer BLAST Hit *P. bivia* strain DSM 20514 show slightly improved alignment in comparison to when the sequences are aligned against ATCC *P. bivia* reference strain DNF00188 with little difference between the direction of the sequences.

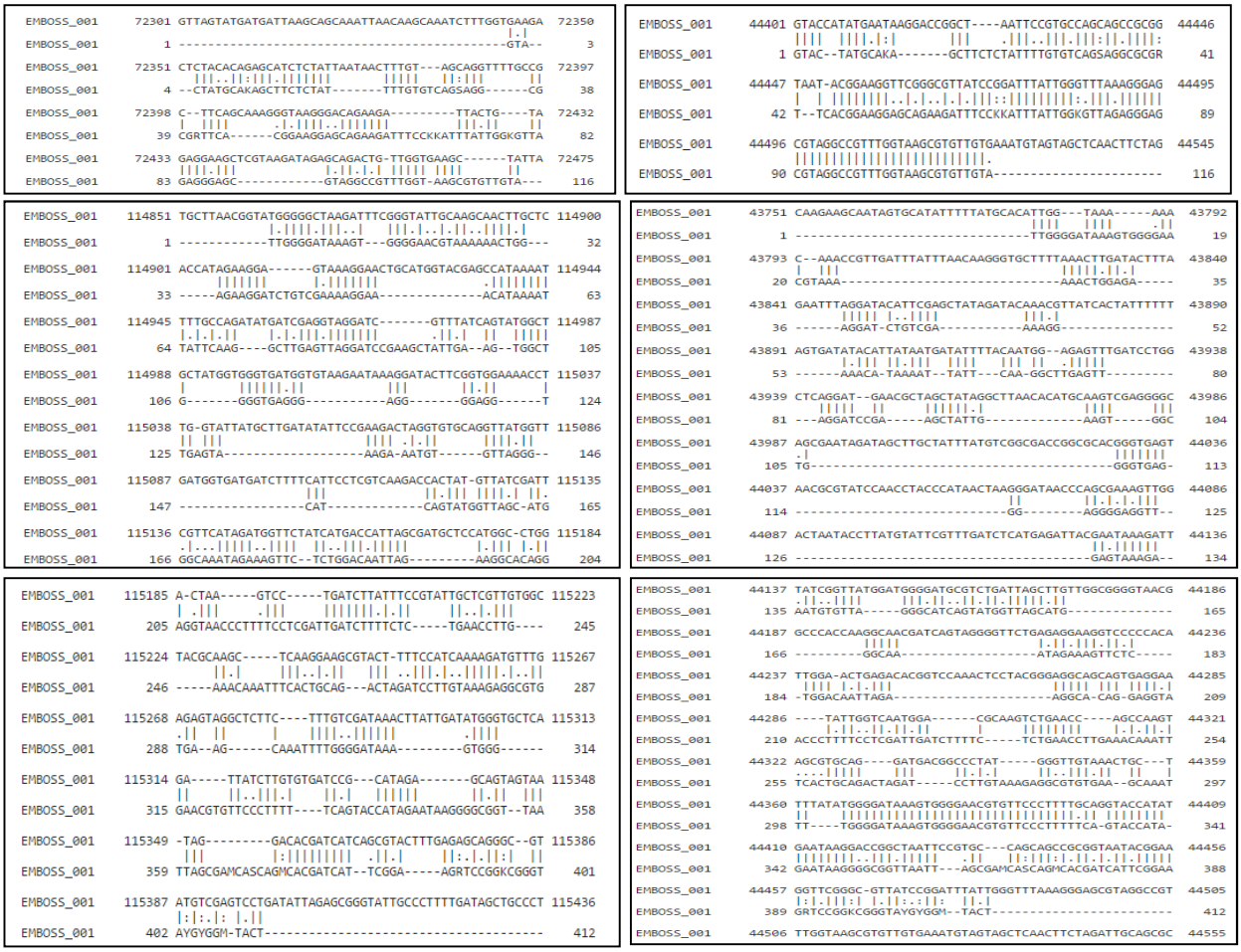

Figure 4.1.2.7: Comparison of the forward (top __ and …) and reverse compliment (bottom _ _ and __) sequence alignments for W174 F11 V2.4 against the ATCC *P. bivia* reference strain DNF00188 (left) and the NCBI Primer BLAST Hit *P. bivia* strain DSM 20514 (right).

The last sample analyzed showed improved alignment to both alignment sequences with improved alignment to NCBI Primer BLAST Hit *P. bivia* strain DSM 20514 in comparison to when the sequences are aligned against ATCC *P. bivia* reference strain DNF00188 for both the forward and reverse compliment sequences. This indicates the primers have a higher specificity for the *P. bivia* strain DSM 20514, to which the samples should be compared to.

From the above data, it can be seen that there are multiple products and sizes that are amplified by the set of primers that were eventually used to assess the WISH samples, which indicates their non-specificity, as indicated by the poor alignments. This means that the primers are not reliable and should not be used for future research, with further effort going into designing species specific primers. This variability of the primers can be seen in the high readings of quantified *P. bivia* (copies/ng) indicated by the lack of significant difference in any of the above associations. As such, the *P. bivia* results have not been included in the category figures for comparison between the bacterium. The individual figures for the *P. bivia* results for each category have been included for referral, but should be interpreted with strong criticism and not compared to the other bacterium figures, with any future progress involving optimized primers.

4.2 Real-Time PCR (qPCR) Results

For all amplification, standard and melt curves for qPCR results see appendix D qPCR Results.

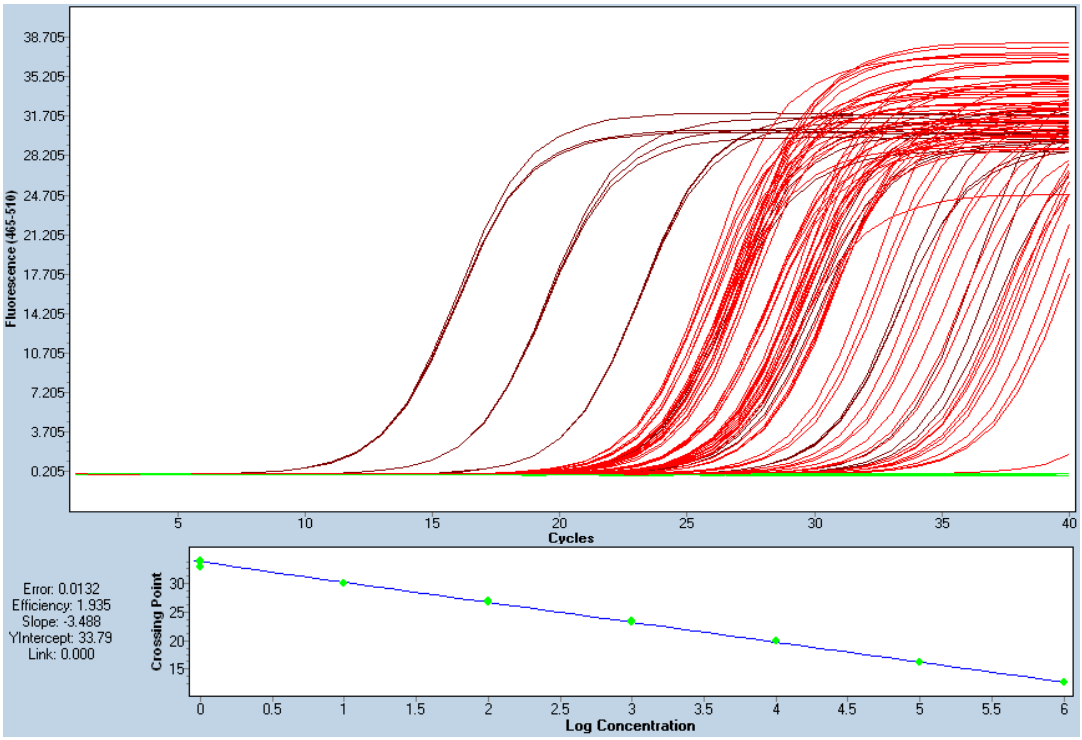

Figure 4.2: Example of an amplification and standard curve run with the WISH samples. Amplification and standard curves of *L. iners* qPCR Plate V2.5 generated based on all wells and the standard curve is generated based on the amplification curve of the standard positive controls ranging from 10^6 to 10^0 copies/µL. Red and brown indicate positive amplification in the

unknown samples and the positive control standards respectively, blue indicates uncertainty and green indicates negative amplification in the wells.

4.2.1 Descriptive statistics

All six bacterial species DNA quantities in the WISH samples had a $p<0.0001$ for the Shapiro-Wilk normality test, indicating none of the bacterial species were normally distributed across the participant samples, which can be seen by the large discrepancies between the mean and median values across the bacteria (Table 4.2.1). The box plots in the figure below illustrate the $\log_{10}$-transformed values for copies/ng DNA of each of the bacteria. As illustrated below, the medians of *L. iners, G. vaginalis* copies/ng are consistently higher and more evenly distributed than *L. crispatus, L. jensenii* and *L. gasseri,* which are skewed left towards the lower range of copies/ng, except for *L. gasseri.* This shows a distinct separation of the bacteria into two different groups of low and high quantity, further associated with a 'healthy' or dysbiotic vaginal microbiome, respectively.

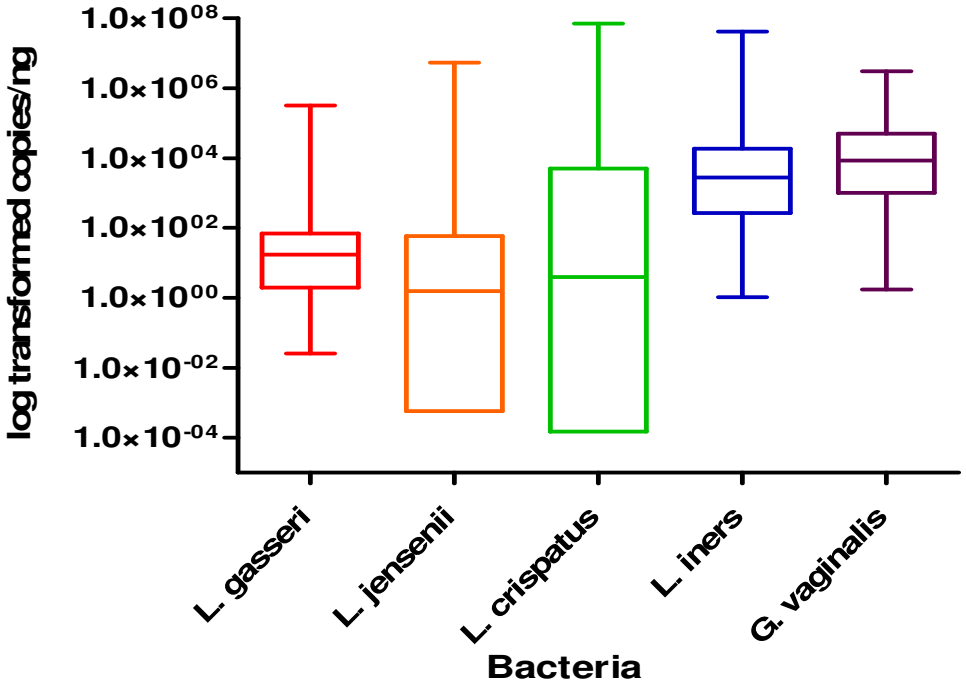

Figure 4.2.1: Box plot comparison of the copies of each bacterial species of interest quantified in the DNA extracted from WISH participants' lateral wall swabs; showing the entire cohort reported as log transformed copies/ng total DNA for *L. gasseri* (red), *L. jensenii* (orange), *L. crispatus* (green), *L. iners* (blue), and *G. vaginalis* (purple). The 'box' component of each plot

indicates the interquartile range (IQR) of the data set and the 'whiskers' which are the two lines (bottom and top) extending from the box component of each block that end with a horizontal stroke, indicate the range from the smallest and largest non-outliers to the 25% and 75% percentile components, respectively. The middle line indicates the median value for each data set.

Table 4.2.1: Descriptive statistics for each bacterial species, quantified from DNA extracted from the WISH lateral wall swab for each participant.

	Bacteria					
	L. crispatus	*L. gasseri*	*L. jensenii*	*L. iners*	*G. vaginalis*	*P. bivia*
Min	0.0	0.0	0.0	1.034	1.738	1.738
25% Percentile	0.0	1.976	1.570e-016	266.7	1015	3667
Median	3.957	17.58	1.568	2807	8540	11073
75% Percentile	4980	64.67	59.00	18727	49867	75533
Max	7.113e+007	320000	5.440e+006	4.167e+007	3.033e+006	2.553e+007
Mean	858412	3327	48743	337988	151382	750128
Std. Deviation	7.157e+006	27908	462042	3.485e+006	414156	3.405e+006
Std. Error	598472	2334	38638	291468	34633	284714

Although we only measured the most common vagina-associated bacteria, using these as markers for total lactobacillus bacterial load we can assume this cohort of adolescent females had predominantly non-lactobacillus species dominating their vaginal microbiome, indicating a shift in what is considered the 'normal' vaginal microbiome in terms of the standard 'healthy' Lactobacillus dominated microbiome.

Due to the data set being non-parametric, all figures below represent the $\log_{10}$ transformed values for each area of comparison. The comparisons were considered statistically significantly different if the p-values were lower than 0.05; medians and 95% confidence intervals are reported.

For all of the following analyses, the same shapes have been used for each bacterium; *L crispatus* (equilateral triangle), *L. gasseri* (square), *L. jensenii* (circle), *L. iners* (square balanced at 45° angle) *G. vaginalis* (isosceles right triangle) and *P. bivia* (square with an x through the center).

4.3 Comparison of absolute bacterial quantities to BV status, inflammation levels, age, hormonal contraceptive and STI status, bacterial versus viral STIs and HPV

4.3.1 Association between the quantities of the bacteria of interest and BV status

Participants were categorized as being BV positive, intermediate or negative based on Nugent scoring. A Nugent score of 0-3 is BV negative, a score of 4-6 is BV intermediate and a score of 7-10 is BV positive.

The median copies/ng for each bacterium were compared using a Friedman's ANOVA with a Dunn's Multiple Comparison test for BV positive (n=56, 39.16%), BV intermediate (n=17, 11.89%) and BV negative (n=70, 48.95%) groups. All ANOVA tests were statistically significant ($p<0.0001$) indicating an overall significant difference between the copies/ng of the bacteria in each BV group. For the p-values of the Friedman's ANOVA test with a Dunn's Multiple Comparison test run across all BV groups, see Appendix D qPCR results, Section 2.1. Asterisk stars were used in the following figures where one start (*) indicates a p-value lower than 0.05, two stars (**) indicate a p-value lower than 0.01 and three stars (***) indicate a p-value lower than 0.001.

Within the BV positive group (Figure 4.3.1A), *L. iners* and *G. vaginalis* both showed significantly higher copies/ng in comparison to *L. gasseri* ($p<0.0001$), *L. jensenii* ($p<0.0001$) and *L. crispatus* ($p<0.0001$). *G. vaginalis* was significantly more abundant than *L. iners* ($p=0.007$) and *L. gasseri* was more abundant than *L. jensenii* ($p=0.0157$). *G. vaginalis* had significantly higher copies/ng within the BV intermediate group (Figure 4.3.1B), with higher copies/ng in comparison to *L. gasseri* ($p=0.0123$), and *L. jensenii* ($p=0.0074$), with both *G. vaginalis* and *L. iners* being significantly greater than *L. crispatus* ($p=0.0001$, $p=0.0044$). The BV negative group (Figure 4.3.1C) had greater copies/ng of *L. crispatus, L. iners* and *G. vaginalis* in comparison to *L. gasseri* ($p=0.0009$, $p<0.0001$, $p=0.0002$ respectively). *L. crispatus, L. iners* and *G. vaginalis* had higher median copies/ng with a significant difference of $p<0.0001$ in comparison to *L. jensenii*. Overall, the greatest differences occurred between the high median copies/ng of *G. vaginalis* in comparison to *L. gasseri, L. jensenii,* and *L. crispatus,* with *L. iners* to varying degrees across the BV positive, intermediate and negative groups. The increased copies/ng of *L. crispatus* within the BV negative group follows the literature of a 'healthy' FGT microbiome.

Interestingly, *L. crispatus* and *L. iners* were the most prevalent of the lactobacilli species we quantified in the BV negative group, however this trend is further followed by *L. iners* and *G. vaginalis* across all three BV groups which differs strongly from the general lactobacilli dominated FGT within a 'healthy' FGT microbiome. This could indicate a difference in what is considered the 'normal' microbiome within this adolescent population.

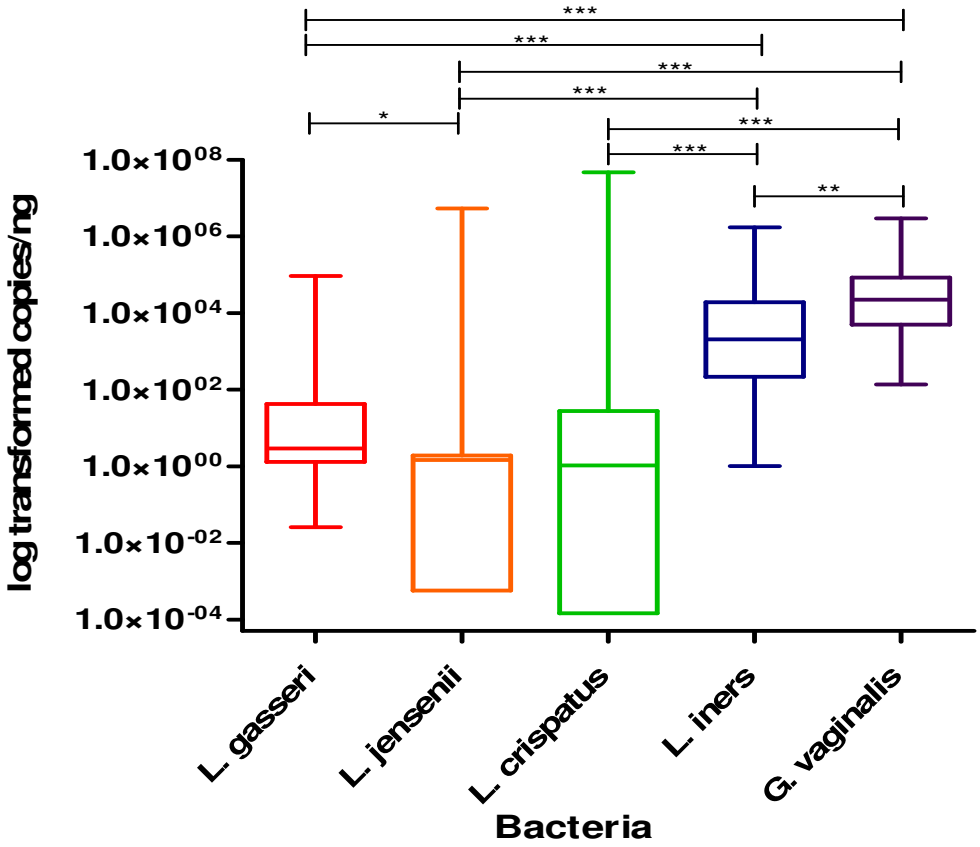

Figure 4.3.1A: Box-plot of *L. gasseri* (red), *L. jensenii* (orange), *L. crispatus* (green), *L. iners* (blue), and *G. vaginalis* (purple) quantities for BV positive participants reported as log transformed copies/ng total DNA. The 'box' component of each plot indicates the interquartile range (IQR) of the data set and the 'whiskers' which are the two lines (bottom and top) extending from the box component of each block that end with a horizontal stroke, indicate the range from the smallest and largest non-outliers to the 25% and 75% percentile components, respectively. The middle line indicates the median value for each data set.

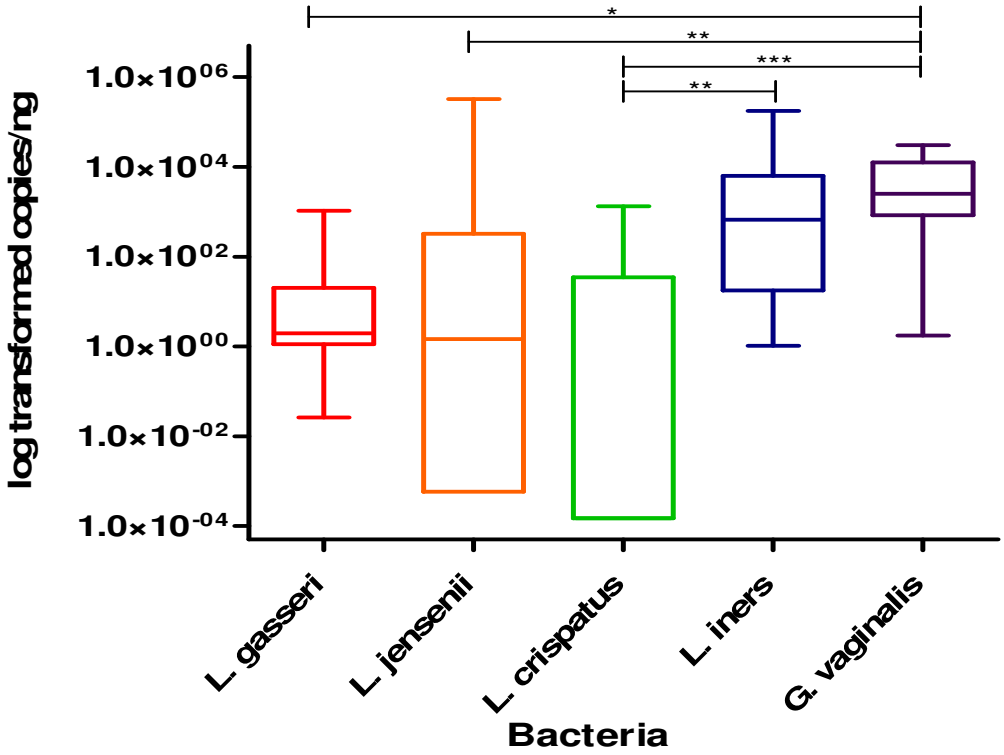

Figure 4.3.1B: Box-plot of *L. gasseri* (red), *L. jensenii* (orange), *L. crispatus* (green), *L. iners* (blue), and *G. vaginalis* (purple) quantities for BV intermediate participants reported as log transformed copies/ng total DNA. The 'box' component of each plot indicates the interquartile range (IQR) of the data set and the 'whiskers' which are the two lines (bottom and top) extending from the box component of each block that end with a horizontal stroke, indicate the range from the smallest and largest non-outliers to the 25% and 75% percentile components, respectively. The middle line indicates the median value for each data set.

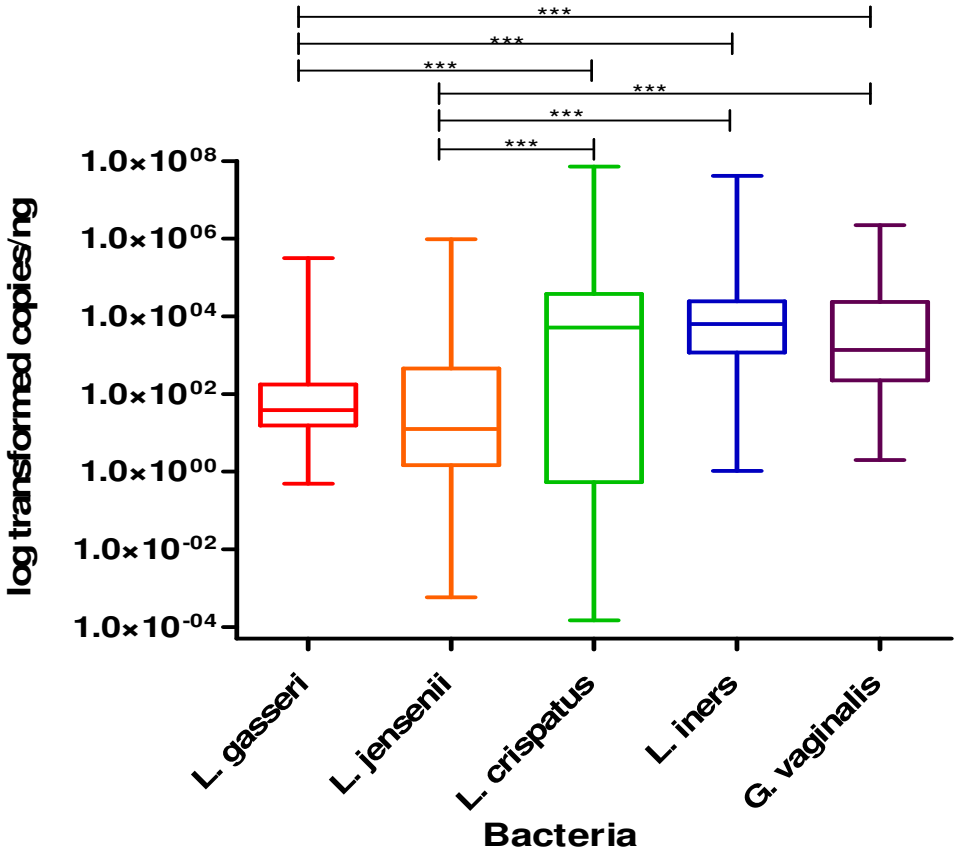

Figure 4.3.1C: Box-plot of *L. gasseri* (red), *L. jensenii* (orange), *L. crispatus* (green), *L. iners* (blue), and *G. vaginalis* (purple) quantities for BV negative participants reported as log transformed copies/ng total DNA. The 'box' component of each plot indicates the interquartile range (IQR) of the data set and the 'whiskers' which are the two lines (bottom and top) extending from the box component of each block that end with a horizontal stroke, indicate the range from the smallest and largest non-outliers to the 25% and 75% percentile components, respectively. The middle line indicates the median value for each data set.

4.3.1.1 *Lactobacillus crispatus*

We compared the quantified log copies/ng of *L. crispatus* between the BV groups. BV negative participants had a significantly higher median value of *L. crispatus* (copies/ng) compared to those in the BV intermediate (p=0.0004) and BV positive (p=0.0002) participant groups. There was an overall significant difference in *L. crispatus* between the BV groups (Kruskal-Wallis ANOVA p<0.0001) (Figure 4.3.1.1).

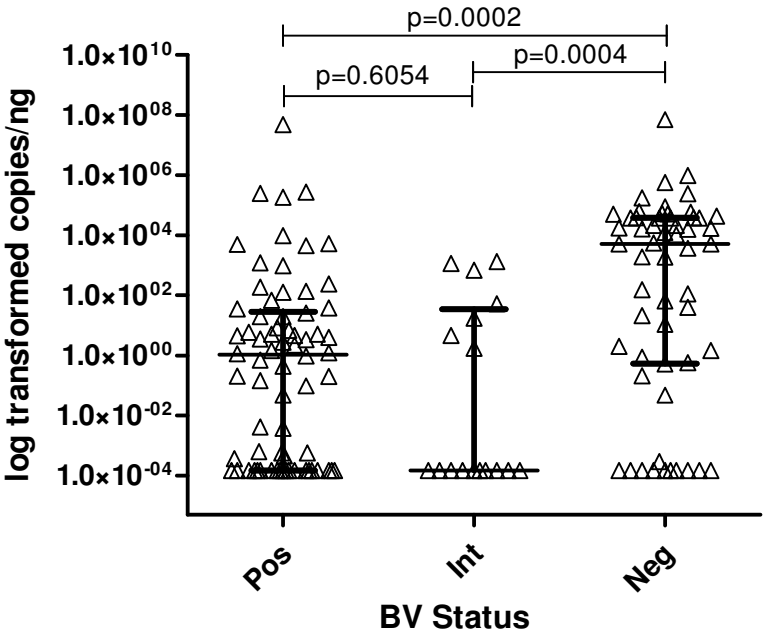

Figure 4.3.1.1: Comparison of the quantities of *L. crispatus* (log transformed copies/ng DNA) measured in the DNA extracted from vaginal lateral wall swabs from participants in the WISH study, between BV positive, intermediate and negative groups. All p-value comparisons were based on an unpaired, non-parametric Dunn's Multiple Comparison test. Each point in the figure represents an individual participant. The three horizontal bars represent the median value (middle bar), upper interquartile range (top bar) and lower interquartile range (bottom bar).

4.3.1.2 *Lactobacillus gasseri*

We compared the quantified log copies/ng of *L. gasseri* between the BV groups. The BV negative participants had a significantly higher median value of *L. gasseri* (copies/ng) compared to those in the BV intermediate (p=0.0016) and BV positive (p<0.0001) participant groups. There was an overall significant difference between the BV groups (Kruskal-Wallis ANOVA p<0.0001) (Figure 4.3.1.2).

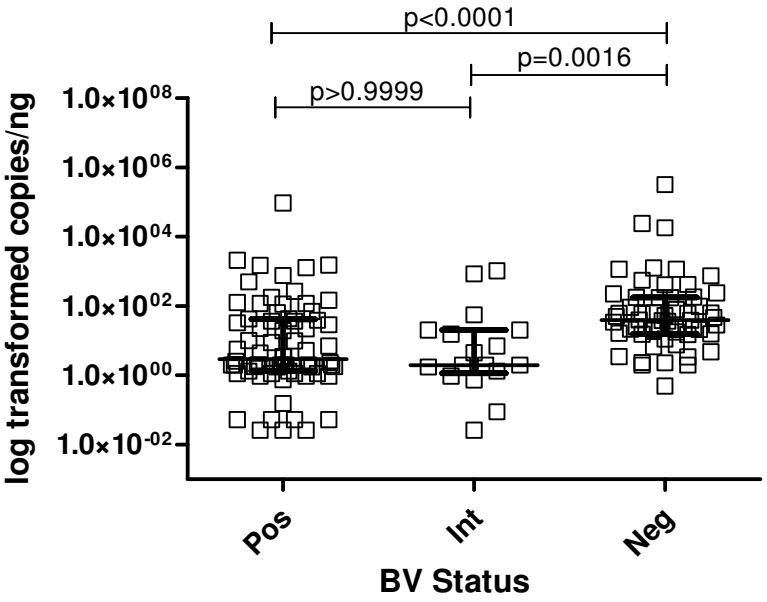

Figure 4.3.1.2: Comparison of the quantities of *L. gasseri* (log transformed copies/ng DNA) measured in the DNA extracted from vaginal lateral wall swabs from participants in the WISH study, between BV positive, intermediate and negative groups. All p-value comparisons were based on an unpaired, non-parametric Dunn's Multiple Comparison test. Each point in the figure represents an individual participant. The three horizontal bars represent the median value (middle bar), upper interquartile range (top bar) and lower interquartile range (bottom bar).

4.3.1.3 *Lactobacillus jensenii*

We compared the quantified log copies/ng of *L. jensenii* between the BV groups. BV negative participants had a significantly higher median value of *L. jensenii* (copies/ng) compared to those in the BV positive ($p<0.0001$) participant group. There was an overall significant difference in *L. jensenii* between the BV groups (Kruskal-Wallis ANOVA $p<0.0001$) (Figure 4.3.1.3).

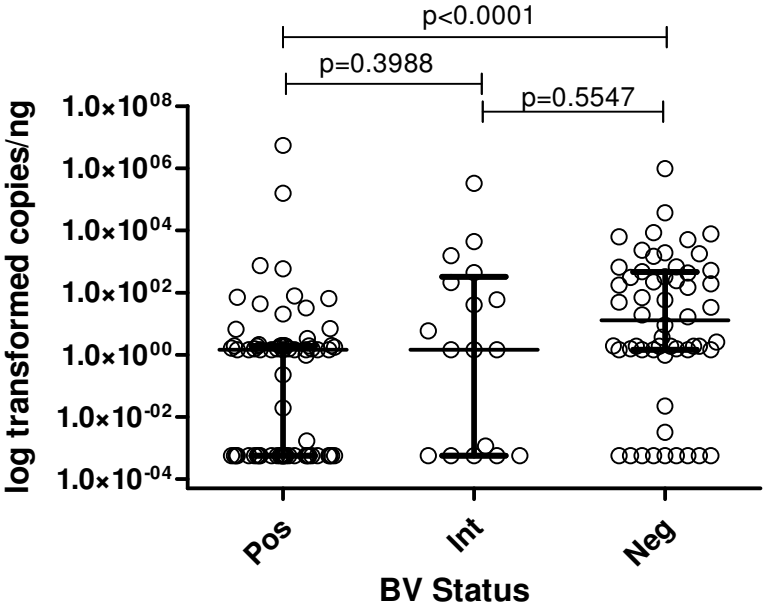

Figure 4.3.1.3: Comparison of the quantities of *L. jensenii* (log transformed copies/ng DNA) measured in the DNA extracted from vaginal lateral wall swabs from participants in the WISH study, between BV positive, intermediate and negative groups. All p-value comparisons were based on an unpaired, non-parametric Dunn's Multiple Comparison test. Each point in the figure represents an individual participant. The three horizontal bars represent the median value (middle bar), upper interquartile range (top bar) and lower interquartile range (bottom bar).

4.3.1.4 *Lactobacillus iners*

We compared the quantified log copies/ng of *L. iners* between the BV groups. BV negative participants had a significantly higher median value of *L. iners* (copies/ng) compared to those in the BV intermediate (p=0.0461) participant group. There was an overall significant difference in *L. iners* between the BV groups (Kruskal-Wallis ANOVA p=0.0358) (Figure 4.3.1.4).

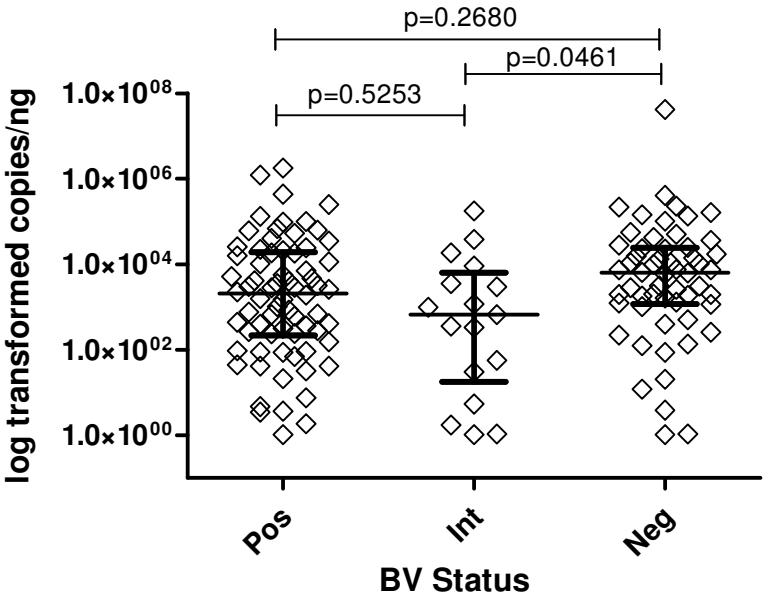

Figure 4.3.1.4: Comparison of the quantities of *L. iners* (log transformed copies/ng DNA) measured in the DNA extracted from vaginal lateral wall swabs from participants in the WISH study, between BV positive, intermediate and negative groups. All p-value comparisons were based on an unpaired, non-parametric Dunn's Multiple Comparison test. Each point in the figure represents an individual participant. The three horizontal bars represent the median value (middle bar), upper interquartile range (top bar) and lower interquartile range (bottom bar).

4.3.1.5 *Gardnerella vaginalis*

We compared the quantified log copies/ng of *G. vaginalis* between the BV groups. BV positive participants had significantly higher copies/ng of *G. vaginalis* compared to those in the BV intermediate (p=0.0059) and BV negative (p<0.0001) participant groups. There was an overall significant difference in *G. vaginalis* between the BV groups (Kruskal-Wallis ANOVA p<0.0001) (Figure 4.3.1.5).

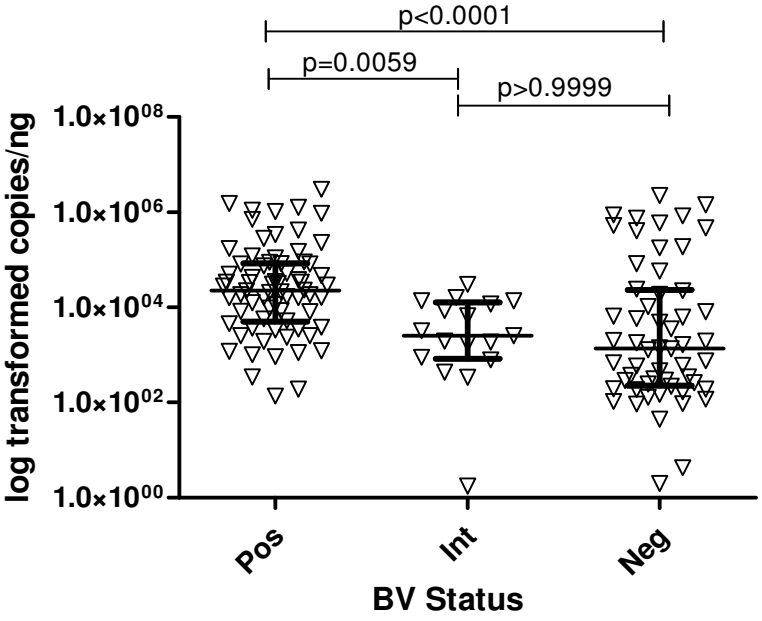

Figure 4.3.1.5: Comparison of the quantities of *G. vaginalis* (log transformed copies/ng DNA) measured in the DNA extracted from vaginal lateral wall swabs from participants in the WISH study, between BV positive, intermediate and negative groups. All p-value comparisons were based on an unpaired, non-parametric Dunn's Multiple Comparison test. Each point in the figure represents an individual participant. The three horizontal bars represent the median value (middle bar), upper interquartile range (top bar) and lower interquartile range (bottom bar).

Therefore, we can conclude than women without BV had higher median levels of *L. crispatus* (copies/ng) and *L. gasseri* (copies/ng) compared to those in the BV intermediate and BV positive groups. Further, the BV negative group had higher median levels of *L. jensenii* (copies/ng) and *L. iners* (copies/ng) compared to the BV positive and intermediate groups, respectively. Overall, *L. crispatus, L. iners* and *G. vaginalis*, which are associated with both dysbiosis and a 'healthy' vaginal microbiome, dominated the BV negative group. The BV positive group had higher median levels of *G. vaginalis* (copies/ng) compared to those in the BV intermediate and BV

positive groups, with none of the BV groups having any difference in the median levels of *P. bivia* (copies/ng) present. This follows the expected trend of association between the presence of increased *G. vaginalis* copies/ng with BV positive literature and increased *L. crispatus, L. gasseri* and *L. jensenii* and BV negative literature.

Due to the unreliability of the qPCR amplification results, the *P. bivia* data regarding BV has not been included and can be found in Appendix E: Results, page 186.

4.3.2 Association between bacteria of interest and inflammatory immunological factor levels

The two inflammatory groups were defined based on the unsupervised analysis of the 47 immunological factors of interest in the cervicovaginal fluid of women in the WISH cohort. These immunological factors were categorized into high and low inflammation by partitioning around medoids (PAM) using an R package 'cluster' with a k-value of 2. The samples were originally separated into high and low inflammation based on the levels of only the pro-inflammatory and chemokine factors measured. However, the inflammation separation of the participant samples showed little difference between the two pro-inflammatory and chemokine groups of immunological factor analysis in comparison to using all of the factors to determine high and low inflammation. Thus the final inflammation categorization was done using all 47 immunological factors.

The immunological factors measured in this study can be generally grouped into five different categories. The immunological factors considered as pro-inflammatory were IL-1a, IL-1b, IL-6, IL-12p40, IL-12(p70), IL-18, MIF, TNF-a, TNF-b and TRAIL. The immunological factors considered chemokines were CTACK, Eotaxin, GROa, IL-8, IL-16, IP-10, MCP-1, MCP-3, MIG, MIP-1a, MIP-1b, IFN-a2, and RANTES. The immunological factors considered growth factors were b-NGF, FGF basic, G-CSF, GM-CSF, HGF, IL-3, IL-7, IL-9, LIF, M-CSF, PDGF-bb, SCF, SCGF-b, SDF-1a and VEGF. The immunological factors considered adaptive were IFN-g, IL-4, IL-13, IL-17, IL-2Ra, IL-2, and IL-5. The immunological factors considered regulatory were IL-10 and IL-1ra.

The median log transformed copies/ng for each bacterium were compared using a Friedman's ANOVA with a Dunn's Multiple Comparison test for high (n=98, 70%) and low (n=42, 30%)

inflammation groups. Both ANOVA tests were significant ($p<0.0001$) indicating statistically different median values for the bacterial copies/ng in the low and high genital inflammation groups. For the p-values of the Friedman's ANOVA test with a Dunn's Multiple Comparison test run across the inflammation groups, see Appendix D qPCR results, Section 2.2. Asterisk stars were used in the following figures where one start (*) indicates a p-value lower than 0.05, two stars (**) indicate a p-value lower than 0.01 and three stars (***) indicate a p-value lower than 0.001.

In the women with low levels of inflammation, both *G. vaginalis* and *L. iners* were significantly higher compared to *L. gasseri* and *L. jensenii* ($p<0.0001$) (Figure 4.3.2A), *L. crispatus* copies/ng were also significantly higher than *L. gasseri* and *L. jensenii* ($p=0.0097$ and $p=0.0005$, respectively). There were no differences between *L. iners, L. crispatus* and *G. vaginalis* in the low inflammation group. The high inflammation group (Figure 4.3.2B) also had the significantly higher copies/ng of *G. vaginalis* and *L. iners* compared to *L. gasseri* ($p<0.0001$), *L. jensenii* ($p<0.0001$), and *L. crispatus* ($p<0.0001$). *L. gasseri* had higher copies/ng compared to *L. jensenii* ($p=0.0463$). Regardless of inflammatory factor level, copies/ng of *G. vaginalis* and *L. iners* were high. However, the low inflammation group had equivalent copies/ng of *L. crispatus* and the high inflammation group had increased copies/ng of *L. gasseri.*

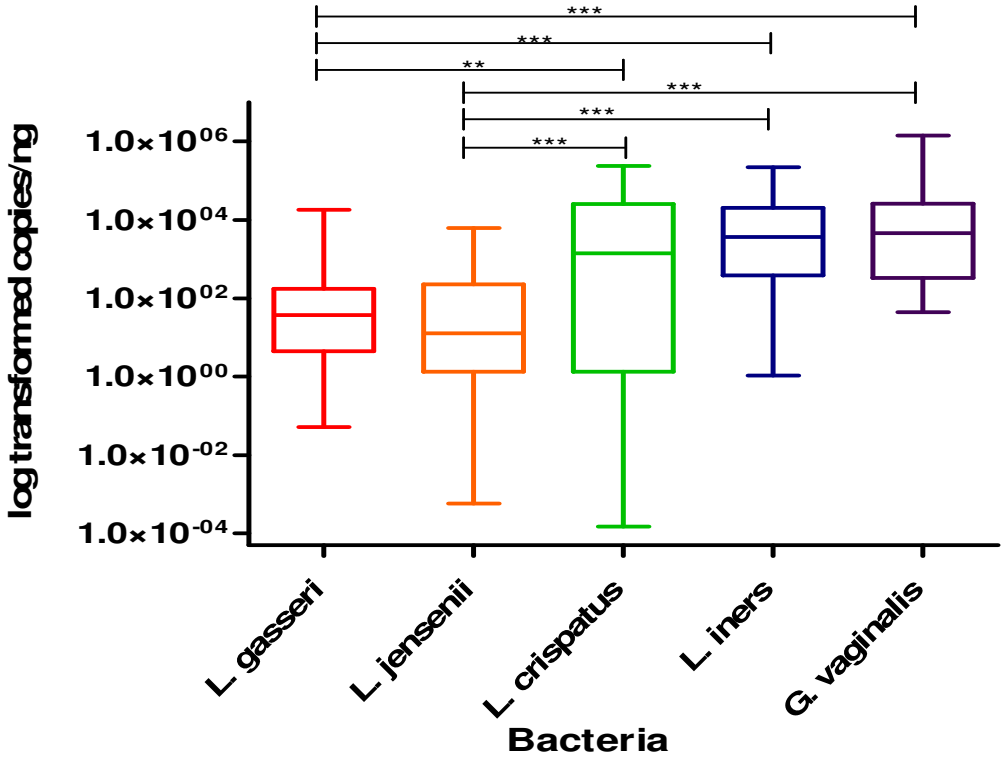

Figure 4.3.2A: Box-plot of the low inflammation for *L. gasseri* (red), *L. jensenii* (orange), *L. crispatus* (green), *L. iners* (blue), and *G. vaginalis* (purple) reported as log transformed copies/ng total DNA. The 'box' component of each plot indicates the interquartile range (IQR) of the data set and the 'whiskers' which are the two lines (bottom and top) extending from the box component of each block that end with a horizontal stroke, indicate the range from the smallest and largest non-outliers to the 25% and 75% percentile components, respectively. The middle line indicates the median value for each data set.

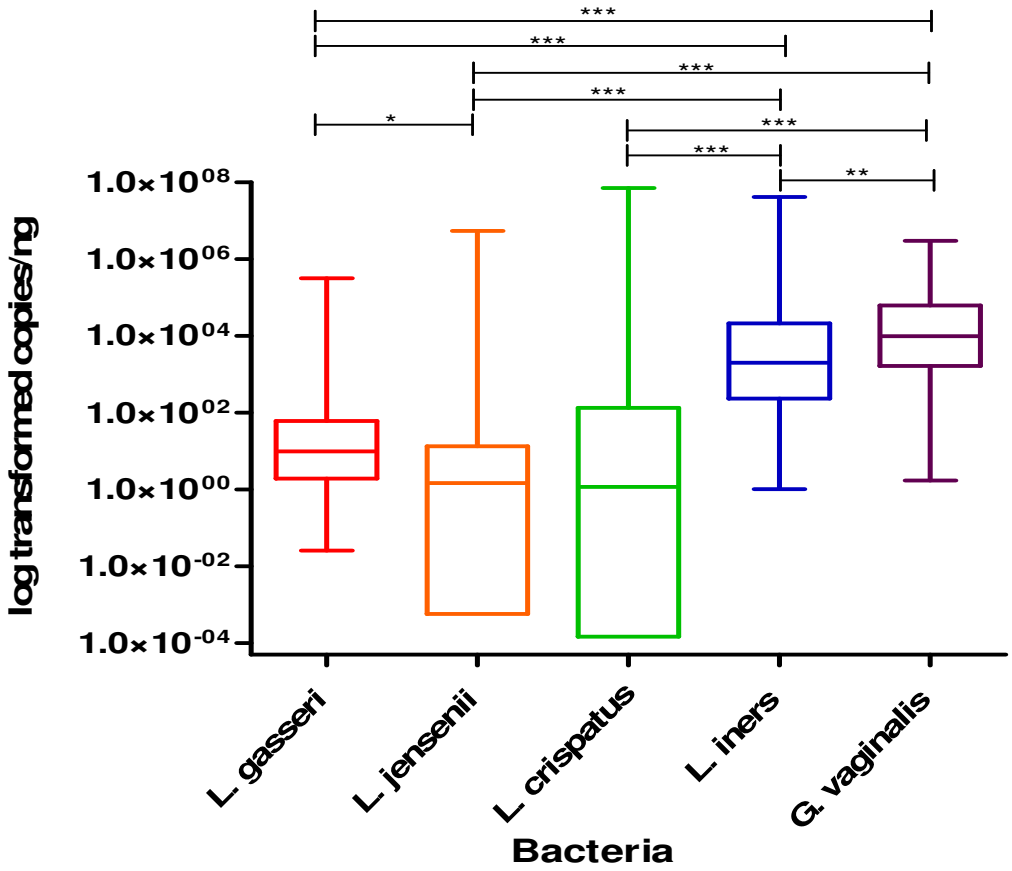

Figure 4.3.2B: Box-plot of the high inflammation for *L. gasseri* (red), *L. jensenii* (orange), *L. crispatus* (green), *L. iners* (blue), and *G. vaginalis* (purple) reported as log transformed copies/ng total DNA. The 'box' component of each plot indicates the interquartile range (IQR) of the data set and the 'whiskers' which are the two lines (bottom and top) extending from the box component of each block that end with a horizontal stroke, indicate the range from the smallest and largest non-outliers to the 25% and 75% percentile components, respectively. The middle line indicates the median value for each data set.

4.3.2.1 *Lactobacillus crispatus*

We compared the quantified log copies/ng of *L. crispatus* between the inflammation groups. The low inflammation group had significantly higher copies/ng compared to those in the high inflammation group (p=0.0005) (Figure 4.3.2.1).

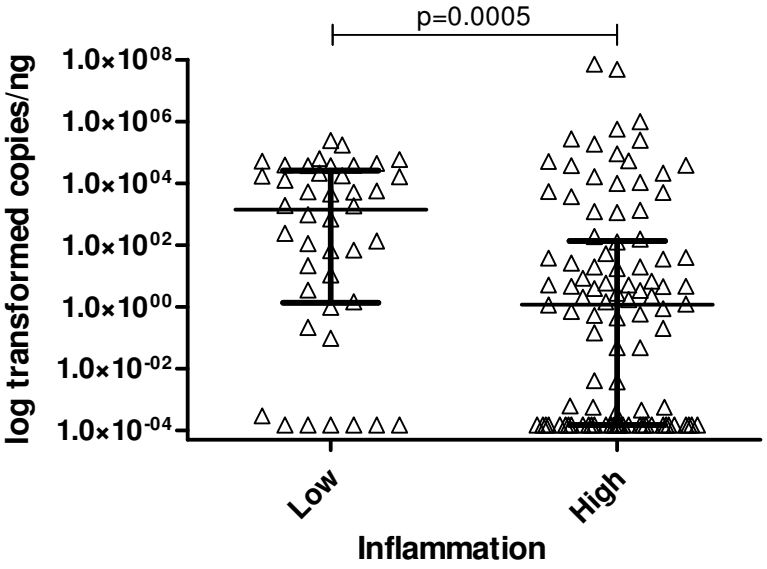

Figure 4.3.2.1: Comparison of the quantities of *L. crispatus* (log transformed copies/ng DNA) measured in the DNA extracted from vaginal lateral wall swabs from participants in the WISH study, between women with high and low genital inflammation. All p-value comparisons were based on an unpaired, non-parametric Mann-Whitney t-test statistic. Each point in the figure represents an individual participant. The three horizontal bars represent the median value (middle bar), upper interquartile range (top bar) and lower interquartile range (bottom bar).

4.3.2.2 *Lactobacillus gasseri*

We compared the quantified log copies/ng of *L. gasseri* between the inflammation groups. The low inflammation group had significantly higher copies/ng of *L. gasseri* compared to those in the high inflammation group (p=0.033) (Figure 4.3.2.2).

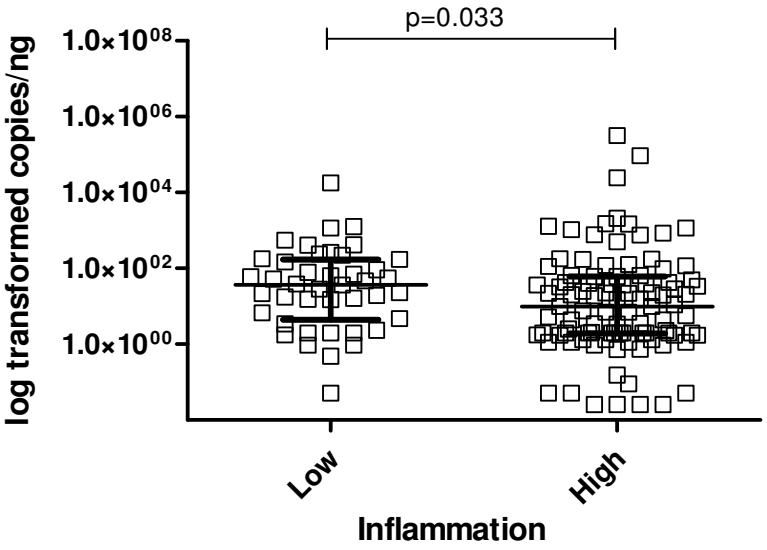

Figure 4.3.2.2: Comparison of the quantities of *L. gasseri* (log transformed copies/ng DNA) measured in the DNA extracted from vaginal lateral wall swabs from participants in the WISH study, between women with high and low genital inflammation. All p-value comparisons were based on an unpaired, non-parametric Mann-Whitney t-test statistic. Each point in the figure represents an individual participant. The three horizontal bars represent the median value (middle bar), upper interquartile range (top bar) and lower interquartile range (bottom bar).

4.3.2.3 *Lactobacillus jensenii*

We compared the quantified log copies/ng of *L. jensenii* between the inflammation groups. The low inflammation group had significantly higher copies/ng compared to those in the high inflammation group (p=0.0046) (Figure 4.3.2.3).

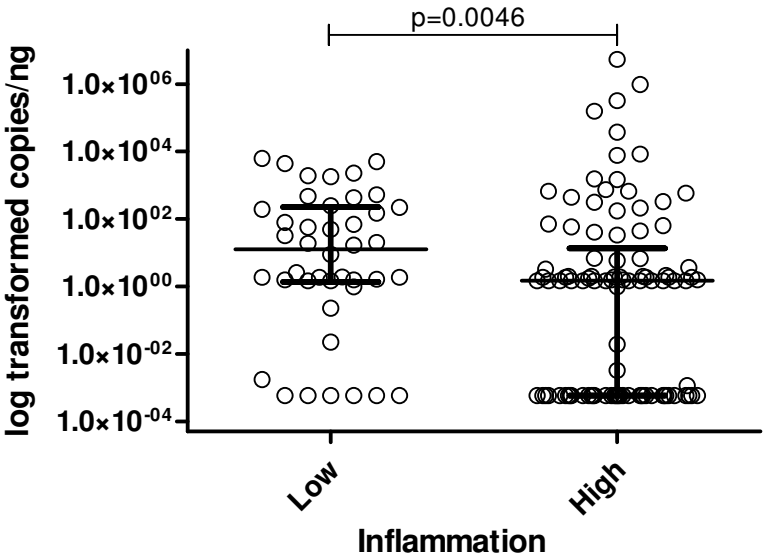

Figure 4.3.2.3: Comparison of the quantities of *L. jensenii* (log transformed copies/ng DNA) measured in the DNA extracted from vaginal lateral wall swabs from participants in the WISH study, between women with high and low genital inflammation. All p-value comparisons were based on an unpaired, non-parametric Mann-Whitney t-test statistic. Each point in the figure represents an individual participant. The three horizontal bars represent the median value (middle bar), upper interquartile range (top bar) and lower interquartile range (bottom bar).

4.3.2.4 *Lactobacillus iners*

We compared the quantified log copies/ng of *L. iners* between the inflammation groups. There was no significant difference in *L. iners* between the high inflammation group and the low inflammation group (p=0.5689) (Figure 4.3.2.4).

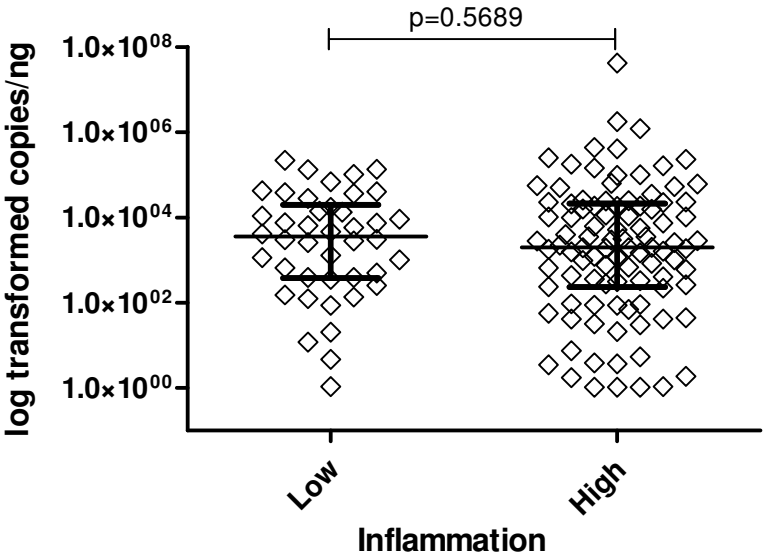

Figure 4.3.2.4: Comparison of the quantities of *L. iners* (log transformed copies/ng DNA) measured in the DNA extracted from vaginal lateral wall swabs from participants in the WISH study, women with high and low genital inflammation. All p-value comparisons were based on an unpaired, non-parametric Mann-Whitney t-test statistic. Each point in the figure represents an individual participant. The three horizontal bars represent the median value (middle bar), upper interquartile range (top bar) and lower interquartile range (bottom bar).

4.3.2.5 *Gardnerella vaginalis*

We compared the quantified log copies/ng of *G. vaginalis* between the inflammation groups. The high inflammation group and the low inflammation group had no significant difference (p=0.1227) (Figure 4.3.2.5).

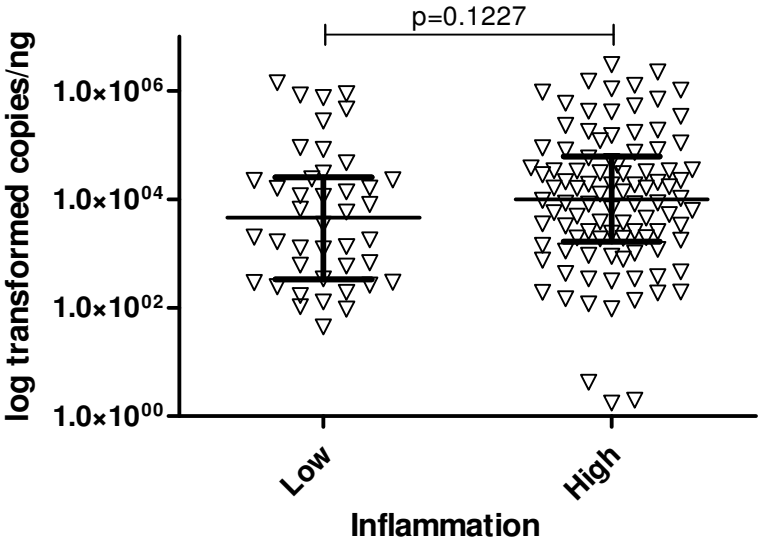

Figure 4.3.2.5: Comparison of the quantities of *G. vaginalis* (log transformed copies/ng DNA) measured in the DNA extracted from vaginal lateral wall swabs from participants in the WISH study, between women with high and low genital inflammation. All p-value comparisons were based on an unpaired, non-parametric Mann-Whitney t-test statistic. Each point in the figure represents an individual participant. The three horizontal bars represent the median value (middle bar), upper interquartile range (top bar) and lower interquartile range (bottom bar).

In summary, consistent with our hypothesis, participants with low inflammation in their genital tract fluid had significantly higher copies/ng of *L. crispatus, L. gasseri,* and *L. jensenii* compared to those present in the high inflammation group. Conversely, there were no significant differences in the copies/ng for *L. iners* or *G. vaginalis* between women with high or low inflammation. Thus there is an association with the presence of lactobacilli and low inflammation. This begs the question of whether the presence of bacteria such as *G. vaginalis*, versus the absence of lactobacilli bacterium playing any role in high genital inflammation

Due to the unreliability of the qPCR amplification results, the *P. bivia* data regarding Inflammation has not been included and can be found in Appendix E: Results, page 189.

4.3.3 Association between the quantities (copies/ng) of bacteria of interest and age

The age of all participants was recorded upon screening for participation within the study. For this analysis, age was binarised into 16-18 years of age versus 19-22 years of age.

The median copies/ng for each bacterium were compared using a Friedman's ANOVA with a Dunn's Multiple Comparison test for the two age groups 16-18 years (n=75, 52.45%) and 19-22 years (n=68, 47.55%). Both ANOVA tests were significant ($p<0.0001$), indicating the bacterial copies/ng in each age group were statistically different from each other. For the p-values of the Friedman's ANOVA test with a Dunn's Multiple Comparison test run across the inflammation groups, see Appendix D qPCR results, Section 2.2.3. Asterisk stars were used in the following figures where one start (*) indicates a p-value lower than 0.05, two stars (**) indicate a p-value lower than 0.01 and three stars (***) indicate a p-value lower than 0.001.

In both the 16-18 years (Figure 4.3.3A) and 19-22 years (Figure 4.3.3B) age groups, *G. vaginalis* and *L. iners* were significantly higher compared to *L. gasseri* ($p<0.0001$), *L. jensenii* ($p<0.0001$) and *L. crispatus* ($p<0.0001$). *L. crispatus* was significantly higher to *L. jensenii* ($p=0.0419$) in the 16-18 years' group. This data set is similar to the study cohort as a whole.

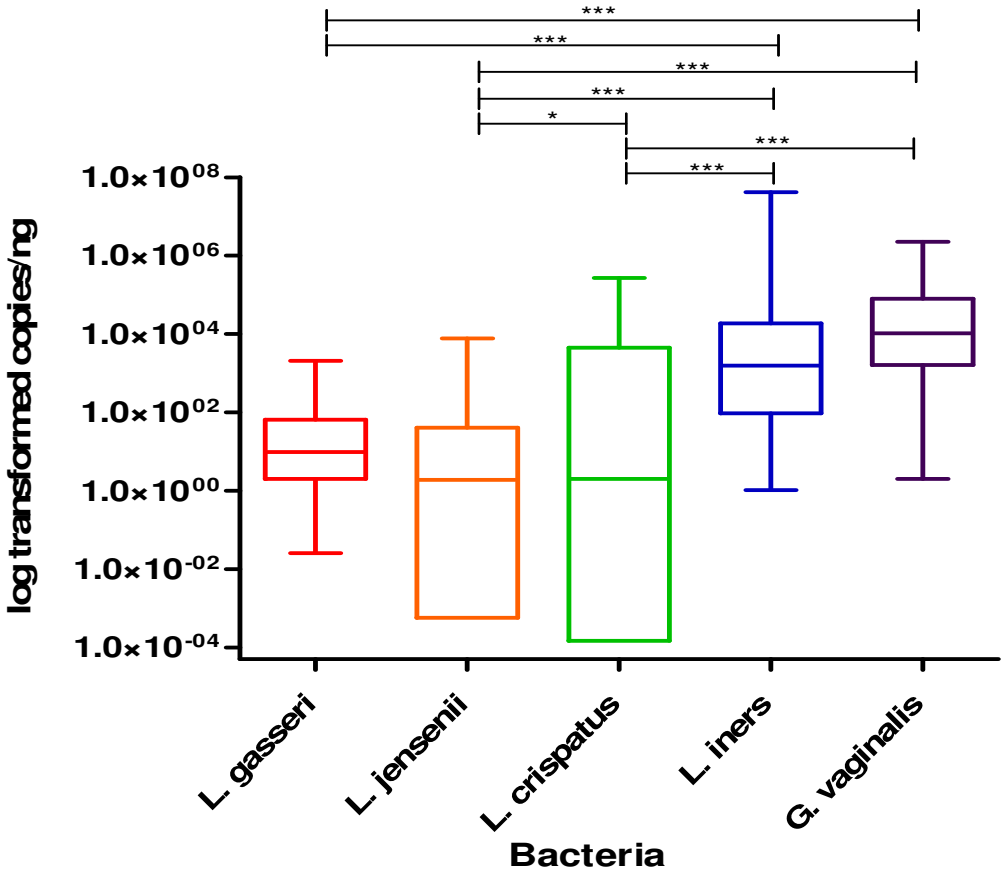

Figure 4.3.3A: Box-plot of the 16-18 years for *L. gasseri* (red), *L. jensenii* (orange), *L. crispatus* (green), *L. iners* (blue), and *G. vaginalis* (purple) reported as log transformed copies/ng total DNA. The 'box' component of each plot indicates the interquartile range (IQR) of the data set and the 'whiskers' which are the two lines (bottom and top) extending from the box component of each block that end with a horizontal stroke, indicate the range from the smallest and largest non-outliers to the 25% and 75% percentile components, respectively. The middle line indicates the median value for each data set.

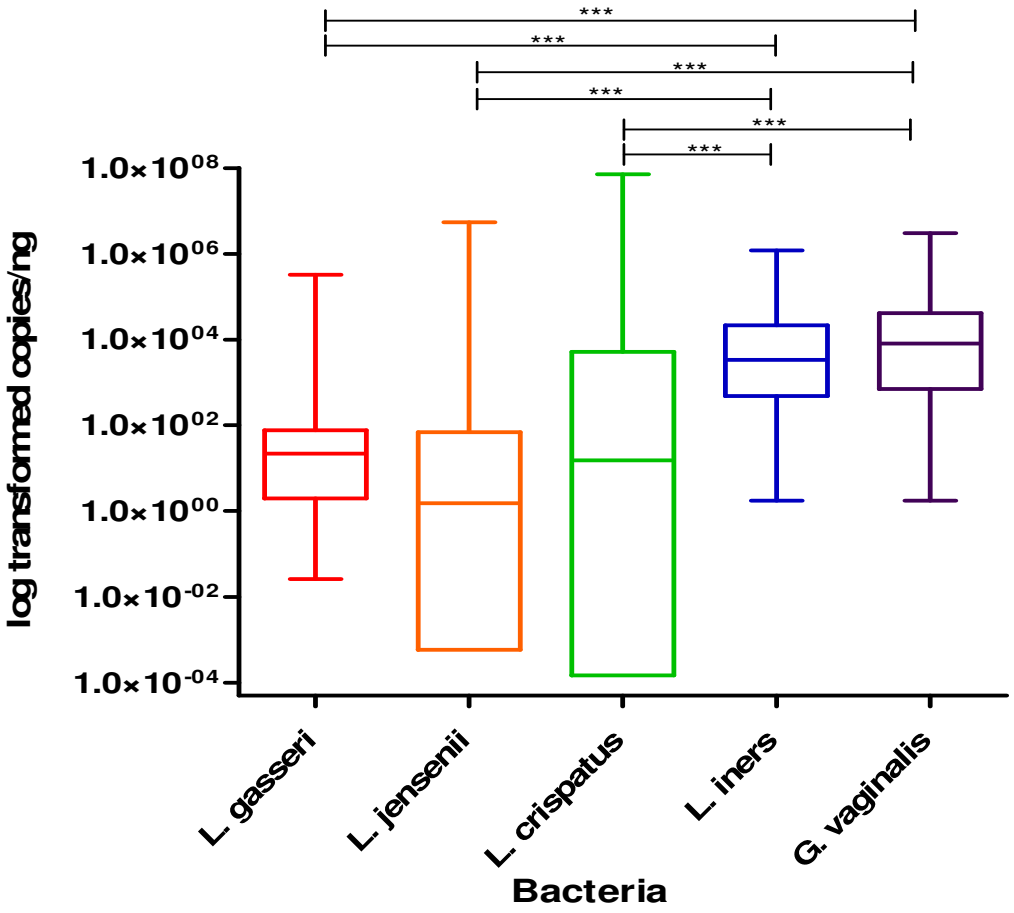

Figure 4.3.3B: Box-plot of the 19-22 years for *L. gasseri* (red), *L. jensenii* (orange), *L. crispatus* (green), *L. iners* (blue), and *G. vaginalis* (purple) reported as log transformed copies/ng total DNA. The 'box' component of each plot indicates the interquartile range (IQR) of the data set and the 'whiskers' which are the two lines (bottom and top) extending from the box component of each block that end with a horizontal stroke, indicate the range from the smallest and largest non-outliers to the 25% and 75% percentile components, respectively. The middle line indicates the median value for each data set.

4.3.3.1 *Lactobacillus crispatus*

The 16-18 years old age group and the 19-22 years old age group had no significant difference in log copies/ng (p=0.6861) (Figure 4.3.3.1).

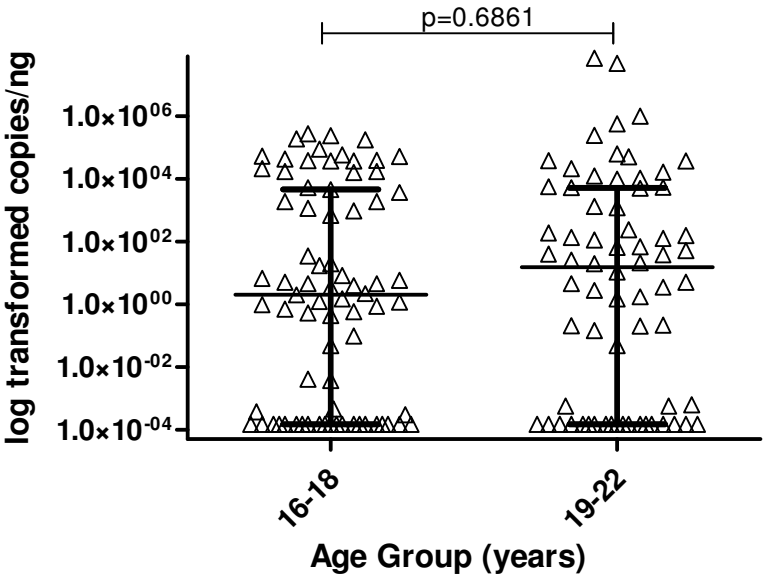

Figure 4.3.3.1: Comparison of the quantities of *L. crispatus* (log transformed copies/ng DNA) measured in the DNA extracted from vaginal lateral wall swabs from participants in the WISH study, between the two 16-18 years old and 19-22 years old age groups. All p-value comparisons were based on an unpaired, non-parametric Mann-Whitney t-test statistic. Each point in the figure represents an individual participant. The three horizontal bars represent the median value (middle bar), upper interquartile range (top bar) and lower interquartile range (bottom bar).

4.3.3.2 *Lactobacillus gasseri*

We compared the quantified copies/ng of *L. gasseri* between the age groups. The 16-18 years old age group and the 19-22 years old age group had no significant difference in log copies/ng (p=0.2991) (Figure 4.3.3.2).

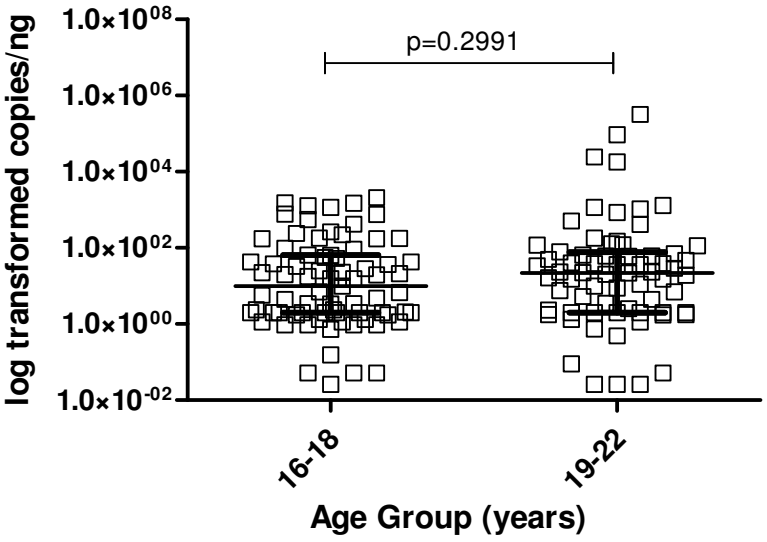

Figure 4.3.3.2: Comparison of the quantities of *L. gasseri* (log transformed copies/ng DNA) measured in the DNA extracted from vaginal lateral wall swabs from participants in the WISH study, between the two 16-18 years old and 19-22 years old age groups. All p-value comparisons were based on an unpaired, non-parametric Mann-Whitney t-test statistic. Each point in the figure represents an individual participant. The three horizontal bars represent the median value (middle bar), upper interquartile range (top bar) and lower interquartile range (bottom bar).

4.3.3.3 *Lactobacillus jensenii*

The 16-18 years old age group and the 19-22 years old age group had no significant difference in log copies/ng (p=0.7909) (Figure 4.3.3.3).

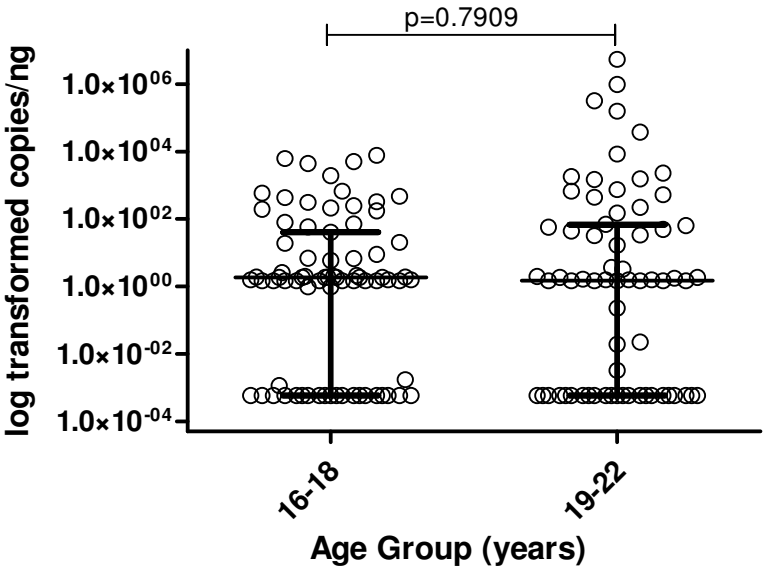

Figure 4.3.3.3: Comparison of the quantities of *L. jensenii* (log transformed copies/ng DNA) measured in the DNA extracted from vaginal lateral wall swabs from participants in the WISH study, between the two 16-18 years old and 19-22 years old age groups. All p-value comparisons were based on an unpaired, non-parametric Mann-Whitney t-test statistic. Each point in the figure represents an individual participant. The three horizontal bars represent the median value (middle bar), upper interquartile range (top bar) and lower interquartile range (bottom bar).

4.3.3.4 *Lactobacillus iners*

We compared the quantified copies/ng of *L. iners* between the age groups. The 16-18 years old age group and the 19-22 years old age group had no significant difference in log copies/ng (p=0.1664) (Figure 4.3.3.4).

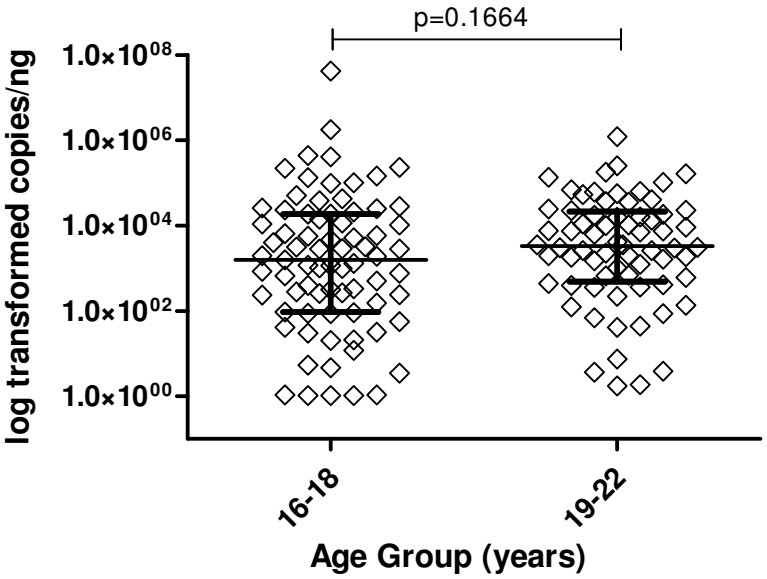

Figure 4.3.3.4: Comparison of the quantities of *L. iners* (log transformed copies/ng DNA) measured in the DNA extracted from vaginal lateral wall swabs from participants in the WISH study, between the two 16-18 years old and 19-22 years old age groups. All p-value comparisons were based on an unpaired, non-parametric Mann-Whitney t-test statistic. Each point in the figure represents an individual participant. The three horizontal bars represent the median value (middle bar), upper interquartile range (top bar) and lower interquartile range (bottom bar).

4.3.3.5 *Gardnerella vaginalis*

We compared the quantified copies/ng of *G. vaginalis* between the age groups. The 16-18 years old age group and the 19-22 years old age group had no significant difference in log copies/ng (p=0.3788) (Figure 4.3.3.5).

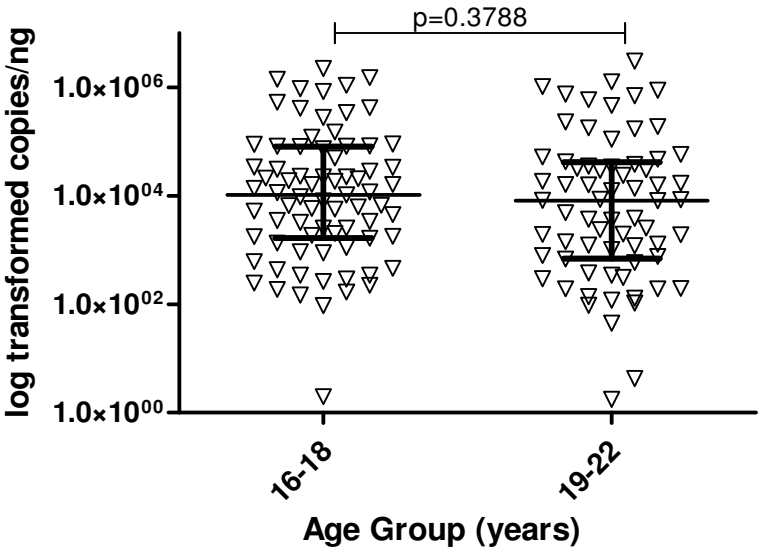

Figure 4.3.3.5: Comparison of the quantities of *G. vaginalis* (log transformed copies/ng DNA) measured in the DNA extracted from vaginal lateral wall swabs from participants in the WISH study, between the two 16-18 years old and 19-22 years old age groups. All p-value comparisons were based on an unpaired, non-parametric Mann-Whitney t-test statistic. Each point in the figure represents an individual participant. The three horizontal bars represent the median value (middle bar), upper interquartile range (top bar) and lower interquartile range (bottom bar).

Therefore, age did not influence the bacterial quantities (copies/ng) regardless of the species associated with health or dysbiosis, as the comparisons between the median quantified values of the two different age groups 16-18 years old and 19-22 years old, did not significantly differ in any way towards a particular age set. Analyzing age as continuous variable, yielded similar results.

Due to the unreliability of the qPCR amplification results, the *P. bivia* data regarding age has not been included and can be found in Appendix E: Results, page 190.

4.3.4 Association between the quantities (copies/ng) of vaginal bacteria and hormonal contraceptives

The hormonal contraceptive that each participant was using was recorded at the first visit of the WISH Cohort study process. The three hormonal contraceptives of particular interest within this study include DMPA, the Implanon and Nur Isterate.

The median copies/ng for each bacterium were compared using a Friedman's ANOVA with a Dunn's Multiple Comparison test for hormonal contraceptive use of DMPA (n=25, 18.38%), Implanon (n=9, 6.62%) and Nur Isterate (n=102, 75%). The copies/ng between the bacteria in each hormonal contraceptive usage group were significantly different to each other (ANOVA $p<0.0001$). For the p-values of the Friedman's ANOVA test with a Dunn's Multiple Comparison test run across all hormonal contraceptive usage groups, see Appendix D qPCR results, Section 2.4. Asterisk stars were used in the following figures where one start (*) indicates a p-value lower than 0.05, two stars (**) indicate a p-value lower than 0.01 and three stars (***) indicate a p-value lower than 0.001.

The copies/ng of *G. vaginalis* and *L. iners* in the DMPA (Figure 4.3.4A) and Nur Isterate (Figure 4.3.4C) hormonal contraceptive groups were significantly higher compared to *L. gasseri* ($p=0.0057$, $p<0.0001$), *L. jensenii* ($p<0.0001$, $p<0.0001$) and *L. crispatus* ($p=0.0132$, $p<0.0001$). The Implanon hormonal contraceptive (Figure 4.3.4B) had significantly higher copies/ng of *G. vaginalis* in comparison to *L. gasseri* ($p=0.0375$) *L. jensenii* ($p<0.0001$) and *L. crispatus* ($p=0.003$) with *L. iners* having significantly higher copies/ng in comparison to *L. jensenii* ($p=0.0375$). The Implanon hormonal contraceptive had the least association with the bacterial copes/ng with DMPA and Nur Isterate having similar patterns between *G. vaginalis* and *L. iners.*

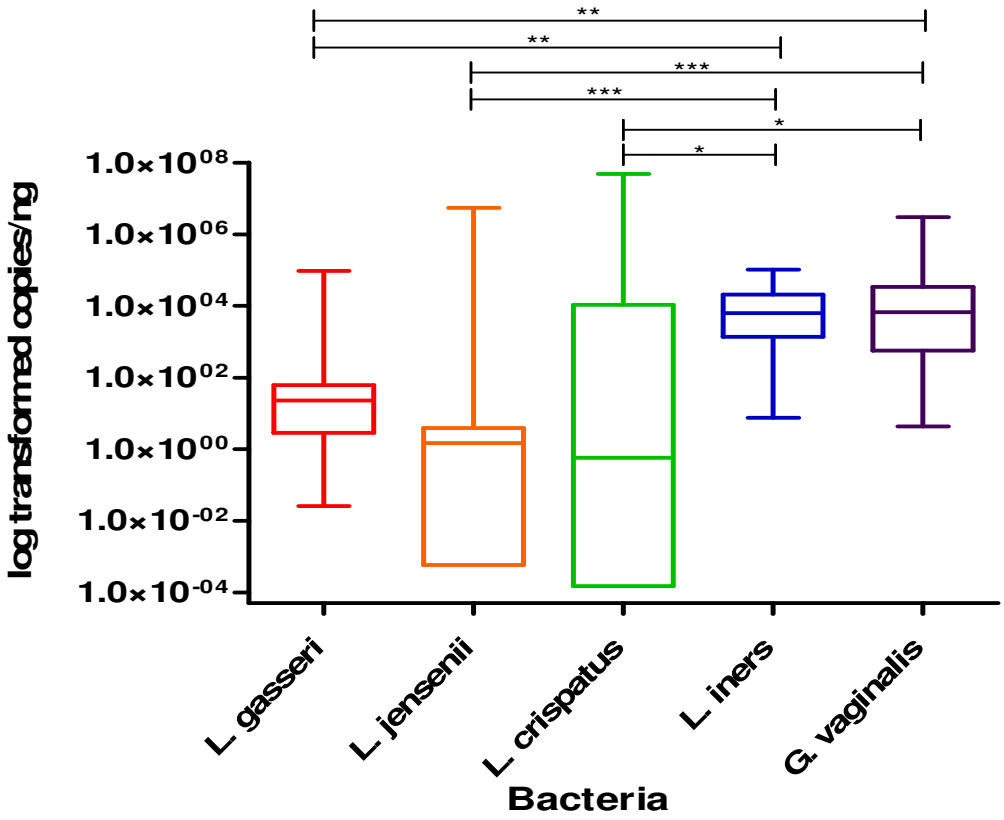

Figure 4.3.4A: Box-plot of hormonal contraceptive use of DMPA for *L. gasseri* (red), *L. jensenii* (orange), *L. crispatus* (green), *L. iners* (blue), and *G. vaginalis* (purple) reported as log transformed copies/ng total DNA. The 'box' component of each plot indicates the interquartile range (IQR) of the data set and the 'whiskers' which are the two lines (bottom and top) extending from the box component of each block that end with a horizontal stroke, indicate the range from the smallest and largest non-outliers to the 25% and 75% percentile components, respectively. The middle line indicates the median value for each data set.

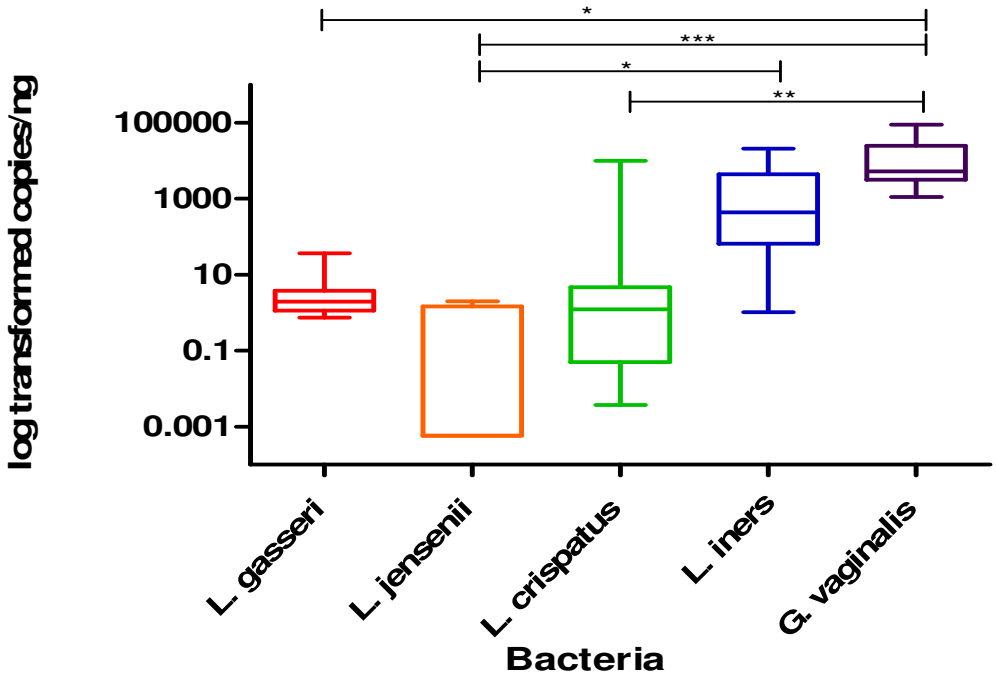

Figure 4.3.4B: Box-plot of hormonal contraceptive use of the Implanon for *L. gasseri* (red), *L. jensenii* (orange), *L. crispatus* (green), *L. iners* (blue), and *G. vaginalis* (purple) reported as log transformed copies/ng total DNA. The 'box' component of each plot indicates the interquartile range (IQR) of the data set and the 'whiskers' which are the two lines (bottom and top) extending from the box component of each block that end with a horizontal stroke, indicate the range from the smallest and largest non-outliers to the 25% and 75% percentile components, respectively. The middle line indicates the median value for each data set.

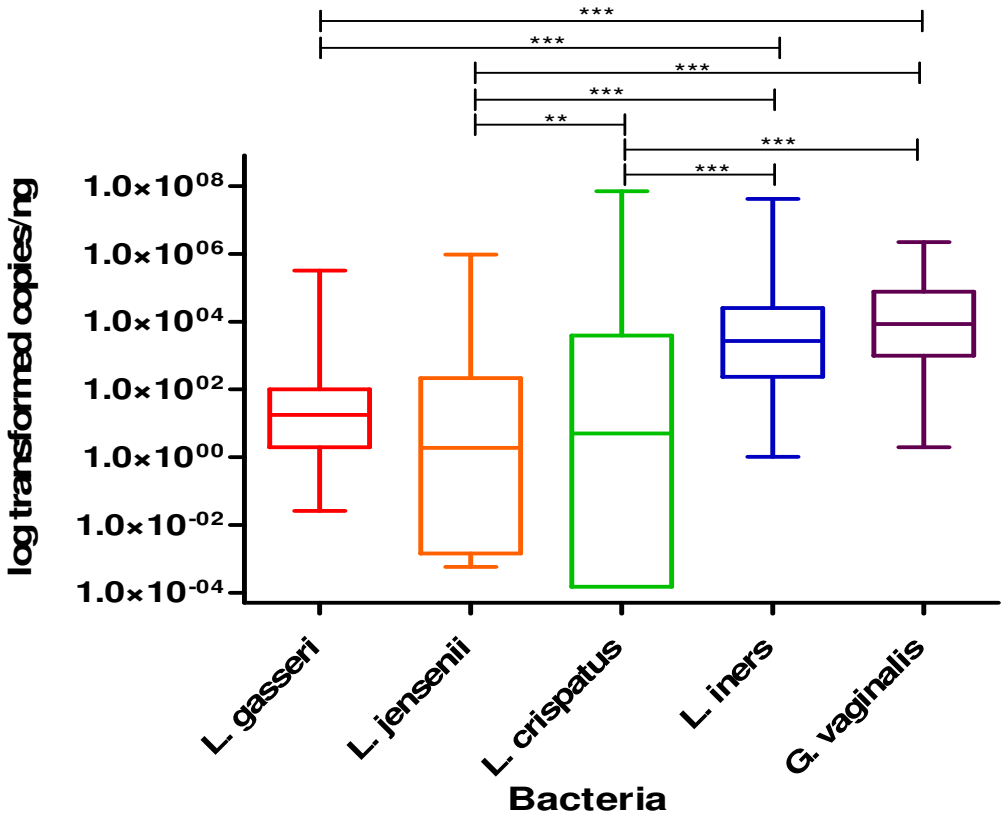

Figure 4.3.4C: Box-plot of hormonal contraceptive use of Nur Isterate for *L. gasseri* (red), *L. jensenii* (orange), *L. crispatus* (green), *L. iners* (blue), and *G. vaginalis* (purple) reported as log transformed copies/ng total DNA. The 'box' component of each plot indicates the interquartile range (IQR) of the data set and the 'whiskers' which are the two lines (bottom and top) extending from the box component of each block that end with a horizontal stroke, indicate the range from the smallest and largest non-outliers to the 25% and 75% percentile components, respectively. The middle line indicates the median value for each data set.

4.3.4.1 *Lactobacillus crispatus*

We compared the quantified log copies/ng of *L. crispatus,* and found no significant differences between the hormonal contraceptive groups (Kruskal-Wallis ANOVA p=0.276) (Figure 4.3.4.1).

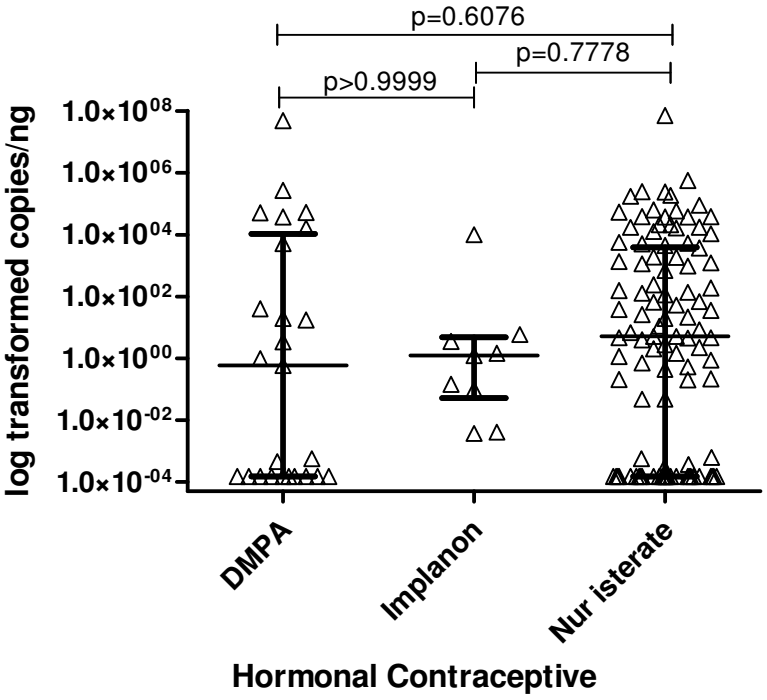

Figure 4.3.4.1: Comparison of the quantities of *L. crispatus* (log transformed copies/ng DNA) measured in the DNA extracted from vaginal lateral wall swabs from participants in the WISH study, between the hormonal contraceptives DMPA, Nur Isterate and the Implanon. All p-value comparisons were based on an unpaired, non-parametric Dunn's Multiple Comparison test. Each point in the figure represents an individual participant. The three horizontal bars represent the median value (middle bar), upper interquartile range (top bar) and lower interquartile range (bottom bar).

4.3.4.2 *Lactobacillus gasseri*

We compared the quantified log copies/ng of *L. gasseri* between the contraceptive groups, and we noted that levels of *L. gasseri* were much lower in the Implanon group that the DMPA group, but the difference did not achieve statistical significance (Kruskal-Wallis ANOVA p=0.0918) (Figure 4.3.4.2).

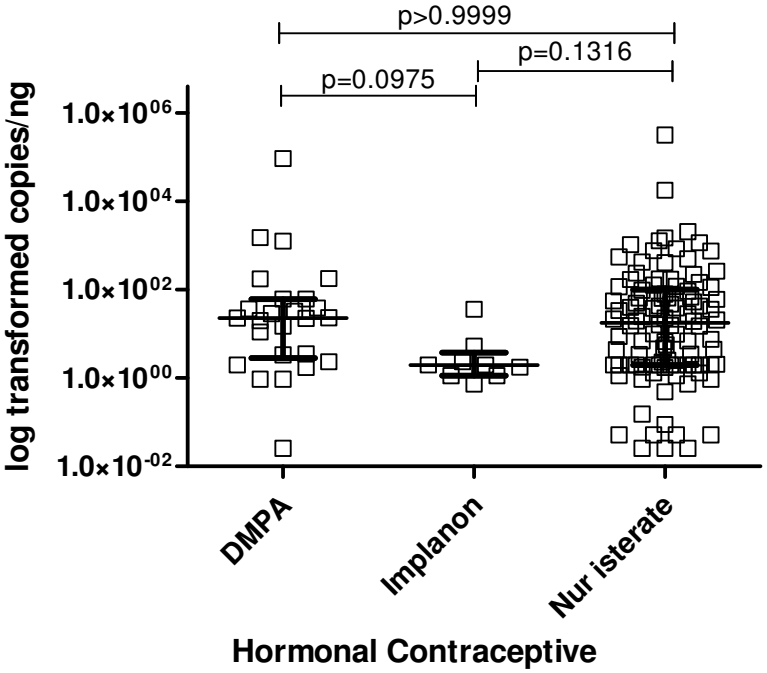

Figure 4.3.4.2: Comparison of the quantities of *L. gasseri* (log transformed copies/ng DNA) measured in the DNA extracted from vaginal lateral wall swabs from participants in the WISH study, between hormonal contraceptives DMPA, Nur Isterate and the Implanon. All p-value comparisons were based on an unpaired, non-parametric Dunn's Multiple Comparison test. Each point in the figure represents an individual participant. The three horizontal bars represent the median value (middle bar), upper interquartile range (top bar) and lower interquartile range (bottom bar).

4.3.4.3 *Lactobacillus jensenii*

We compared the quantified log copies/ng of *L. jensenii* between the hormonal contraceptive groups, which had an overall significant difference (Kruskal-Wallis ANOVA p=0.0222) (Figure 4.3.4.3).

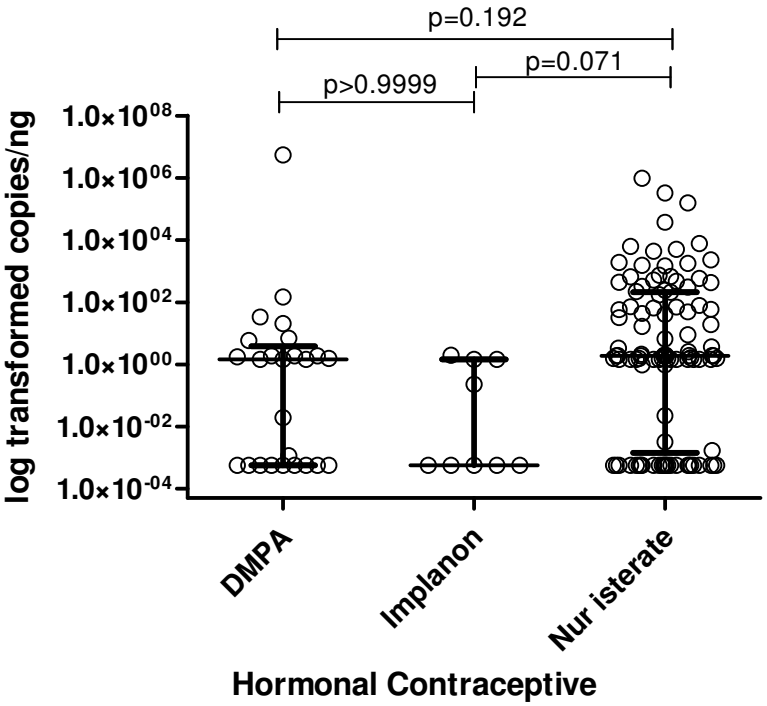

Figure 4.3.4.3: Comparison of the quantities of *L. jensenii* (log transformed copies/ng DNA) measured in the DNA extracted from vaginal lateral wall swabs from participants in the WISH study, between hormonal contraceptives DMPA, Nur Isterate and the Implanon. All p-value comparisons were based on an unpaired, non-parametric Dunn's Multiple Comparison test. Each point in the figure represents an individual participant. The three horizontal bars represent the median value (middle bar), upper interquartile range (top bar) and lower interquartile range (bottom bar).

4.3.4.4 *Lactobacillus iners*

We compared the quantified log copies/ng of *L. iners* and found no significant differences between the hormonal contraceptive groups (Kruskal-Wallis ANOVA p=0.1721) (Figure 4.3.4.4).

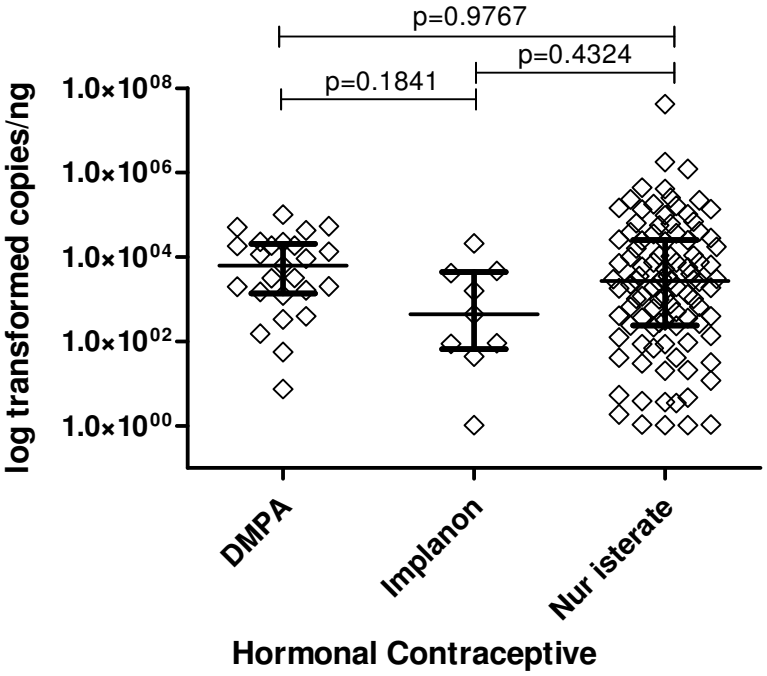

Figure 4.3.4.4: Comparison of the quantities of *L. iners* (log transformed copies/ng DNA) measured in the DNA extracted from vaginal lateral wall swabs from participants in the WISH study, between hormonal contraceptives DMPA, Nur Isterate and the Implanon. All p-value comparisons were based on an unpaired, non-parametric Dunn's Multiple Comparison test. Each point in the figure represents an individual participant. The three horizontal bars represent the median value (middle bar), upper interquartile range (top bar) and lower interquartile range (bottom bar).

4.3.4.5 *Gardnerella vaginalis*

We compared the quantified log copies/ng of *G. vaginalis,* and found no difference between the hormonal contraceptive groups (Kruskal-Wallis ANOVA p=0.9144) (Figure 4.3.4.5).

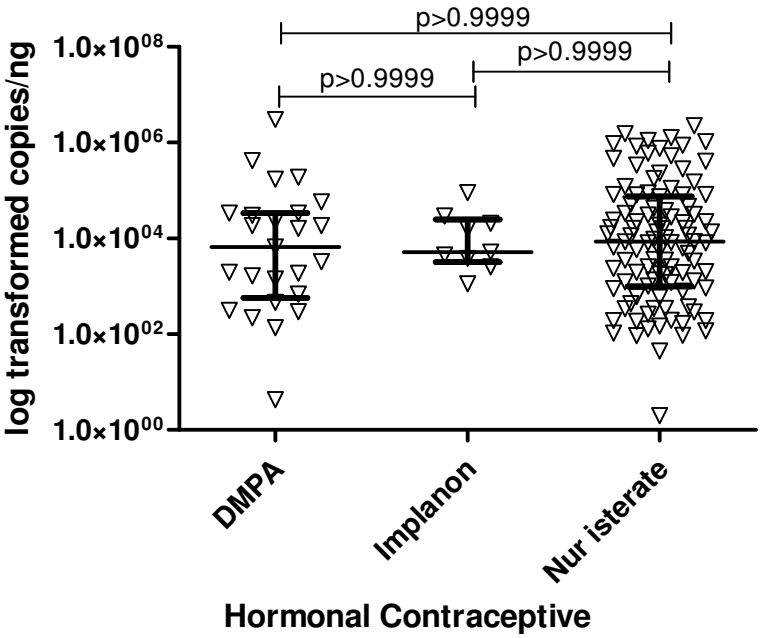

Figure 4.3.4.5: Comparison of the quantities of *G. vaginalis* (log transformed copies/ng DNA) measured in the DNA extracted from vaginal lateral wall swabs from participants in the WISH study, between the hormonal contraceptives DMPA, Nur Isterate and the Implanon. All p-value comparisons were based on an unpaired, non-parametric Dunn's Multiple Comparison test. Each point in the figure represents an individual participant. The three horizontal bars represent the median value (middle bar), upper interquartile range (top bar) and lower interquartile range (bottom bar).

Therefore, the hormonal contraceptives DMPA, Implanon and Nur Isterate showed no patterns of significantly different copies/ng of bacteria, except for an overall significant Kruskal-Wallis statistic for *L. jensenii* (p=0.00222). There is no specific association between the hormonal contraceptive usage and bacterial log copes/ng. However, the sample size for Implanon was small and as such the computing power of the Kruskal-Wallis statistic could be less accurate than with a larger sample size due to weakened statistical power. Thus it can be postulated that the

type of hormonal contraceptive used by female adolescents does not have a direct impact on the FGT microbiota.

Due to the unreliability of the qPCR amplification results, the *P. bivia* data regarding hormonal contraceptives has not been included and can be found in Appendix E: Results, page 192.

4.3.5 Association between the quantities (copies/ng) of the bacteria of interest and the absence or presence of any one STI in the WISH cohort

The STI status was determined based on the absence or presence of any one bacterial (*Chlamydia trachomatis, Neisseria gonorrhea,* and *Mycoplasma genitalium*), viral (Herpes Simplex Virus 2, and Human Papilloma Virus) or parasitic (*Trichomonas vaginalis*) STI for each participant.

The median copies/ng for each bacterium were compared using a Friedman's ANOVA with a Dunn's Multiple Comparison test for the absence or presence of any one STI. The bacterial copies/ng in the women with (n=78, 55.71%) and without (n=62, 44.29%) any one STI were significantly different to each other (ANOVA $p<0.0001$). For the p-values of the Friedman's ANOVA test with a Dunn's Multiple Comparison test run across both STI groups, see Appendix D qPCR results, Section 2.5. Asterisk stars were used in the following figures where one start (*) indicates a p-value lower than 0.05, two stars (**) indicate a p-value lower than 0.01 and three stars (***) indicate a p-value lower than 0.001.

In the absence of any one STI (Figure 4.3.5A), *G. vaginalis* and *L. iners* had a significant higher in copies/ng with a p-value of >0.0001 in comparison to *L. gasseri, L. jensenii* and *L. crispatus.* The same pattern was followed by *G. vaginalis* and *L. iners* in the presence of any one STI (Figure 4.3.5B), except *L. iners* had significantly higher p-value of 0.0002 compared to *L. crispatus,* which in turn was significantly higher to *L. jensenii* (p=0.0079). The absence of or presence of any one STI is similar to the overall cohort.

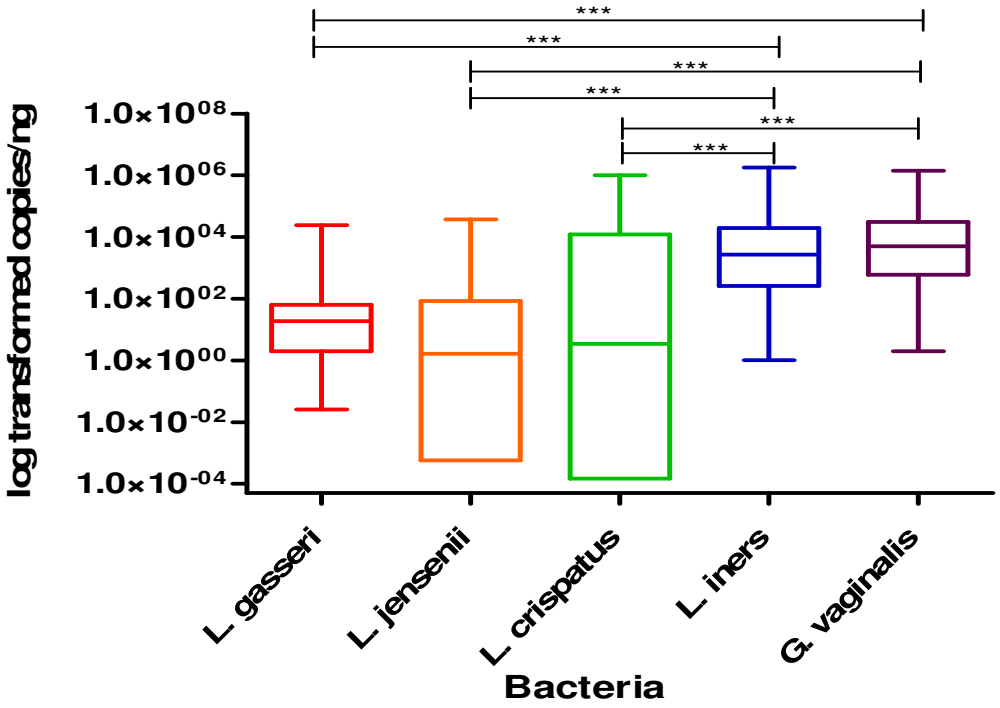

Figure 4.3.5A: Box-plot of the absence of any one STI for *L. gasseri* (red), *L. jensenii* (orange), *L. crispatus* (green), *L. iners* (blue), and *G. vaginalis* (purple) reported as log transformed copies/ng total DNA. The 'box' component of each plot indicates the interquartile range (IQR) of the data set and the 'whiskers' which are the two lines (bottom and top) extending from the box component of each block that end with a horizontal stroke, indicate the range from the smallest and largest non-outliers to the 25% and 75% percentile components, respectively. The middle line indicates the median value for each data set.

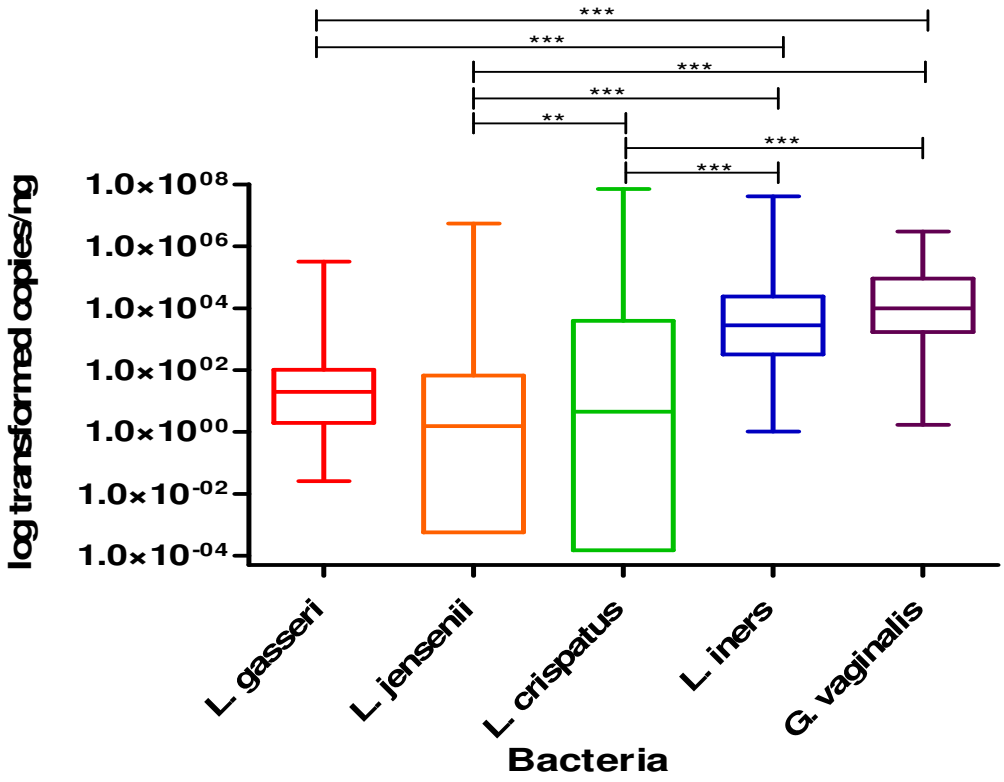

Figure 4.3.5B: Box-plot of the presence of any one STI for *L. gasseri* (red), *L. jensenii* (orange), *L. crispatus* (green), *L. iners* (blue), and *G. vaginalis* (purple) reported as log transformed copies/ng total DNA. The 'box' component of each plot indicates the interquartile range (IQR) of the data set and the 'whiskers' which are the two lines (bottom and top) extending from the box component of each block that end with a horizontal stroke, indicate the range from the smallest and largest non-outliers to the 25% and 75% percentile components, respectively. The middle line indicates the median value for each data set.

4.3.5.1 *Lactobacillus crispatus*

We compared the quantified log copies/ng of *L. crispatus,* and found no difference between the participants with and without any one STI (p=0.9655) (Figure 4.3.5.1).

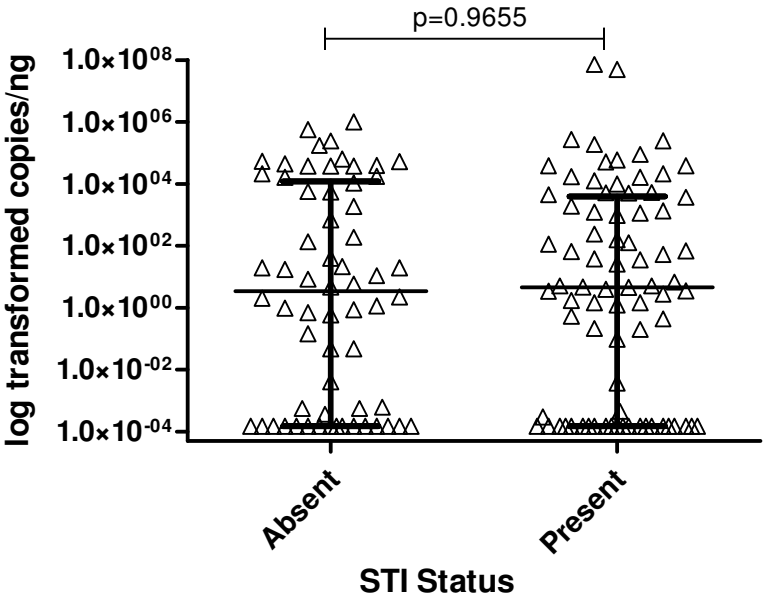

Figure 4.3.5.1: Comparison of the quantities of *L. crispatus* (log transformed copies/ng DNA) measured in the DNA extracted from vaginal lateral wall swabs from participants in the WISH study, where the samples have been separated based on absence or presence of any one of the WISH cohort STIs present. All p-value comparisons were based on an unpaired, non-parametric Mann-Whitney t-test statistic. Each point in the figure represents an individual participant. The three horizontal bars represent the median value (middle bar), upper interquartile range (top bar) and lower interquartile range (bottom bar).

4.3.5.2 *Lactobacillus gasseri*

We compared the quantified log copies/ng of *L. gasseri* and found no significant differences between the participants with and without any one STI (p=0.6386) (Figure 4.3.5.2).

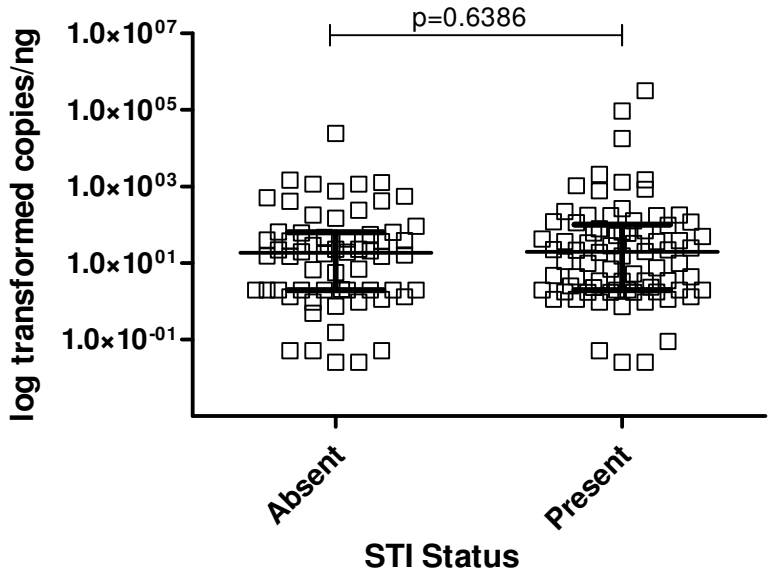

Figure 4.3.5.2: Comparison of the quantities of *L. gasseri* (log transformed copies/ng DNA) measured in the DNA extracted from vaginal lateral wall swabs from participants in the WISH study, where the samples have been separated based on absence or presence of any one of the WISH cohort STIs present. All p-value comparisons were based on an unpaired, non-parametric Mann-Whitney t-test statistic. Each point in the figure represents an individual participant. The three horizontal bars represent the median value (middle bar), upper interquartile range (top bar) and lower interquartile range (bottom bar).

4.3.5.3 *Lactobacillus jensenii*

We compared the quantified log copies/ng of *L. jensenii* and found no difference between the participants with and without any one STI (p=0.735) (Figure 4.3.5.3).

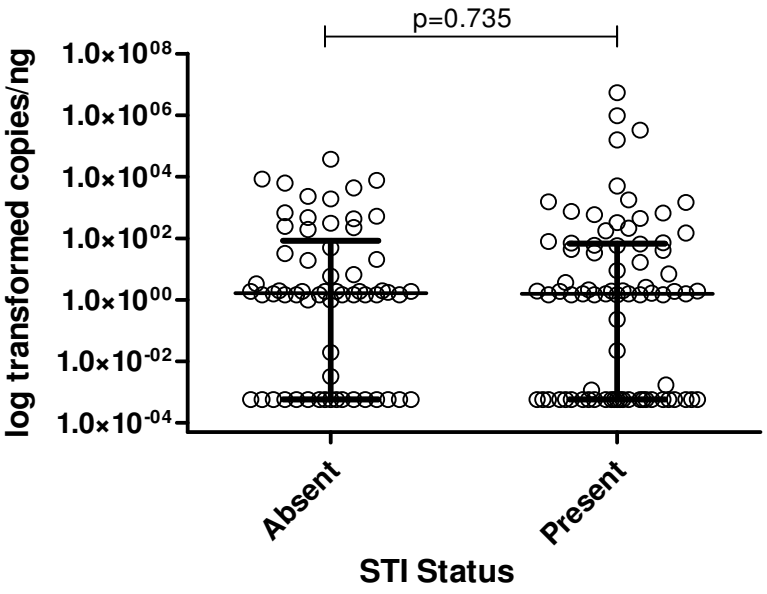

Figure 4.3.5.3: Comparison of the quantities of *L. jensenii* (log transformed copies/ng DNA) measured in the DNA extracted from vaginal lateral wall swabs from participants in the WISH study, where the samples have been separated based on absence or presence of any one of the WISH cohort STIs present. All p-value comparisons were based on an unpaired, non-parametric Mann-Whitney t-test statistic. Each point in the figure represents an individual participant. The three horizontal bars represent the median value (middle bar), upper interquartile range (top bar) and lower interquartile range (bottom bar).

4.3.5.4 *Lactobacillus iners*

We compared the quantified log copies/ng of *L. iners* and found no difference between the participants with and without any one STI (p=0.9525) (Figure 4.3.5.4).

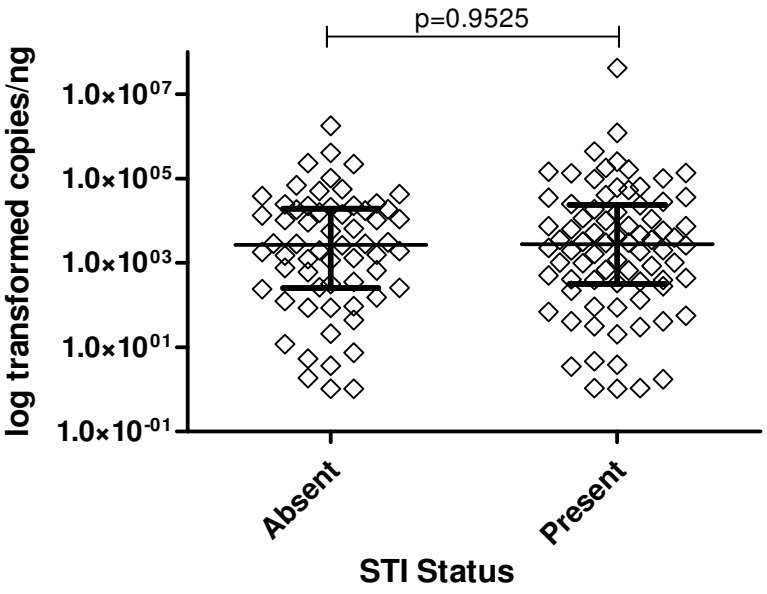

Figure 4.3.5.4: Comparison of the quantities of *L. iners* (log transformed copies/ng DNA) measured in the DNA extracted from vaginal lateral wall swabs from participants in the WISH study, where the samples have been separated based on absence or presence of any one of the WISH cohort STIs present. All p-value comparisons were based on an unpaired, non-parametric Mann-Whitney t-test statistic. Each point in the figure represents an individual participant. The three horizontal bars represent the median value (middle bar), upper interquartile range (top bar) and lower interquartile range (bottom bar).

4.3.5.5 *Gardnerella vaginalis*

We compared the quantified log copies/ng of *G. vaginalis* and found no significant differences between the participants with and without any one STI (p=0.1040) (Figure 4.3.5.5).

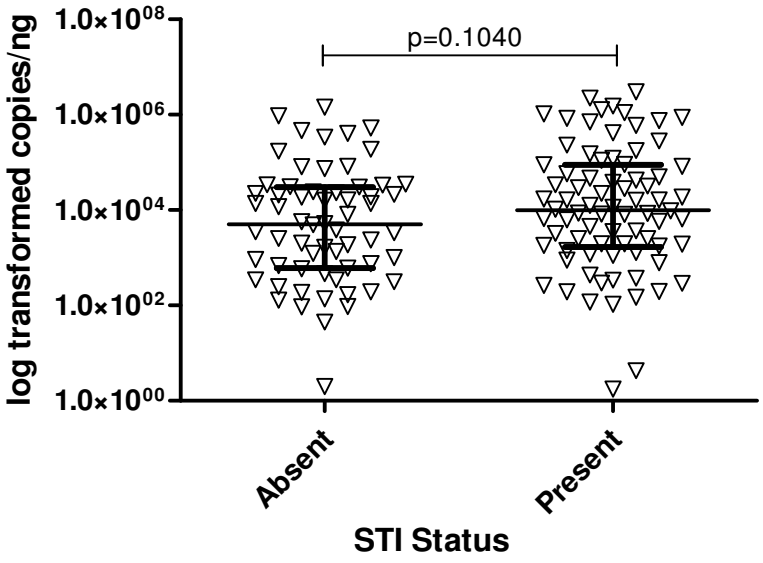

Figure 4.3.5.5: Comparison of the quantities of *G. vaginalis* (log transformed copies/ng DNA) measured in the DNA extracted from vaginal lateral wall swabs from participants in the WISH study, where the samples have been separated based on absence or presence of any one of the WISH cohort STIs present. All p-value comparisons were based on an unpaired, non-parametric Mann-Whitney t-test statistic. Each point in the figure represents an individual participant. The three horizontal bars represent the median value (middle bar), upper interquartile range (top bar) and lower interquartile range (bottom bar).

Therefore, the absence of, or presence of any one of the STIs i.e. bacterial (*Chlamydia trachomatis, Neisseria gonorrhea,* and *Mycoplasma genitalium*), viral (Herpes Simplex Virus 2, and Human Papilloma Virus) or parasitic (*Trichomonas vaginalis*), showed no association with the copies/ng of *L. crispatus, L. gasseri, L. jensenii, L. iners*, *G. vaginalis,* and *P. bivia.* This could correlate with a lack of interaction between the STIs and the bacterium studied in this cohort within the FGT.

Due to the unreliability of the qPCR amplification results, the *P. bivia* data regarding STIs has not been included and can be found in Appendix E: Results, page 193.

4.3.6 Association between the quantities (copies/ng) of the bacteria of interest and the presence of bacterial or viral STIs in the WISH cohort

The STI status was determined based on the sum value of the presence or absence of all bacterial (*Chlamydia trachomatis, Neisseria gonorrhea,* and *Mycoplasma genitalium*), or viral (Herpes Simplex Virus 2, and Human Papilloma Virus) for each participant within the WISH cohort.

The median copies/ng for each bacterium were compared using a Friedman's ANOVA with a Dunn's Multiple Comparison test for the absence (n=77, 53.85%), presence of one (n=51, 35.66%) or presence of two or more (n=15, 10.49%) bacterial STIs. Further, the median copies/ng for each bacterium were compared using a Friedman's ANOVA with a Dunn's Multiple Comparison test for the absence (n=46, 32.17%), presence of one (n=91, 63.63%) or presence of two (n=6, 4.20%) viral STIs. There was an overall significant difference between the copies/ng of the bacteria in the bacterial STI groups (ANOVA $p<0.0001$). The ANOVA tests were significantly different for copies/ng of the bacteria in both the absence of and presence of one viral STI ($p<0.0001$) and the presence of two viral STIs ($p=0.0162$). The figures comparing the bacterium copies/ng per bacterial and viral STI group followed the same trends as the absence or presence of any one STI as well as the overall cohort and as such have not been included within this chapter. For the representative figures and p-values of the Friedman's ANOVA test with a Dunn's Multiple Comparisons run across the bacterial and viral STI groups, see Appendix D qPCR results, Section 2.6.

4.3.6.1 *Lactobacillus crispatus*

We compared log copies/ng of *L. crispatus* between those with none, one or two (or more) bacterial or viral STI groups. There was no significant difference in *L. crispatus* between the bacterial STI groups (Kruskal-Wallis ANOVA p=0.8469). There was no significant difference in *L. crispatus* between the viral STI groups (Kruskal-Wallis ANOVA p=0.2327) (Figure 4.3.6.1)

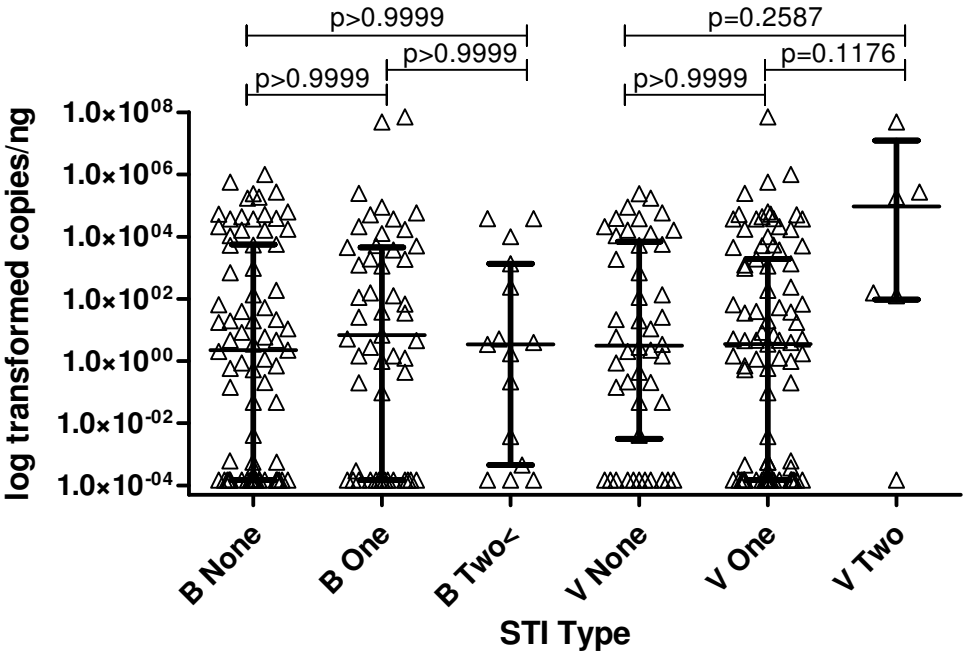

Figure 4.3.6.1: Comparison of the quantities of *L. crispatus* (log transformed copies/ng DNA) measured in the DNA extracted from vaginal lateral wall swabs from participants in the WISH study, where the samples have been separated based on none, one, two (or more <) of the WISH cohort Bacterial (B) versus Viral (V) STIs being present. All p-value comparisons were based on an unpaired, non-parametric Dunn's Multiple Comparison test. Each point in the figure represents an individual participant. The three horizontal bars represent the median value (middle bar), upper interquartile range (top bar) and lower interquartile range (bottom bar).

4.3.6.2 *Lactobacillus gasseri*

We compared the quantified log copies/ng of *L. gasseri* between those with none, one or two (or more) bacterial or viral STI groups. There was no significant difference in *L. gasseri* between the bacterial STI groups (Kruskal-Wallis ANOVA p=0.8184) and the viral STI groups (Kruskal-Wallis ANOVA p=0.2327) (Figure 4.3.6.2).

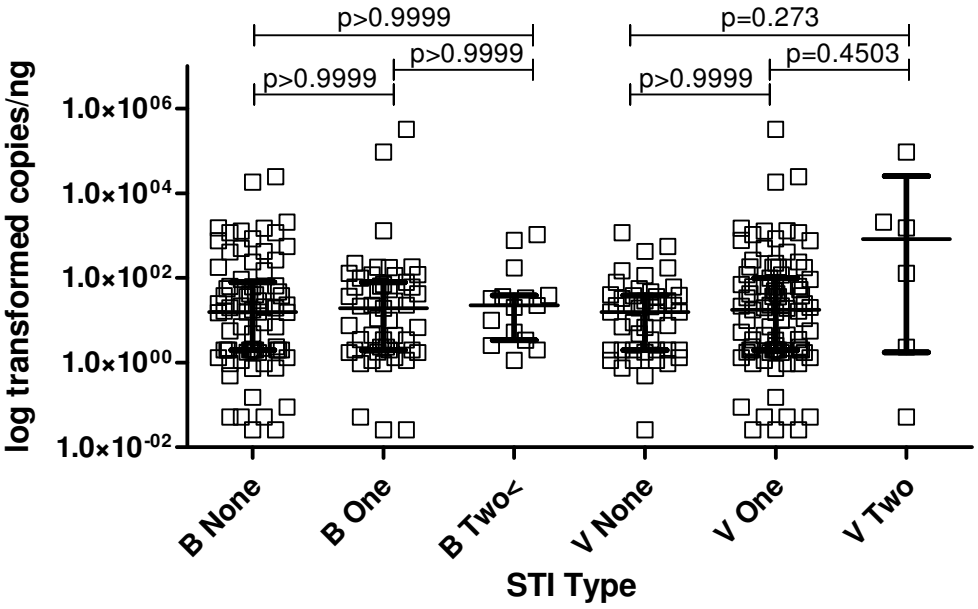

Figure 4.3.6.2: Comparison of the quantities of *L. gasseri* (log transformed copies/ng DNA) measured in the DNA extracted from vaginal lateral wall swabs from participants in the WISH study, where the samples have been separated based on none, one, two (or more <) of the WISH cohort Bacterial (B) versus Viral (V) STIs being present. All p-value comparisons were based on an unpaired, non-parametric Dunn's Multiple Comparison test. Each point in the figure represents an individual participant. The three horizontal bars represent the median value (middle bar), upper interquartile range (top bar) and lower interquartile range (bottom bar).

4.3.6.3 *Lactobacillus jensenii*

We compared the quantified log copies/ng of *L. jensenii* between those with none, one or two (or more) bacterial or viral STI groups. The bacterial STI groups had no significant difference in *L. jensenii* between the bacterial STI groups (Kruskal-Wallis ANOVA p=0.4743) and the viral STI groups (Kruskal-Wallis ANOVA p=0.2219) (Figure 4.3.6.3).

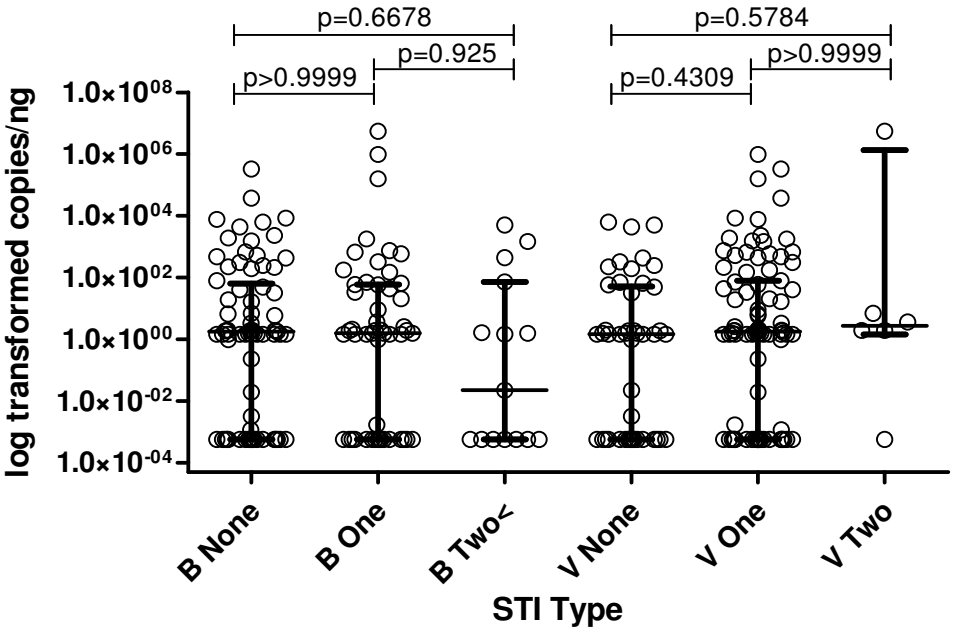

Figure 4.3.6.3: Comparison of the quantities of *L. jensenii* (log transformed copies/ng DNA) measured in the DNA extracted from vaginal lateral wall swabs from participants in the WISH study, where the samples have been separated based on none, one, two (or more <) of the WISH cohort Bacterial (B) versus Viral (V) STIs being present. All p-value comparisons were based on an unpaired, non-parametric Dunn's Multiple Comparison test. Each point in the figure represents an individual participant. The three horizontal bars represent the median value (middle bar), upper interquartile range (top bar) and lower interquartile range (bottom bar).

4.3.6.4 *Lactobacillus iners*

We compared the quantified log copies/ng of *L. iners* between those with none, one or two (or more) bacterial or viral STI groups. Both the bacterial and viral STI groups had no significant difference in *L. iners* (Kruskal-Wallis ANOVA p=0.5727 and p=0.7316, respectively) (Figure 4.3.6.4).

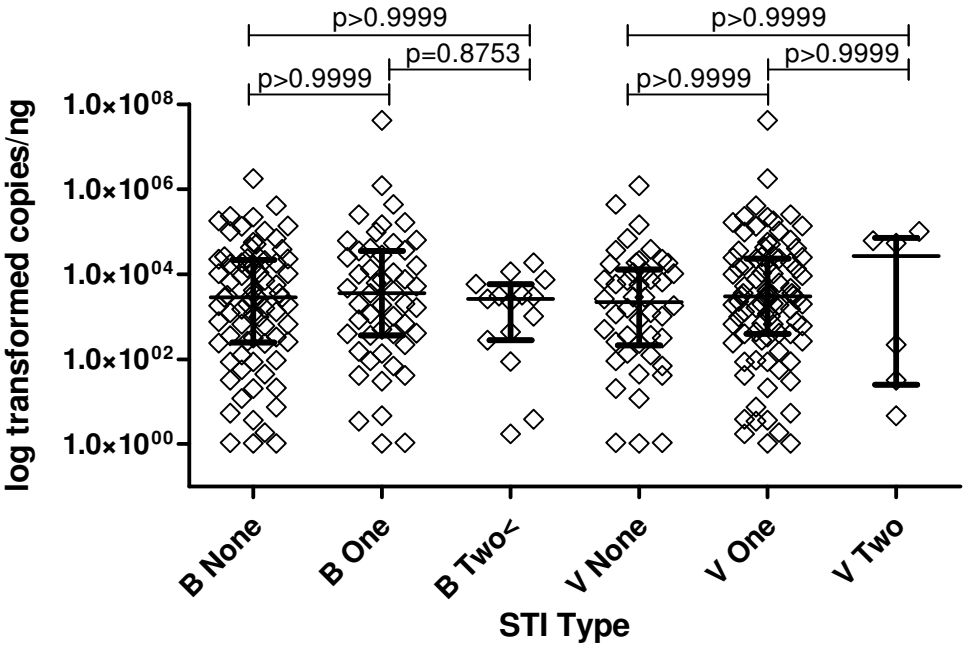

Figure 4.3.6.4: Comparison of the quantities of *L. iners* (log transformed copies/ng DNA) measured in the DNA extracted from vaginal lateral wall swabs from participants in the WISH study, where the samples have been separated based on none, one, two (or more <) of the WISH cohort Bacterial (B) versus Viral (V) STIs being present. All p-value comparisons were based on an unpaired, non-parametric Dunn's Multiple Comparison test. Each point in the figure represents an individual participant. The three horizontal bars represent the median value (middle bar), upper interquartile range (top bar) and lower interquartile range (bottom bar).

4.3.6.5 *Gardnerella vaginalis*

We compared the quantified log copies/ng of *G. vaginalis* between those with none, one or two (or more) bacterial or viral STI groups. In the bacterial STI groups there was no significant difference in *G. vaginalis* (Kruskal-Wallis ANOVA p=0.2239). The group with two viral STIs had significantly different copies/ng of *G. vaginalis* compared to no viral STI (p=0.0098) and one viral STI (p=0.0324). There was an overall significant difference in *G. vaginalis* between the viral STI groups (Kruskal-Wallis ANOVA p=0.0126) (Figure 4.3.6.5). This significance could be skewed due to the reduced participants with two viral STIs.

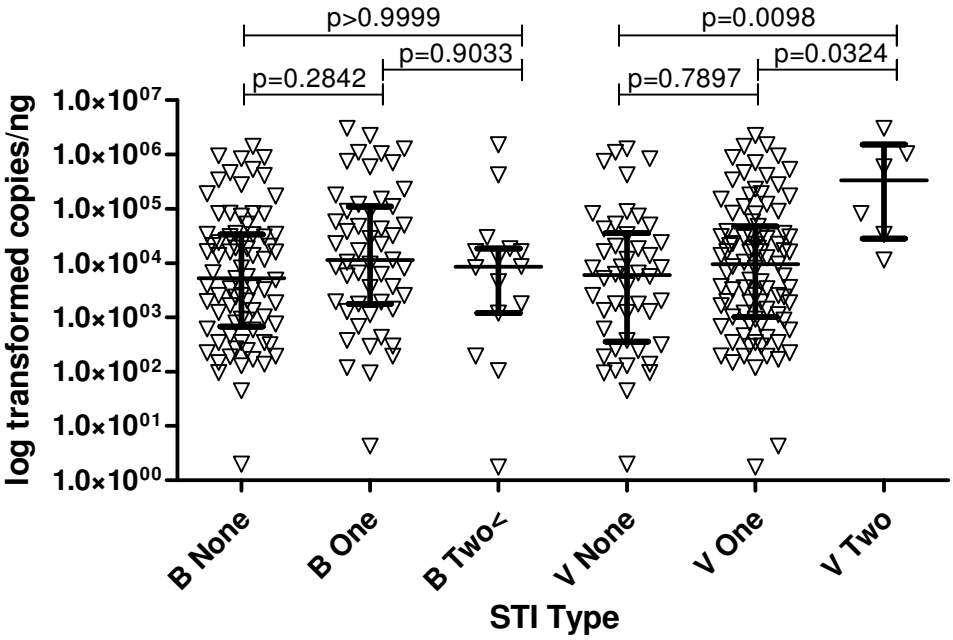

Figure 4.3.6.5: Comparison of the quantities of *G. vaginalis* (log transformed copies/ng DNA) measured in the DNA extracted from vaginal lateral wall swabs from participants in the WISH study, where the samples have been separated based on none, one, two (or more <) of the WISH cohort Bacterial (B) versus Viral (V) STIs being present. All p-value comparisons were based on an unpaired, non-parametric Dunn's Multiple Comparison test. Each point in the figure represents an individual participant. The three horizontal bars represent the median value (middle bar), upper interquartile range (top bar) and lower interquartile range (bottom bar).

The above figures thus indicate that the presence of none, one or two or more bacterial STIs (*Chlamydia trachomatis, Neisseria gonorrhea,* and *Mycoplasma genitalium),* have no association

with the copies/ng of *L. crispatus, L. gasseri, L. jensenii, L. iners, G. vaginalis* and *P. bivia*. The absence or presence of one or two viral STIs (Herpes Simplex Virus 2, and Human Papilloma Virus) showed no association with the copies/ng of *L. crispatus, L. gasseri, L. jensenii,* and *L. iners*. There was an association between the presence of two viral STIs and the copies/ng of *G. vaginalis* and *P. bivia,* which was not seen in the comparison of the copies/ng of the bacteria within the group. However, this could be due to the low participant number within the group and the statistical significance may decrease with an increase in number of participants. The bacterial and viral STI groups had increased copies/ng of *G. vaginalis* and *L. iners* in comparison to the other four bacteria. From this data it can be estimated that neither the absence, nor the increasing presence of bacterial or viral STIs have any association with the copies/ng of the bacterium quantified in this cohort.

Due to the unreliability of the qPCR amplification results, the *P. bivia* data regarding bacterial and viral STIs has not been included and can be found in Appendix E: Results, page 201.

4.3.7 Association between the quantities (copies/ng) of bacteria of interest and the absence or presence of low and high risk HPV subtypes in the WISH cohort

The HPV status was considered negative in the absence of all HPV subtypes amplified by the Roche linear array, low risk if 6, 11, 40, 42, 54, 55, 61, 62, 64, 67, 69, 70, 71, 72, 81, 83, 84, 89(CP6109) and IS39 HPV subtypes were present, and high risk if 16, 18, 26, 31, 33, 35, 39, 45, 51, 52, 53, 56, 58, 59, 66, 68, 73 and 82 HPV subtypes were present.

The median copies/ng for each bacterium were compared using a Friedman's ANOVA with a Dunn's Multiple Comparison test for the negative (n=29, 32.22%), low risk (n=27, 30%) and high risk (n=34, 37.78%) HPV groups. The comparison of the copies/ng between the bacteria in each category, were significantly different to each other overall (ANOVA $p<0.0001$). For the p-values of the Friedman's ANOVA test with a Dunn's Multiple Comparison test run across the HPV groups, see Appendix D qPCR results, Section 2.7. Asterisk stars were used in the following figures where one start (*) indicates a p-value lower than 0.05, two stars (**) indicate a p-value lower than 0.01 and three stars (***) indicate a p-value lower than 0.001.

Within the negative HPV group (Figure 4.3.7A), *G. vaginalis* and *L. iners* had significantly higher copies/ng in comparison to *L. gasseri* (p=0.0023) and *L. jensenii* (p<0.0001), with *L. crispatus* having a significantly higher copies/ng with p=0.0023 in comparison to *L. jensenii.* Within the low risk HPV group (Figure 4.3.7B), *G. vaginalis* and *L. iners* were significantly higher than *L. jensenii* (p<0.0001), *L. crispatus* (p<0.0001) and *L. gasseri* (p=0.0001, p=0.0017 respectively). *G. vaginalis* and *L. iners* were significantly higher than *L. jensenii* (p<0.0001) and *L. gasseri* (p<0.0001) in the high risk HPV group (Figure 4.3.7C) with *G. vaginalis* and *L. crispatus* showing significantly higher copies/ng in comparison to *L. crispatus* (p=0.00112) and *L. jensenii* (p=0.0089) respectively. The low and high risk HPV groups showed similar trends in the copies/ng of the bacteria with only a slight difference with *L. crispatus* in relation to the negative HPV group.

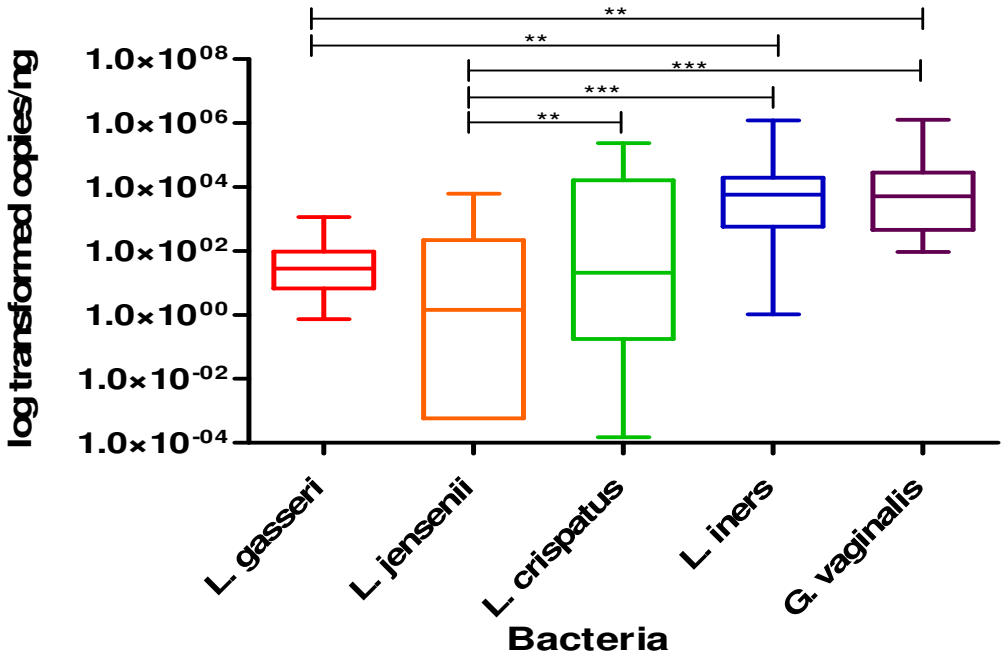

Figure 4.3.7A: Box-plot of the negative HPV group for *L. gasseri* (red), *L. jensenii* (orange), *L. crispatus* (green), *L. iners* (blue), and *G. vaginalis* (purple) reported as log transformed copies/ng total DNA. The 'box' component of each plot indicates the interquartile range (IQR) of the data set and the 'whiskers' which are the two lines (bottom and top) extending from the box component of each block that end with a horizontal stroke, indicate the range from the smallest and largest non-outliers to the 25% and 75% percentile components, respectively. The middle line indicates the median value for each data set.

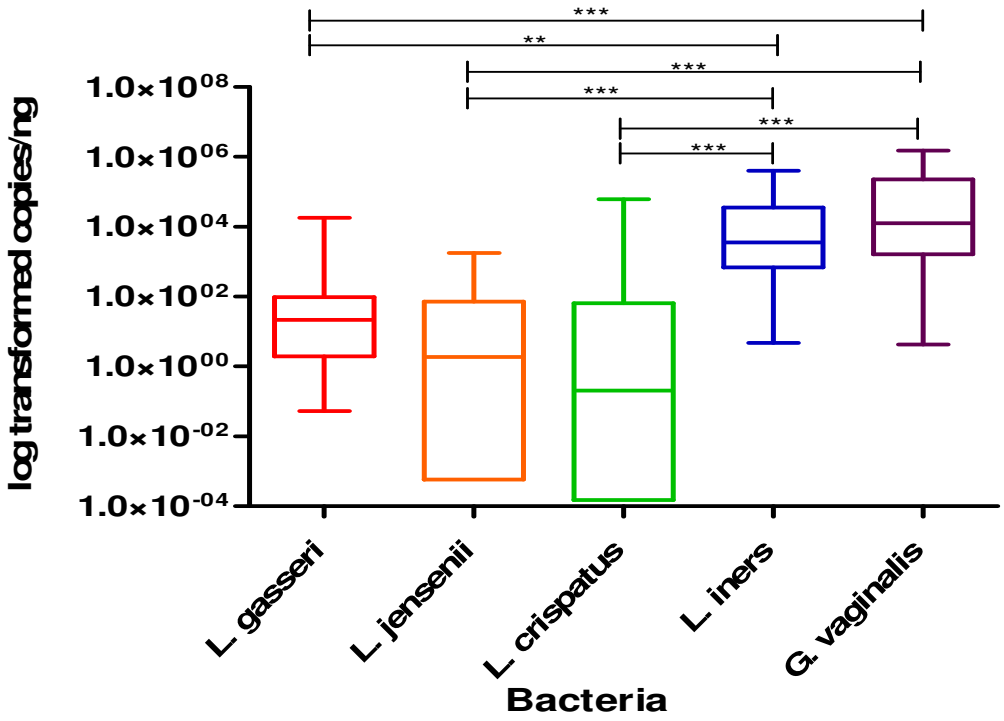

Figure 4.3.7B: Box-plot of the low risk HPV group for *L. gasseri* (red), *L. jensenii* (orange), *L. crispatus* (green), *L. iners* (blue), and *G. vaginalis* (purple) reported as log transformed copies/ng total DNA. The 'box' component of each plot indicates the interquartile range (IQR) of the data set and the 'whiskers' which are the two lines (bottom and top) extending from the box component of each block that end with a horizontal stroke, indicate the range from the smallest and largest non-outliers to the 25% and 75% percentile components, respectively. The middle line indicates the median value for each data set.

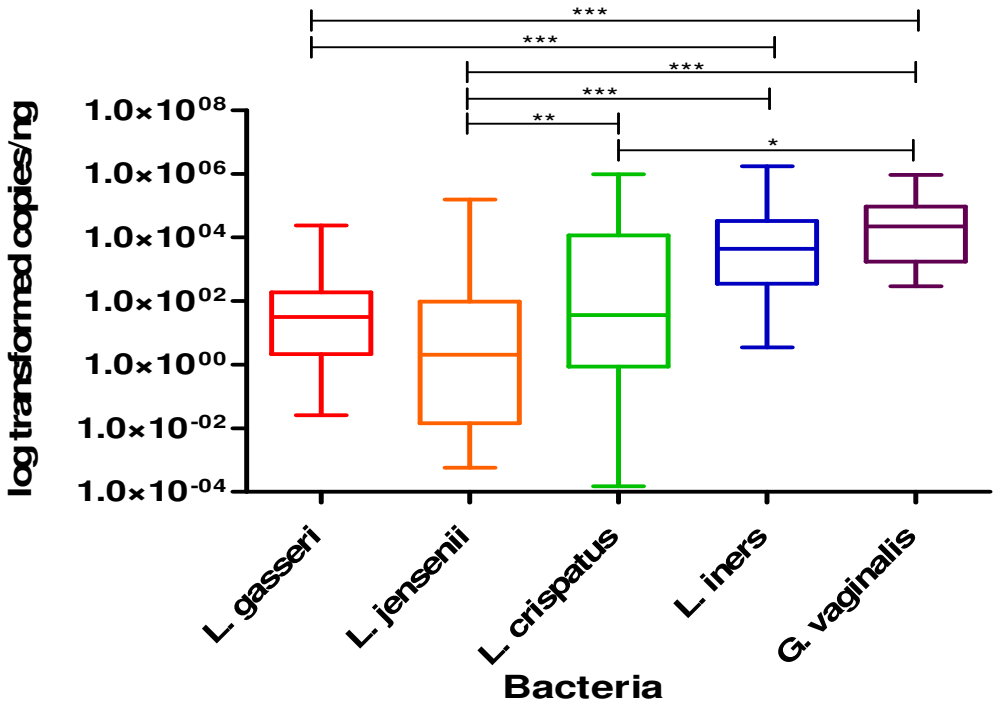

Figure 4.3.7C: Box-plot of the high risk HPV group for *L. gasseri* (red), *L. jensenii* (orange), *L. crispatus* (green), *L. iners* (blue), and *G. vaginalis* (purple) reported as log transformed copies/ng total DNA. The 'box' component of each plot indicates the interquartile range (IQR) of the data set and the 'whiskers' which are the two lines (bottom and top) extending from the box component of each block that end with a horizontal stroke, indicate the range from the smallest and largest non-outliers to the 25% and 75% percentile components, respectively. The middle line indicates the median value for each data set.

4.3.7.1 *Lactobacillus crispatus*

The log copies/ng of *L. crispatus* within the high risk HPV group were significantly higher than the copies/ng in the low risk HPV group. There was an overall significant difference in *L. crispatus* between the HPV groups (Kruskal-Wallis ANOVA p=0.0145) (Figure 4.3.7.1).

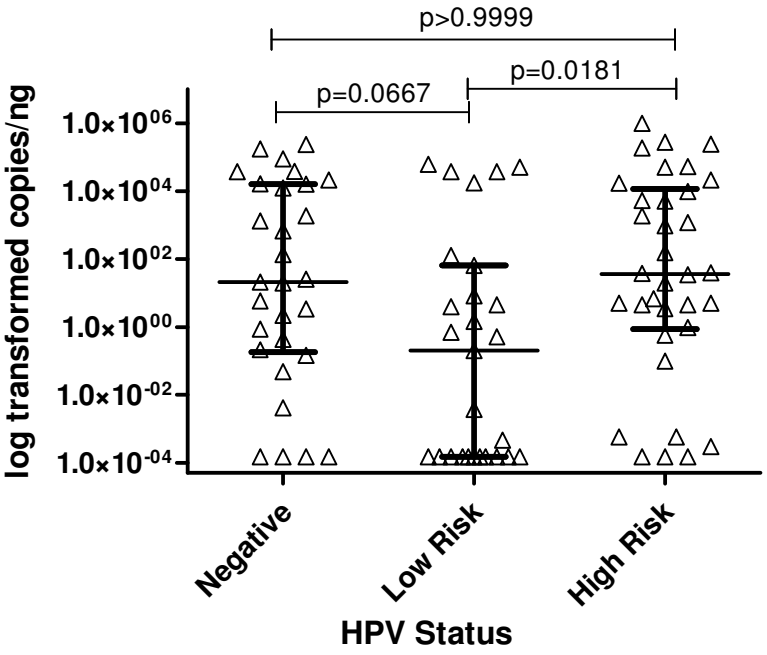

Figure 4.3.7.1: Comparison of the quantities of *L. crispatus* (log transformed copies/ng DNA) measured in the DNA extracted from vaginal lateral wall swabs from participants in the WISH study, between the negative, low risk and high risk HPV groups. All p-value comparisons were based on an unpaired, non-parametric Dunn's Multiple Comparison test. Each point in the figure represents an individual participant. The three horizontal bars represent the median value (middle bar), upper interquartile range (top bar) and lower interquartile range (bottom bar).

4.3.7.2 *Lactobacillus gasseri*

The quantified log copies/ng of *L. gasseri* had no significant difference between the HPV groups (Kruskal-Wallis ANOVA p=0.6824) (Figure 4.3.7.2).

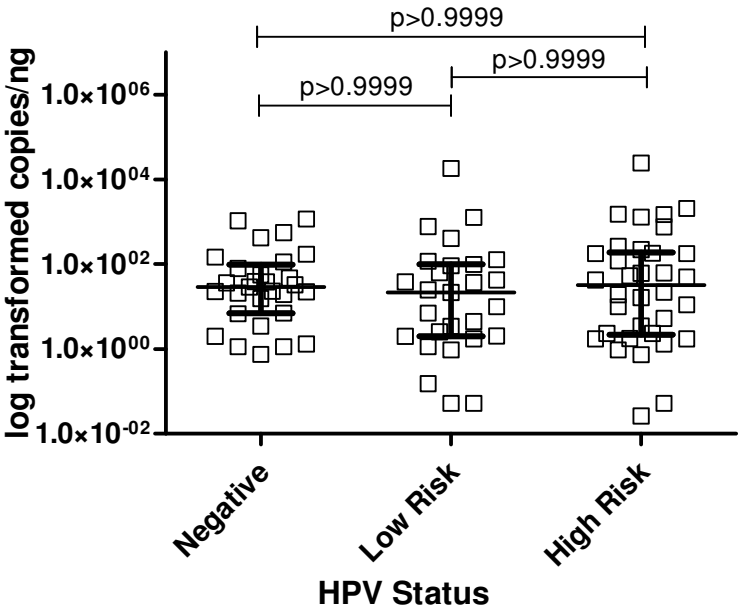

Figure 4.3.7.2: Comparison of the quantities of *L. gasseri* (log transformed copies/ng DNA) measured in the DNA extracted from vaginal lateral wall swabs from participants in the WISH study, between the negative, low risk and high risk HPV groups. All p-value comparisons were based on an unpaired, non-parametric Dunn's Multiple Comparison test. Each point in the figure represents an individual participant. The three horizontal bars represent the median value (middle bar), upper interquartile range (top bar) and lower interquartile range (bottom bar).

4.3.7.3 *Lactobacillus jensenii*

The compared quantified log copies/ng of *L. jensenii* between the HPV groups had no significant difference (Kruskal-Wallis ANOVA p=0.4648) (Figure 4.3.7.3).

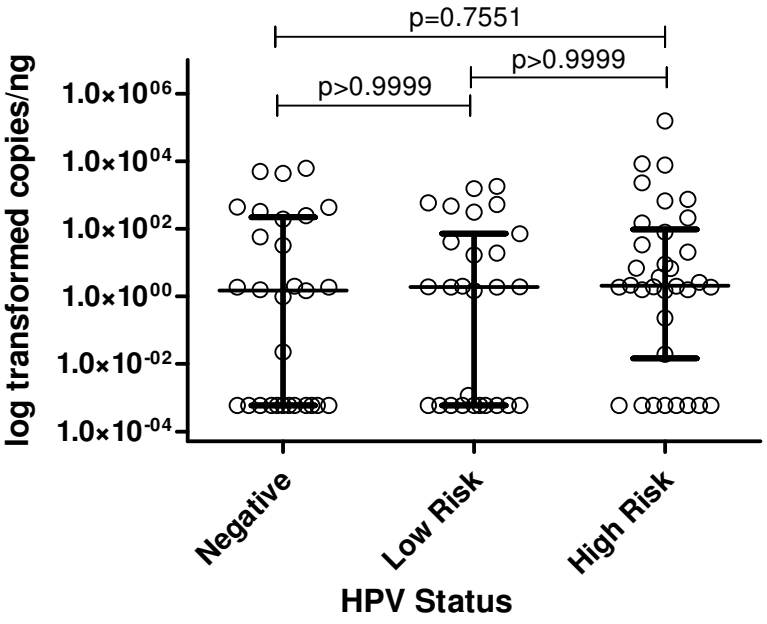

Figure 4.3.7.3: Comparison of the quantities of *L. jensenii* (log transformed copies/ng DNA) measured in the DNA extracted from vaginal lateral wall swabs from participants in the WISH study, between the negative, low risk and high risk HPV groups. All p-value comparisons were based on an unpaired, non-parametric Dunn's Multiple Comparison test. Each point in the figure represents an individual participant. The three horizontal bars represent the median value (middle bar), upper interquartile range (top bar) and lower interquartile range (bottom bar).

4.3.7.4 *Lactobacillus iners*

There was no significant difference in *L. iners* between the HPV groups (Kruskal-Wallis ANOVA p=0.9488) (Figure 4.3.7.4).

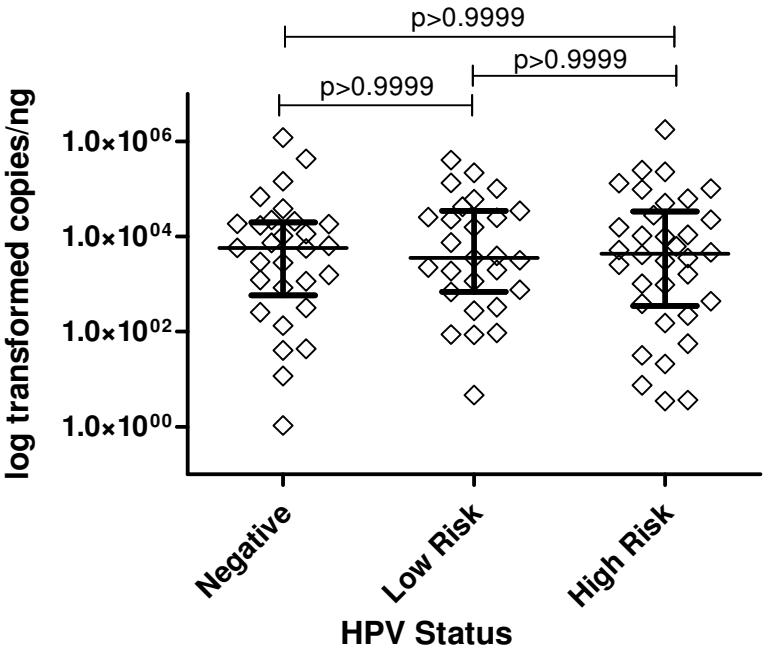

Figure 4.3.7.4: Comparison of the quantities of *L. iners* (log transformed copies/ng DNA) measured in the DNA extracted from vaginal lateral wall swabs from participants in the WISH study, between the negative, low risk and high risk HPV groups. All p-value comparisons were based on an unpaired, non-parametric Dunn's Multiple Comparison test. Each point in the figure represents an individual participant. The three horizontal bars represent the median value (middle bar), upper interquartile range (top bar) and lower interquartile range (bottom bar).

4.3.7.5 *Gardnerella vaginalis*

The compared quantified log copies/ng of *G. vaginalis* between the HPV groups had no significant difference (Kruskal-Wallis ANOVA p=0.1756) (Figure 4.3.7.5).

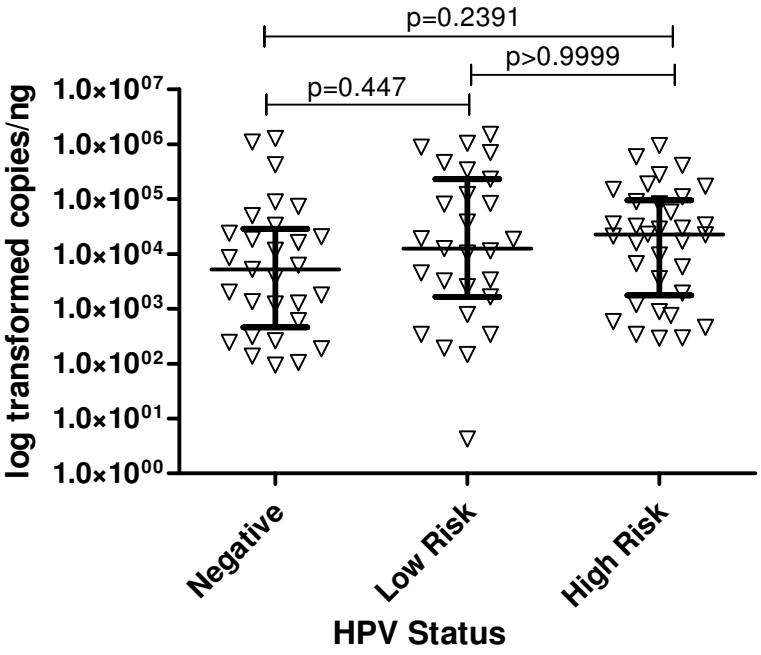

Figure 4.3.7.5: Comparison of the quantities of *G. vaginalis* (log transformed copies/ng DNA) measured in the DNA extracted from vaginal lateral wall swabs from participants in the WISH study, between the negative, low risk and high risk HPV groups. All p-value comparisons were based on an unpaired, non-parametric Dunn's Multiple Comparison test. Each point in the figure represents an individual participant. The three horizontal bars represent the median value (middle bar), upper interquartile range (top bar) and lower interquartile range (bottom bar).

Therefore, the absence of HPV, as well as the presence of low risk or high risk HPV sub-types showed no association with the bacterial copies/ng of *L. gasseri, L. jensenii, L. iners, G. vaginalis,* and *P. bivia*. There were significantly higher copies/ng of *L. crispatus* in the high risk HPV in comparison to the low risk HPV group, with an overall significant difference between the negative, low risk and high risk HPV groups (ANOVA p=0.0145). Thus high-risk HPV subtypes indicate an association with increased *L. crispatus* copies/ng, with no further associations with the other bacterium within this cohort.

Due to the unreliability of the qPCR amplification results, the *P. bivia* data regarding HPV has not been included and can be found in Appendix E: Results, page 203.

4.4 Overview

Overall, within the cohort, *G. vaginalis* and *L. iners* had high copies/ng in vaginal samples in comparison to the other bacteria. There was a diverse effect of the BV status on the quantities (copies/ng) of bacteria measured on the adolescent female lateral wall swab DNA. As expected, participants who were BV negative had increased levels of *L. crispatus* (copies/ng) and *L. gasseri* (copies/ng) in comparison to both the BV intermediate and BV positive participants while *L. jensenii* (copies/ng) and *L. iners* (copies/ng) showed increased levels in comparison to the BV positive and BV intermediate participants, respectively. The participants in the BV positive group showed the opposite traits with increased levels of *G. vaginalis* (copies/ng) in comparison to both the BV intermediate and BV negative groups. *L. iners*, although significantly higher in BV negative versus BV intermediate, did not differ between BV positive and BV negative, and was ubiquitously present. The low inflammation group showed increased copies/ng of *L. crispatus*, *L. gasseri*, and *L. jensenii* in comparison to the high inflammation group. The two inflammatory groups indicated no association with the copies/ng of *L. iners*, and *G. vaginalis*, within the FGT of these adolescent participants.

There was a slight association between *L. jensenii* and hormonal contraceptive usage, *G. vaginalis* and the presence of two viral STIs in comparison to none and one, *P. bivia* and the presence of two viral STIs in comparison to none present, and *L. iners* with the low risk and high risk HPV groups. Furthermore, no category of interest within this study showed any impact on with the copies/ng of *P. bivia* with non-significant p-values in all group comparisons, except for the presence of the two viral STIs. From the above data, we can conclude that within this cohort, the quantities (copies/ng DNA) of the bacteria we measured within the FGT microbiome are do not have a distinct association with age, the absence or present of any one STI, absence or presence of any one, two or more bacterial STIs (*Chlamydia trachomatis, Neisseria gonorrhea,* and *Mycoplasma genitalium*) in the adolescent females based in Masiphumelele who were part of the WISH cohort.

Finally, research should be undertaken to design and optimize primers for *P. bivia* that are species specific, have low levels of self-complementarity and are reliable in order to validate the results and allow for accurate and direct analyses.

Chapter 5: Discussion

Adolescent and young adult women are at extreme risk for HIV infection (Jaspan et al. 2011; Seutlwadi et al. 2012), the cause of which has yet to be determined (Jaspan 2011; Pettifor et al. 2005). Within our South African cohort different factors such as BV status, genital inflammation, age, hormonal contraceptive (HC) usage, and the absence or presence of bacterial or viral STIs were investigated. The absolute quantified log copies/ng of *L. crispatus, L. gasseri, L. jensenii, L. iners, G. vaginalis* and *P. bivia* were compared between the subset groups of these factors in order to determine any associations with HIV acquisition risk. We hypothesized that individuals with vaginal microbiota dominated by *L. crispatus, L. jensenii* and *L. gasseri* were more likely BV negative, had low genital low inflammation, had no STIs, were using either the hormonal contraceptive Nur Isterate or Implanon, and were between the ages of 16-18 years old. We further hypothesized that *L. iners, G. vaginalis* and *P. bivia* would be relatively more abundant in females with high levels of genital inflammatory cytokines, in individuals who were BV positive, had one or more STIs, and/or were using the hormonal contraceptive DMPA and/or were between the ages of 19-22 years old.

The most fundamental step in the development of the qPCR protocols for the six bacteria involved was to ensure pure colonies and the correct growth conditions in order to guarantee accurate and reliable standard curves. If the serially diluted pure positive control DNA was incorrectly extracted from contaminated bacterial colonies, the entire standard curve which was the basis for the bacterial quantification would have been unreliable, rendering all the results null and void. The accuracy of the DNA extraction and quantification process further have a large influence on the data. Errors and contamination during this stage of the assay development would have resulted in inaccurate readings, preventing any reliable analyses of the data. The optimization of the qPCR protocols for the first *Lactobacillus* spp. required the most time. Seven optimization runs were performed in order to ensure the most accurate quantification readings of *L. crispatus*, after which three were generally required for *L. jensenii, L. iners* and *L. gasseri* as the protocol conditions were very similar. The qPCR protocols for the *L. crispatus*, followed by *G. vaginalis* and *P. bivia* were optimized through single step-by-step changes. The guidance for optimization was based on the error (≤ 0.05) and efficiency (2) values being as close to target as possible. The first step take with the optimization process would be to either increase and/or

decrease the annealing temperatures by up to 5℃ to improve the amplification peaks. If the change in annealing temperature did not yield sufficient improvements, the length of the initial denaturation step was adjusted in order to determine if the DNA was not denaturing sufficiently. The next step would be to increase the number of cycles in the amplification step of the protocol in order to improve the amplification curves as well as the error and efficiency value readings. The next step would be to be to either re-dilute the serially diluted standard curves in order to determine of the standard curve DNA was inaccurate, or to change the protocol entirely based from published literature research. The last step in the optimization process would be to change the primers, this was only necessary for *L. crispatus*, and *P. bivia,* after which the above steps would need to be repeated in order to finalize the qPCR protocol. Most differences occurred between primers, and the cycling conditions in terms of temperatures, length of and number of cycles per step in the qPCR protocol.

In this cohort, it was established that in general, *L. iners* and *G. vaginalis* were present at significantly higher copy numbers in comparison to the other *Lactobacillus* species in the adolescent FGT. *L. gasseri* and *L. jensenii* were present at particularly low levels in the majority of the adolescents, compared to other *Lactobacilli.* There were significantly higher copies/ng of *L. crispatus* in participants who were BV negative, had low genital inflammation levels, were 16-18 years of age, and were using the hormonal contraceptive Nur Isterate in comparison to the copies/ng of *L. jensenii*. Further, participants with no STI present, any one bacterial STI present (*N. gonorrhea, C. trachomatis,* HSV-2, *T. vaginalis, M. genitalium, T. pallidum, H. ducreyi*), and who were either negative or had high risk HPV subtypes present within their vaginal secretions, had significantly higher copies/ng of *L. crispatus* in comparison to *L. jensenii.* These increased copy numbers could be due to the dominance of *L. crispatus* within the FGT and its relation to maintaining health and preventing any infections. Nevertheless, *L. iners* remained the dominant lactobacilli species even in these "healthy" women. It is possible that since we only assessed four of the main lactobacilli species from the genital tract, the ratio of increased copies/ng of *L. crispatus* and the decreased copies/ng of *L. gasseri* and *L. jensenii* could change in relation to other lactobacilli when quantified. Most publications associate lactobacilli dominance with a healthy FGT microbiome (Jespers et al. 2015; Ravel et al. 2011; Lopes dos Santos Santiago et al. 2012).

The increased copy numbers of *L. iners* in comparison to the other measured lactobacilli in this cohort, is consistent with other studies conducted in South African women (Anahtar et al. 2015), with another study indicating that African and Asian women who had low Nugent scores, had increased levels of *G. vaginalis,* and decreased *Lactobacillus* species, except for *L. iners* (Jespers et al. 2012). It has been established that women of African descent have a different FGT microbiota profile compared with Caucasian women, which is in agreement with the *L. iners* dominance seen in our cohort. Moreover, Caucasian and Asian women are reportedly more likely to have FGT dominated by lactobacilli than Hispanic or black women who are more likely to have FGT microbiota dominated by *L. iners* and increased vaginal pH (R. F. Lamont et al. 2011; Ma et al. 2013; Ravel et al. 2011; Srinivasan et al. 2012). A study based on black South African women between the ages of 18-23 reported four cervicotypes; including one-dominated by non-*iners* lactobacilli species*,* another *L. iners*-dominated*,* a predominantly *G. vaginalis* group and a *Prevotella*-mixed group was present in all communities (Anahtar et al. 2015). This indicates that ethnicity and the increased risk status of adolescents influences the FGT microbiota profile (Jespers et al. 2012). Research should compare the vaginal microbiota of African women across different age groups beyond 16-22 years of age in order to determine any trends across different African races in combination with different dietary factors and vaginal hygiene practices, and whether any of these factors influence differences in FGT microbiota.

As expected from previous studies, the FGT microbiota of BV-negative participants were dominated by *L. crispatus, L. gasseri,* and *L. jensenii*, while BV-positive participants were dominated by *G. vaginalis* (Datcu 2014; Fredricks et al. 2015; Fredricks et al. 2007; Marrazzo et al. 2012; Mayer et al. 2015; Srinivasan et al. 2010). Interestingly, *L. iners* had the highest quantified log copies/ng across the cohort as well as in the BV negative and BV intermediate participants. Although both *L. crispatus* and *L. iners* are associated with a healthy FGT microbiota and there may be some overlap, they do not share the same niche. Studies have shown that *L. iners* is the first lactobacilli species to establish after BV within the mucosa of the vagina, restoring pH through the production of lactate, allowing for the growth of the normal dominant lactobacilli species such as *L. crispatus, L. gasseri* and *L. jensenii* (France et al. 2016; Jakobsson & Forsum 2008; Mayer et al. 2015; Petrova et al. 2015). This has been demonstrated by the differential production of L- and D- lactic acid by *L. crispatus,* and only L- lactic acid by *L. iners*; and the genetic inability of *L. iners* to oxidize pyruvate to produce hydrogen peroxide

(France et al. 2016). In addition, *L. crispatus* contains genes for an iron transport system within its genome while *L. iners* does not, while *L. crispatus* is able to break down putrescine, an amino acid associated with BV. This indicates differential competition for the dominance of the shared FGT microbiota possibly through nutrient sources, ability to respond to invading pathogens and menses (France et al. 2016).

As hypothesized, increased log transformed copies/ng readings of *L. crispatus, L. gasseri* and *L. jensenii* were observed in participants with low levels of genital inflammation, indicating an inferred negative association with participants with high levels of genital inflammation. However, there was no direct association between any log transformed copies/ng readings for the bacteria and participants with high levels of genital inflammation, contradicting our second hypothesis that adolescents with high levels of genital inflammation have FGT microbiota profiles dominated by *L. iners, G. vaginalis* and *P. bivia*. This could indicate that high levels of genital inflammation are not due to the presence of pathogenic bacteria such as BV-associated *G. vaginalis,* but rather due to the absence of health-associated lactobacilli species. Further research would be required as this does not agree with current literature.

It was hypothesized that young adolescents between the ages of 16-18years would have increased *L. jensenii, L. gasseri* and *L. crispatus* while adolescents between the ages of 19-22 would have increased *L. iners, G. vaginalis* and *P. bivia.* However, there were no differences in bacterial quantities when stratifying participants by age (16-18 versus 19-22 years), or when considering age as a continuous variable (data not included). This lack of age-specific FGT microbiota could also however, be due to the tight age range that we studied. Indeed, women 30 years and older (who are many years past menarche, are experiencing menses or have been pregnant), reportedly have different FGT microbiota profiles compared with adolescents (Chaban et al. 2014; Ma et al. 2013; MacIntyre et al. 2015). Studies have shown that the presence and relative abundance of lactobacilli within the FGT microbiota profile changes with age (Cauci et al. 2002; Madan et al. 2012; Thoma et al. 2011). A cohort involving older women should be studied in order to determine whether the trend of fewer lactobacilli species and the increased copies/ ng of *G. vaginalis* are possibly culture-dependent, due to personal hygiene and bathing habits, or age. The point at which sexual debut occurs could further influence the FGT microbiota through the increase in BV-associated bacteria such as *G. vaginalis* (Mitchell et al.

2012), however, other studies indicate that bacteria such as *G. vaginalis* could colonize the FGT prior to the onset of menarche (Hickey et al. 2015). The data suggest that the driving factor for increased HIV acquisition risk may be something age.

Progestin-only hormonal contraceptives are the most commonly prescribed hormonal contraceptive in South Africa (Byrne et al. 2016; Murphy et al. 2014; van de Wijgert et al. 2013). These are particularly popular among adolescents due to their long-lasting effects. However, observational data suggest that injectable progestin-only hormonal contraceptives may increase risk for HIV (Byrne et al. 2016; Murphy et al. 2014; Roxby et al. 2016). There are contradicting data regarding the difference in HIV acquisition risk between DMPA and Nur Isterate, with suggestions that the active agent of Nur Isterate is the safer alternative (Govender et al. 2014; Tomasicchio et al. 2013). It was hypothesized that adolescents prescribed the contraceptives Nur Isterate or Implanon would have increased levels of *L. jensenii, L. gasseri,* and *L. crispatus*, while those prescribed DMPA would have increased levels of *L. iners, G. vaginalis* and *P. bivia.* However, there were no significant differences in abundance for any of the bacteria studied here between adolescents on DMPA versus those on Nur Isterate. Although the active agents are very similar, the difference in initial dosage due to the 8 week, versus 12week activity could possibly influence the level of association with the bacteria, as well as reduced numbers of participants prescribed DMPA (n=25) in comparison to those prescribed Nur Isterate (n=102). There were no differences in copy number for any of the bacteria for participants prescribed Implanon. However, there were fewer participants within this group (n=9) than those using DMPA and Nur Isterate which may have resulted in inaccurate differences. The only association identified was an overall significant difference in *L. jensenii* copies/ng across the three hormonal contraceptive groups; based on higher copies/ng in participants prescribed DMPA and Nur Isterate compared to those prescribed Implanon.

A better comparison would be to compare the copies/ng of the participants using the different hormonal contraceptives in comparison the participants who were using non-hormonal contraceptive methods. In order to increase the reliability of the results, repeats would need to be run, with equal numbers of participants in each three hormonal group. Further, as part of the WISH cohort through Masiphumelele, there were no girls who were not on a form of contraceptive. The larger study collected samples from Johannesburg where participants were

not taking any form of oral/injectable contraceptive. Further analysis could compare overall participants taking a form of contraceptive versus those participants not taking a hormonal contraceptive. However, this would require crossing location samples which was not a part of this master's thesis study and thus only inter-hormonal contraceptive comparisons could be performed.

The copies/ng of the bacteria were compared between women with and without any one laboratory-diagnosed STI. We hypothesized that the FGT microbiota of participants who had no STI would be more abundant in *L. jensenii, L. gasseri,* and *L. crispatus*, while participants who had one or more STIs would have a FGT microbiota dominated by *L. iners, G. vaginalis* and *P. bivia.* No such association was found in relation to the absence or presence of any one STI; the absence, presence of one, or presence of two or more bacterial STIs, or the absence or presence of one viral STI. There was an association between increased copies/ng of *G. vaginalis* and the presence of two viral STIs; however, the number of participants within this group was small. This trend was further observed for *P. bivia;* however, because the primers were not reliable the data should be interpreted with caution. The serological data for HSV-2 was not included within the results, nor incorporated within the statistical analyses, thus further associations cannot be conducted with the abundance of the bacteria and HSV-2. The serological status of HSV-2 is important as studies have shown a link with BV as well as multiple immunological changes within the immune system with further associations with HIV acquisition (Kaul et al. 2007; Keller et al. 2012). The presence of HPV was not associated with any of the bacteria studied here. However, participants who had high risk HPV subtypes had increased levels of *L. crispatus* compared with their HPV low risk counterparts. Research has established that HPV is essentially a marker for sexual debut, and it is unlikely to see any major difference between the bacteria for this STI (Aujo et al. 2014; Bednarczyk et al. 2012; Houlihan et al. 2014). Validation of the STI results would be recommended as the small sample size could possibly have influenced the results.

Multiple factors likely drive increased risk of HIV acquisition in South African adolescent females. Within the U.S.A, male adolescents within the same age group with the same number of reported sexual partners have a lower risk of HIV acquisition in comparison to their South African counterparts (Cohen et al. 2012; Jaspan 2011; Pettifor et al. 2011). The increased

copies/ng of *G. vaginalis* within these adolescents could indicate a shift in the FGT microbiota profile in comparison to what is generally seen in adults as an indicator for BV (Datcu 2014; Hickey et al. 2015). Different FGT microbiota trends can be influenced by the use of agents to dry, tighten or warm the vagina having a possible link to vaginal health and HIV risk. The misuse of such agents through misunderstanding, could lead to decreased vaginal health in adolescents. Studies have shown than adolescents as well as older women, insert agents such as ice, newspaper, snuff, menthol-based ointments, washing with sunlight soap, cleansing with Disprin and tissues, and using traditional herbs as ointments, ingestion or smoking and douching in order to remove any 'excess' vaginal wetness and increase friction and the 'dryness' of sexual intercourse (Scorgie et al. 2009; Hilber et al. 2010; Jespers et al. 2016b; Mitchell et al. 2011; Smit et al. 2002). Further factors that should be taken into consideration include the living conditions and cultural practices within Masiphumelele (Cauci et al. 2002; Madan et al. 2012; Thoma et al. 2011).

Limitations of this study include uneven numbers of participants for each of the factors compared, as well large differences between group participant numbers, especially the viral STIs. Future statistical analyses should be performed using category groups with more even numbers of participants for comparison and validation of these results. Further, a larger age range as well as more lactobacilli species would have benefitted the understanding of dominant abundance. The comparison for association between bacterial copy number and HC would have benefitted with a non-HC base group of adolescents. Finally, the *P. bivia* primers were not reliable and thus the data cannot be used for comparison or association with the factors of interest within this study. Multiple changes were implemented in order to try and optimize the qPCR protocol for *P. bivia*, however, none of the changes performed resulted in sufficient identification of the bacterium in order to produce reliable results. Any further work with *P. bivia* will involve more in-depth research into more reliable primers, possibly TaqMan probes, in order to improve specificity and reliability. Further limitations of this study include the simple statistical analyses performed. More multivariate comparisons could have been performed in order to better understand the relationships between the classification types and their groups, rather than simply in direct relation to the copies/ng of the bacterium. Potential associations could have been missed due to statistical analyses that did not take into account interrelatedness and confounding variables.

Chapter 6: Conclusion

In conclusion, the FGT microbiota of the adolescent population of females in Masiphumelele is dominated by *L. iners* relative to the other bacteria within this cohort, similar to previous studies with black women, and *G. vaginalis,* which does not follow the normal 'healthy' microbiome. This trend is shifted by *L. crispatus,* which had increased copy numbers across the different factors such as BV status, low levels of genital inflammation and the presence of two viral STIs, with a slight association with high risk HPV subtypes. The age of the participants, high levels of genital inflammation, absence or presence of any one STI, the absence or presence of one, or two or more bacterial STIs, and the absence of or presence of one viral STI do not have any association with the copies/ng of *L. crispatus, L. gasseri, L. jensenii, L. iners,* and *G. vaginalis.*

The FGT microbiota profile is different within the Masiphumelele female adolescents in comparison to many publications based on different ethnicities and geographical locations based on the increased copy numbers of *L. iners* and *G. vaginalis*.

References

AFSA, 2011. HIV/AIDS in South Africa. Available at: http://www.aids.org.za/hivaids-in-south-africa/ [Accessed August 10, 2016].

Amsel, R. et al., 1983. Nonspecific vaginitis. Diagnostic criteria and microbial and epidemiologic associations. *American Journal of Medicine*, 74, pp.14–22.

Anahtar, M.N. et al., 2015. Cervicovaginal Bacteria Are a Major Modulator of Host Inflammatory Responses in the Female Genital Tract. *Immunity*, 42(5), pp.965–976. Available at: http://dx.doi.org/10.1016/j.immuni.2015.04.019.

Anjuère, F. et al., 2012. B cell and T cell immunity in the female genital tract: Potential of distinct mucosal routes of vaccination and role of tissue-associated dendritic cells and natural killer cells. *Clinical Microbiology and Infection*, 18(SUPPL. 5), pp.117–122.

Arnold, K.B. et al., 2015. Increased levels of inflammatory cytokines in the female reproductive tract are associated with altered expression of proteases, mucosal barrier proteins, and an influx of HIV-susceptible target cells. *Mucosal immunology*, 9(February), pp.1–12. Available at: http://www.ncbi.nlm.nih.gov/pubmed/26104913.

Atashili, J. et al., 2008. Bacterial vaginosis and HIV acquisition: a meta-analysis of published studies. *AIDS (London, England)*, 22(12), pp.1493–1501.

Aujo, J.C. et al., 2014. No difference in sexual behavior of adolescent girls following Human Papilloma Virus vaccination: a case study two districts in Uganda; Nakasongola and Luwero. *BMC Public Health*, 14, p.155. Available at: internal-pdf://aujo-1346692352/Aujo.pdf.

De Backer, E. et al., 2007. Quantitative determination by real-time PCR of four vaginal Lactobacillus species, Gardnerella vaginalis and Atopobium vaginae indicates an inverse relationship between L. gasseri and L. iners. *BMC microbiology*, 7, p.115. Available at: http://www.ncbi.nlm.nih.gov/pubmed/18093311.

Balkus, J.E. et al., 2012. Detection of hydrogen peroxide-producing Lactobacillus species in the vagina: a comparison of culture and quantitative PCR among HIV-1 seropositive women. *BMC infectious diseases*, 12(1), p.188. Available at: http://www.biomedcentral.com/1471-2334/12/188.

Beagley, K.W. & Gockel, C.M., 2003. Regulation of innate and adaptive immunity by the female sex hormones oestradiol and progesterone. *FEMS Immunology and Medical Microbiology*, 38(1), pp.13–22.

Bednarczyk, R.A. et al., 2012. Sexual activity-related outcomes after human papillomavirus vaccination of 11- to 12-year-olds. *Pediatrics*, 130, pp.798–805. Available at: http://internal-pdf//Bednarczyk-2012-Sexual activity-rela-1596887809/Bednarczyk-2012-Sexual activity-rela.pdf%5Cnhttp://pediatrics.aappublications.org/content/130/5/798.full.pdf.

Borgdorff, H. et al., 2015. The impact of hormonal contraception and pregnancy on sexually transmitted infections and on cervicovaginal microbiota in African sex workers. *Sexually transmitted diseases*, 42(5), pp.143–152.

Breen, E.C., 2002. Pro- and anti-inflammatory cytokines in human immunodeficiency virus infection and acquired immunodeficiency syndrome. *Pharmacol.Ther.*, 95(3), pp.295–304. Available at: http://www.ncbi.nlm.nih.gov/pubmed/12243799.

Bustin, S.A., 2010. Why the need for qPCR publication guidelines?-The case for MIQE. *Methods*, 50(4), pp.217–226. Available at: http://dx.doi.org/10.1016/j.ymeth.2009.12.006.

Byrne, E.H. et al., 2016. Association between injectable progestin-only contraceptives and HIV acquisition and HIV target cell frequency in the female genital tract in South African women: A prospective cohort study. *The Lancet Infectious Diseases*, 16(4), pp.441–448. Available at: http://dx.doi.org/10.1016/S1473-3099(15)00429-6.

Byun, R. et al., 2004. Quantitative Analysis of Diverse Lactobacillus Species Present in Advanced Dental Caries Quantitative Analysis of Diverse Lactobacillus Species Present in Advanced Dental Caries. *J. Clin. Microbiol.*, 42(7), pp.3128–3136.

Cauci, S. et al., 2002. Prevalence of Bacterial Vaginosis and Vaginal Flora Changes in Peri- and Postmenopausal Women. *JOURNAL OF CLINICAL MICROBIOLOGY,*, 40(6), pp.2147–2152.

Cavaillon, J.-M., 2000. Pro-versus Anti-inflammatory cytokines: myth or reality. *Cellular and Molecular Biology*, 47(4), pp.695–702. Available at: http://www.ncbi.nlm.nih.gov/pubmed/15237199.

CDC, 2014a. Bacterial Vaginosis – CDC Fact Sheet. *Center of Disease Control and Prevention*, p.2.

CDC, 2014b. Genital HPV Infection – CDC Fact Sheet. *Center of Disease Control and Prevention*, pp.1–2.

CDC, 2014c. Gonorhea – CDC Fact Sheet. *Center of Disease Control and Prevention*, pp.1–2.

CDC, 2014d. Trichomoniasis Fact Sheet. *Center of Disease Control and Prevention*.

Chaban, B. et al., 2014. Characterization of the vaginal microbiota of healthy Canadian women through the menstrual cycle. *Microbiome*, 2(1), p.23. Available at: http://www.pubmedcentral.nih.gov/articlerender.fcgi?artid=4106219&tool=pmcentrez&rendertype=abstract.

Chiaffarino, F. et al., 2004. Risk factors for bacterial vaginosis. *European Journal of Obstetrics Gynecology and Reproductive Biology*, 117(2), pp.222–226.

Chinsembu, K.C., 2009. Sexually transmitted infections in adolescents. *Contemporary Reviews in Obstetrics and Gynaecology*, 3(1), pp.107–117.

Cohen, C.R. et al., 2012. Bacterial vaginosis associated with increased risk of female-to-male HIV-1 transmission: A prospective cohort analysis among african couples. *PLoS Medicine*, 9(6), p.18.

Czerniecki, J. & Wołczyński, S., 2011. Deep sequencing – a new method and new requirements of gene expression analysis. *STUDIES IN LOGIC, GRAMMAR AND RHETORIC*, 25(38), pp.41–48.

Datcu, R., 2014. Characterization of the vaginal microflora in health and disease. *Danish Medical Journal*, 61(4), pp.1–24.

Department of Health, 2012. *National Contraception Clinical Guidelines*,

Dinarello, C.A., 2000. Proinflammatory cytokines. *Chest*, 118(2), pp.503–508. Available at: http://dx.doi.org/10.1378/chest.118.2.503.

Dr Manto Tshabalala-Msimang, 2013. *National Contraception Polivy Guidelines*,

Cape Town.

Draper, L., 2006. Working women and contraception: History, health, and choices. *Aaohn J*, 54(7), pp.316–317.

Dumonceaux, T.J. et al., 2009. Multiplex detection of bacteria associated with normal microbiota and with bacterial vaginosis in vaginal swabs by use of oligonucleotide-coupled fluorescent microspheres. *Journal of Clinical Microbiology*, 47(12), pp.4067–4077.

Eschenbach, D.A. et al., 1988. Diagnosis and clinical manifestations of bacterial vaginosis. *American journal of obstetrics and gynecology*, 158(4), pp.819–28. Available at: http://www.ncbi.nlm.nih.gov/pubmed/3259075.

Family Planning Western Australia, 2012. Contraceptive Implant. , (7), pp.1–4.

Fanales-Belasio, E. et al., 2010. HIV virology and pathogenetic mechanisms of infection: a brief overview. *Ann Ist Super Sanità*, 46(1), pp.5–14.

Faust, K. et al., 2012. Microbial Co-occurrence Relationships in the Human Microbiome. *PLoS Computational Biology*, 8(7), pp.1–14.

Fethers, K.A. et al., 2008. Sexual Risk Factors and Bacterial Vaginosis: A Systematic Review and Meta-Analysis. *Clin. Infect. Dis.*, 47(11), pp.1426–1435. Available at: http://www.ncbi.nlm.nih.gov/pubmed/18947329.

Filippo, C. De et al., 2010. Impact of diet in shaping gut microbiota revealed by a comparative study in children from Europe and rural Africa. *PNAS*, 107(33), pp.14691–14696.

Firestein, G.S. et al., 2013. Cytokines. *Kelley's Textbook of Rheumatology*, 285(18), pp.367–377.

France, M.T., Mendes-Soares, H. & Forney, L.J., 2016. *Genomic comparisons of Lactobacillus crispatus and Lactobacillus iners* reveal potential ecological drivers of community composition in the vagina. *Applied and Environmental Microbiology*, (September), p.AEM.02385-16. Available at: http://aem.asm.org/lookup/doi/10.1128/AEM.02385-16.

Fredricks, D.N. et al., 2009. Changes in vaginal bacterial concentrations with intravaginal metronidazole therapy for bacterial vaginosis as assessed by quantitative PCR. *Journal of Clinical Microbiology*, 47(3), pp.721–726.

Fredricks, D.N. et al., 2007. Targeted PCR for detection of vaginal bacteria associated with bacterial vaginosis. *Journal of Clinical Microbiology*, 45(10), pp.3270–3276.

Fredricks, D.N., Fiedler, T.L. & Marrazzo, J.M., 2015. Molecular Identification of Bacteria Associated with Bacterial Vaginosis. , pp.1899–1911.

FSRH Clinical Effectivesness Unit, 2017. CEU Statement: UK MEC 2016 Update Change of UKMEC category for use of progestogen-only injectable contraception by women at high risk of HIV infection from UKMEC1 to UKMEC2 28. *CEU Statement: UK MEC 2016 Update*, (March), pp.28–30.

Gad, G.F.M. et al., 2014. Evaluation of different diagnostic methods of bacterial vaginosis. *IOSR Journal of Dental and Medical Sciences*, 13(1), pp.15–23. Available at: www.iosrjournals.org.

Govender, Y. et al., 2014. The injectable-only contraceptive medroxyprogesterone acetate, unlike norethisterone acetate and progesterone, regulates inflammatory genes in endocervical cells via the glucocorticoid receptor. *PLoS ONE*, 9(5).

Grabowski, M.K. et al., 2015. Use of injectable hormonal contraception and

women ’ s risk of herpes simplex virus type 2 acquisition : a prospective study of couples in Rakai , Uganda. *The Lancet Global Health*, 3(8), pp.e478–e486. Available at: http://dx.doi.org/10.1016/S2214-109X(15)00086-8.

Griffith, J.W., Sokol, C.L. & Luster, A.D., 2014. Chemokines and chemokine receptors: positioning cells for host defense and immunity. *Annual review of immunology*, 32, pp.659–702. Available at: http://www.ncbi.nlm.nih.gov/pubmed/24655300.

Grunenwald, H. & Kramer, K., Cloning a Real-Time PCR Product ; Does SYBR ® Green I Dye Interfere ? *Epicentre*, 11(4), pp.17–19.

Gupta, V.K. et al., 2015. Divergences in gene repertoire among the reference Prevotella genomes derived from distinct body sites of human. *BMC genomics*, 16(153), pp.1350–1356.

Hayashi, H. et al., 2007. Prevotella copri sp . nov . and Prevotella stercorea sp . nov ., isolated from human faeces. *International Journal of Systematic and Evolutionary Microbiology*, (57), pp.941–946.

Hermann-bank, M.L. et al., 2013. The Gut Microbiotassay : a high-throughput qPCR approach combinable with next generation sequencing to study gut microbial diversity. *BMC Genomics*, 14(788), pp.1–14.

Hickey, D.K. et al., 2011. Innate and adaptive immunity at mucosal surfaces of the female reproductive tract: Stratification and integration of immune protection against the transmission of sexually transmitted infections. *Journal of Reproductive Immunology*, 88(2), pp.185–194.

Hickey, R.J. et al., 2015. Vaginal microbiota of adolescent girls prior to the onset of menarche resemble those of reproductive-age women. *mBio*, 6(2), pp.1–14.

Hilber, M.A. et al., 2010. A cross cultural study of vaginal practices and sexuality: Implications for sexual health. *Social Science and Medicine*, 70(3), pp.392–400.

Houlihan, C.F. et al., 2014. Prevalence of human papillomavirus in adolescent girls before reported sexual debut. *Journal of Infectious Diseases*, 210(6), pp.837–845.

Hunt, P.W. et al., 2011. HIV-specific CD4+ T cells may contribute to viral persistence in HIV controllers. *Clinical Infectious Diseases*, 52(5), pp.681–687.

Idziorek, T. et al., 1998. Recombinant human IL-16 inhibits HIV-1 replication and protects against activation-induced cell death (AICD). *Clinical and Experimental Immunology*, 112(1), pp.84–91.

Illumina, 2013. An Introduction to Next-Generation Sequencing Technology Welcome to Next-Generation Sequencing. , (Journal of Experimental Botany).

Jakobsson, T. & Forsum, U., 2008. Changes in the predominant human Lactobacillus flora during in vitro fertilisation. *Annals of Clinical Microbiology and Antimicrobials*, 7(14), pp.1–9. Available at: http://www.embase.com/search/results?subaction=viewrecord&from=export&id=L352069146%5Cnhttp://dx.doi.org/10.1186/1476-0711-7-16.

Jaspan, H., 2011. The wrong place at the wrong time: Geographic disparities in young people's HIV risk. *Journal of Adolescent Health*, 49(3), pp.227–229. Available at: http://dx.doi.org/10.1016/j.jadohealth.2011.07.004.

Jaspan, H.B. et al., 2011. Immune activation in the female genital tract during HIV infection predicts mucosal CD4 depletion and HIV shedding. *Journal of*

Infectious Diseases, 204(10), pp.1550–1556.

Jaspan, H.B. et al., 2011. Sexual health, HIV risk, and retention in an adolescent HIV prevention trial preparatory cohort. *J Adolesc Health*, 49(1), pp.42–46.

Jespers, V. et al., 2016a. Association of Sexual Debut in Adolescents With Microbiota and Inflammatory Markers. *Obstetrics & Gynecology*, 128(1), pp.22–31. Available at: http://content.wkhealth.com/linkback/openurl?sid=WKPTLP:landingpage&an=00006250-201607000-00005.

Jespers, V. et al., 2016b. Association of Sexual Debut in Adolescents With Microbiota and Inflammatory Markers. *Obstetrics & Gynecology*, 128(1), pp.22–31. Available at: http://content.wkhealth.com/linkback/openurl?sid=WKPTLP:landingpage&an=00006250-201607000-00005.

Jespers, V. et al., 2012. Quantification of bacterial species of the vaginal microbiome in different groups of women, using nucleic acid amplification tests. *BMC microbiology*, 12(1), p.83. Available at: ???

Jespers, V. et al., 2015. The significance of Lactobacillus crispatus and L. vaginalis for vaginal health and the negative effect of recent sex: A cross-sectional descriptive study across groups of African women. *BMC Infectious Diseases*, 15(1), p.115. Available at: http://ovidsp.ovid.com/ovidweb.cgi?T=JS&PAGE=reference&D=prem&NEWS=N&AN=25879811%5Cnhttp://www.biomedcentral.com/bmcinfectdis/%5Cnhttp://ovidsp.ovid.com/ovidweb.cgi?T=JS&PAGE=reference&D=emed13&NEWS=N&AN=2015001066.

Jones, M.B. et al., 2015. Library preparation methodology can influence genomic and functional predictions in human microbiome research. *Proc Natl Acad Sci U S A*, 112(45), p.1519288112-. Available at: http://www.pnas.org/content/early/2015/10/27/1519288112.abstract.

Jung, H.C. et al., 1995. A distinct array of proinflammatory cytokines is expressed in human colon epithelial cells in response to bacterial invasion. *The Journal of clinical investigation*, 95(1), pp.55–65.

Kaul, R. et al., 2007. Prevalent herpes simplex virus type 2 infection is associated with altered vaginal flora and an increased susceptibility to multiple sexually transmitted infections. *The Journal of infectious diseases*, 196(11), pp.1692–1697.

Keller, M.J. et al., 2012. Changes in the Soluble Mucosal Immune Environment during Genital Herpes Outbreaks. *J Acquir Immune Defic Syndr*, 61(2), pp.194–202.

Kolenbrander, P.E. et al., 2002. Communication among Oral Bacteria. *MICROBIOLOGY AND MOLECULAR BIOLOGY REVIEWS*, 66(3), pp.486–505.

Lambert, J.A. et al., 2013. Novel PCR-Based Methods Enhance Characterization of Vaginal Microbiota in a Bacterial Vaginosis Patient before and after Treatment. *Applied and Environmental Microbiology*, 79(13), pp.4181–4185.

Lamont et al., 2011. The vaginal microbiome: New information about genital tract flora using molecular based techniques. *BJOG: An International Journal of Obstetrics and Gynaecology*, 118(5), pp.533–549.

Lamont, R.F. et al., 2011. The vaginal microbiome: New information about genital

tract using molecular based techniques. *Brit. J. Obstet. Gynaec.*, 118(5), pp.533–549.

Lawn, S.D. et al., 2006. Impact of HIV infection on the epidemiology of tuberculosis in a peri-urban community in South Africa: the need for age-specific interventions. *Clinical infectious diseases : an official publication of the Infectious Diseases Society of America*, 42(7), pp.1040–7. Available at: http://www.ncbi.nlm.nih.gov/pubmed/16511773.

Lewis, D.A., 2000. Diagnostic tests for chancroid Diagnostics. *Sex Transm Inf*, 76, pp.137–141.

Lopes dos Santos Santiago, G. et al., 2012. Longitudinal qPCR Study of the Dynamics of L. crispatus, L. iners, A. vaginae, (Sialidase Positive) G. vaginalis, and P. bivia in the Vagina. *PLoS ONE*, 7(9).

loveLife, 1999. loveLife. Available at: http://www.lovelife.org.za/ [Accessed August 15, 2016].

Ma, B., Forney, L.J. & Ravel, J., 2013. The vaginal microbiome : rethinking health and diseases. *Annu Rev Microbiol*, 66, pp.371–389.

MacIntyre, D.A. et al., 2015. The vaginal microbiome during pregnancy and the postpartum period in a European population. *Scientific reports*, 5(Cst Iv), p.8988. Available at: http://www.nature.com/srep/2015/150311/srep08988/full/srep08988.html.

Macklaim, J.M. et al., 2013. Comparative meta-RNA-seq of the vaginal microbiota and differential expression by Lactobacillus iners in health and dysbiosis. *Microbiome*, 1(1), p.12. Available at: http://www.pubmedcentral.nih.gov/articlerender.fcgi?artid=3971606&tool=pm

centrez&rendertype=abstract.

Madan, R.P. et al., 2012. Altered biomarkers of mucosal immunity and reduced vaginal lactobacillus concentrations in sexually active female adolescents. *PLoS ONE*, 7(7), pp.1–10.

Malaguti, N. et al., 2015. Sensitive Detection of Thirteen Bacterial Vaginosis-Associated Agents Using Multiplex Polymerase Chain Reaction. , 2015.

Marrazzo, J.M. et al., 2012. Extravaginal reservoirs of vaginal bacteria as risk factors for incident bacterial vaginosis. *Journal of Infectious Diseases*, 205(10), pp.1580–1588.

Masson, L. et al., 2015. Relationship between female genital tract infections, mucosal interleukin-17 production and local T helper type 17 cells. *Immunology*, 146(4), pp.557–567.

Mayer, B.T. et al., 2015. Rapid and profound shifts in the vaginal microbiota following antibiotic treatment for bacterial vaginosis. *Journal of Infectious Diseases*, 212(5), pp.793–802.

Mestecky, J. & Fultz, P.N., 1999. Mucosal Immune System of the Human Genital Tract. *The Journal of Infectious Diseases*, 179(Suppl 3), pp.S470-4.

Minnesota, U. of, 2005. Web Anatomy. *14 November*. Available at: http://msjensen.cbs.umn.edu/webanatomy/image_database/Reproductive/default.htm [Accessed August 8, 2016].

Mirmonsef, P. et al., 2011. The Effects of Commensal Bacteria on Innate Immune Responses in the Female Genital Tract. *American Journal of Reproductive Immunology*, 65(3), pp.190–195.

Mitchell, C. et al., 2011. Effect of sexual activity on vaginal colonization with hydrogenperoxide producing Lactobacilli and Gardnerella vaginalis. *Sexually Transmitted Diseases*, 38(12), pp.1137–1144.

Mitchell, C.M. et al., 2012. Effect of Sexual Debut on Vaginal Microbiota in a Cohort of Young Women. *Obstet Gynecol*, 120(6), pp.1306–1313.

Mitchell, C.M. & Marrazzo, J., 2014. Bacterial vaginosis and the cervicovaginal immune system. *American Journal of Reproductive Immunology*, 71(6), pp.555–563.

Mitchell, S., 2008. Contraception. , p.38.

Mlisana, K. et al., 2012. Symptomatic vaginal discharge is a poor predictor of sexually transmitted infections and genital tract inflammation in high-risk women in South Africa. *Journal of Infectious Diseases*, 206(1), pp.6–14.

Murphy, K., Irvin, S.C. & Herold, B.C., 2014. Research Gaps in Defining the Biological Link between HIV Risk and Hormonal Contraception. , 2(72), pp.228–235.

Myer, L. et al., 2005. Bacterial vaginosis and susceptibility to HIV infection in South African women: A nested case-control study. *Journal of Infectious Diseases*, 192(8), pp.1372–1380.

Newman, L. et al., 2013. Global Estimates of Syphilis in Pregnancy and Associated Adverse Outcomes: Analysis of Multinational Antenatal Surveillance Data. *PLoS Medicine*, 10(2).

Noguchi, L.M. et al., 2015. Risk of HIV-1 acquisition among women who use diff erent types of injectable progestin contraception in South Africa: A

prospective cohort study. *The Lancet HIV*, 2(7), pp.e279–e287. Available at: http://dx.doi.org/10.1016/S2352-3018(15)00058-2.

Nugent, R.P., Krohn, M.A. & Hillier, S.L., 1991. Reliability of diagnosing bacterial vaginosis is improved by a standardized method of gram stain interpretation. *Journal of Clinical Microbiology*, 29(2), pp.297–301.

O'Farrell, N., 2008. Control of sexually transmitted infections for HIV prevention. *The Lancet*, 372(9646), p.1297. Available at: http://dx.doi.org/10.1016/S0140-6736(08)61540-8.

Ochiel, D.O. et al., 2008. Innate Immunity in the Female Reproductive Tract: Role of Sex Hormones in Regulating Uterine Epithelial Cell Protection Against Pathogens. *Current Womens Health Rev.iew*, 4(2), pp.102–117.

Ohene, S. & Akoto, I., 2008. Factors associated with sexually transmitted infections among young ghanaian women. *Ghana medical journal*, 42(3), pp.96–100. Available at: http://www.pubmedcentral.nih.gov/articlerender.fcgi?artid=2643428&tool=pmcentrez&rendertype=abstract.

Organon Pharmaceuticals USA, 2011. IMPLANON® (etonogestrel implant). Available at: https://dailymed.nlm.nih.gov/dailymed/archives/fdaDrugInfo.cfm?archiveid=63647 [Accessed September 6, 2016].

Pabinger, S. et al., 2014. A survey of tools for the analysis of quantitative PCR (qPCR) data. *Biomolecular Detection and Quantification*, 1(1), pp.23–33. Available at: http://dx.doi.org/10.1016/j.bdq.2014.08.002.

Patterson, B.K. et al., 2002. Susceptibility to human immunodeficiency virus-1

infection of human foreskin and cervical tissue grown in explant culture. *The American journal of pathology*, 161(3), pp.867–873.

Petricevic, L. et al., 2014. Characterisation of the vaginal Lactobacillus microbiota associated with preterm delivery. *Scientific reports*, 4, p.5136. Available at: http://www.pubmedcentral.nih.gov/articlerender.fcgi?artid=4038809&tool=pmcentrez&rendertype=abstract.

Petrova, M.I. et al., 2015. Lactobacillus species as biomarkers and agents that can promote various aspects of vaginal health. *Frontiers in Physiology*, 6(MAR), pp.1–18.

Pettifor, A.E. et al., 2011. A tale of two countries: Rethinking sexual risk for HI. *J Adolesc Health*, 49(3), pp.237–243.

Pettifor, A.E. et al., 2005. Young people's sexual health in South Africa: HIV prevalence and sexual behaviors from a nationally representative household survey. *Aids*, 19(14), pp.1525–1534.

Pfaffl, M.W.., 2004. *Quantification strategies in real-time PCR*.

Pfaffl, M.W.. & Wittwer, C., 2015. QPCR, dPCR, NGS - A journey. *Biomolecular Detection and Quantification*, 3(September 2005), pp.A1–A5.

Pfizer, 2011. Depo-Provera. , pp.1–17.

Pharmaceutical/Industry, 2005. NUR-ISTERATE. Available at: http://home.intekom.com/pharm/schering/nur-ist.html [Accessed September 5, 2016].

Polis, C.B. et al., 2016. An updated systematic review of epidemiological evidence on hormonal contraceptive methods and HIV acquisition in women. *AIDS*,

30(17), p.19.

Premaraj, T. et al., 1999. Use of PCR and sodium dodecyl sulfate-polyacrylamide gel electrophoresis techniques for differentiation of Prevotella intermedia sensu stricto and Prevotella nigrescens. *Journal of Clinical Microbiology*, 37(4), pp.1057–1061.

Ravel, J. et al., 2011. Vaginal microbiome of reproductive-age women. *Proceedings of the National Academy of Sciences*, 108(Supplement_1), pp.4680–4687. Available at: http://www.pnas.org/cgi/doi/10.1073/pnas.1002611107.

Reis Machado, J. et al., 2014. Mucosal Immunity in the Female Genital Tract, HIV/AIDS. *BioMed Research International*, 2014, p.20.

Reproductive Health and Research & Who, 2005. Sexually transmitted and other reproductive tract infections: a guide to essential practice. *World Health Organization*. Available at: http://whqlibdoc.who.int/publications/2005/9241592656.pdf?ua=1.

Riou, C. et al., 2012. Distinct kinetics of Gag-specific CD4+ and CD8+ T cell responses during acute HIV-1 infection. *Journal of immunology (Baltimore, Md. : 1950)*, 188(5), pp.2198–206. Available at: http://www.pubmedcentral.nih.gov/articlerender.fcgi?artid=3288487&tool=pmcentrez&rendertype=abstract.

Roberts, L. et al., 2012. Vaginal microbicides to prevent human immunodeficiency virus infection in women: Perspectives on the female genital tract, sexual maturity and mucosal inflammation. *Best Practice and Research: Clinical Obstetrics and Gynaecology*, 26(4), pp.441–449. Available at:

http://dx.doi.org/10.1016/j.bpobgyn.2012.02.002.

Roche, 2003. *Creating Standard Curves with Genomic DNA or Plasmid DNA Templates for Use in Quantitative PCR*,

Roxby, A., Fredricks, D. & Odem-Davis, K., 2016. Changes in vaginal microbiota and immune mediators in HIV-1-seronegative Kenyan Women initiating depot medroxyprogesterone acetate. *JAIDS Journal of*, 71(4), pp.359–366. Available at: http://journals.lww.com/jaids/Abstract/2016/04010/Changes_in_Vaginal_Microbiota_and_Immune_Mediators.2.aspx.

Roy, C.C. et al., 2006. Short-Chain Fatty Acids: Ready for Prime Time? *NCP - Nutrition in Clinical Practice*, 21(4), pp.351–366. Available at: http://ncp.aspenjournals.org/cgi/content/abstract/21/4/351.

Saito, D. et al., 2006. Identification of bacteria in endodontic infections by sequence analysis of 16S rDNA clone libraries. *Journal of Medical Microbiology*, 55(1), pp.101–107.

Salipante, S.J. et al., 2013. Rapid 16S rRNA Next-Generation Sequencing of Polymicrobial Clinical Samples for Diagnosis of Complex Bacterial Infections. *PLoS ONE*, 8(5).

Scher, J.U. et al., 2013. Expansion of intestinal Prevotella copri correlates with enhanced susceptibility to arthritis. *eLIFE*, (e01202), pp.1–20.

Scorgie, F. et al., 2009. In search of sexual pleasure and fidelity: vaginal practices in KwaZulu-Natal, South Africa. *Culture, health & sexuality*, 11(3), pp.267–283.

Selle, K. et al., 2014. Development of an integration mutagenesis system in Lactobacillus gasseri. *Gut Microbes*, 5(3), pp.326–332.

Seutlwadi, L., Karl, P. & Gugu, M., 2012. Contraceptive use and associated factors among South African youth (18 - 24 years): A population-based survey. *South African Journal of Obstetrics & Gynaecology*, 18(2), pp.43–47.

Smit, J. et al., 2002. Vaginal wetness: An underestimated problem experienced by progestogen injectable contraceptive users in South Africa. *Social Science and Medicine*, 55(9), pp.1511–1522.

Smith, C.J. & Osborn, A.M., 2009. Advantages and limitations of quantitative PCR (Q-PCR) -based approaches in microbial ecology. *FEMS Microbiological Ecology*, 67(1991), pp.6–20.

Spiegel, C.A., Amsel, R. & Holmes, K.K., 1983. Diagnosis of bacterial vaginosis by direct gram stain of vaginal fluid . Diagnosis of Bacterial Vaginosis by Direct Gram Stain of Vaginal Fluid. *JOURNAL OF CLINICAL MICROBIOLOGY,*, 18(1), pp.170–177.

Srinivasan, S. et al., 2012. Bacterial communities in women with bacterial vaginosis: High resolution phylogenetic analyses reveal relationships of microbiota to clinical criteria. *PLoS ONE*, 7(6).

Srinivasan, S. et al., 2010. Temporal variability of human vaginal bacteria and relationship with bacterial vaginosis. *PLoS ONE*, 5(4).

Srinivasan, S. & Fredricks, D.N., 2008. The human vaginal bacterial biota and bacterial vaginosis. *Interdisciplinary perspectives on infectious diseases*, 2008, p.750479. Available at: http://www.pubmedcentral.nih.gov/articlerender.fcgi?artid=2648628&tool=pm

centrez&rendertype=abstract.

Su, D.L. et al., 2012. Roles of pro- and anti-inflammatory cytokines in the pathogenesis of SLE. *Journal of Biomedicine and Biotechnology*, 2012.

Sultani, M. et al., 2012. Anti-Inflammatory Cytokines: Important Immunoregulatory Factors Contributing to Chemotherapy-Induced Gastrointestinal Mucositis. *Chemotherapy Research and Practice*, 2012, pp.1–11.

Tamrakar, R. et al., 2007. Association between Lactobacillus species and bacterial vaginosis-related bacteria, and bacterial vaginosis scores in pregnant Japanese women. *BMC infectious diseases*, 7, p.128.

Tan, B. et al., 2015. Next-generation sequencing (NGS) for assessment of microbial water quality: Current progress, challenges, and future opportunities. *Frontiers in Microbiology*, 6(SEP).

Thoma, M.E. et al., 2011. Longitudinal changes in vaginal microbiota composition assessed by Gram-stain among never sexually active pre- and postmenarcheal adolescents in Rakai, Uganda. *Pediatr Adolesc Gynecol.*, 24(1), pp.42–47.

Tomasicchio, M. et al., 2013. The Progestin-Only Contraceptive Medroxyprogesterone Acetate, but Not Norethisterone Acetate, Enhances HIV-1 Vpr-Mediated Apoptosis in Human CD4+ T Cells through the Glucocorticoid Receptor. *PLoS ONE*, 8(5).

UNAIDS, 2015. HIV and AIDS estimates. Available at: http://www.unaids.org/en/regionscountries/countries/southafrica [Accessed August 10, 2016].

Vitali, B. et al., 2007. Dynamics of vaginal bacterial communities in women developing bacterial vaginosis, candidiasis, or no infection, analyzed by PCR-denaturing gradient gel electrophoresis and real-time PCR. *Applied and Environmental Microbiology*, 73(18), pp.5731–5741.

Voelkerding, K. V, Dames, S. & Durtschi, J.D., 2010. Next Generation Sequncing for Clinical Diagnostics - Principles and Application to Targeted Resequencing for Hypertrophic Cardiomyopathy. *The Journal of Molecular Diagnostics*, 12(5), pp.539–551. Available at: http://dx.doi.org/10.2353/jmoldx.2010.100043.

Wang, Y. & Rice, A.P., 2006. Interleukin-10 inhibits HIV-1 LTR-directed gene expression in human macrophages through the induction of cyclin T1 proteolysis. *Virology*, 352(2), pp.485–492.

Western Cape Government, 2015. Contraception (family planning). Available at: https://www.westerncape.gov.za/service/contraception-family-planning [Accessed October 12, 2016].

Wienkoop, S. & Weckwerth, W., 2006. Relative and absolute quantitative shotgun proteomics : targeting low-abundance proteins in Arabidopsis thaliana. *Journal of Experimental Botany*, 57(7), pp.1529–1535.

van de Wijgert, J.H.H.M. et al., 2013. Hormonal contraception decreases bacterial vaginosis but oral contraception may increase candidiasis: implications for HIV transmission. *AIDS (London, England)*, 27(13), pp.2141–53.

Wira, C.R., Fahey, J. V., et al., 2005. Innate and adaptive immunity in female genital tract: Cellular responses and interactions. *Immunological Reviews*, 206, pp.306–335.

Wira, C.R., Grant-Tschudy, K.S. & Crane-Godreau, M.A., 2005. Epithelial cells in the female reproductive tract: a central role as sentinels of immune protection. *American journal of reproductive immunology (New York, N.Y. : 1989)*, 53(2), pp.65–76. Available at: http://doi.wiley.com/10.1111/j.1600-0897.2004.00248.x%5Cnpapers3://publication/doi/10.1111/j.1600-0897.2004.00248.x.

World Health Organization, 2017. *Hormonal contraceptive eligibility for women at high risk of HIV Guidance*,

Wu, G.D. et al., 2011. Linking Long-Term Dietary Patterns with Gut Microbial Enterotypes. *Science*, 334(6052), pp.105–108.

Xu, H., Wang, X. & Veazey, R.S., 2013. Mucosal immunology of HIV infection. *Immunological Reviews*, 254(1), pp.10–33.

Zhang, Z.-Q. et al., 2004. Roles of substrate availability and infection of resting and activated CD4+ T cells in transmission and acute simian immunodeficiency virus infection. *Proceedings of the National Academy of Sciences of the United States of America*, 101(15), pp.5640–5645.

Appendix A – DNA Concentrations

The DNA from the majority of the lateral wall swab participant samples from the adolescent females who took part of the WISH cohort had been extracted by Enock Bugaye Havyarimana and Anna Blakney. The DNA was extracted from the remaining samples during this study. The DNA was extracted using the MoBio Powersoil® DNA Isolation Kit.

Table 1: List of DNA concentrations (ng/µL) extracted from WISH participant lateral wall swab vaginal samples collected at Visit 1.

Count	Participant sample:	DNA concentration (ng/µL)
1	W001 V1	0.053
2	W002 V1	0.17
3	W004 V1	2.62
4	W005 V1	0.13
5	W006 V1	0.47
6	W007 V1	8.24
7	W008V1	0.6
8	W009 V1	9.40
9	W010 V1	8.84
10	W011 V1	2.88
11	W012 V1 Rep B	7.82
12	W013 V1	0.452
13	W015 V1	2.31
14	W016 V1	3.3
15	W017 V1	2.42
16	W019 V1	0.188
17	W021 V1	3.02
18	W022 V1	2.6
19	W023 V1	0.93
20	W024 V1	1.28
21	W025 V1	0.79
22	W026 V1	7.54
23	W027 V1	6.48
24	W028 V1	4.40
25	W030 V1	0.288
26	W031 V1	0.86
27	W032 V1	2.26
28	W033 V1	2.64
29	W034 V1	0.005
30	W035 V1	0.15
31	W036 V1	16.3
32	W037 V1	1.40
33	W038 V1	3.6
34	W039 V1	4.0

35	W040 V1	1.7
36	W041 V1	6.06
37	W043 V1	4.20
38	W044 V1	6.32
39	W045 V1	0.22
40	W046 V1	0.005
41	W047 V1	37.2
42	W048 V1	3.76
43	W050 V1	0.17
44	W051 V1	0.68
45	W052 V1	4.08
46	W053 V1	0.80
47	W054 V1	0.25
48	W055 V1	0.53
49	W056 V1	0.80
50	W057 V1	3.48
51	W059 V1	0.64
52	W060 V1	1.79
53	W061V1	0.48
54	W062 V1	0.46
55	W063V1	0.20
56	W064 V1	0.52
57	W065 V1	0.52
58	W066 V1	2.20
59	W067 V1	2.20
60	W068 V1	2.66
61	W070 V1	10.40
62	W071 V1	1.02
63	W072 V1	1.64
64	W073 V1	10.2
65	W074 V1	0.96
66	W076 V1	8.76
67	W077 V1	5.20
68	W079 V1	1.46
69	W080 V1	0.005
70	W081 V1	1.80
71	W082 V1	6.32
72	W083 V1 Rep A	19.38
73	W084 V1	1.07
74	W085 V1	4.52
75	W086 V1	2.05
76	W087 V1	5.72
77	W088 V1	2.71
78	W089 V1	5.12
79	W091 V1	1.23
80	W092 V1	7.84

81	W094 V1	3.82
82	W095 V1	3.04
83	W096 V1	3.24
84	W097 V1	0.76
85	W098 V1	1.11
86	W099 V1	0.005
87	W100 V1	0.30
88	W101 V1	1.61
89	W102 V1	1.01
90	W104 V1	7.0
91	W105 V1	1.40
92	W106 V1	6.28
93	W107 V1	4.36
94	W108 V1	7.28
95	W110 V1	3.4
96	W112 V1	1.06
97	W113 V1	5.12
98	W114 V1	6.96
99	W115 V1	3.83
100	W116 V1	4.44
101	W117 V1	6.48
102	W118 V1	4.84
103	W119 V1 Rep A	25
104	W120 V1	8.24
105	W121 V1	1.44
106	W122 V1	1.14
107	W123 V1	0.038
108	W124 V1	1.36
109	W125 V1	0.60
110	W126 V1	9.76
111	W127 V1	5
112	W128 V1	1.38
113	W129 V1	4.68
114	W130 V1	7.24
115	W131 V1	4.68
116	W132 V1 Rep B	25.2
117	W135 V1Rep A	10.42
118	W136 V1	11.7
119	W137 V1	3.3
120	W138 V1 Rep A	88.7
121	W139 V1	7.40
122	W141 V1	1.62
123	W147 V1	9.68
124	W148 V1 Rep A	17.44
125	W149 V1	2.92
126	W150 V1 Rep B	20.8

127	W152 V1	13.2
128	W154 V1	8.4
129	W156 V1 Rep A	4.5
130	W157 V1 Rep B	30.4
131	W158 V1 Rep B	2.28
132	W159 V1 Rep A	15.56
133	W160 V1 Rep B	15.06
134	W161 V1 Rep B	5.94
135	W163 V1 Rep B	45
136	W164 V1 Rep A	9.44
137	W165 V1 Rep A	5.14
138	W166 V1 Rep A	0.1
139	W167 V1 Rep A	32.8
140	W168 V1 Rep A	3.84
141	W170 V1 Rep A	15.74
142	W171 V1 Rep B	0.78
143	W172 V1 Rep A	4.4
144	W173 V1 Rep B	7.88
145	W174 V1 Rep A	1.6
146	W176 V1 Rep A	7.06

Appendix B – Primer Confirmation

A PCR was run using the DNA extracted from the growth of each bacterial positive control in duplicate with a Non-Template Control (NTC) (Qiagen Blood and Tissue DNA Maxi Extraction Kit with Buffers B1 and B2). The PCR products were then run on a 1.6% agarose gel at 130V for 1 h with a 100 bp ladder to visualize the size of the bands to confirm the species specific primer product sizes for each species.

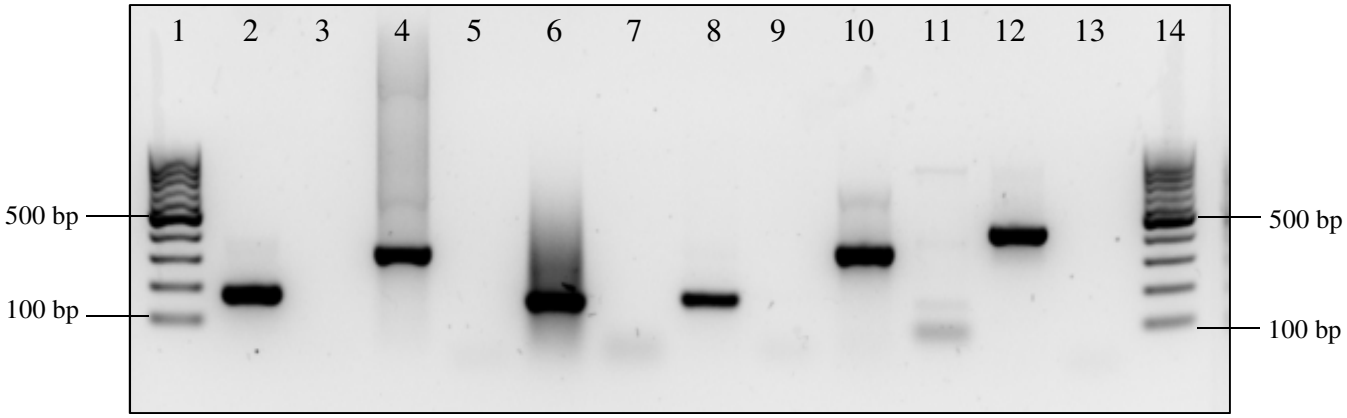

Figure 1: Gel electrophoresis of the standard positive control species specific PCR to confirm primer specificity and product size. 1 and 14 indicate a ThermoFisher O'Gene 100 bp ruler, lanes 2, 4, 6, 8, 10, and 12 indicates the PCR products for *L. crispatus, L. gasseri, L. jensenii, L. iners, G. vaginalis* and *P. bivia*, and lanes 3, 5, 7, 9, and 11 indicate their respective NTC's.

Appendix C: qPCR Optimization

For the optimization of each bacterial specific absolute qPCR, multiple plates were run with different conditions until the error and efficiency values were as close to 0.05 and 2 respectively, as could be optimized. The following figures illustrate each trial plate that was run for each bacterial species, as well as the changes that were made for each plate.

The optimization figures for *L. crispatus, G. vaginalis* and *P. bivia* can be found in Chapter 4, Results, 4.1 Real-Time PCR (qPCR) Optimization.

Real-Time PCR (qPCR) Optimization:

1 *Lactobacillus gasseri*

A total of three trial plates were run to finalize the optimization of *L. gasseri* qPCR conditions. The first trial plate (V1.1) was run using the same reagent volumes as the finalized conditions for *L. crispatus* (V1.7). The following qPCR conditions were followed, 95℃ for 15 min initial denaturation, followed by 40 cycles of 95℃ for 15 s, 57℃ for 1 min and 65℃ for 1 min (Figure 1.1 A, Figure 1.2 A). The replicates for the positive controls showed some inaccuracies and thus required a second run. The second trial plate for *L. gasseri* (1.2) was run under the same conditions as qPCR trial plate V1.1 in order to improve efficiency and pipetting accuracy with the exception of the initial denaturation being for 5 min (Figure 1.1 B, Figure 1.2 B). The error and efficiency values showed good readings and the positive controls amplified well. The third and final optimization plate for *L. gasseri* was run using the same conditions as V1.2 in order to determine whether the lack of amplification in the positive controls at 10^{-2} copies/µL was due to a pipetting error or the concentration threshold for amplification of the standard control DNA (Figure 1.1 C, Figure 1.2 C). The final standard curve error and efficiency readings were good with single peaks in the melt curves and thus accepted to run samples.

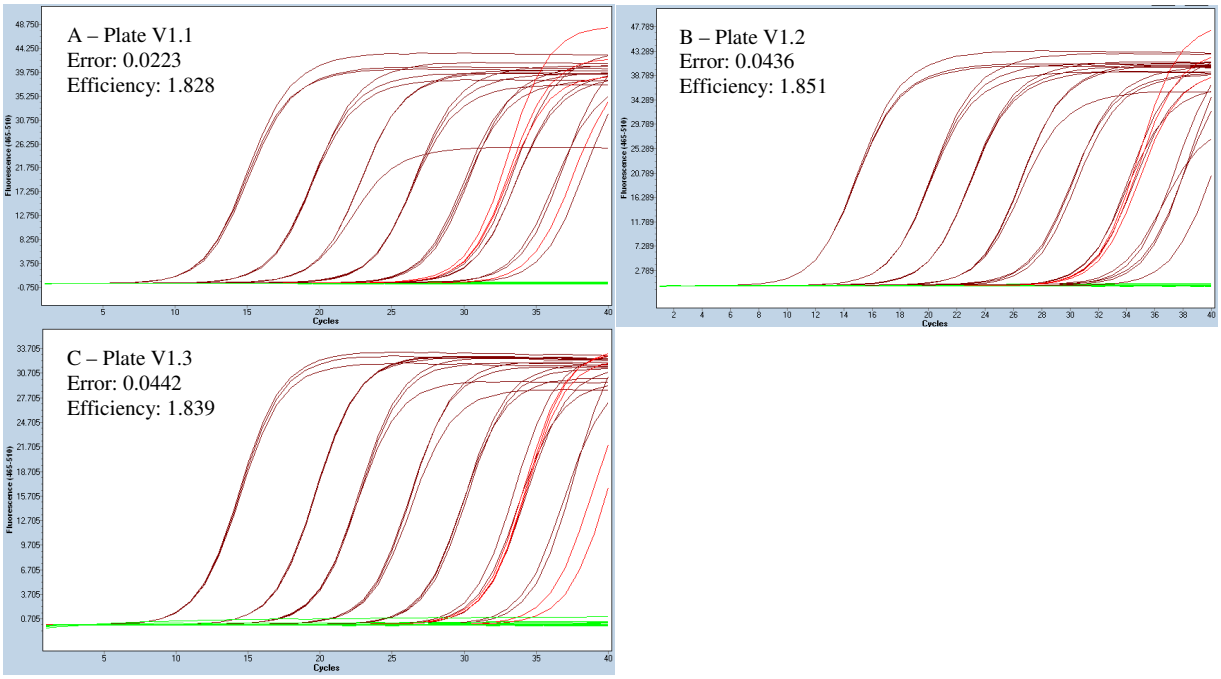

Figure 1.1: Roche LightCycler® 480 absolute quantitative derivative max amplification curve for the three *L. gasseri* optimization plates (V1.1-V1.3). The fluorescence (465-510 nm) is indicated on the y-axis and the number of cycles is indicated on the x-axis. Red and brown indicate positive amplification in the unknown sample and the positive control standards respectively, and green indicates negative amplification in the wells.

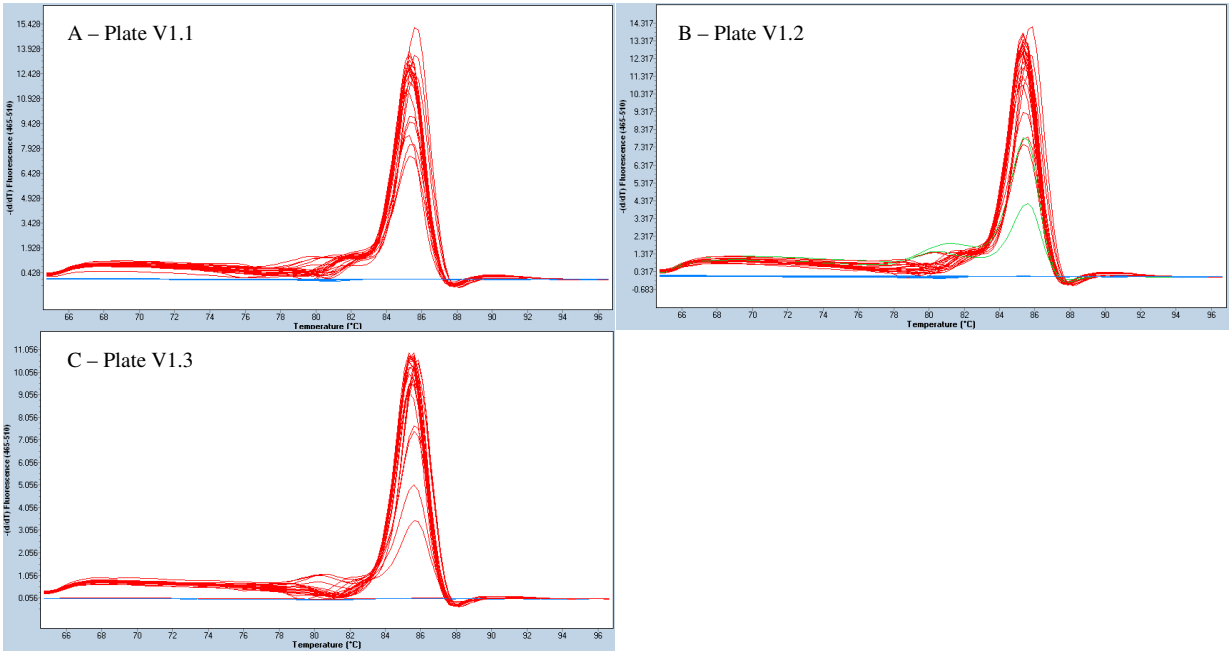

Figure 1.2: Roche LightCycler® 480 melt curve for the three *L. gasseri* optimization plates (V1.1-V1.3). The –d/dT fluorescence (465-510 nm) is indicated on the y-axis and the

temperature (℃) is indicated on the x-axis. Red indicates a single peak (product), green indicates two peaks and blue indicates no peak for each well.

2 *Lactobacillus jensenii*

Two qPCR trial plates were run for *L. jensenii* where the first (V1.1) was run using the same reagent volumes as the finalized conditions for *L. crispatus* (V1.7). The following qPCR conditions were followed, 95℃ for 5 min for initial denaturation, followed by 40 cycles of 95℃ for 15 s, 60℃ for 55 s, and 72℃ for 1 min (Figure 2.1 A, Figure 2.2 A). The error value was higher than optimum despite the clean amplification curves of the positive controls. The second *L. jensenii* qPCR trial plate (V1.2) was run under the same conditions as qPCR trial V1.1 to try and improve efficiency and pipetting accuracy (Figure 2.1 B, Figure 2.2 B). The error and efficiency values were close to optimum with a good standard curve and single melt curve peaks.

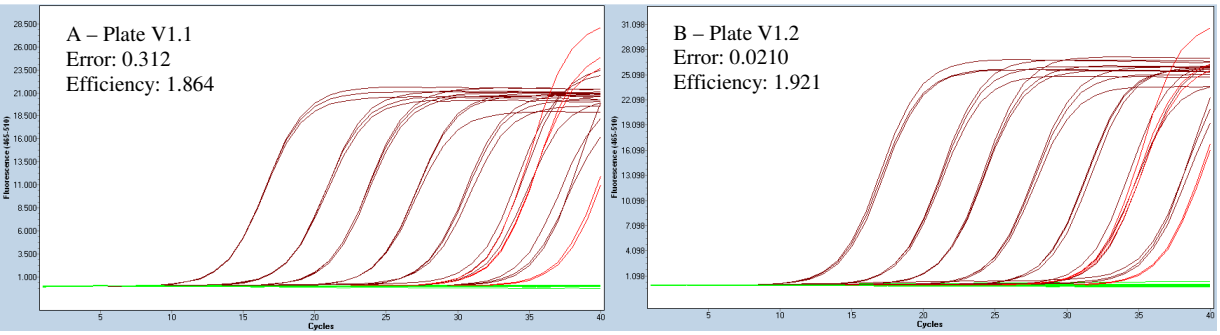

Figure 2.1: Roche LightCycler® 480 absolute quantitative derivative max amplification curve for the two *L. jensenii* optimization plates (V1.1-V1.2). The fluorescence (465-510 nm) is indicated on the y-axis and the number of cycles is indicated on the x-axis. Red and brown indicate positive amplification in the unknown sample and the positive control standards respectively, and green indicates negative amplification in the wells.

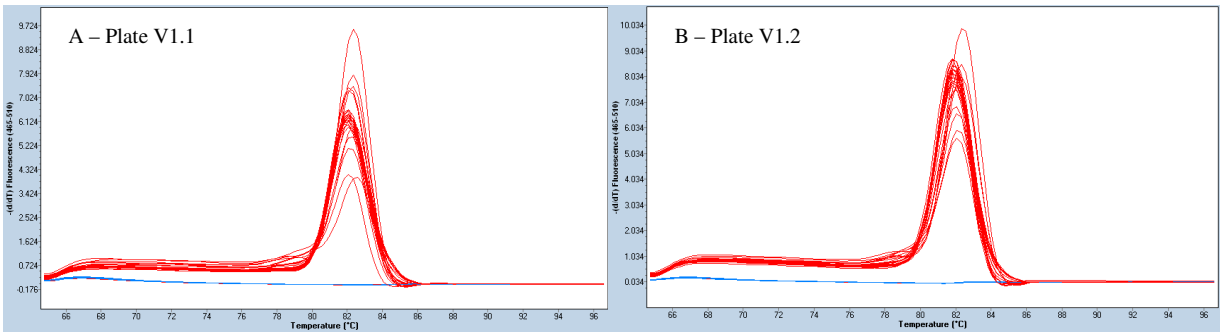

Figure 2.2: Roche LightCycler® 480 melt curve for the two *L. jensenii* optimization plates (V1.1-V1.2). The –d/dT fluorescence (465-510 nm) is indicated on the y-axis and the temperature (℃) is indicated on the x-axis. Red indicates a single peak (product), green indicates two peaks and blue indicates no peak for each well.

3 *Lactobacillus iners*

As seen above for *L. jensenii, L. iners* was optimized with two trial plates with the first trial plate (V1.1) being run using the same reagent volumes and concentrations as set up in the final trial run for *L. crispatus* (V1.7) with the following qPCR conditions 95℃ for 15 min for the initial denaturation, followed by 40 cycles of 95℃ for 15 s, 60℃ for 55s and 69℃ for 1 min (Figure 3.1 A, Figure 3.2 A). The efficiency was slightly higher than expected with some dimerization present within the melt curve. The second trial plate for *L. iners* (V1.2) was run using the same conditions as in V1.1 in order to confirm the error and efficiency values before running samples (Figure 3.1 B, Figure 3.2 B). The error and efficiency were of sufficient readings with a single melt curve peak.

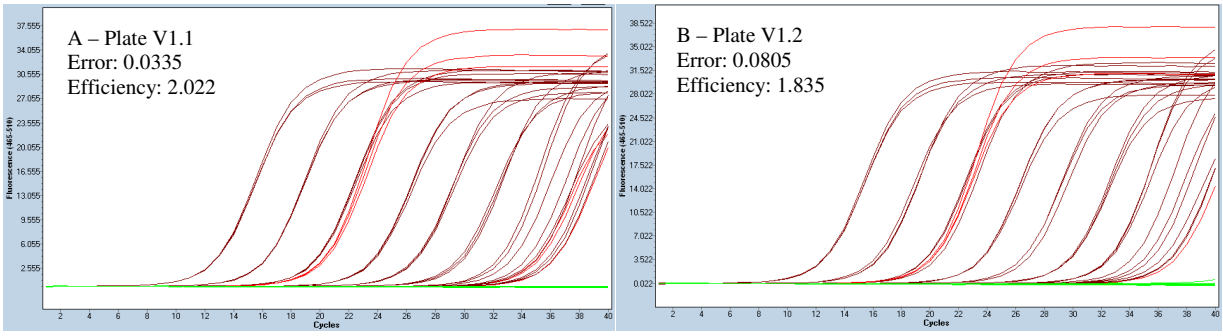

Figure 3.1: Roche LightCycler® 480 absolute quantitative derivative max amplification curve for the two *L. iners* optimization plates (V1.1-V1.2). The fluorescence (465-510 nm) is indicated on the y-axis and the number of cycles is indicated on the x-axis. Red and brown indicate positive amplification in the unknown sample and the positive control standards respectively, and green indicates negative amplification in the wells.

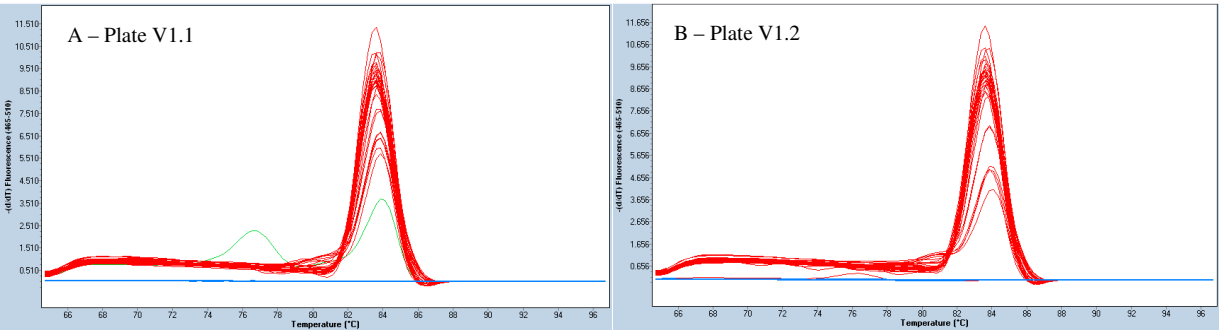

Figure 3.2: Roche LightCycler® 480 melt curve for the two *L. iners* optimization plates (V1.1-V1.2). The –d/dT fluorescence (465-510 nm) is indicated on the y-axis and the temperature (℃) is indicated on the x-axis. Red indicates a single peak (product), green indicates two peaks and blue indicates no peak for each well.

For all result amplification and melt curves, see Appendix D, qPCR Results.

Appendix D: qPCR Results

Thhis appendix serves as a refrence for the raw qPCR results for the absolute quantitifcation od each bacterial species of interest i.e. *L. crispatus* (copies/ng), *L. gasseri* (copies/ng), *L. jensenii* (copies/ng), *L. iners* (copies/ng), *G. vaginalis* (copies/ng), and *P. bivia* (copies/ng) in the DNA extracted from the lateral wall swabs from adolescent females who partook in the WISH Cohort at the Masiphumelele Youth Centre.

1. Real-Time PCR (qPCR) Results:

Table 1.1: Summary table for the WISH sample run qPCR standard curve statistics for the following bacteria of interest:

Bacteria	qPCR Plate	Error	Efficiency
L. crispatus	V2.1	0.244	1.704
	V2.2	0.259	1.807
	V2.3	0.0130	1.896
	V2.4	0.0264	1.903
	V2.5	0.488	1.521
	V2.6	0.0215	1.867
	V2.7	0.0393	1.819
	V2.8	0.0290	1.865
L. gasseri	V2.1	0.0557	1.803
	V2.2	0.0672	1.741
	V2.3	0.0565	1.743
	V2.4	0.0592	1.691
	V2.5	0.0609	1.695
	V2.6	0.0511	1.701
	V2.7	0.122	1.801
	V2.8	0.0328	1.858
	V2.9	0.0261	1.846
L. jensenii	V2.1	0.0256	1.897
	V2.2	0.0521	1.962
	V2.3	0.0498	1.912
	V2.4	0.0458	1.901
	V2.5	0.0521	1.930
	V2.6	0.0508	1.686
	V2.7	0.0466	1.961
	V2.8	0.0401	1.941
L. iners	V2.1	0.0139	1.810
	V2.2	0.0237	1.764
	V2.3	0.0203	1.698
	V2.4	0.0143	1.825
	V2.5	0.0832	1.867

	V2.6	0.0132	1.935
G. vaginalis	V2.1	0.0252	1.895
	V2.2	0.0151	1.856
	V2.3	0.0375	1.902
	V2.4	0.0601	1.892
	V2.5	0.0255	1.901
	V2.6	0.0751	1.821
	V2.7	0.0805	1.835
P. bivia	V2.1-V2.6	0.0608	1.993

1.1 *Lactobacillus crispatus*

Eight plates were run in total for the 143 samples in triplicate with the positive controls for *L. crispatus*. For instances where either one or two replicates showed primer dimers, no amplification or different values in comparison to the other replicates for the sample, the sample was re-run on another plate to confirm the readings (Figure 1.1.1, Figure 1.1.2).

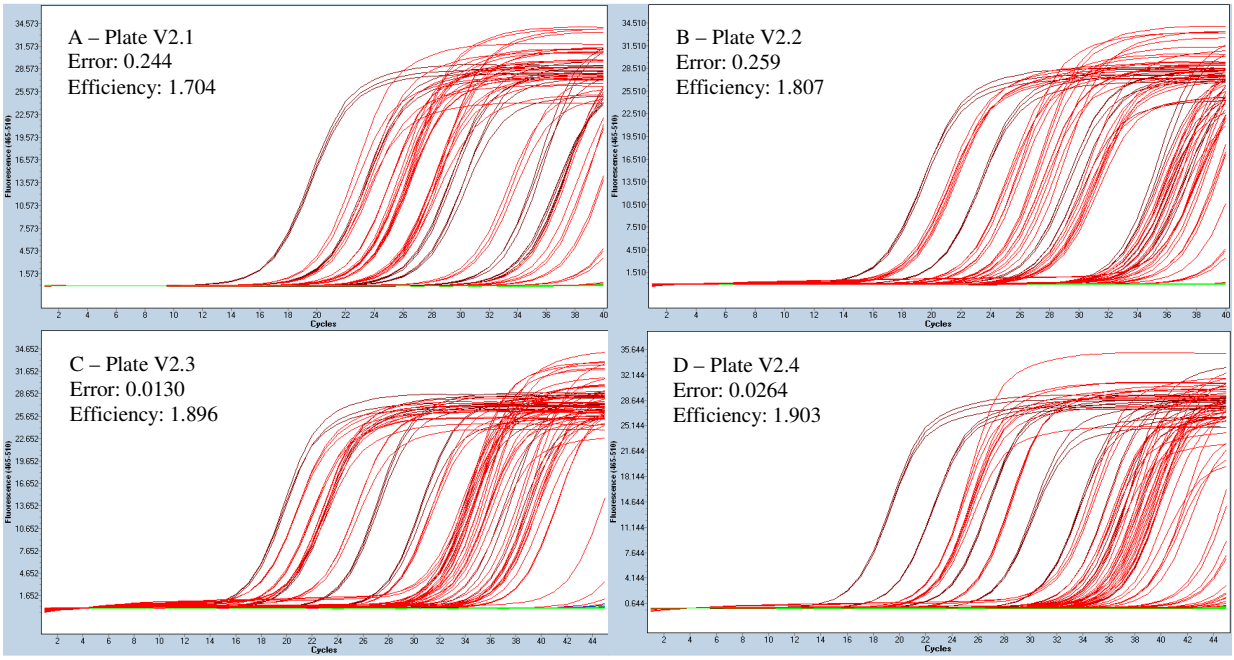

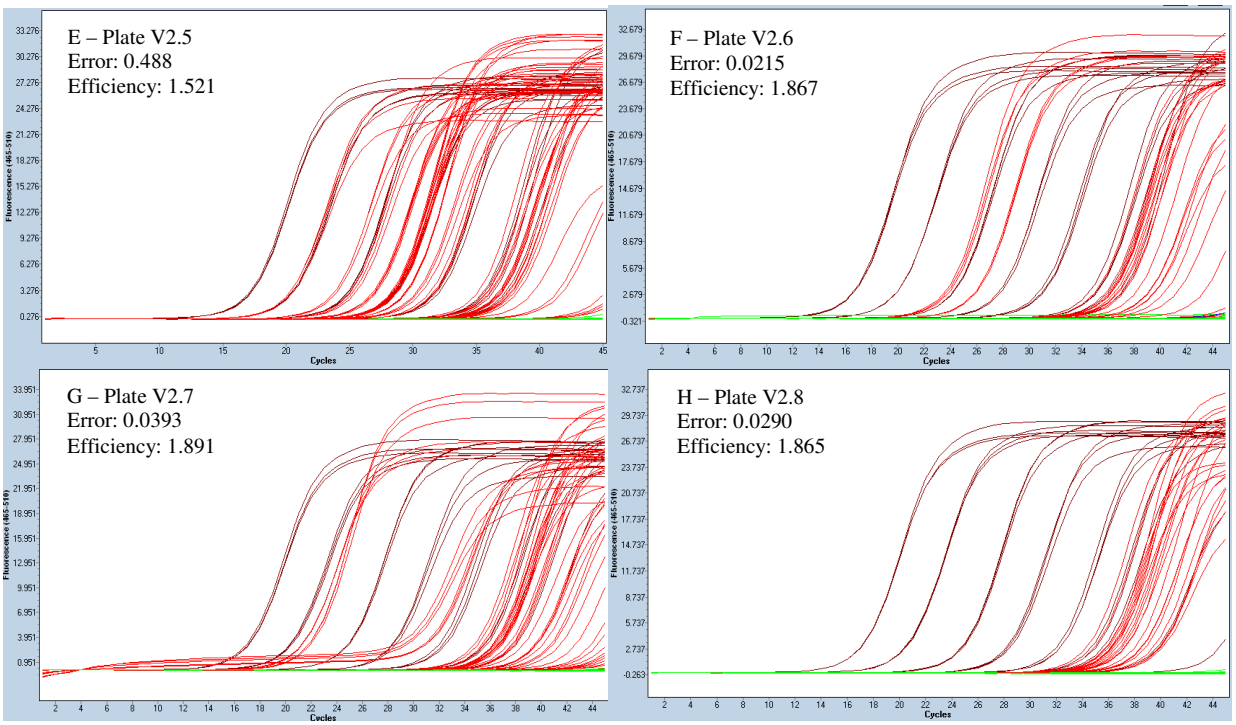

Figure 1.1.1: Absolute quantitative derivative max amplification curve of *L. crispatus* qPCR (V2.1-V2.8) reported as log transformed copies/ng total DNA, generated based on all wells and the standard curve is generated based on the amplification curve of the standard positive controls ranging from 10^6 to 10^0 copies/µL. The fluorescence (465-510 nm) is indicated on the y-axis and the number of cycles is indicated on the x-axis. Red and brown indicate positive amplification in the unknown samples and the positive control standards respectively; blue indicates uncertainty and green indicates negative amplification in the wells.

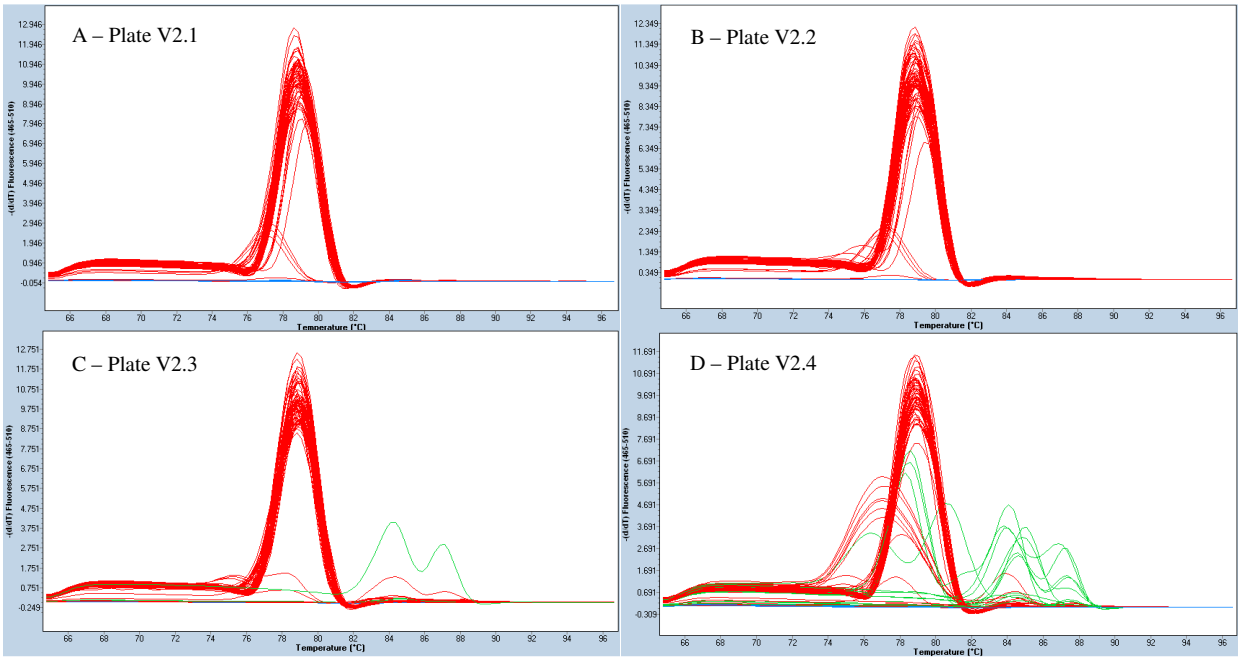

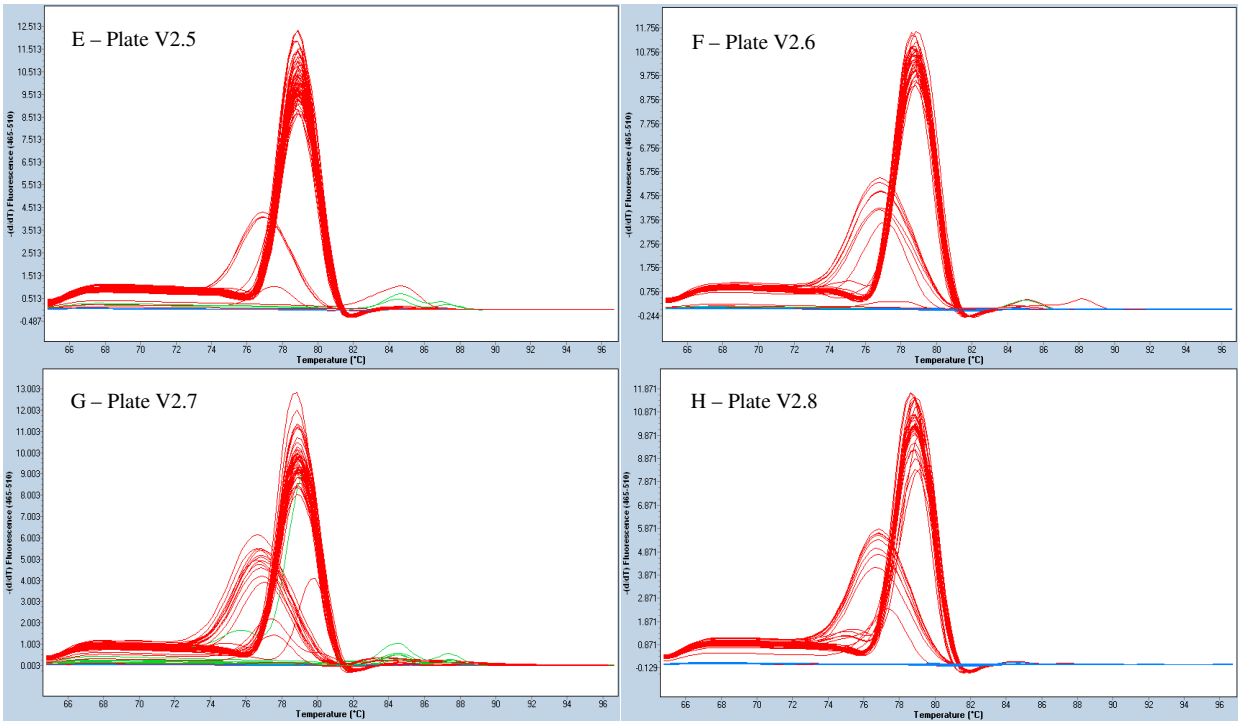

Figure 1.1.2: Melt curve of *L. crispatus*, qPCR (V2.1-V2.8) generated based on the amplification curve of all wells where red indicates a single product (peak) and blue indicates no product. The –d/dT fluorescence (465-510 nm) is indicated on the y-axis and the temperature (℃) is indicated on the x-axis.

1.2 *Lactobacillus gasseri*

Nine plates were run in total for the 143 samples in triplicate with the positive controls for *L. gasseri* due to more samples requiring confirmation of their replicate consistency. For instances where either one or two replicates showed primer dimers, no amplification or different values in comparison to the other replicates for the sample, the sample was re-run on another plate to confirm the readings (Figure 1.2.1, Figure 1.2.2).

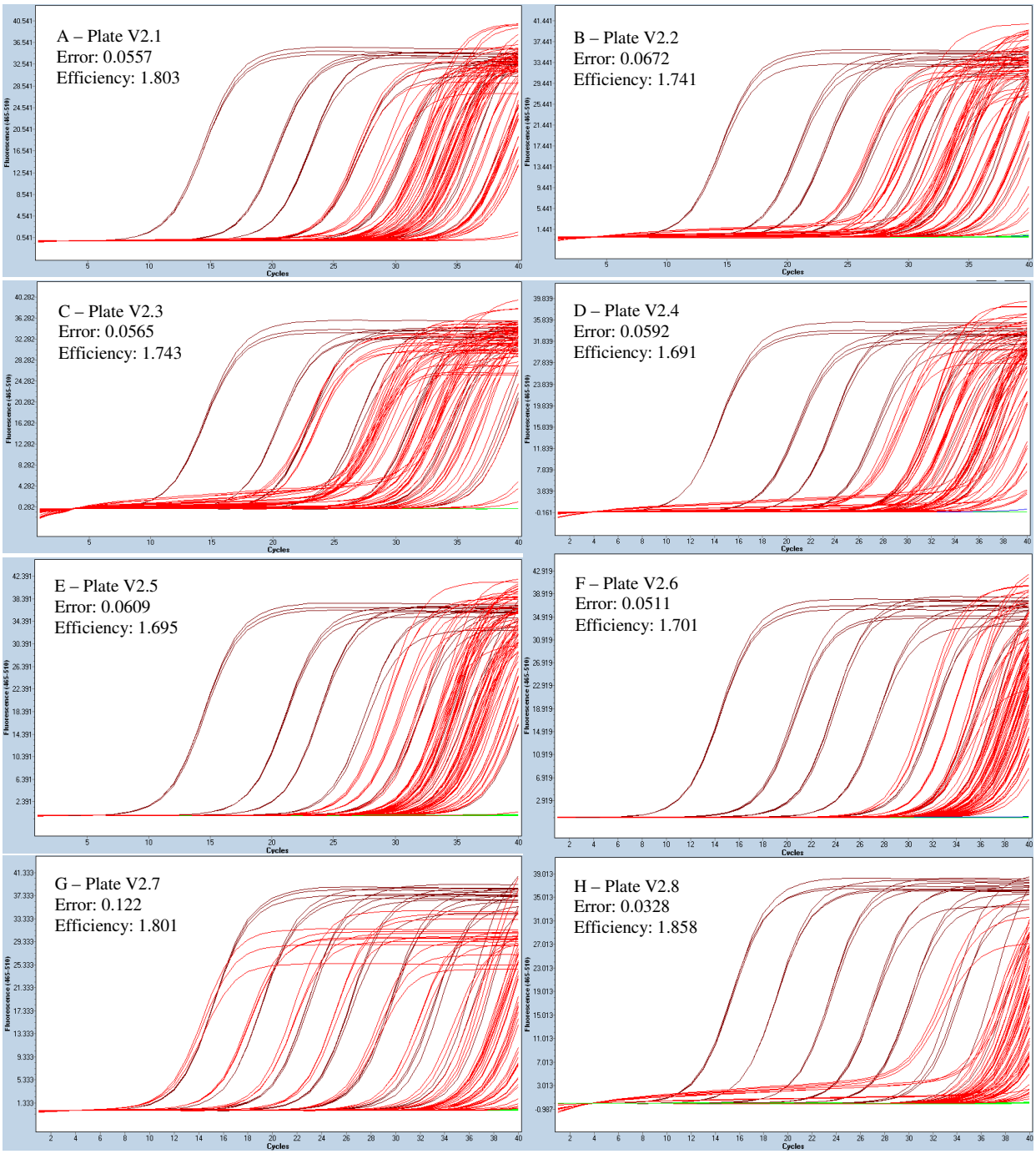
A – Plate V2.1
Error: 0.0557
Efficiency: 1.803
B – Plate V2.2
Error: 0.0672
Efficiency: 1.741
C – Plate V2.3
Error: 0.0565
Efficiency: 1.743
D – Plate V2.4
Error: 0.0592
Efficiency: 1.691
E – Plate V2.5
Error: 0.0609
Efficiency: 1.695
F – Plate V2.6
Error: 0.0511
Efficiency: 1.701
G – Plate V2.7
Error: 0.122
Efficiency: 1.801
H – Plate V2.8
Error: 0.0328
Efficiency: 1.858
Cycles
Fluorescence (465-510)

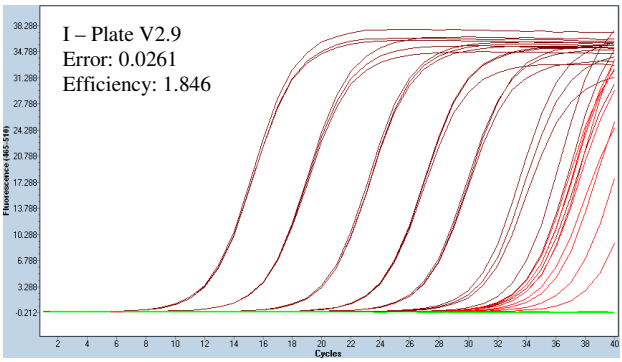

Figure 1.2.1: Absolute quantitative derivative max amplification curve of *L. gasseri* qPCR (V2.1-V2.9) reported as log transformed copies/ng total DNA, generated based on all wells and the standard curve is generated based on the amplification curve of the standard positive controls ranging from 10^6 to 10^0 copies/µL. The fluorescence (465-510 nm) is indicated on the y-axis and the number of cycles is indicated on the x-axis. Red and brown indicate positive amplification in the unknown samples and the positive control standards respectively; blue indicates uncertainty and green indicates negative amplification in the wells.

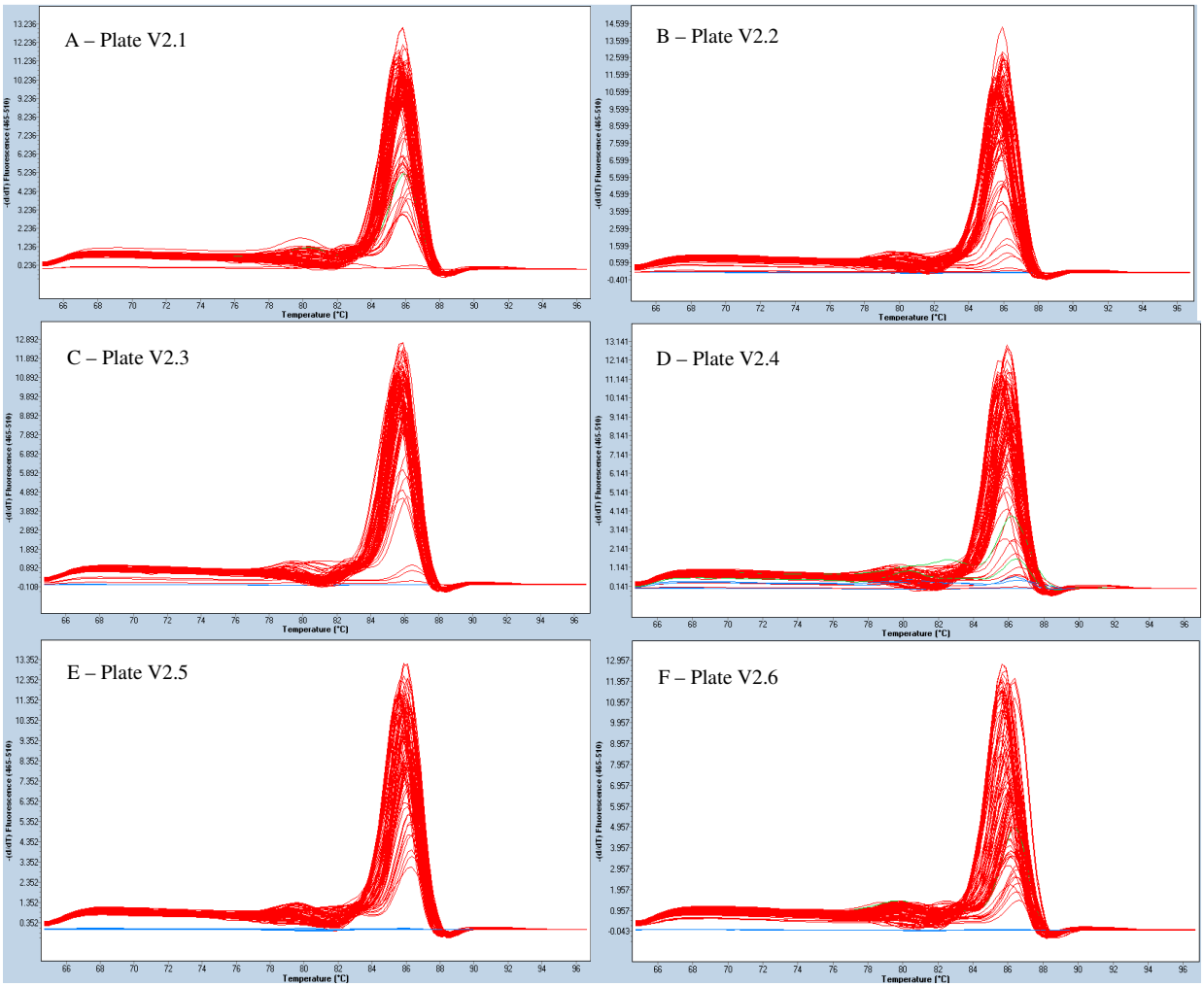

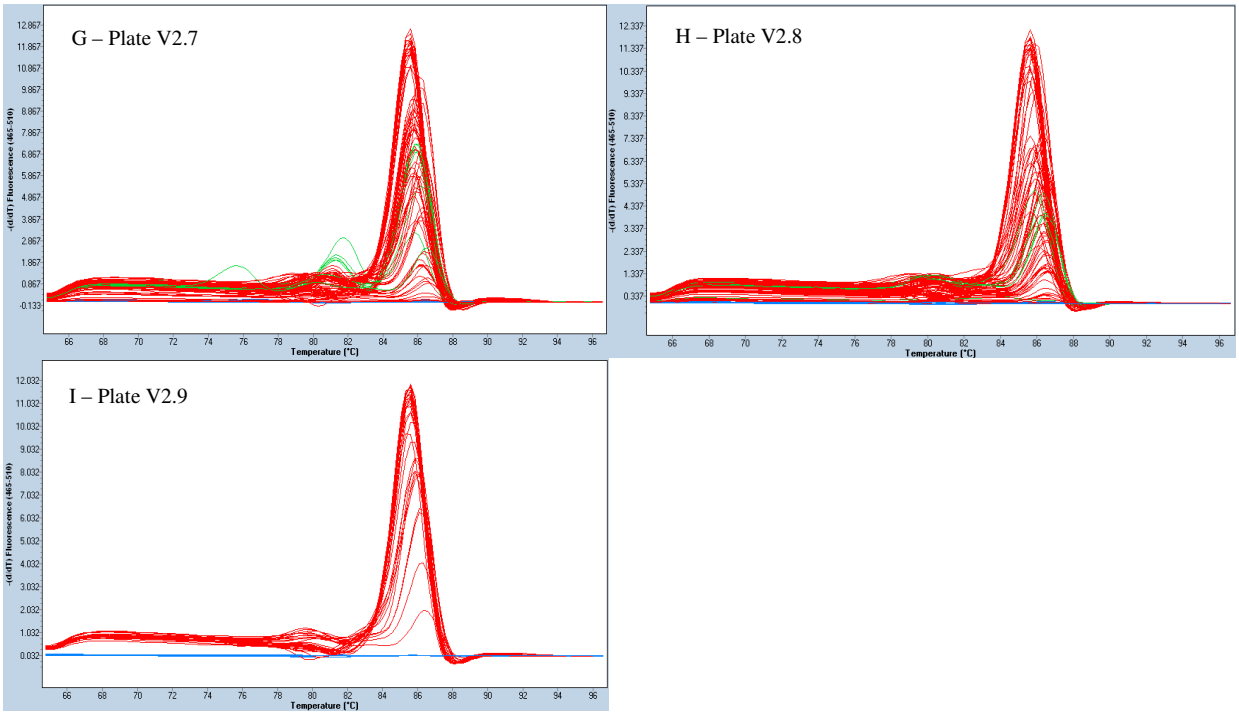

Figure 1.2.2: Melt curve of *L. gasseri* qPCR (V2.1-V2.9) generated based on the amplification curve of all wells where red indicates a single product (peak) and blue indicates no product. The –d/dT fluorescence (465-510 nm) is indicated on the y-axis and the temperature (℃) is indicated on the x-axis.

1.3 *Lactobacillus jensenii*

Eight plates were run in total for the 143 samples in triplicate with the positive controls for *L. jensenii* due to more samples requiring confirmation of their replicate consistency. For instances where either one or two replicates showed primer dimers, no amplification or different values in comparison to the other replicates for the sample, the sample was re-run on another plate to confirm the readings (Figure 1.3.1, Figure 1.3.2).

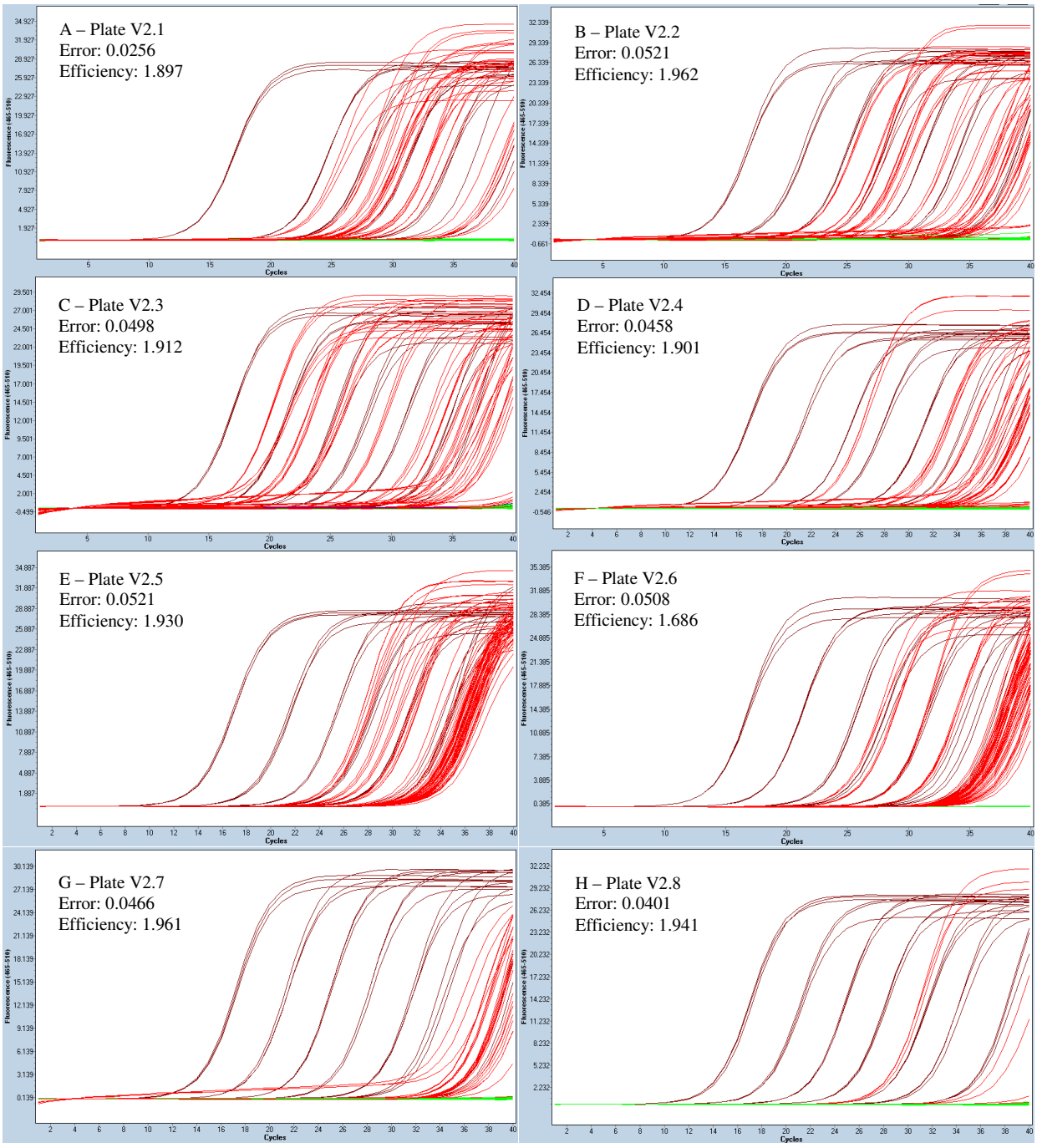

Figure 1.3.1: Absolute quantitative derivative max amplification curve of *L. jensenii* qPCR (V2.1-V2.8) reported as log transformed copies/ng total DNA, generated based on all wells and the standard curve is generated based on the amplification curve of the standard positive controls ranging from 10^6 to 10^0 copies/µL. The fluorescence (465-510 nm) is indicated on the y-axis and the number of cycles is indicated on the x-axis. Red and brown indicate positive amplification in the unknown samples and the positive control standards respectively; blue indicates uncertainty and green indicates negative amplification in the wells.

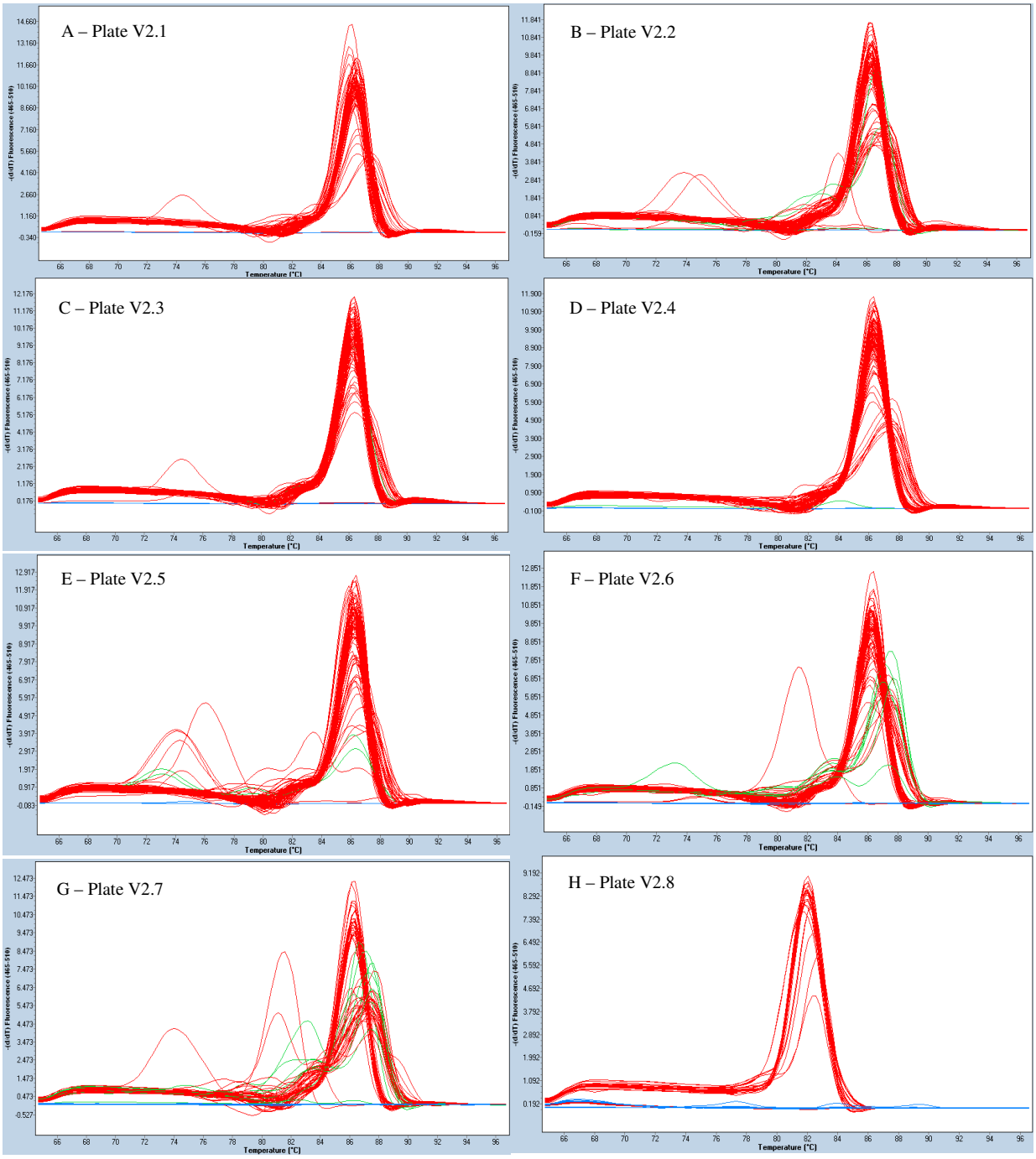

Figure 1.3.2: Melt curve of *L. jensenii* qPCR (V2.1-V2.8) generated based on the amplification curve of all wells where red indicates a single product (peak) and blue indicates no product. The –d/dT fluorescence (465-510 nm) is indicated on the y-axis and the temperature (℃) is indicated on the x-axis.

1.4 *Lactobacillus iners*

Six plates were run in total for the 143 samples in triplicate with the positive controls for *L. iners*. Repeats were not run for *L. iners* as it was established with the previous three bacteria that the majority of the negatives were due to lower readings for the bacteria in comparison to *L. iners* (Figure 1.4.1, Figure 1.4.2).

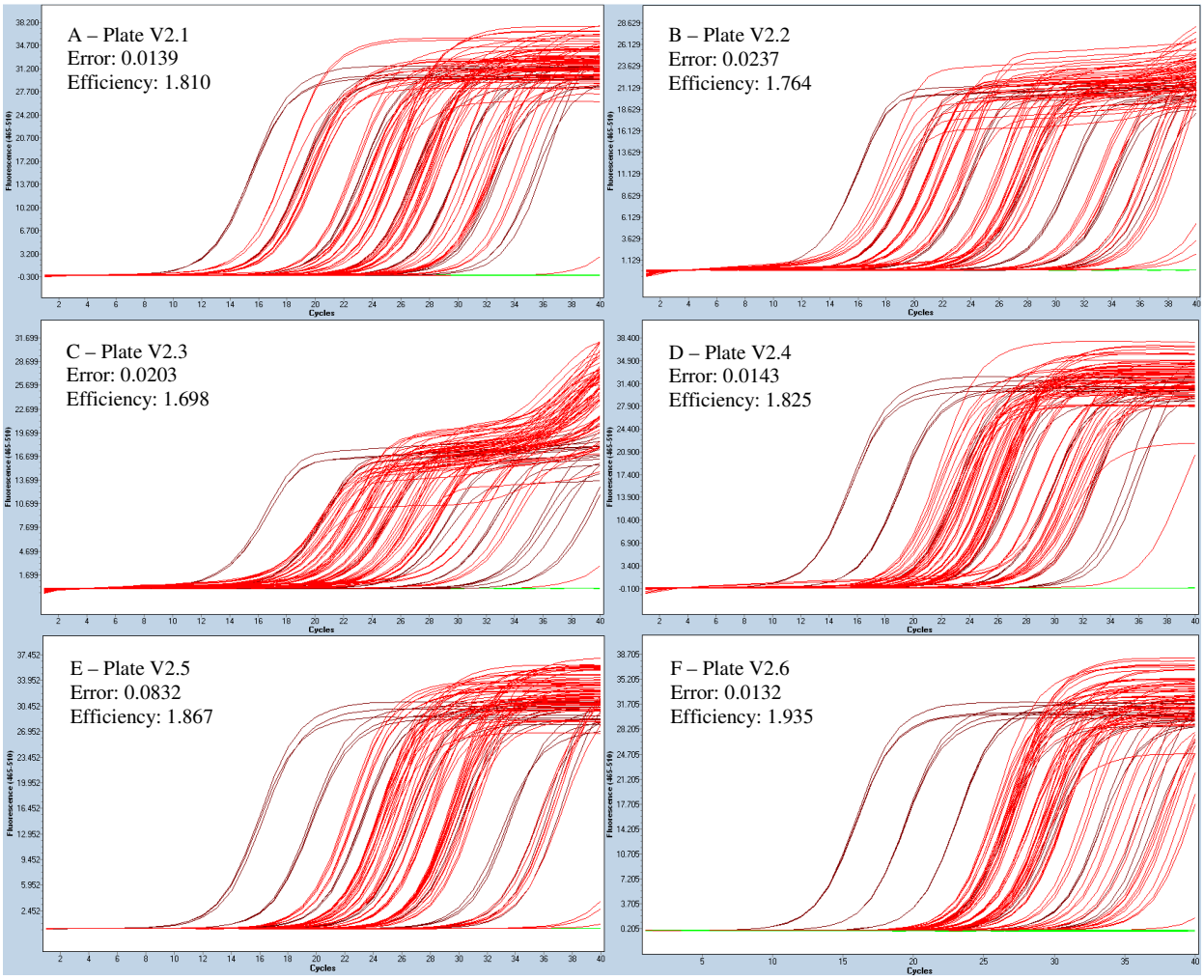

Figure 1.4.1: Absolute quantitative derivative max amplification curve of *L. iners* qPCR (V2.1-V2.6) reported as log transformed copies/ng total DNA, generated based on all wells and the standard curve is generated based on the amplification curve of the standard positive controls ranging from 10^6 to 10^0 copies/µL. The fluorescence (465-510 nm) is indicated on the y-axis and the number of cycles is indicated on the x-axis. Red and brown indicate positive amplification in the unknown samples and the positive control standards respectively; blue indicates uncertainty and green indicates negative amplification in the wells.

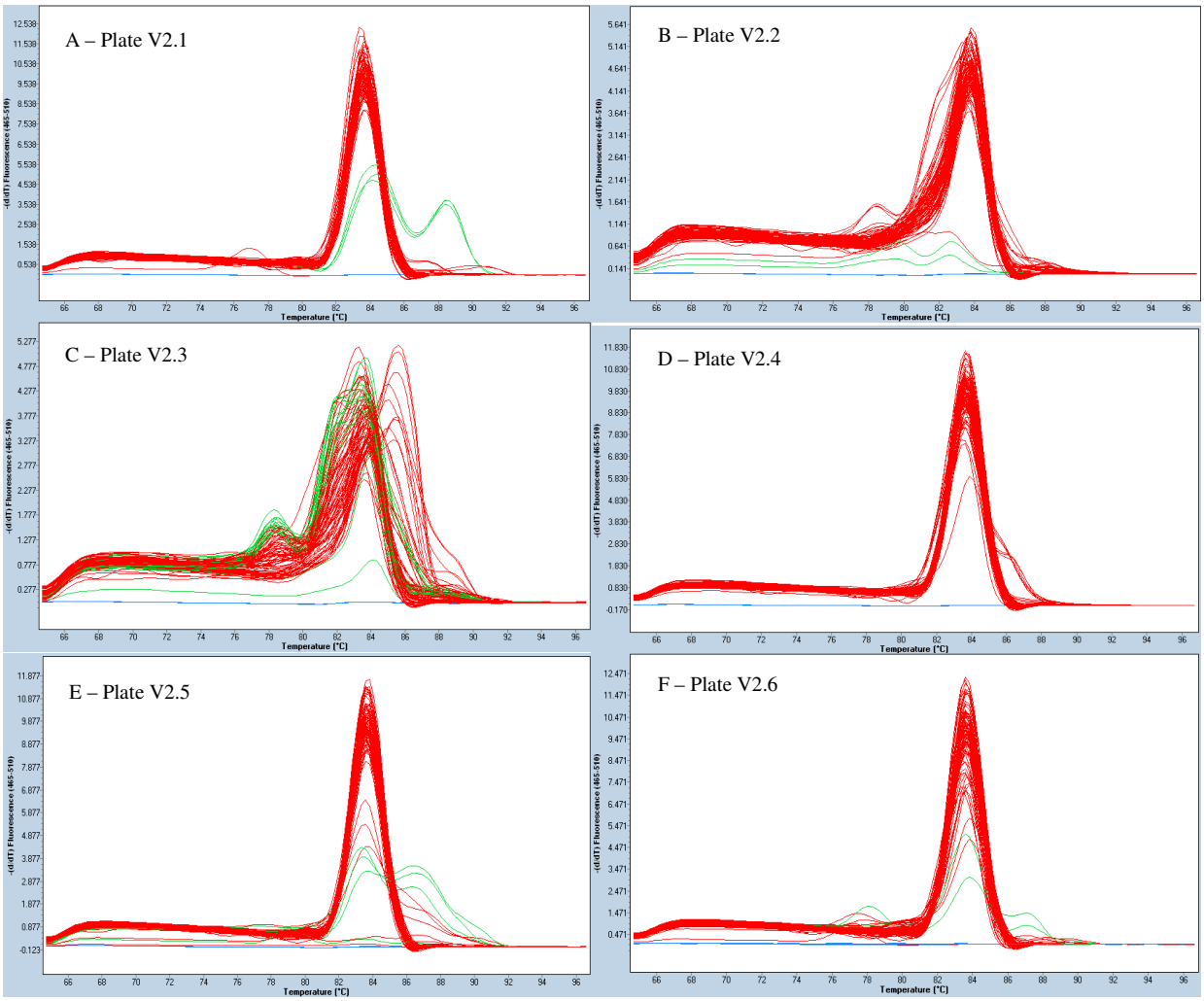

Figure 1.4.2: Melt curve of *L. iners* qPCR (V2.1-V2.6) generated based on the amplification curve of all wells where red indicates a single product (peak) and blue indicates no product. The –d/dT fluorescence (465-510 nm) is indicated on the y-axis and the temperature (℃) is indicated on the x-axis.

1.5 *Gardnerella vaginalis*

A total of seven plates were run for *G. vaginalis* in order to quantify the number of copies/ng present within the samples. For instances where either one or two replicates showed primer dimers, no amplification or different values in comparison to the other replicates for the sample, the sample was re-run on another plate to confirm the readings (Figure 1.5.1, Figure 1.5.2).

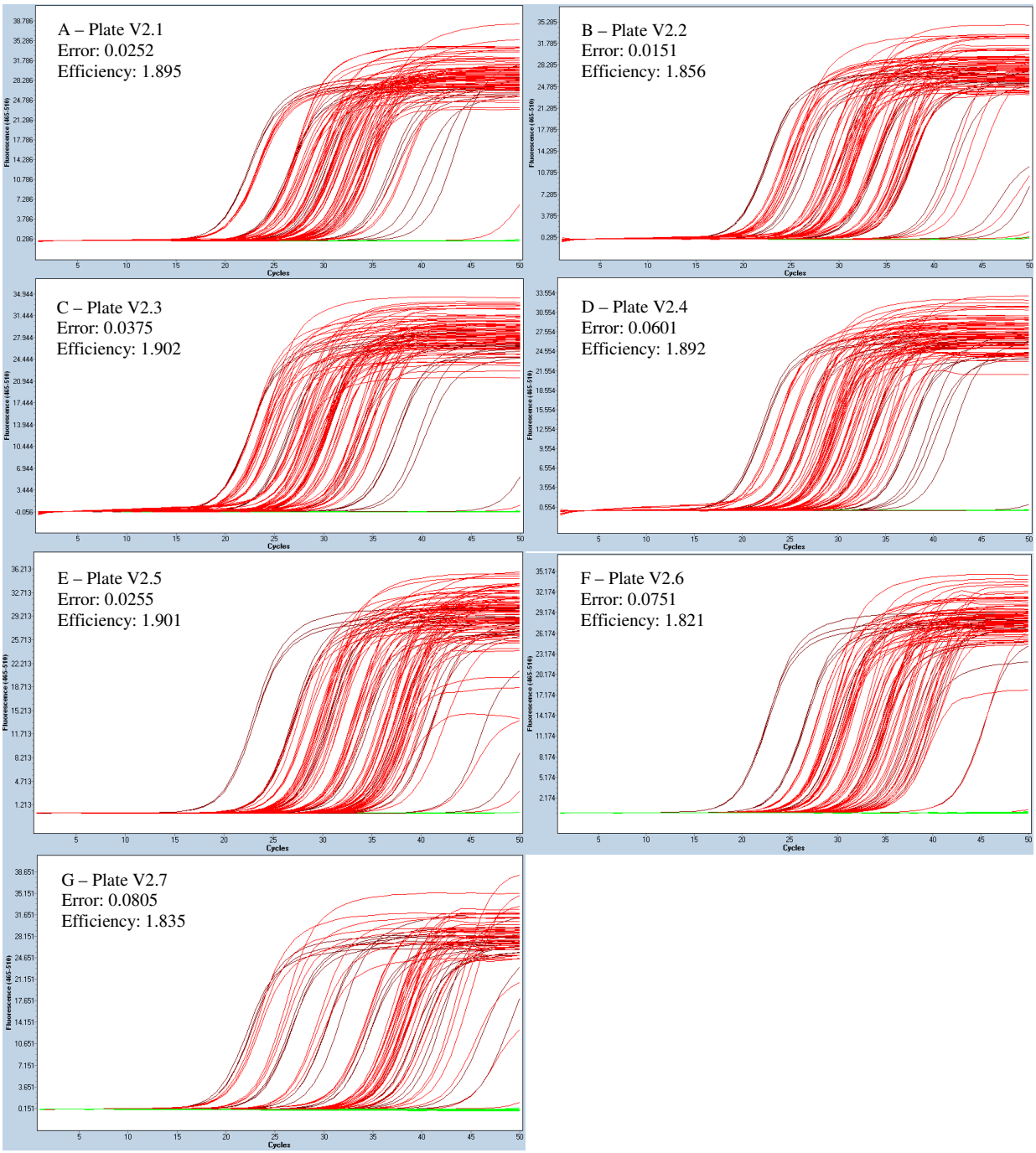

Figure 1.5.1: Absolute quantitative derivative max amplification curve of *G. vaginalis* qPCR (V2.1-V2.7) reported as log transformed copies/ng total DNA generated based on all wells and the standard curve is generated based on the amplification curve of the standard positive controls ranging from 10^6 to 10^0 copies/µL. The fluorescence (465-510 nm) is indicated on the y-axis and the number of cycles is indicated on the x-axis. Red and brown indicate positive amplification in the unknown samples and the positive control standards respectively; blue indicates uncertainty and green indicates negative amplification in the wells.

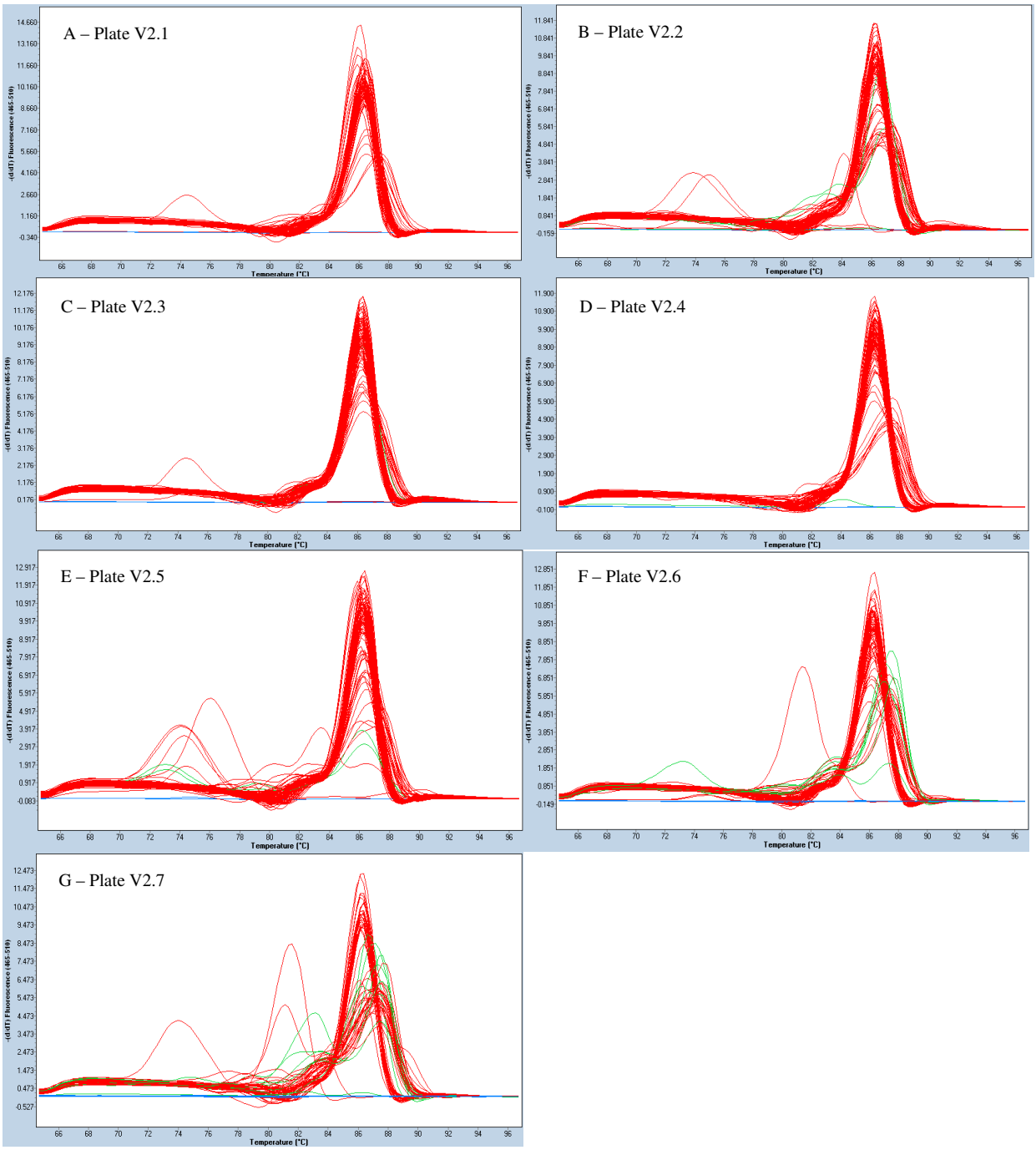

Figure 1.5.2: Melt curve of *G. vaginalis* qPCR (V2.1-V2.7) generated based on the amplification curve of all wells where red indicates a single product (peak) and blue indicates no product. The –d/dT fluorescence (465-510 nm) is indicated on the y-axis and the temperature (℃) is indicated on the x-axis.

1.6 *Prevotella bivia*

Five plates were run in total for the 143 samples in triplicate with the positive controls for *P. bivia*. There were no instances where either one or two replicates showed primer dimers, no amplification or different values in comparison to the other replicates for the samples, thus no samples were repeated. There was not enough standard control DNA to run repeats of all the dilutions each time, thus a reference standard curve was used to quantify the samples (Figure 1.6.1, Figure 1.6.2).

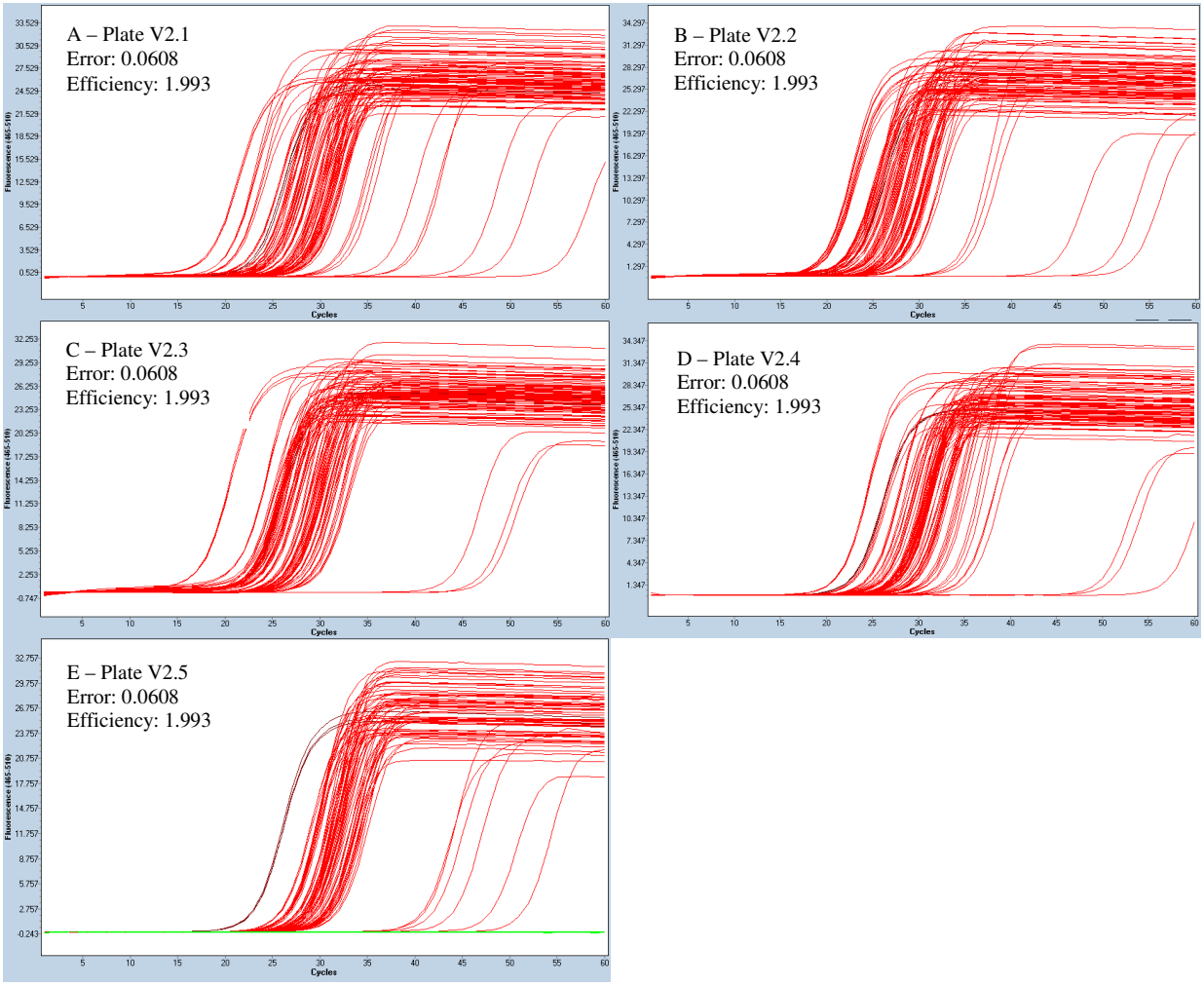

Figure 1.6.1: Absolute quantitative derivative max amplification curve of *P. bivia* qPCR (V2.1-V2.5) reported as log transformed copies/ng total DNA, generated based on all wells and the standard curve is generated based on the amplification curve of the standard positive controls ranging from 10^6 to 10^0 copies/µL. The fluorescence (465-510 nm) is indicated on the y-axis and the number of cycles is indicated on the x-axis. Red and brown indicate positive amplification in

the unknown samples and the positive control standards respectively; blue indicates uncertainty and green indicates negative amplification in the wells.

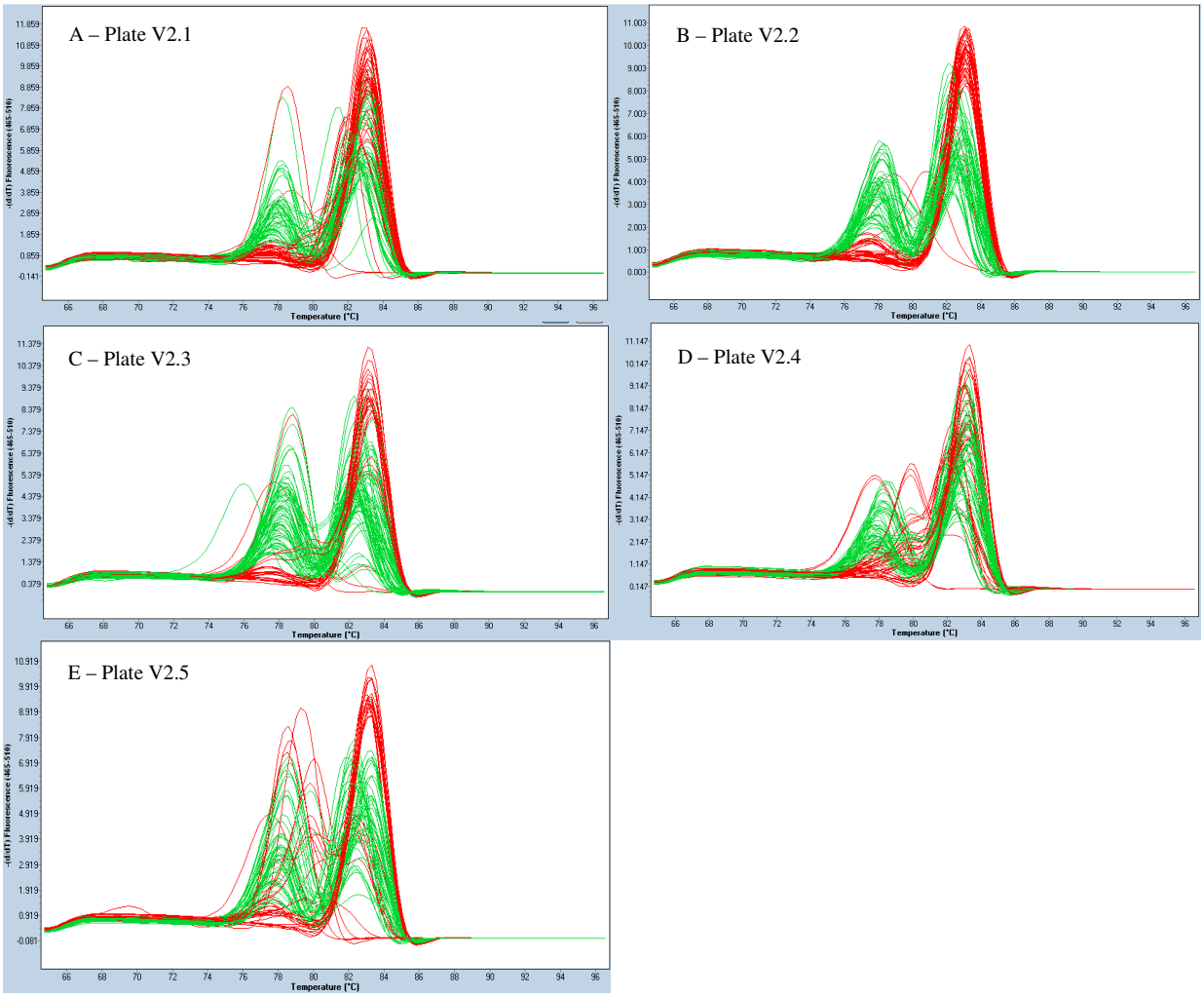

Figure 1.6.2: Melt curve of *P. bivia* qPCR (V2.1-V2.5) generated based on the amplification curve of all wells where red indicates a single product (peak) and blue indicates no product. The –d/dT fluorescence (465-510 nm) is indicated on the y-axis and the temperature (℃) is indicated on the x-axis.

Appendix E: Results

This appendix contains all of the data not included within Chapter 4: Results, as well as all of the *P. bivia* data.

1 Descriptive statistics

Table 1.1: Descriptive statistics for each bacterial species, quantified from DNA extracted from the WISH lateral wall swab for each participant.

	Bacteria					
	L. crispatus	*L. gasseri*	*L. jensenii*	*L. iners*	*G. vaginalis*	*P. bivia*
Min	0.0	0.0	0.0	1.034	1.738	1.738
25% Percentile	0.0	1.976	1.570e-016	266.7	1015	3667
Median	3.957	17.58	1.568	2807	8540	11073
75% Percentile	4980	64.67	59.00	18727	49867	75533
Max	7.113e+007	320000	5.440e+006	4.167e+007	3.033e+006	2.553e+007
Mean	858412	3327	48743	337988	151382	750128
Std. Deviation	7.157e+006	27908	462042	3.485e+006	414156	3.405e+006
Std. Error	598472	2334	38638	291468	34633	284714

2. Comparison of absolute bacterial quantities to BV status, inflammation levels, age, hormonal contraceptive and STI status, bacterial versus viral STI's and HPV

2.1 Association levels between the quantities of the bacteria of interest and BV status

Participants were categorized as being BV positive, intermediate or negative based on Nugent scoring. A Nugent score of 0-3 is BV negative, a score of 4-6 is BV intermediate and a score of 7-10 is BV positive.

Table 2.1: Comparison of the non-parametric paired Friedman's ANOVA test across all bacterial groups with a Dunn's Multiple Comparison test for BV positive, BV intermediate and BV negative groups:

Bacterial comparisons	BV Group p-values		
	Positive	Intermediate	Negative
L. gasseri vs *L. jensenii*	0.0158*	>0.9999	>0.9999
L. gasseri vs *L. crispatus*	>0.9999	>0.9999	0.0009*

L. gasseri vs *L. iners*	<0.0001*	0.1756	<0.0001*
L. gasseri vs *G. vaginalis*	<0.0001*	0.0123*	0.0002*
L. gasseri vs *P. bivia*	<0.0001*	0.0001*	<0.0001*
L. jensenii vs *L. crispatus*	0.741	>0.9999	<0.0001*
L. jensenii vs *L. iners*	<0.0001*	0.1178	<0.0001*
L. jensenii vs *G. vaginalis*	<0.0001*	0.0074*	<0.0001*
L. jensenii vs *P. bivia*	<0.0001*	<0.0001*	<0.0001*
L. crispatus vs *L. iners*	<0.0001*	0.0044*	>0.9999
L. crispatus vs *G. vaginalis*	<0.0001*	0.0001*	>0.9999
L. crispatus vs *P. bivia*	<0.0001*	<0.0001*	0.0012*
L. iners vs *G. vaginalis*	0.007	>0.9999	>0.9999
L. iners vs *P. bivia*	0.0274	0.8133	0.3939
G. vaginalis vs *P. bivia*	>0.9999	>0.9999	0.0041*
ANOVA p-value	<0.0001*	<0.0001*	<0.0001*

*The asterisk indicates a p-value lower than the standardized p-value of 0.05 with a 95% confidence interval.

2.1.1 *Prevotella bivia*

We compared the quantified log copies/ng of *P. bivia* between the BV groups. There was no significant difference in *P. bivia* between the BV groups (Kruskal-Wallis ANOVA p=0.8031) (Figure 2.1.1). This is one of the reasons that *P. bivia* was not included in the comparison between the bacteria per category. The results are not reliable and indicate and oversensitivity of the primers, resulting in increased copies/ng between all thee BV groups.

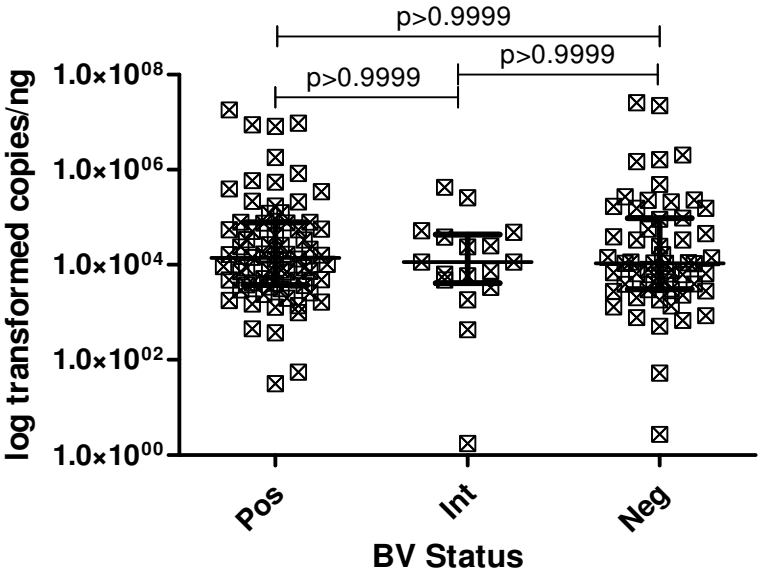

Figure 2.1.1: Comparison of the quantities of *P. bivia* (log transformed copies/ng DNA) measured in the DNA extracted from vaginal lateral wall swabs from participants in the WISH study, between BV positive, intermediate and negative groups. All p-value comparisons were based on an unpaired, non-parametric Dunn's Multiple Comparison test. Each point in the figure represents an individual participant. The three horizontal bars represent the median value (middle bar), upper interquartile range (top bar) and lower interquartile range (bottom bar).

2.2 Association levels between bacteria of interest and inflammatory immunological factor levels

The two inflammatory groups were defined based on the unsupervised analysis of the 47 immunological factors of interest in the cervicovaginal fluid of women in the WISH cohort. These immunological factors were categorized into high and low inflammation by partitioning around medoids (PAM) using an R package 'cluster' with a k-value of 2. The samples were originally separated into high and low inflammation based on the levels of only the pro-inflammatory and chemokine factors measured. However, the inflammation separation of the participant samples showed little difference between the two pro-inflammatory and chemokine groups of immunological factor analysis in comparison to using all of the factors to determine high and low inflammation. Thus the final inflammation categorization was done using all 47 immunological factors.

The immunological factors measured in this study can be generally grouped into five different categories. The immunological factors considered as pro-inflammatory were IL-1a, IL-1b, IL-6, IL-12p40, IL-12(p70), IL-18, MIF, TNF-a, TNF-b and TRAIL. The immunological factors considered chemokines were CTACK, Eotaxin, GROa, IL-8, IL-16, IP-10, MCP-1, MCP-3, MIG, MIP-1a, MIP-1b, IFN-a2, and RANTES. The immunological factors considered growth factors were b-NGF, FGF basic, G-CSF, GM-CSF, HGF, IL-3, IL-7, IL-9, LIF, M-CSF, PDGF-bb, SCF, SCGF-b, SDF-1a and VEGF. The immunological factors considered adaptive were IFN-g, IL-4, IL-13, IL-17, IL-2Ra, IL-2, and IL-5. The immunological factors considered regulatory were IL-10 and IL-1ra.

Table 2.2: Comparison of the non-parametric, paired Friedman's ANOVA test across all bacterial groups with a Dunn's Multiple Comparison test for the Inflammation high and low groups:

Bacterial comparisons	Inflammation Level p-values	
	Low	High
L. gasseri vs *L. jensenii*	>0.9999	0.0463
L. gasseri vs *L. crispatus*	0.0097*	>0.9999
L. gasseri vs *L. iners*	<0.0001*	<0.0001*
L. gasseri vs *G. vaginalis*	<0.0001*	<0.0001*
L. gasseri vs *P. bivia*	<0.0001*	<0.0001*
L. jensenii vs *L. crispatus*	0.0005*	0.23
L. jensenii vs *L. iners*	<0.0001*	<0.0001*
L. jensenii vs *G. vaginalis*	<0.0001*	<0.0001*
L. jensenii vs *P. bivia*	<0.0001*	<0.0001*
L. crispatus vs *L. iners*	>0.9999	<0.0001*
L. crispatus vs *G. vaginalis*	0.9929	<0.0001*
L. crispatus vs *P. bivia*	0.0007*	<0.0001*
L. iners vs *G. vaginalis*	>0.9999	0.8439
L. iners vs *P. bivia*	0.1302	0.0117*
G. vaginalis vs *P. bivia*	0.3712	>0.9999
ANOVA p-value	<0.0001*	<0.0001*

* The asterisk indicates a p-value lower than the standardized p-value of 0.05 with a 95% confidence interval.

2.2.1 *Prevotella bivia*

We compared the quantified log copies/ng of *P. bivia* between the inflammation groups. The high inflammation group and the low inflammation group had no significant difference (p=0.8438) (Figure 2.2.1). The copies/ng within this inflammatory group should not be compared against the other five bacteria due to unreliable primers.

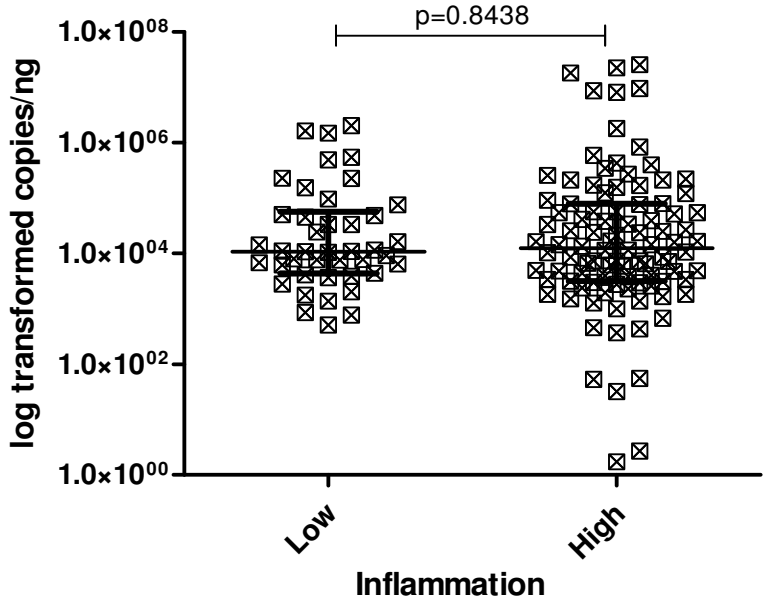

Figure 2.2.1: Comparison of the quantities of *P. bivia* (log transformed copies/ng DNA) measured in the DNA extracted from vaginal lateral wall swabs from participants in the WISH study, between women with high and low genital inflammation. All p-value comparisons were based on an unpaired, non-parametric Mann-Whitney t-test statistic. Each point in the figure represents an individual participant. The three horizontal bars represent the median value (middle bar), upper interquartile range (top bar) and lower interquartile range (bottom bar).

2.3 Association levels between the quantities (copies/ng) of bacteria of interest and age

The age of all participants was recorded upon screening for participation within the study. For this analysis, age was binarised into 16-18 years of age versus 19-22 years of age.

Table 2.3: Comparison of the non-parametric paired Friedman's ANOVA test across all bacterial groups with Dunn's Multiple Comparison test p-values for the two age groups 16 to 18 years old compared to 19 to 22 years old:

Bacterial comparisons	Age Group p-values	
	16-18 years old	19-22 years old
L. gasseri vs *L. jensenii*	0.2457	>0.9999
L. gasseri vs *L. crispatus*	>0.9999	>0.9999
L. gasseri vs *L. iners*	<0.0001*	<0.0001*
L. gasseri vs *G. vaginalis*	<0.0001*	<0.0001*

L. gasseri vs *P. bivia*	<0.0001*	<0.0001*
L. jensenii vs *L. crispatus*	0.0419*	0.0582
L. jensenii vs *L. iners*	<0.0001*	<0.0001*
L. jensenii vs *G. vaginalis*	<0.0001*	<0.0001*
L. jensenii vs *P. bivia*	<0.0001*	<0.0001*
L. crispatus vs *L. iners*	<0.0001*	<0.0001*
L. crispatus vs *G. vaginalis*	<0.0001*	<0.0001*
L. crispatus vs *P. bivia*	<0.0001*	<0.0001*
L. iners vs *G. vaginalis*	0.8223	>0.9999
L. iners vs *P. bivia*	0.0117*	0.1348
G. vaginalis vs *P. bivia*	>0.9999	0.7713
ANOVA p-value	<0.0001*	<0.0001*

* The asterisk indicates a p-value lower than the standardized p-value of 0.05 with a 95% confidence interval.

2.3.1 *Prevotella bivia*

We compared the quantified copies/ng of *P. bivia* between the age groups. The 16-18 years old age group and the 19-22 years old age group had no difference in log copies/ng (p=0.2629) (Figure 2.3.1). Although the *P. bivia* age data follows the same trend as the other bacteria, this analysis should be repeated with new primers.

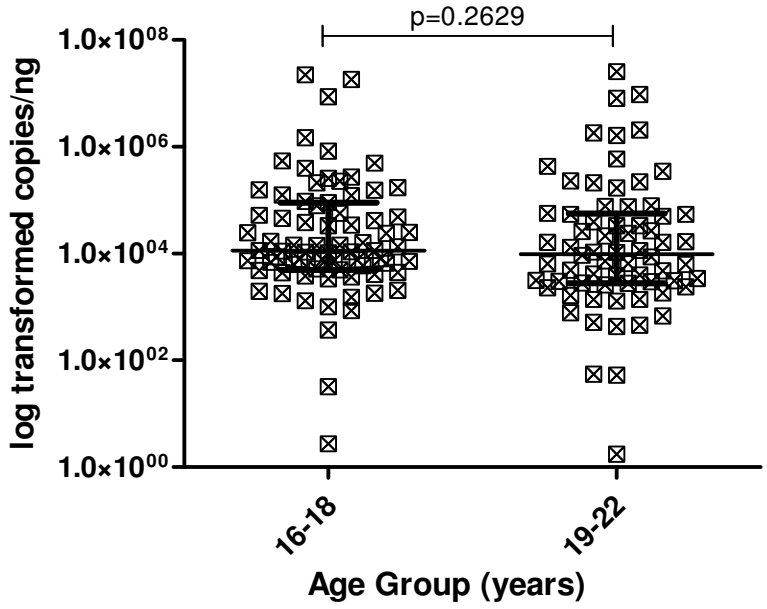

Figure 2.3.1: Comparison of the quantities of *P. bivia* (log transformed copies/ng DNA) measured in the DNA extracted from vaginal lateral wall swabs from participants in the WISH

study, between the two 16-18 years old and 19-22 years old, age groups. All p-value comparisons were based on an unpaired, non-parametric Mann-Whitney t-test statistic. Each point in the figure represents an individual participant. The three horizontal bars represent the median value (middle bar), upper interquartile range (top bar) and lower interquartile range (bottom bar).

2.4 Association levels between the quantities (copies/ng) of vaginal bacteria and hormonal contraceptives

The hormonal contraceptive that each participant was using was recorded at the first visit of the WISH Cohort study process. The three hormonal contraceptives of particular interest within this study include DMPA, the Implanon and Nur Isterate.

Table 2.4: Comparison of the non-parametric paired Friedman's ANOVA test across all bacterial groups with a Dunn's Multiple Comparison test for the DMPA, Implanon and Nur Isterate hormonal contraceptive groups:

Bacterial comparisons	Hormonal Contraceptive p-values		
	DMPA	Implanon	Nur Isterate
L. gasseri vs *L. jensenii*	0.8817	>0.9999	>0.9999
L. gasseri vs *L. crispatus*	>0.9999	>0.9999	0.1923
L. gasseri vs *L. iners*	0.0057*	>0.9999	<0.0001*
L. gasseri vs *G. vaginalis*	0.0057*	0.0375*	<0.0001*
L. gasseri vs *P. bivia*	<0.0001*	0.2103	<0.0001*
L. jensenii vs *L. crispatus*	0.5144	>0.9999	0.0065*
L. jensenii vs *L. iners*	<0.0001*	0.0375*	<0.0001*
L. jensenii vs *G. vaginalis*	<0.0001*	<0.0001*	<0.0001*
L. jensenii vs *P. bivia*	<0.0001*	0.0003*	<0.0001*
L. crispatus vs *L. iners*	0.0132*	0.8817	<0.0001*
L. crispatus vs *G. vaginalis*	0.0132*	0.003*	<0.0001*
L. crispatus vs *P. bivia*	<0.0001*	0.0245*	<0.0001*
L. iners vs *G. vaginalis*	>0.9999	>0.9999	>0.9999
L. iners vs *P. bivia*	>0.9999	>0.9999	0.0015*
G. vaginalis vs *P. bivia*	>0.9999	>0.9999	0.3366
ANOVA p-value	<0.0001*	<0.0001*	<0.0001*

* The asterisk indicates a p-value lower than the standardized p-value of 0.05 with a 95% confidence interval.

2.4.1 *Prevotella bivia*

We compared the quantified log copies/ng of *P. bivia,* and found no significant differences between the hormonal contraceptive groups (Kruskal-Wallis ANOVA p=0.2820) (Figure 2.4.1).

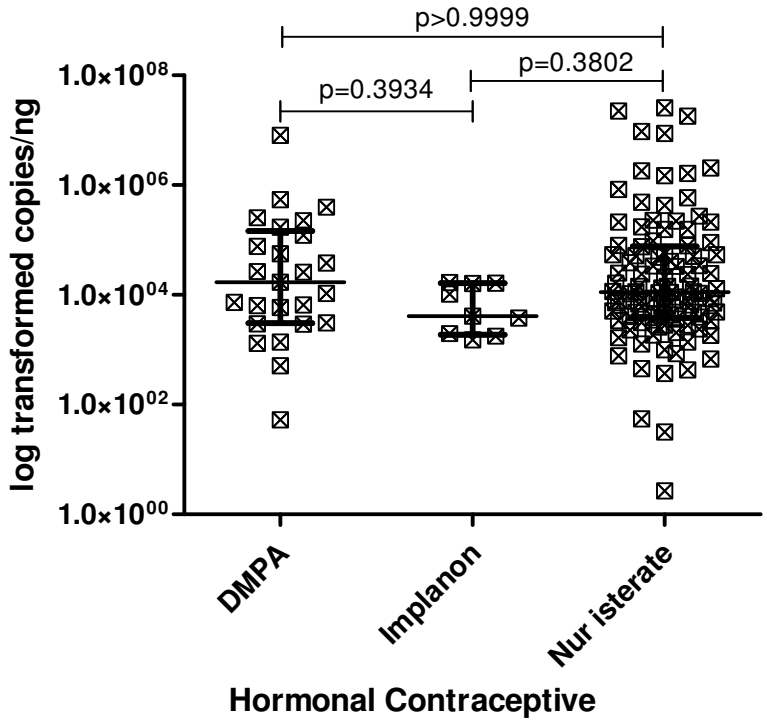

Figure 2.4.1: Comparison of the quantities of *P. bivia* (log transformed copies/ng DNA) measured in the DNA extracted from vaginal lateral wall swabs from participants in the WISH study, between the hormonal contraceptives DMPA, Nur Isterate and the Implanon. All p-value comparisons were based on an unpaired, non-parametric Dunn's Multiple Comparison test. Each point in the figure represents an individual participant. The three horizontal bars represent the median value (middle bar), upper interquartile range (top bar) and lower interquartile range (bottom bar).

2.5 Association levels between the quantities (copies/ng) of the bacteria of interest and the absence or presence of any once STI in the WISH cohort

The STI status was determined based on the absence or presence of any one bacterial (*Chlamydia trachomatis, Neisseria gonorrhea,* and *Mycoplasma genitalium*), viral (Herpes

Simplex Virus 2, and Human Papilloma Virus) or parasitic (*Trichomonas vaginalis*) STI for each participant.

Table 2.5: Comparison of the non-parametric, paired Friedman's ANOVA test across all bacterial groups with a Dunn's Multiple Comparison test for the absence or presence of any one STI of interest in the WISH study.

Bacterial comparisons	STI Status Group p-values	
	Absent	Any one Present
L. gasseri vs *L. jensenii*	0.918	0.436
L. gasseri vs *L. crispatus*	>0.9999	>0.9999
L. gasseri vs *L. iners*	<0.0001*	<0.0001*
L. gasseri vs *G. vaginalis*	<0.0001*	<0.0001*
L. gasseri vs *P. bivia*	<0.0001*	<0.0001*
L. jensenii vs *L. crispatus*	0.1534	0.0079*
L. jensenii vs *L. iners*	<0.0001*	<0.0001*
L. jensenii vs *G. vaginalis*	<0.0001*	<0.0001*
L. jensenii vs *P. bivia*	<0.0001*	<0.0001*
L. crispatus vs *L. iners*	<0.0001*	0.0002*
L. crispatus vs *G. vaginalis*	<0.0001*	<0.0001*
L. crispatus vs *P. bivia*	<0.0001*	<0.0001*
L. iners vs *G. vaginalis*	>0.9999	0.9398
L. iners vs *P. bivia*	0.1884	0.0079*
G. vaginalis vs *P. bivia*	0.918	>0.9999
ANOVA p-value	<0.0001*	<0.0001*

* The asterisk indicates a p-value lower than the standardized p-value of 0.05 with a 95% confidence interval.

2.5.1 *Prevotella bivia*

We compared the quantified log copies/ng of *P. bivia* and found no significant differences between the participants with and without any one STI (p=0.1905) (Figure 2.5.1). Although this follows the trend of the other bacterium within this cohort, due to the lack of accuracy of the primers this data should not be taken as reliable.

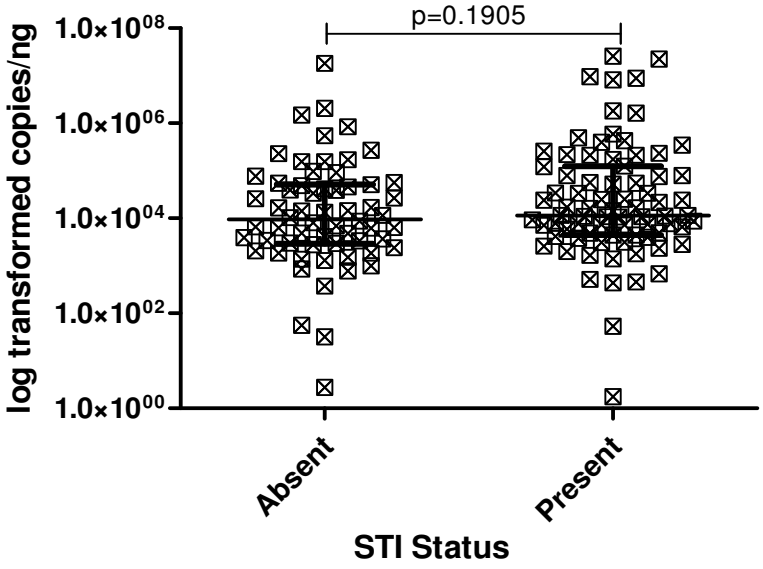

Figure 2.5.1: Comparison of the quantities of *P. bivia* (log transformed copies/ng DNA) measured in the DNA extracted from vaginal lateral wall swabs from participants in the WISH study, where the samples have been separated based on absence or presence of any one of the WISH cohort STIs present. All p-value comparisons were based on an unpaired, non-parametric Mann-Whitney t-test statistic. Each point in the figure represents an individual participant. The three horizontal bars represent the median value (middle bar), upper interquartile range (top bar) and lower interquartile range (bottom bar).

2.6 Association levels between the quantities (copies/ng) of the bacteria of interest and the presence of bacterial or viral STI's in the WISH cohort

The STI status was determined based on the sum value of the presence or absence of all bacterial (*Chlamydia trachomatis, Neisseria gonorrhea,* and *Mycoplasma genitalium*), or viral (Herpes Simplex Virus 2, and Human Papilloma Virus) for each participant within the WISH cohort.

Asterisk stars were used in the following figures where one start (*) indicates a p-value lower than 0.05, two stars (**) indicate a p-value lower than 0.01 and three stars (***) indicate a p-value lower than 0.001.

Table 2.6.1: Comparison of the non-parametric, paired Friedman's ANOVA test across all bacterial groups with a Dunn's Multiple Comparison test for the three STI groups, none, one and two or more bacterial STI's of interest in the WISH study is present.

Bacterial comparisons	Bacterial STI grouping p-values		
	None	One	Two<
L. gasseri vs *L. jensenii*	0.5221	>0.9999	0.6815
L. gasseri vs *L. crispatus*	>0.9999	0.9595	>0.9999
L. gasseri vs *L. iners*	<0.0001*	<0.0001*	>0.9999
L. gasseri vs *G. vaginalis*	<0.0001*	<0.0001*	0.0812
L. gasseri vs *P. bivia*	<0.0001*	<0.0001*	0.0055*
L. jensenii vs *L. crispatus*	0.2835	0.0294*	>0.9999
L. jensenii vs *L. iners*	<0.0001*	<0.0001*	0.0095*
L. jensenii vs *G. vaginalis*	<0.0001*	<0.0001*	<0.0001*
L. jensenii vs *P. bivia*	<0.0001*	<0.0001*	<0.0001*
L. crispatus vs *L. iners*	<0.0001*	0.0117*	>0.9999
L. crispatus vs *G. vaginalis*	<0.0001*	0.0001*	0.0437*
L. crispatus vs *P. bivia*	<0.0001*	<0.0001*	0.0026*
L. iners vs *G. vaginalis*	>0.9999	>0.9999	>0.9999
L. iners vs *P. bivia*	0.129	0.1043	0.4769
G. vaginalis vs *P. bivia*	>0.9999	>0.9999	>0.9999
ANOVA p-value	<0.0001*	<0.0001*	<0.0001*

* The asterisk indicates a p-value lower than the standardized p-value of 0.05 with a 95% confidence interval.

The absence of any bacterial STI group (Figure 2.6.1A) had significantly different copies/ng of *G. vaginalis* and *L. iners* in comparison to *L. gasseri* (p<0.0001)*, L. jensenii* (p<0.0001) and *L. crispatus* (p<0.0001). This trend was followed by the group with one bacterial STI present (Figure 2.6.1B) except *G. vaginalis* and *L. iners* had a significance of p=0.0001 and p=0.0117 in comparison to *L. crispatus* respectively, with *L. crispatus* having significantly different copies/ng in comparison to *L. jensenii* (p=0.0294). In the presence of two or more bacterial STIs (Figure 2.6.1C), *G. vaginalis* and *L. iners* had significantly higher copies/ng in comparison to *L. jensenii* (p<0.0001, p=0.0095) with *G. vaginalis* further having higher copies/ng in comparison to *L. crispatus* (p=0.0437). The absence of, or presence of one bacterial STI, show similar trends in bacterial copies/ng with the presence of two or more bacterial STIs having fewer differences between the bacterial copies/ng.

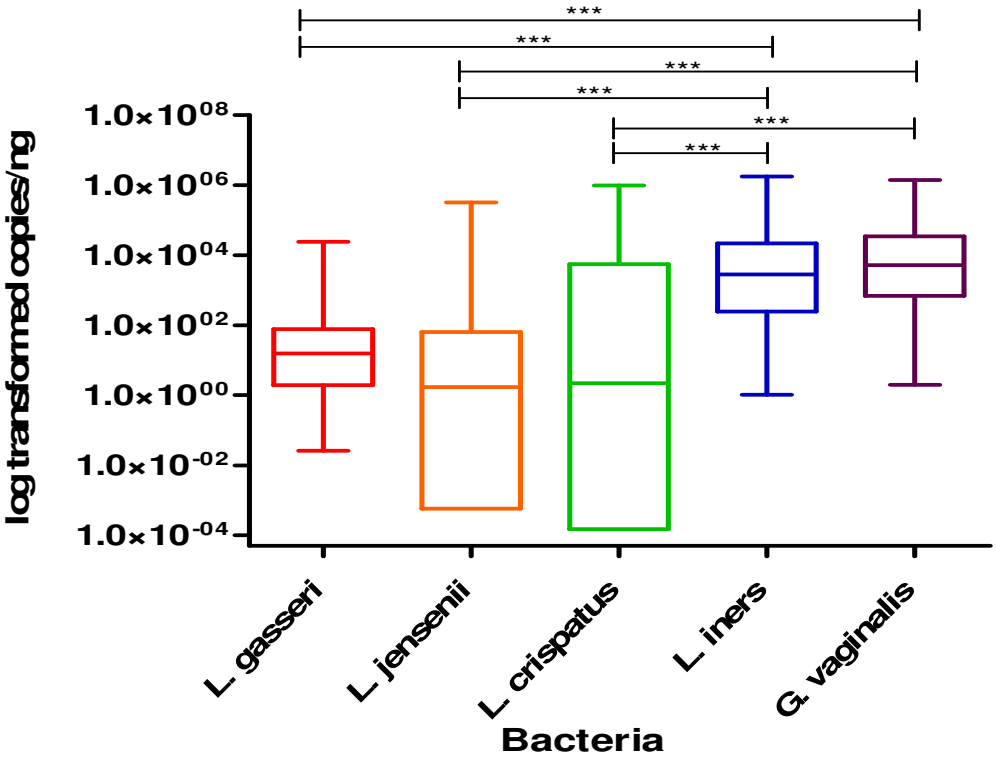

Figure 2.6.1A: Box-plot of the absence of any one bacterial STI for *L. gasseri* (red), *L. jensenii* (orange), *L. crispatus* (green), *L. iners* (blue), *G. vaginalis* (purple) reported as log transformed copies/ng total DNA. The 'box' component of each plot indicates the interquartile range (IQR) of the data set and the 'whiskers' which are the two lines (bottom and top) extending from the box component of each block that end with a horizontal stroke, indicate the range from the smallest and largest non-outliers to the 25% and 75% percentile components, respectively. The middle line indicates the median value for each data set.

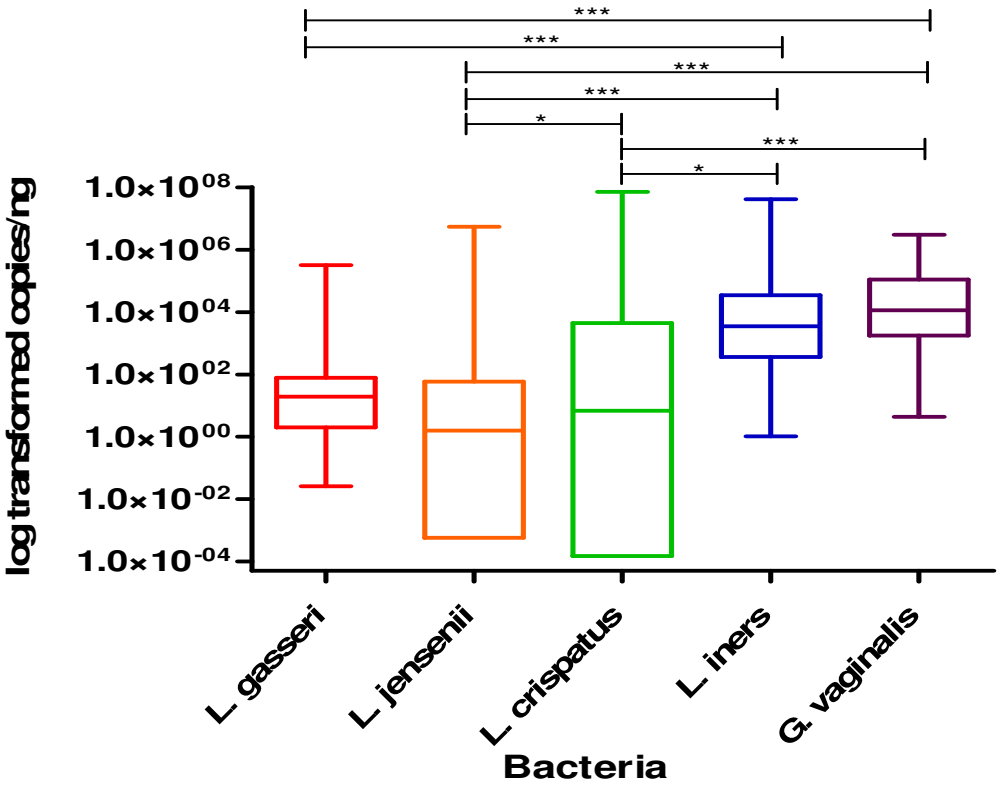

Figure 2.6.1B: Box-plot of the presence of any one bacterial STI for *L. gasseri* (red), *L. jensenii* (orange), *L. crispatus* (green), *L. iners* (blue), *G. vaginalis* (purple) reported as log transformed copies/ng total DNA. The 'box' component of each plot indicates the interquartile range (IQR) of the data set and the 'whiskers' which are the two lines (bottom and top) extending from the box component of each block that end with a horizontal stroke, indicate the range from the smallest and largest non-outliers to the 25% and 75% percentile components, respectively. The middle line indicates the median value for each data set.

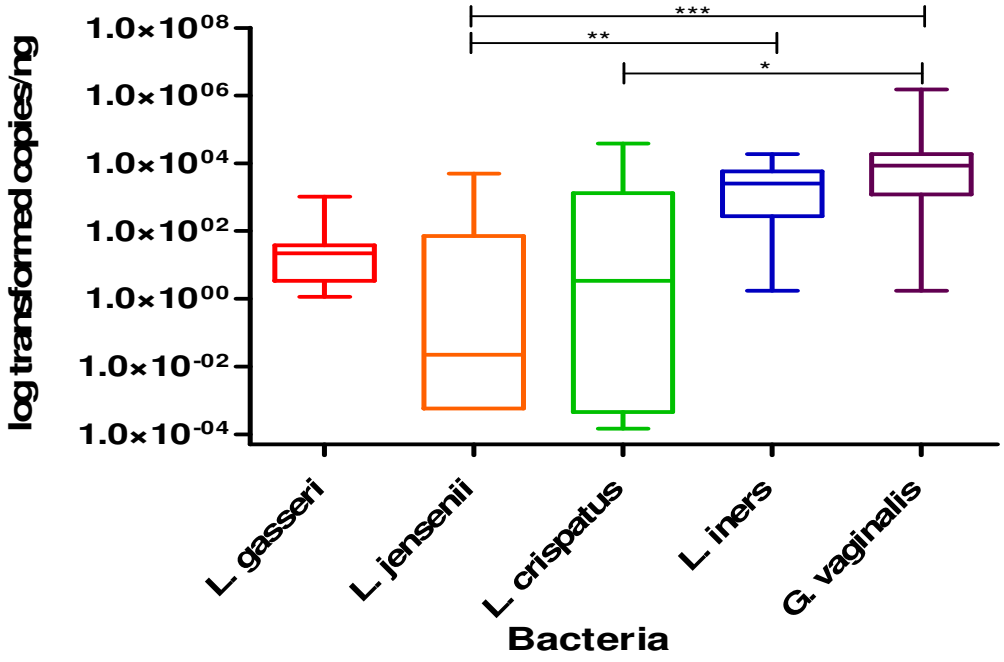

Figure 2.6.1C: Box-plot of two or more bacterial STIs for *L. gasseri* (red), *L. jensenii* (orange), *L. crispatus* (green), *L. iners* (blue), *G. vaginalis* (purple) reported as log transformed copies/ng total DNA. The 'box' component of each plot indicates the interquartile range (IQR) of the data set and the 'whiskers' which are the two lines (bottom and top) extending from the box component of each block that end with a horizontal stroke, indicate the range from the smallest and largest non-outliers to the 25% and 75% percentile components, respectively. The middle line indicates the median value for each data set.

Table 2.6.2: Comparison of the non-parametric, paired Friedman's ANOVA test across all viral groups with a Dunn's Multiple Comparison test for the three STI groups, none, one or two viral STI's of interest in the WISH.

Bacterial comparisons	Viral STI grouping p-values		
	None	One	Two
L. gasseri vs *L. jensenii*	0.4463	0.4859	>0.9999
L. gasseri vs *L. crispatus*	>0.9999	>0.9999	0.6729
L. gasseri vs *L. iners*	<0.0001*	<0.0001*	>0.9999
L. gasseri vs *G. vaginalis*	<0.0001*	<0.0001*	0.1307
L. gasseri vs *P. bivia*	<0.0001*	<0.0001*	0.2033
L. jensenii vs *L. crispatus*	0.0083*	0.3777	0.6729
L. jensenii vs *L. iners*	<0.0001*	<0.0001*	>0.9999
L. jensenii vs *G. vaginalis*	<0.0001*	<0.0001*	0.1307
L. jensenii vs *P. bivia*	<0.0001*	<0.0001*	0.2033

L. crispatus vs *L. iners*	0.0184*	<0.0001*	>0.9999
L. crispatus vs *G. vaginalis*	0.0011*	<0.0001*	>0.9999
L. crispatus vs *P. bivia*	<0.0001*	<0.0001*	>0.9999
L. iners vs *G. vaginalis*	>0.9999	>0.9999	>0.9999
L. iners vs *P. bivia*	0.6725	0.0054*	>0.9999
G. vaginalis vs *P. bivia*	>0.9999	0.5104	>0.9999
ANOVA p-value	< 0.0001*	< 0.0001*	0.0038*

* The asterisk indicates a p-value lower than the standardized p-value of 0.05 with a 95% confidence interval.

In the presence of one viral STI (Figure 2.6.2A), *G. vaginalis* and *L. iners* had significantly different copies/ng in comparison to *L. gasseri* (p<0.0001), *L. jensenii* (p<0.0001) and *L. crispatus* (p<0.0001). A similar pattern was followed in the absence of any viral STI (Figure 2.6.2B), except *G. vaginalis* and *L. iners* had a significance of p=0.0011 and p=0.0184 in comparison to *L. crispatus,* respectively. Further, *L. crispatus* had significantly different copies/ng in comparison to *L. jensenii* (p=0.0083). The presence of two viral STIs (Figure 2.6.2C) showed no association with the copies/ng of the bacterium which showed no difference.

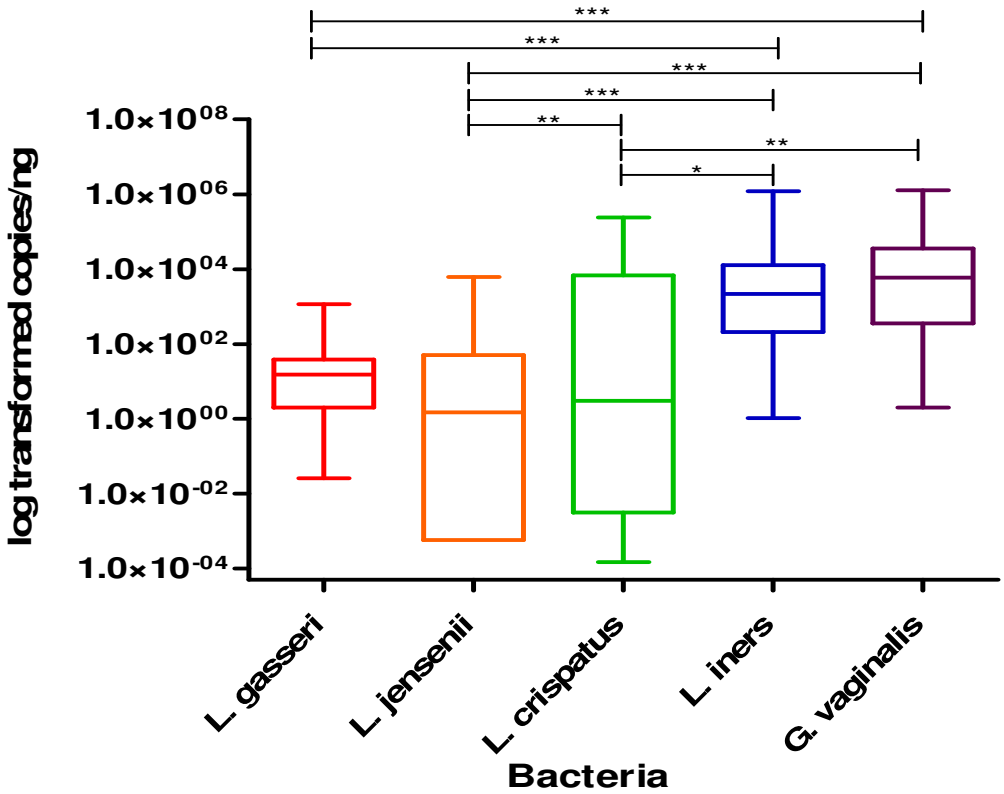

Figure 2.6.2A: Box-plot of the absence of any one viral STI for *L. gasseri* (red), *L. jensenii* (orange), *L. crispatus* (green), *L. iners* (blue), *G. vaginalis* (purple) reported as log transformed copies/ng total DNA. The 'box' component of each plot indicates the interquartile range (IQR) of the data set and the 'whiskers' which are the two lines (bottom and top) extending from the box component of each block that end with a horizontal stroke, indicate the range from the smallest and largest non-outliers to the 25% and 75% percentile components, respectively. The middle line indicates the median value for each data set.

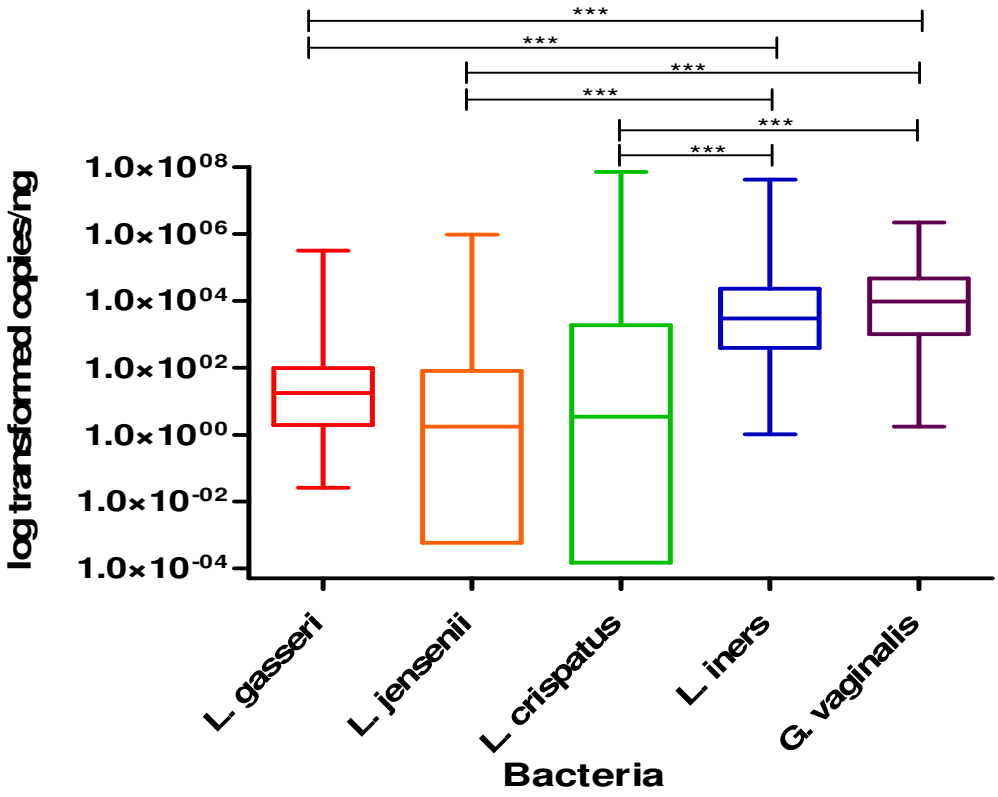

Figure 2.6.2B: Box-plot of the presence of any one viral STI for *L. gasseri* (red), *L. jensenii* (orange), *L. crispatus* (green), *L. iners* (blue), *G. vaginalis* (purple) reported as log transformed copies/ng total DNA. The 'box' component of each plot indicates the interquartile range (IQR) of the data set and the 'whiskers' which are the two lines (bottom and top) extending from the box component of each block that end with a horizontal stroke, indicate the range from the smallest and largest non-outliers to the 25% and 75% percentile components, respectively. The middle line indicates the median value for each data set.

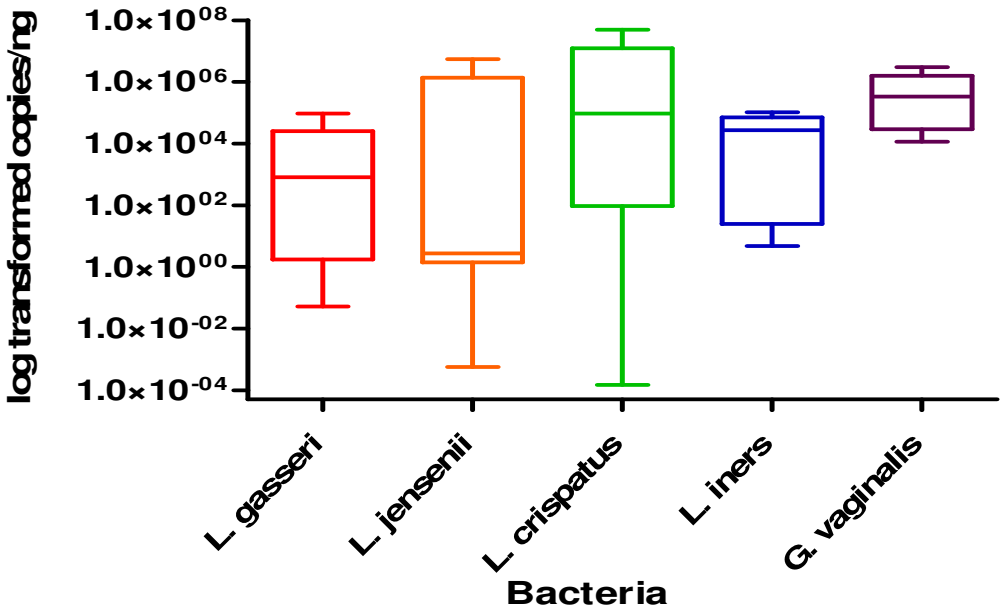

Figure 2.6.2C: Box-plot of two viral STIs for *L. gasseri* (red), *L. jensenii* (orange), *L. crispatus* (green), *L. iners* (blue), *G. vaginalis* (purple) reported as log transformed copies/ng total DNA. The 'box' component of each plot indicates the interquartile range (IQR) of the data set and the 'whiskers' which are the two lines (bottom and top) extending from the box component of each block that end with a horizontal stroke, indicate the range from the smallest and largest non-outliers to the 25% and 75% percentile components, respectively. The middle line indicates the median value for each data set.

2.6.3 *Prevotella bivia*

We compared the quantified log copies/ng of *P. bivia* between those with none, one or two (or more) bacterial or viral STI groups s. The bacterial STI groups had no significant difference in *P. bivia* (Kruskal-Wallis ANOVA p=0.5566). The copies/ng of *P. bivia* in the viral STI group with no STI differed significantly from the presence of two viral STIs (p=0.0488). There was no significant difference in *P. bivia* between the viral STI groups (Kruskal-Wallis ANOVA p=0.0526) (Figure 2.6.3). This data should not be taken as reliable due to the primer errors discussed previously.

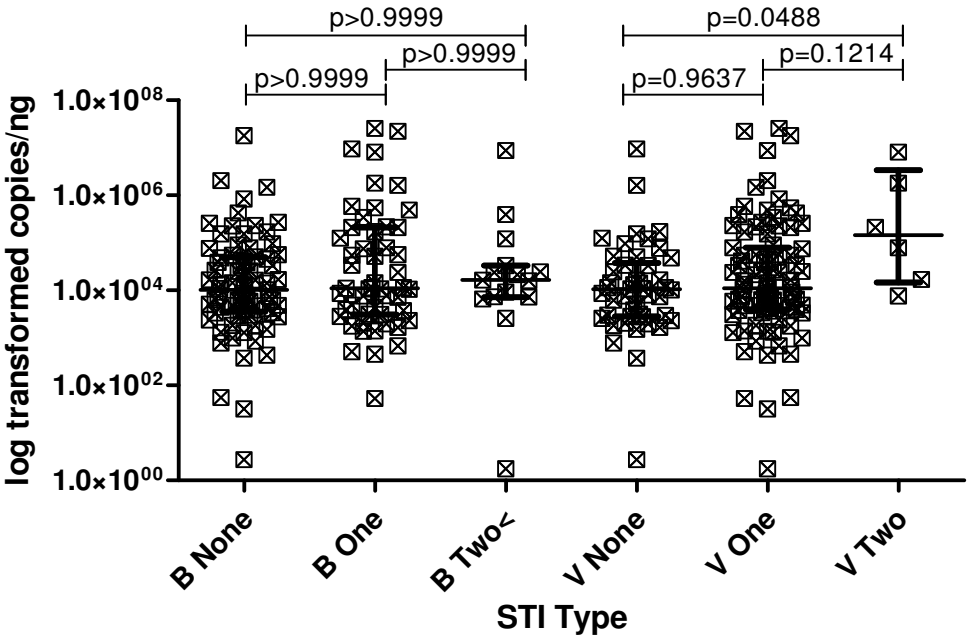

Figure 2.6.3: Comparison of the quantities of *P. bivia* (log transformed copies/ng DNA) measured in the DNA extracted from vaginal lateral wall swabs from participants in the WISH study, where the samples have been separated based on none, one, two (or more <) of the WISH cohort Bacterial (B) versus Viral (V) STIs being present. All p-value comparisons were based on an unpaired, non-parametric Dunn's Multiple Comparison test. Each point in the figure represents an individual participant. The three horizontal bars represent the median value (middle bar), upper interquartile range (top bar) and lower interquartile range (bottom bar).

2.7 Association levels between the quantities (copies/ng) of bacteria of interest and the absence or presence of low and high risk HPV subtypes in the WISH cohort

The HPV status was considered negative in the absence of all HPV subtypes amplified by the Roche linear array, low risk if 6, 11, 40, 42, 54, 55, 61, 62, 64, 67, 69, 70, 71, 72, 81, 83, 84, 89(CP6109) and IS39 HPV subtypes were present, and high risk if 16, 18, 26, 31, 33, 35, 39, 45, 51, 52, 53, 56, 58, 59, 66, 68, 73 and 82 HPV subtypes were present.

Table 2.7: Comparison of the non-parametric paired Friedman's ANOVA test across all bacterial groups with a Dunn's Multiple Comparison test for the HPV groups.

Bacterial comparisons	HPV Group p-values		
	Negative	Low Risk	High Risk
L. gasseri vs *L. jensenii*	0.4845	>0.9999	>0.9999

L. gasseri vs *L. crispatus*	>0.9999	>0.9999	0.6674
L. gasseri vs *L. iners*	0.0023*	0.0017*	<0.0001*
L. gasseri vs *G. vaginalis*	0.0023*	0.0001*	<0.0001*
L. gasseri vs *P. bivia*	<0.0001*	<0.0001*	<0.0001*
L. jensenii vs *L. crispatus*	0.0023*	>0.9999	0.0089*
L. jensenii vs *L. iners*	<0.0001*	<0.0001*	<0.0001*
L. jensenii vs *G. vaginalis*	<0.0001*	<0.0001*	<0.0001*
L. jensenii vs *P. bivia*	<0.0001*	<0.0001*	<0.0001*
L. crispatus vs *L. iners*	0.4845	<0.0001*	0.0881
L. crispatus vs *G. vaginalis*	0.4845	<0.0001*	0.0112*
L. crispatus vs *P. bivia*	0.0034*	<0.0001*	0.0002*
L. iners vs *G. vaginalis*	>0.9999	>0.9999	>0.9999
L. iners vs *P. bivia*	>0.9999	>0.9999	>0.9999
G. vaginalis vs *P. bivia*	>0.9999	>0.9999	>0.9999
ANOVA p-value	<0.0001*	<0.0001*	<0.0001

* The asterisk indicates a p-value lower than the standardized p-value of 0.05 with a 95% confidence interval.

2.7.1 *Prevotella bivia*

We compared the quantified log copies/ng of *P. bivia* between the HPV groups. There was no significant difference in *P. bivia* between the HPV groups (Kruskal-Wallis ANOVA p=0.7775) (Figure 2.7.1). The lack of difference between the copies/ng in each group has been attributed to the inaccurate primers and thus the results are unreliable until validated with new, accurate primers.

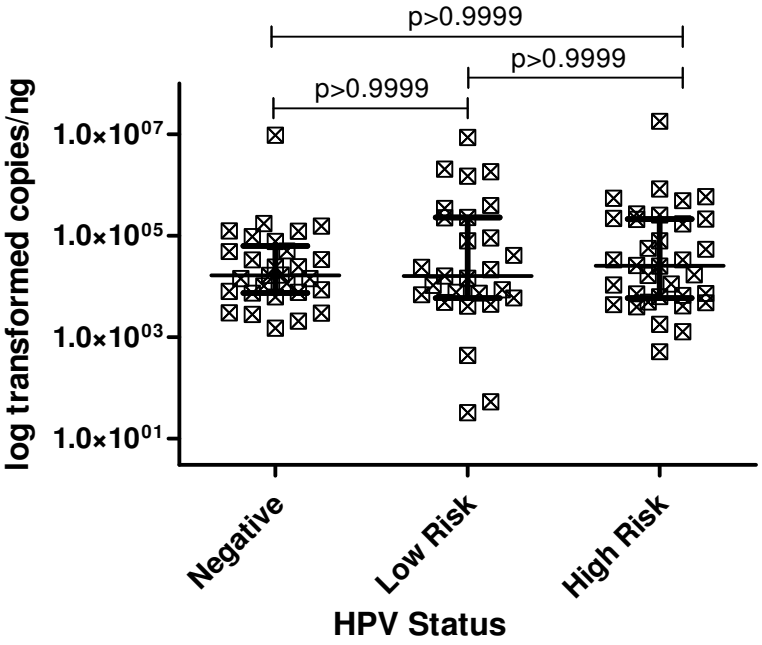

Figure 2.7.1: Comparison of the quantities of *P. bivia* (log transformed copies/ng DNA) measured in the DNA extracted from vaginal lateral wall swabs from participants in the WISH study, between the negative, low risk and high risk HPV groups. All p-value comparisons were based on an unpaired, non-parametric Dunn's Multiple Comparison test. Each point in the figure represents an individual participant. The three horizontal bars represent the median value (middle bar), upper interquartile range (top bar) and lower interquartile range (bottom bar).